MONASH University

Prefabricated modular beam-to-hybrid columns connections under quasi-static loading

Seyed Nima Sadeghi

B.Sc., M.Sc. in Mechanical Engineering

A thesis submitted for the degree of Doctor of Philosophy at Monash University in 2018

Department of Civil Engineering

Copyright notice

© The author (2018). Except as provided in the Copyright Act 1968, this thesis may not be reproduced in any form without the written permission of the author.

Synopsis

Using hollow sections, namely fabricated hollow columns, due to the higher load-bearing capacities is becoming more popular in the construction industry. An innovative hybrid-fabricated column (HFC) was recently developed at Civil Engineering Department of Monash University. In this column, four ultra-high strength steel (UHSS) tubes are welded to thin mild steel (MS) plates at corners to form a closed section. Although the superior performance of the HFCs has been demonstrated, due to their geometry, the subject of connecting I-beams to the HFCs is challenging.

In this research, an innovative prefabricated modular connection was developed based on the geometrical characteristics of the HFCs. First, this patented connection was modelled using the FE model. The HFC used in the simulations had four corner tubes with material properties of MS or UHSS. The geometry of the plates connecting the corner tubes was chosen to be either flat or corrugated in different cases, but their material was chosen to be MS in all cases.

Thus, experimental tests were conducted on the proposed prefabricated modular connection under monotonic loading to validate the finite element modelling. The connection was tested in two different versions in which the beam was either bolted or welded to other components. Material properties of the FE model were chosen similar to the properties of the materials used in the experiments. Combination of these parameters has shown the impact of material properties and attachment methods on the behaviour of the connection.

Using the validated finite element model, the behaviour of the proposed connection was compared to that of some conventional connections. Furthermore, a topology optimisation has been conducted on two aforementioned versions of the connection with different thicknesses. The behaviour of the connection (original and a thinned version) used along the HFC consisting of corrugated plates, and corner tubes was also studied using the FE model. Whereas corrugated plates show less stiffness under loads perpendicular to the corrugation, the effect of bidirectional connections along with corrugated HFCs was also investigated. Thus, the effect of the dimensions of the connection components on the joint behaviour was investigated.

A component-based model was also developed for simulating the behaviour of the connection. The results of this model have been compared to the results of the finite

element model, showing a good agreement. The component-based model has the potential to accurately predict the moment resistance and rotation capacity of the connection.

The innovative connection proposed in this research has been able to satisfy the requirements and constraints dictated by the geometry of the hybrid fabricated columns. It utilises the superior material properties of the corner tubes and efficiently transfers the load from the beam to the column through them, as the strong components of the column. It also can be adjusted for different levels of capacity required in the construction. However, it should be designed to satisfy the full-strength connection status. Although the behaviour of the patented connection under cyclic loading should be investigated in future, it might have a potential to be used in seismic region as the rotation capacity of the connection is beyond the prerequisite limits in standards for moment frames used in these areas. The modularity and reusability of the connection are two other significant benefits of the connection, which improve the building quality and construction time, cost, and safety.

Thesis including published works declaration

In accordance with Monash University Doctorate Regulation 17.2 Doctor of Philosophy and Research Masters regulations the following declarations are made:

I hereby declare that this thesis contains no material which has been accepted for the award of any other degree or diploma at any university or equivalent institution and that, to the best of my knowledge and belief, this thesis contains no material previously published or written by another person, except where due reference is made in the text of the thesis.

This thesis includes two original papers published in peer-reviewed journals and one submitted publications. The core theme of the thesis is structural mechanics. The ideas, development and writing up of all the papers in the thesis were the principal responsibility of myself, the student, working within the Department of Civil Engineering under the supervision of Dr Amin Heidarpour.

The inclusion of co-authors reflects the fact that the work came from an active collaboration between researchers and acknowledges input into team-based research.

In the case of chapters two and three my contribution to the work involved the following:

Thesis Chapter	**Publication Title**	**Status**	**Nature and % of student contribution**	**Co-author name(s) Nature and % of Co-author's contribution***	**Co-author(s), Monash student Y/N***
Two	An innovative I-beam to hybrid fabricated column connection: Experimental investigation	Published	(70%) Development of ideas; Establishing the methodology; Experimental work; Data analysis; Writing up and revisions.	1) Dr A. Heidarpour (20%) Financial support; Input into manuscript; Revision 2) Prof. X.L. Zhao (5%) Financial support; Revision 3) Prof. R. Al-Mahaidi (5%) Financial support; Revision	No

Three	A comparative numerical study on the innovative I-beam to thin-walled hybrid fabricated column connection	Published	(70%) Development of ideas; Establishing the methodology; Data analysis; Writing up and revisions.	1) Dr A. Heidarpour (20%) Financial support; Input into manuscript; Revision 2) Prof. X.L. Zhao (5%) Financial support; Revision 3) Prof. R. Al-Mahaidi (5%) Financial support; Revision	No

I have renumbered sections of submitted or published papers in order to generate a consistent presentation within the thesis.

Student signature: 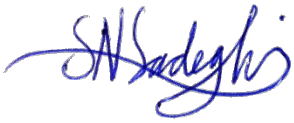 **Date:** 13-June-2018

The undersigned hereby certify that the above declaration correctly reflects the nature and extent of the student's and co-authors' contributions to this work. In instances where I am not the responsible author, I have consulted with the responsible author to agree on the respective contributions of the authors.

Main Supervisor signature:  **Date:** 13-June-2018

List of Publications

The results obtained from the research conducted by the candidate have already been summarised and published in the journal and conference papers listed as follows. It is worth mentioning that all the journal papers were published in ISI Quarter 1 (Q1) peer-reviewed journals. Also, a manuscript written based on the outcomes of the numerical investigation of the behaviour of the connection used along with corrugated HFCs is currently under internal review, and it is presented here as the fifth chapter of the thesis.

Peer Reviewed Journal Papers

- Sadeghi SN, Heidarpour A, Zhao XL, Al-Mahaidi R. A comparative numerical study on the innovative I-beam to thin-walled hybrid fabricated column connection. *Thin-Walled Structures*. 2018;127:235-258.

- Sadeghi SN, Heidarpour A, Zhao XL, Al-Mahaidi R. An innovative I-beam to hybrid fabricated column connection: Experimental investigation. *Engineering Structures*, 2017; 148:907-923.

Conference Papers

- Sadeghi SN, Heidarpour A, Zhao X-L, Al-Mahaidi R (2017). Experimental evaluation of moment-rotation response of an innovative modular beam-to-fabricated column connection, In: Heidarpour A., Zhao, XL, editors. *Tubular Structures XVI: Proceedings of the 16th International Symposium for Tubular Structures (ISTS16)*, Melbourne, Australia: Taylor and Francis Group LLC; 2017. p. 193-200.

- Sadeghi N, Heidarpour A, Zhao XL, Al-Mahaidi R. Numerical investigation of innovative modular beam-to-fabricated column connections under monotonic loading. In: Zingoni A, editor. *Insights and Innovations in Structural Engineering, Mechanics and Computations (SEMC2016)*. Cape Town, South Africa: Taylor and Francis Group, LLC; 2016. p. 1247–52.

Journal Paper under Review

- Sadeghi SN, Heidarpour A, Zhao XL, Al-Mahaidi R. A component-based model for innovative prefabricated beam-to-hybrid tubular column connections. *Thin-Walled Structures*; under review.

Journal Paper under Internal Review

- Sadeghi SN, Heidarpour A, Zhao XL, Al-Mahaidi R. Numerical investigation of the behaviour of innovative beam-to-hybrid corrugated columns connection; under internal review.

Other Outputs

- "Connection Arrangement for Connecting a Cross-Member to a Vertical Member" (PCT/AU2017/050923). Inventors: S.N. Sadeghi, A. Heidarpour, X.L. Zhao.

Acknowledgements

Reaching the end of this invaluable chapter of my life, my PhD journey, I firmly believe that it would not have been possible to conclude it successfully without having a fantastic network of support from my family, friends, and colleagues.

In the first place, I would like to express my sincere gratitude towards my main supervisor, Dr Amin Heidarpour. I feel very fortunate for having the opportunity to work with him as he was more than just an academic supervisor. His patience, steadfast support, and creative thinking on top of his broad knowledge of his field of expertise helped me to remain focused and make timely and efficient progress. I would also like to thank my co-supervisors Prof Xiao-ling Zhao and Prof Riadh Al-Mahaidi whom their feedbacks, suggestions and support provided me with means to advance with more confidence and a clear vision of the different stages of my research.

In spite of being on the other side of the planet, my family gave me their unconditional love and support during these years that helped me keep my high spirits and achieve this milestone. Words cannot explain how grateful I am for the blessing of having them in my life. Speaking of the family, I would like to thank my friends who are my family far from home. People from four corners of the world who taught me humanity comes above all our differences in colour, religion or language.

This research work was supported by a grant awarded by the Australian Research Council through a Discovery Project (DP150100442) to my supervisors. I must also acknowledge the technical staff of the Civil Engineering Laboratory for their assistance in conducting the experimental work and SSAB Corporation, CrossLine Engineering, and Fetha Engineering for providing the required material and engineering support.

Table of Contents

List of Figures

Chapter 1

Chapter 2

Chapter 3

Chapter 4

Chapter 5

List of Tables

Chapter 2

Chapter 3

Chapter 4

Chapter 5

INTRODUCTION

CHAPTER 1

Table of Contents

1.1 Motivation

Using hollow sections in structural design, due to lower weight and surface area in comparison with equivalent open sections [1], has become more popular. Add to this the aesthetic appearance of exposed hollow sections and minimal painting and maintenance cost of these sections [2]. On one side, in spite of this increasing demand due to the mentioned advantages, load-bearing capacity of hollow sections is not adequate in many cases for today's applications such as high-rise buildings or bridges, in that, hot-rolled or cold-formed sections have limited sizes. On the other side, the cost of manufacturing sections with desirable capacities increases so much that their usage is not economically feasible in real-world projects. Therefore, fabricated columns are making their way into structural applications more than ever.

One particular type of these fabricated sections, which is of main interest in this research, has a rectangular cross-section and consists of four steel plates welded to one steel tube at each corner. This concept for fabricated sections was first introduced in early 2000 [3] and has been investigated by many researchers, notably in Civil Engineering Department of Monash University [4 - 22]. These research works have proven the superior performance of this hybrid fabricated column (HFC) - shown in Fig. 1-1 - in comparison to conventionally fabricated columns in axial load bearing. Their performance under bending is currently being investigated in Civil Engineering Department of Monash University. This investigation includes not only hollow section with flat faces but also works towards finding other ways of making even further improvements in these columns performance by introducing concrete filled double skin columns and utilising corrugated plates instead of flat plates as column face.

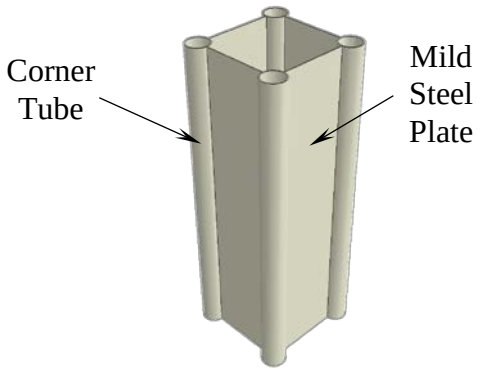

Fig. 1-1. Hybrid Fabricated Column (HFC)

This superior performance makes this type of column a good candidate for use in high-rise buildings subject to extreme events. It is needless to say that due to the loading types in high-rise buildings under extreme scenarios, the moment connections will be discussed and investigated. Bolting and welding are the main two ways of connecting beams to columns where bolting is usually the first preference unless special necessities dictate otherwise. Generally, the welded connection types for hollow structural section (HSS) moment connections are as follows (Fig. 1-2) [23]:

- HSS through-plate flange-plated
- HSS cut out-plate flange-plated
- HSS directly welded
- HSS end plate
- HSS above and below continuous beams
- HSS welded tee flange
- HSS diaphragm plate

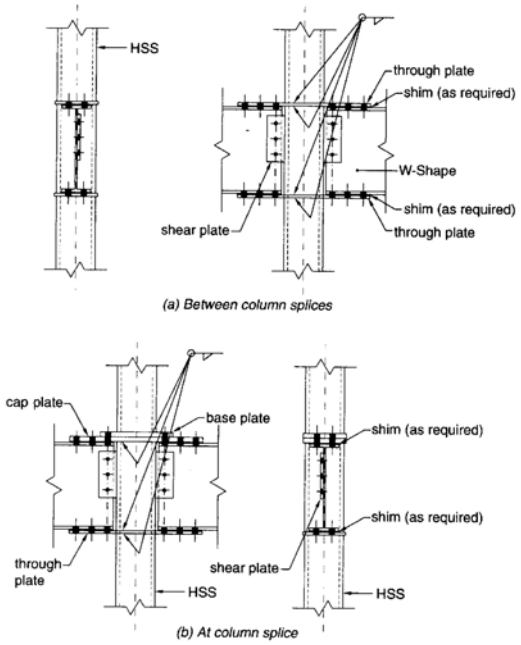

(a) HSS through-plate flange-plated

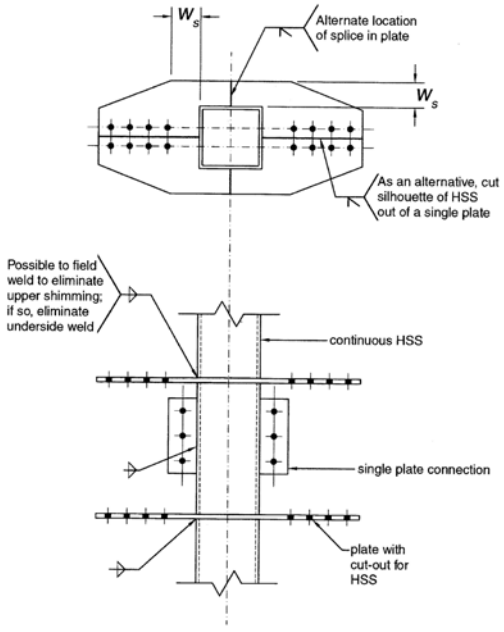

(b) HSS cut out-plate flange-plated

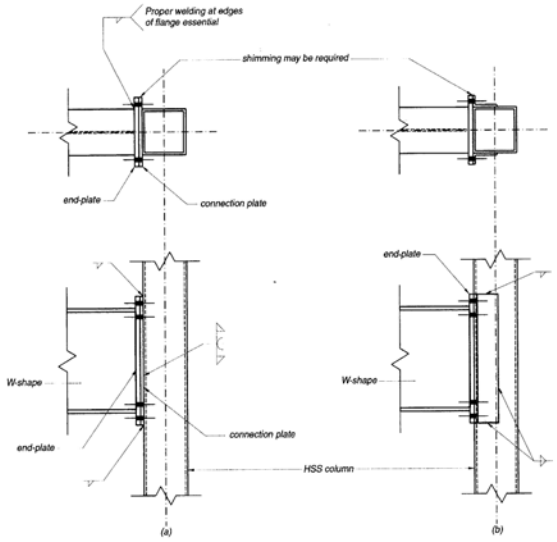

(c) HSS end plate

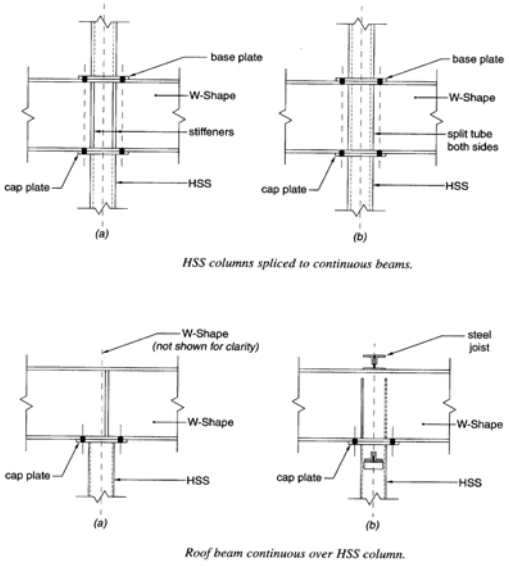

(d) above and below continuous beams

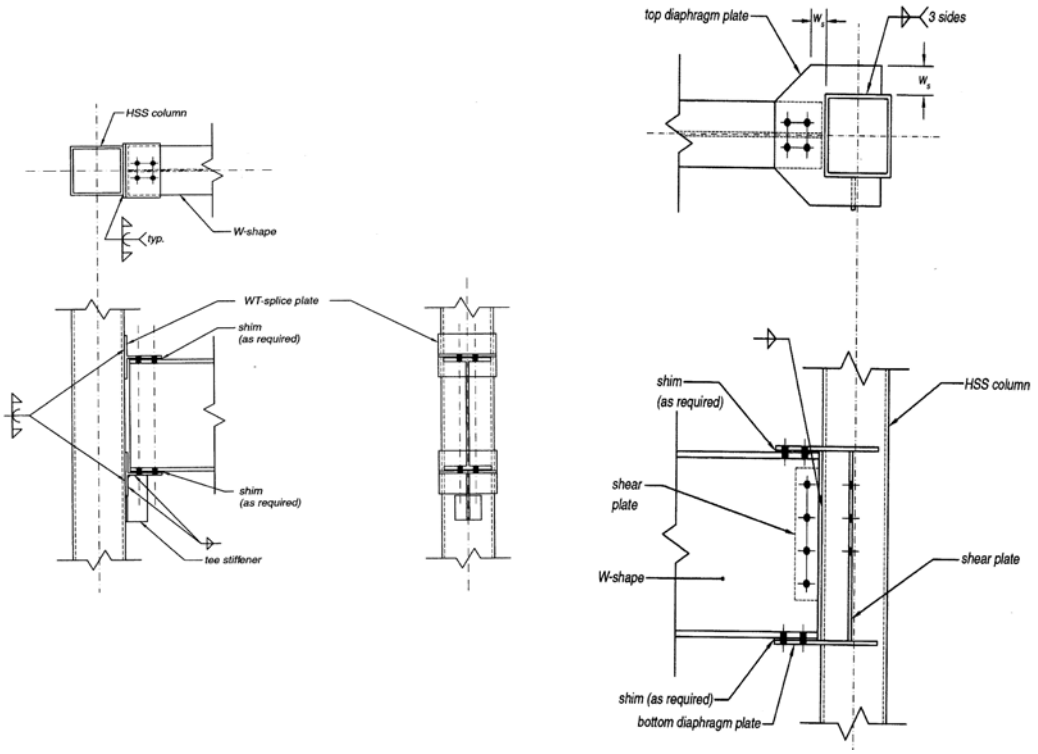

(e) HSS welded tee flange (f) HSS diaphragm plate

Fig. 1-2. HSS Welding Connections [23]

For directly bolted connection to HSS wall several methods can be used such as (Fig. 1-3) [23]:

- Through bolts
- Blind bolts
- Threaded studs
- Flow-drilled bolts
- Nails
- Screws

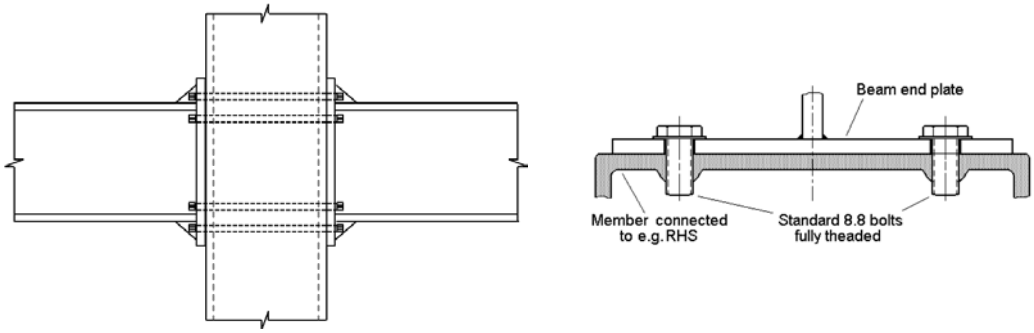

(a) Through bolts (b) Flow drill

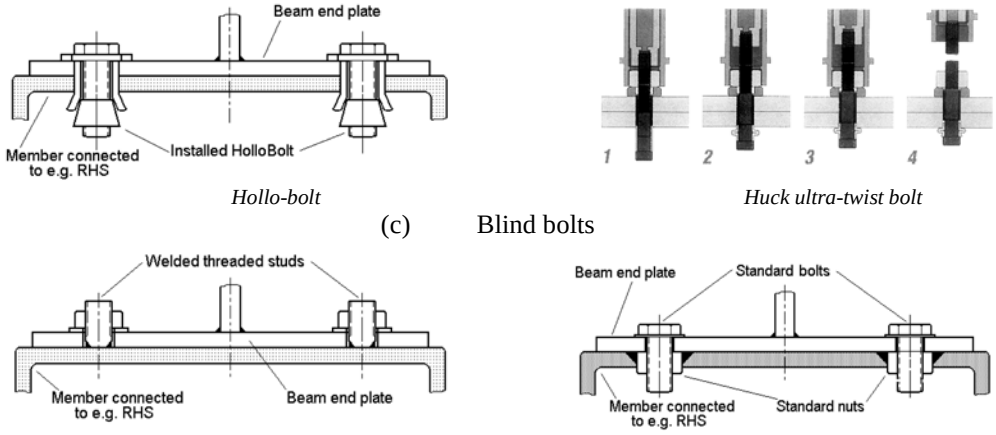

Hollo-bolt *Huck ultra-twist bolt*

(c) Blind bolts

(d) Threaded studs (e) Welded nuts

Fig. 1-3. HSS Direct Bolting Connections [23]

In addition to these special types of connecting methods, usage of standard bolted moment connections, i.e. bolted tee-stub, and end-plate connections are desirable. However, in many cases, inaccessibility of the inside of hollow sections is a real obstacle in construction. This access may be required for inspection purposes (e.g. to check for weld defects) or for tightening the bolts. Making access holes or welding channels/plates on the faces of HSS or employing blind bolts are usually used to tackle this problem.

The majority of previously illustrated connections can be used with the concrete-filled columns, as well. Several other types of connections, which are mostly specific to concrete-filled columns, are depicted in Fig. 1-4.

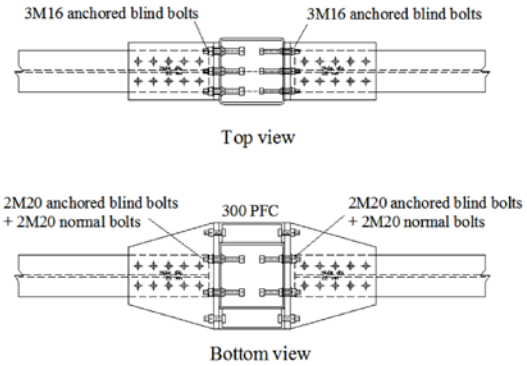

(a) Moment endplate with anchor bolts in concrete [32]

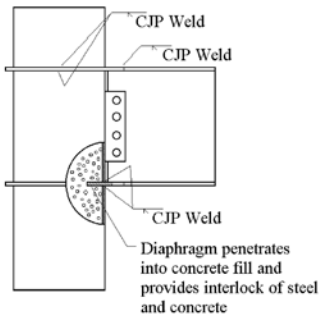

(b) Typical Japanese Style Through Diaphragm

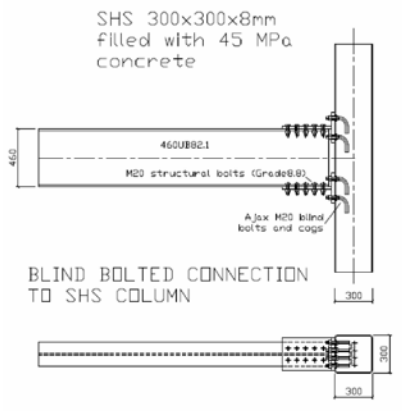

(c) Moment endplate with anchor bolts in concrete [33]

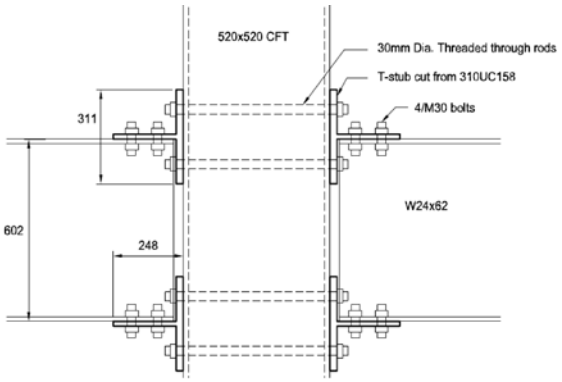

(d) T-Stub [34]

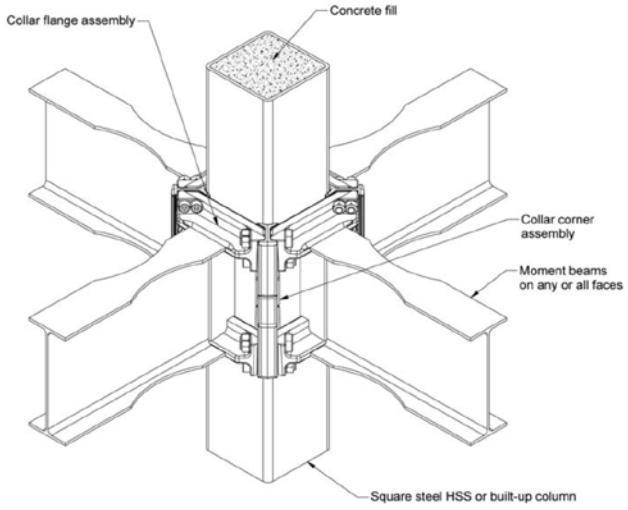

(e) ConXL System[35]

Fig. 1-4. Different Types of Connection to Concrete-filled Columns

As it can be seen, there are many different solutions available to be used for beam-to-column connections. However, the choice of a proper solution lies on the shoulders of the designer, which should be made based on factors such as seismic activity in the area, criticality of the building and alike.

However in the case of HFCs, the topic of connection has not been investigated before. Due to the special geometry of the connection, the suitability of the current conventional connections or the need of designing a new generation of connections to be used along with this column type has been looked into in current study.

1.2 Research aims

Since the introduction of hybrid fabricated columns, researchers have investigated the axial and flexural behaviour of this particular column under monotonic and cyclic loadings [3 - 22]. However, the topic of beam-to-hybrid fabricated column connections is original. This research problem is investigated through numerical simulations and experimental tests.

Different types of bolted connections, including but not limited to conventional connection types such as flush and extended end-plate connections are investigated in this thesis. Due to the particular geometry of this column type (HFC) in which high or ultra-high strength tubes are welded to the thin mild steel plates at corners, conventional types of connections may not be suitable for use. The conventional connections transfer the load to the column faceplates, which are not the strong components in HFCs. Faceplates in this column are deployed to maintain the rotation capacity of the column while corner tubes are considered as load-carrying components. A desirable connection should act in a way that connection load would be transferred to the tubes which count as the strong components.

Numerical simulation in the preliminary stage includes modelling conventional connections (e.g. flush and extended endplate) to find an estimate of how this column would behave under monotonic loading with these types of connections. Using the results of the preliminary study, a robust connection that can easily be fabricated and installed with high moment resistance and rotation capacity is proposed, modelled, and investigated. Following this stage series of experiments under monotonic loading is performed. These experiments are used to validate the numerical modelling as well as to prove the robustness of the proposed connection.

Afterwards, having the experimental test data and using the already validated numerical model, a topology optimisation, and a number of parametric studies on the corner tube material, size of the connection, and shape of the column faceplate is performed. A mechanical model (component-based method) is also developed that can predict the behaviour of the connection (moment-rotation curve) accurately. The generated dataset from experimental tests and numerical simulations could be used to provide a design recommendation for this specific column and its variations and relevant, robust connection(s). In summary, the research aims can be summarised as:

- Suggesting a new generation of robust connections that can be used along with HFCs;
- Experimentally and numerically investigating the behaviour of the proposed connections under monotonic loading in conjunction with different geometries and materials used in the HFCs;
- Providing a component-based model for the connection, which can represent the moment-rotation behaviour of the connection accurately and can be used in further parametric studies or design recommendations.

1.3 Literature review

Cold-formed hollow structural sections were first made in the early 1950s in the United Kingdom. High strength and bending stiffness of fabricated rectangular hollow sections compared to open section members, their torsional stiffness reduces the necessary lateral bracing of these columns [24 , 25]. In addition, higher post-buckling strength, ductility, and energy dissipation capacity due to their less sensitivity to local buckling makes them suitable members to use in moment resisting frames. In spite of possessing the advantages above, finding suitable connections to hollow section members is still under investigation.

Most active areas of research are mainly seismic structural applications, column connections, bolted connections, composite members, and composite connections [26]. The focus of these researches has been on fully restrained welded and bolted connections but when it comes to hollow sections, there is a need for more studies. The concept of innovative fabricated columns, which has been developed during the past two decades, needs more focus in research particularly on finding an appropriate beam to column connections. Now that these structural members are opening their way into the not only steel building structure but also in transportation and highway industry, agricultural equipment, mechanical members, and recreational structures [27], the research should be pursued more proactively. This chapter provides a general overview of related publications mainly on bolted I-beam connections to hollow and concrete filled rectangular sections, connection classifications and commonly used design guidelines and standards.

1.3.1 *Connection Classification*

Different classification systems for connections are available. The system suggested by Bjorhovde [28] is among the first systems proposed as a whole. This system of classification is based on a reference length and in terms of stiffness, ultimate strength, and ductility requirements. This system can be used for frames with the unknown layout. Connections are classified as rigid, semi-rigid, and flexible according to their initial rotational stiffness.

Eurocode 3: Part 1-1 (1992) [29] suggested another system a few years after the system by Bjorhovde. This system which after undergoing some changes now has evolved to Eurocode 3: Part 1-8 (2005) [30], is based on the load-bearing capacity of frame members. In this system, the layout and member sizes should be known. The term "joint" is used as the term referring to all members of a connection together. On the one hand, according to this system connections are classified based on their initial rotational stiffness as rigid, semi-rigid, and nominally pinned. On the other hand, according to the strength (comparing design moment resistance of connection with connected members), joints are classified as full-strength, partially strength and nominally pinned.

A unified system of joint classification has been developed by Nethercot [31] which considers stiffness and strength of the connections simultaneously and classifies joints as fully-connected, partially-connected, pin-connected, and non-structural. This system imposes rotational requirements on the connections. The connection in this system would be checked for both ultimate and serviceability limit states.

1.3.2 *Design Guides and Standards*

CIDECT[1] has published a set of design-guide books under the general title "Construction with Hollow Steel Sections." This series of books consists of nine volumes, each dedicated to one aspect of analysis, design, and construction of structures with hollow (circular/rectangular) sections. CIDECT "Design Guide 9: For structural hollow section

[1] Comité international pour le développement et l'étude de la construction tubulaire

column connections" [36] covers the topic of welded and bolted connection analysis and design.

The American Institute of Steel Construction (AISC) published the Hollow Structural Sections Connections Manual (AISC 310) [37] in 1997 with specifications and commentary specifically focused on onshore HSS design and construction. This publication was later included in AISC Steel Construction Manual (AISC 325) [23] in 2005. Sections J and K of Specification for Structural Steel Buildings (AISC 360:2010a) [38] contain guidelines for designing hollow structural section members and connections. For the purpose of designing for seismic applications, prequalified connections for special and intermediate steel moment frames for seismic applications (AISC 358:2010b) [39] can be used.

AISC Design Guide 24: Hollow Structural Section Connections [1] is another resource for designing hollow section connections. Design guide 24 is a supplementary publication to the 13th edition of the American Institute of Steel Construction (AISC) *Steel Construction Manual* [23]. This reference also provides information for the design of connections for special purposes such as seismic or fatigue applications.

Other major standards that covers the topics related to hollow structural section design are Eurocode 3:Part 1.8 [30], British Standard BS 5950 Part1 [40], Australian Standard AS 4100 [43], Canadian Standard CSA-S16-01 [41], Eurocode 3 Part 1.1 [44], New Zealand Standard NZS 3404 [42] and the Architectural Institute of Japan (AIJ) [45]. The majority of the publications above use the T-stub component method and single or multiple-yield-line mechanism methods in combination with experimental data to analyse the connections and develop the design formulae.

For designing concrete-filled tubes and composite frames, still, a gap for having a reliable, quantitatively justified design guide exists [111]. The recently developed Direct Analysis method for stability design of steel structures (AISC 2010b) has yet to be validated explicitly for use with composite structures. There is little data to justify the structural system response given in the specifications (ASCE 2010; ICC 2012) for seismic design of composite frames, and little guidance is available regarding the value of stiffness that should be used in elastic analyses of composite frames. Provision for the design of composite structures can also be found in Eurocode 4: Part 1-1 (2004), CEN 2009 (Canada), Standards Australia (1998), and AIJ-SRC (Japan-1991).

However, in the case of using conventional connections such as extended or flush end-plate connections, since the bolts do not directly connect the sections, these connections are not special bolted connections. In fact, the connection behaviour is determined by the intermediate connecting steel components, which are welded to the members. Adapting such configurations to tubular columns requires the development of solutions that deal with the issue of local deformations in the column face [113].

1.3.3 *Bolted Connections to Rectangular Hollow Sections*

Moment Frame connections with traditional welded or bolted connection were extensively used from within the 1960s to early 1990s due to the belief that they can show enough ductility. After Northridge, California earthquake (January 17, 1994) this belief went under scrutiny as a result of brittle fracture observed in nearly 150 buildings [46]. A 5-year investigation program was initiated by FEMA[2] to dig into the causes and find the required solutions. Design recommendations and state-of-the-art reports were published in 2000 [47]. Two main strategies were developed to improve the connection performance through relocating the plastic hinge away from the face of the column. The first strategy was strengthening the connection with cover plates, ribs, side plates, and haunches, and the second one was weakening the beam at a short distance away from the column face by reducing the flange width. Achieving this goal in rectangular hollow sections requires the column to be effectively stiffened in a way that load transfer does not impose any yielding or local buckling on the column face. This saves the column undergoing undesirable failure modes.

In practice, connections behave as semi-rigid ones, and their components deformation should be taken into account. Experimental tests are the best possible way (although not always feasible) for recreating the moment-rotation curve and capturing the behaviour of beam-to-column connections. Some of the experimental test results have been gathered in databanks of hundreds of tests. The databank created by Kishi and Chen[48] which includes all the experimental data from 1936 to 1986 or SERICON databank [49 , 50] which

[2] U.S. Federal Emergency Management Agency

contains the data of the tests performed across Europe and also the results on single components and composite joints, are good examples. Individual tests are also available in the literature for different connections such as endplate[51], T-stub joints [52], blind bolted connections [53], reverse channel[54], and through plate[55]. Other methods also used to predict moment-rotation curves of end-plate connections such as T-stub model, yield line model, and finite element analysis. T-stub model was the outcome of early efforts to find non-experimental ways of analysing end-plate connections [59 - 62].

Nonetheless, in the case of connections with multiple components and complex geometries with nonlinearity of material properties, geometry and interactions included, the numerical simulation can be very computationally expensive. Mechanical models or component-based method models are counted as a reliable alternative to the complex three-dimensional finite element models. In this method, the joint is decomposed to its components, which take part in moment capacity and ductility. Each part is attributed a force-displacement characteristic curve that can describe its behaviour reasonably accurately. Assembling these components in the proper way leads to a model that can represent the moment-rotation behaviour of the joint accurately at a computational cost usually less than finite element modelling.

The basics of the component method are based on the analytical and experimental tests performed by Zoetemeijer [63]. Wales and Rossow investigated the behaviour of double-web angle connections using a rigid bar connected by two non-linear springs [64]. Tschemernegg investigated unstiffened welded connections [65]. Tschemmernegg and Humer studied end-plate bolted connections with this method [66]. The research works done by Jaspart[67 , 68] culminated the research studies done before him in this field and it finally was incorporated in Eurocode 3 [30]. Since then, various studies have been done using the component-method approach in different connections such as reverse channel [69], blind bolted [70], and hollow section joints [71]. Shi et al. have performed several experiments and developed a new model based on components method to evaluate the moment-rotation relationship for stiffened and extended steel beam-column end-plate connections [82].

First models developed for finite element analysis of end-plate connections were by Krishnamurthy [72 - 74]. Sherbourne and Bahaari used 3-D finite elements to analyse end-plate connections. In addition to the overall behaviour, the contribution of the bolt, end-plate and column flange flexibility to the connection rotation was singled out [75]. With

the finite element method, they also studied the structural properties of an extended end-plate connected to an unstiffened column flange [76]. Based on 34 stiffened, extended end-plate connections and 19 end-plate connections without stiffeners in the tension region, they produced a single standardised M–φ function for each of these two connection types by curve fitting [77 , 78]. Using many new functions of the finite element method and simulation the mechanical behaviour of end-plate connections and each component more accurately has been performed [79 , 80]. Finite element analysis has also been used to investigate the fundamental behaviour and characteristics of other different connections [83 - 85] as well as performing extensive parametric studies [86 - 88]. Numerous commercial software packages have been used to address this problem such as works performed with ADINA [89], LUSAS [90] and especially in the recent years with ANSYS [91] and ABAQUS [92].

In spite of the extent of studies that have been carried out and have led to several new connection details being proposed for the connection of I-beams to wide-flange columns since the 1994 Northridge earthquake, but research for the connection of I-beams to box-columns has been limited [93]. Among this limited range of publications, a large portion of the researchers has chosen to investigate the behaviour of connections made with the blind bolting system. Flowdrill system is one of the methods of blind bolting the connections to hollow sections that first was introduced in 1996 [94 , 95]. In this system, a hole is drilled in one of the connection faces without removal of the material, and then this hole is threaded to fit a standard bolt. According to recent studies without any stiffening to the hollow section column face, the flexible column face deformation will be the governing failure mode irrespective of the type of fasteners used [36]. Huck blind bolting system (HSBB [3] and Ultra-Twist) is a blind bolting method developed by Huck International in 1990. Researchers have shown that this method requires an even thicker column face to achieve the full tensile strength of the bolt compared to that of the Flowdrill system [96 - 98]. Lindapter Hollobolt as another system of blind bolting was introduced in 1995 [99]. It has been proven to provide a secure grip against pull-out [36]. Reverse

[3] High strength blind bolt

mechanism Hollobolt (RMH) is found to have more grip than the standard one [100]. Ajax ONESIDE bolting system is another method proposed in 2002 [101]. In a hollow section connection, the performance of the ONESIDE may be limited by the thickness of the tube wall [102]. Another disadvantage is that the installation procedure of ONESIDE imposes geometrical limitations to the system [103]. Lee et al. proposed a new blind bolting system to rectangular sections in which channels with side plates connect beam flanges to the side face of HS columns [104].

In addition to the research works regarding the end-plate connections to I-beams, particular works are merely focused on this connection between I-beam to rectangular hollow sections. Ghobara et al. investigated this connection with high-strength bolts and blind bolts [105]. Later on, they proposed a design procedure for extended end-plate connection to hollow rectangular sections [106] and an analytical moment-rotation relationship for this type of connection [107]. A design guide for bolted end-plate connection of hollow rectangular sections [108] and an FE model for the design of bolted hollow structural sections joints [109] have been proposed by Wheeler et al. Achieving a full-resistance connection by attaching the connection directly to the rectangular column face usually needs local strengthening the face. One of the methods used is locally thickening the face by a special procedure invented in Japan [112].

The first efforts to address the problem of connections to concrete-filled columns started in the mid-1980s [110]. Many researchers have investigated the behaviour of connections, whether bolted or welded, to this type of column. Researchers have investigated the feasibility of connection beams to concrete-filled hollow sections using standard high-strength bolts. Ricles led a research work with the purpose of examining the effect that different connection details have on cyclic performance. Various connection details were investigated, including interior diaphragms, exterior extended structural tees, and split tees [114]. Wu et al. proposed a new design of bolted beam-to-column connections for CFT using through bolts [115]. Wu et al. also proposed a new bi-directional connection using thorough bolts [117]. Van et al. have conducted an experimental work about three new joint configurations using standard and through bolts and proposed design guidelines for their developed connections [116]. Denavit and Hajjar recently performed a very extensive research on the behaviour of concrete-filled members and composite frames [111].

Using reverse channel connections is another method of connecting beams to hollow and concrete filled connections. Potential fire and earthquake resistance of structures using

this type of connection have been investigated [118 - 125]. Tizani et al. recently investigated the performance of a new blind bolted connection to concrete-filled hollow sections [126 , 127]. Yao et al. investigated the blind bolted connection to rectangular and circular concrete-filled section using modified blind bolts with cogged ends [33]. Agheshlui et al. investigated the connection to rectangular concrete-filled sections by headed stud anchored blind bolts [32].

ConXL is another connection which has been invented in 2005 [35]. The purpose of this connection is to omit the on-site welding practice, which increases weld quality and tries to introduce more industrialisation into construction projects. This connection is a prequalified connection in AISC 358 [39] for a specific size of I-beams and rectangular hollow section columns. Shahidi et al. [128] recently investigated the behaviour of this connection with an unfilled column under cyclic loading. Eighteen specimens of ConXL moment connections with axial force in single, planar, and bi-axial loading conditions with different arrangements of bolts were tested. Results show that seismic behaviour of specimens with beam section depth less than W30 series under cyclic loading, even with the reduction of the number of the bolts to sixteen, are suitable over 0.04 rad rotations [128]. In another research Rezaeian et al. [129] investigated eleven types of ConXL connections including RBS and normal beams with columns not filled with concrete with axial force in single, planar and biaxial loading conditions. It was found that in addition to satisfying the 0.04 rad condition very low local buckling of the column is observed.

Connection to concrete-filled double skin square tubes has recently investigated by He et al. [130]. They have developed an analytical model to investigate the structural behaviour under seismic loading. It was found that the behaviour is consistent with the expected performance corresponding to current seismic design codes, implying that effective seismic performance of composite CFDST frame with bolted connections can be achieved. Li et al.[131] studied mechanical properties of H-beam connection to concrete-filled double skin rectangular hollow sections using T-stubs and high-strength bolts to find the possible failure modes.

As mentioned before, since every connection has its characteristics depending on the components of that specific connection type, so we have a knowledge gap to see how beam to innovative fabricated column connection works. Whereas connections to the specific case of this research that is an innovative fabricated column have not been investigated before, it sounds necessary to have it numerically and experimentally investigated. Having

these results enables to find out about the behaviour of this column in frames and propose design recommendations based on numerical and test data. This fosters the ground for this type of column, which has been proven to have superior capacities, make its way easier and more effectively into the construction industry.

1.4 Thesis layout

This thesis is divided into six chapters. The main part of the research performed in this work is presented in four consecutive chapters after Chapter 1, which is an introduction to the thesis, including overview, outline, and outcomes. The final chapter (Chapter 6) is a summary of the findings and the outlook. The content of each chapter is as follows:

- **Chapter 1**- Introduction:

  The opening chapter of the thesis provides an overview of the research work undertaken. It also provides an insight into the previous studies available in the literature, pertinent to the field of this study. In addition, the thesis outline and major outcomes of the investigations are pointed out in this chapter.

- **Chapter 2**- An innovative I-beam to hybrid fabricated column connection: Experimental investigation:

  This chapter presents the experimental campaign performed on the innovative connection. The experimental work includes three real-scale tests on the innovative connection attached to the HFC. The first test is on a bolted version of the connection, and the other two tests are on another version of the connection in which the beam is welded to the connection angles. Tests are done on HFCs with mild steel and ultra-high strength steel corner tubes. These tests are also simulated using the finite element method. The finite element model developed for these tests is verified against the results of the experimental tests. This chapter is published as a journal paper.

- **Chapter 3**- A numerical study on the innovative I-beam to hybrid fabricated column connection:

  This chapter deals with the numerical simulation of the different connections attached to the HFCs, using finite element method. The moment-rotation curve of four

conventional connections including flush endplate, extended endplate, reverse channel, and ConXL is numerically extracted. The results of the simulation of these connections are then compared to the results of the innovative connection presented in the previous chapter. The topology of the innovative connection is also optimised, and the performance of the optimised connection is numerically studied. This chapter is accepted for publication as a journal paper.

- **Chapter 4**- A component-based model for the innovative prefabricated beam-to-hybrid tubular column connections:

  The results of a mechanical model developed for the analysis of the innovative connection is presented in this chapter. This model is created using the component method approach in which the connection is broken down into multiple components with their specific stiffness and resistance. The components included in the model are those that play a role in moment capacity or ductility of the connection. These components, based on their location in the connection, are assembled, and the resultant model can estimate the behaviour of the connection, namely its moment-rotation curve. The results presented by the component-based model are compared to those obtained from the finite element in the previous chapters. This chapter is submitted as a journal paper and is currently under review .

- **Chapter 5-** Numerical investigation of the behaviour of innovative beam-to-hybrid corrugated columns connection:

  This chapter includes the analysis of the behaviour of the innovative connection attached to a particular type of HFC, which comprises four corner tubes and corrugated plates. Using the verified finite element model developed in Chapter 1, the connection behaviour under monotonic loading is numerically investigated and compared to the behaviour of the case of HFC with flat plates. A new version of the connection with modified dimensions (thinner components) is also studied in this chapter to investigate how the behaviour of the connection changes when its components are no longer reusable. Thus, the moment-rotation behaviour of this connection, attached to the HFCs with flat plates and corrugated plates are compared. The effect of bidirectional joints on

the moment rotation of the connection attached to HFC with corrugated plates is also investigated in this chapter. This chapter is planned to be submitted as a journal paper.

- **Chapter 6 –** Summary and future works:

  This chapter concludes the thesis by pointing out the summary of the findings and provides an outlook of the possibilities for the future work in the field of the topic of this thesis.

References

[1] AISC (2010). Design Guide 24: Hollow structural Section connections. USA.

[2] Sherman, D.R. (1996). “Designing with Structural Tubing”, *Engineering Journal, AISC*. 33(3), 101–109.

[3] Aoki, T., and Ji, B. (2000). “Experimental Study on Buckling Strength of Tri-Tube Steel Members” *Coupled Instabilities in Metal Structures - CIMS ’2000 - Proceedings of the Third International Conference*, Imperial College Press, Lisbon, Portugal, 283–290.

[4] Javidan, F., Heidarpour, A., Zhao, X.L. and Al-Mahaidi, R. (2017), Bending moment and axial compression interaction of high capacity hybrid fabricated members, Thin-Walled Structures, 121, 89-99.

[5] Nassirnia, M., Heidarpour, A. and Zhao, XL. (2017), A Benchmark analytical approach for evaluating ultimate compressive strength of hollow corrugated stub columns, Thin-Walled Structures, 117, 127-139.

[6] Javidan, F., Heidarpour, A., Zhao, X.L. and Fallahi, H. (2017), Fundamental behaviour of high strength and ultra-high strength steel subjected to low cycle structural damage, Engineering Structures, 143, 427-440.

[7] Farahi, M., Heidarpour, A., Zhao, X.L. and Al-Mahaidi, R. (2017), Effect of ultra-high strength steel on mitigation of non-ductile yielding of concrete-filled double-skin columns, Construction & Building Materials, 147: 736-749.

[8] Farahi, M., Heidarpour, A., Zhao, X.L. and Al-Mahaidi, R. (2016), Parametric study on the static compressive behaviour of concrete-filled double-skin sections consisting of corrugated plates, *Thin-Walled Structures*, 107, 526-542.

[9] Javidan, F., Heidarpour, A., Zhao, X.L. and Minkkinen, J. (2016), Application of high strength and ultra-high strength steel tubes in long hybrid compressive members: Experimental and numerical investigation, *Thin-Walled Structures,* 102, 273-285.

[10] Javidan, F., Heidarpour, A., Zhao, X.L. and Minkkinen, J. (2016), Effect of weld on the mechanical properties of high strength and ultra-high strength steel tubes in fabricate hybrid sections, *Engineering Structures*, 118, 16-27.

[11] Farahi, M., Heidarpour, A., Zhao, XL. and Al-Mahaidi, R. (2016), Compressive behaviour of concrete-filled double-skin sections consisting of corrugated plates, *Engineering Structures*, 111, 467-477.

[12] Nassirnia, M., Heidarpour, A., Zhao, XL. and Minkkinen, J (2016), Innovative hollow corrugated columns comprising corrugated plates and ultra high-strength steel tubes, *Thin-Walled Structures*, 101, 14-25.

[13] Nassirnia, M., Heidarpour, A., Zhao, X.L., and Minkkinen, J. (2015). "Innovative Hollow Corrugated Columns: A Fundamental Study." *Engineering Structures*, Elsevier Ltd, 94, 43–53.

[14] Javidan, F., Heidarpour, A., Zhao, X., and Minkkinen, J. (2015). "Performance of Innovative Fabricated Long Hollow Columns under Axial Compression." *Journal of Constructional Steel Research*, 106, 99–109.

[15] Javidan, F., Heidarpour, A., Zhao, X.L., and Minkkinen, J. (2014). "The Compressive Behaviour of Innovative Hollow Long Columns Consisting of Mild-Steel Plates and Tubes." *EUROSTEEL 2014, Naples, Italy*.

[16] Javidan, F., Heidarpour, A., Zhao, X.L., and Minkkinen, J. (2015). "Compressive Behaviour of Innovative Hollow Long Fabricated Columns Utilizing High Strength and Ultra-High Strength Tubes.", *Tubular Structures XV, Rio de Janeiro, Brazil*.

[17] Nassirnia, M., Heidarpour, A., Zhao, X.L., and Minkkinen, J. (2015). "Innovative Corrugated Hollow Columns Utilizing Ultra-high Strength Steel Tubes" *Tubular Structures XV, Rio de Janeiro, Brazil*.

[18] Binh, D.V., Al-Mahaidi, R., and Zhao, X.L. (2004). "Finite Element Analysis of Fabricated and Triangular Section Stub Columns Utilizing Very High Strength Steel Tubes." *Advances in Structural Engineering an International Journal*, 7(5), 447-460.

[19] Rhodes, J., Zhao, X.L., Binh, D.V., and Al-Mahaidi, R. (2005). "Rational Design Analysis of Stub Columns Fabricated Using Very High Strength Circular Steel Tubes." *Thin-Walled Structures*, 43(3), 445-460.

[20] Ye, J.H., Zhao, X.L., Van Binh, D., and Al-Mahaidi, R. (2007). "Plastic Mechanism Analysis of Fabricated Square and Triangular Sections under Axial Compression." *Thin-Walled Structures*, 45(2), 135-148.

[21] Heidarpour, A., Cevro, S., Song, Q.Y., and Zhao, X.L. (2014). "Behaviour of Stub Columns Utilising Mild-Steel Plates and VHS Tubes under Fire." *Journal of Constructional Steel Research*, 95, 220-229.

[22] Heidarpour, A., Cevro, S., Song, Q.Y., and Zhao, X.L. (2013). "Behaviour of Innovative Stub Columns Utilising Mild-Steel Plates and Stainless Steel Tubes at Ambient and Elevated Temperatures." *Engineering Structures*, 57, 416-427.

[23] AISC, Steel Construction Manual, 13th ed. USA (2006).

[24] Sherman, D. R. (1996). "Designing With Structural Tubing." *Engineering Journal*, 33(3), 101–109.

[25] FEMA-355D. (2000). State of the Art Report on Connection Performance. Washington (DC): Federal Emergency Management Agency.

[26] Packer, J. (2000). "Tubular Construction." *Progress in Structural Engineering and Materials*, 2(1), 41–49.

[27] Zhao, X.-L., Wilkinson, T., and Hancock, G. (2005). Cold-Formed Tubular Members and Connections, Elsevier.

[28] Bjorhovde, R., Colson, A., and Brozzetti, J. (1990). "Classification System for Beam To-Column Connections." *Journal of Structural Engineering*, 116(11), 3059-3076.

[29] European Committee for Standardisation (CEN). (1992). Eurocode 3. Design of Steel Structures, Part 1-1: General Rules and Rules for Building. Brussels.

[30] European Committee for Standardisation (CEN). (2005). Eurocode 3. Design of Steel Structures, Part 1-8: Design of Joints. Brussels: CEN.

[31] Nethercot, D. A., Li, T. Q., and Ahmed, B. (1998). "Unified Classification System for Beam-to-Column Connections." *Journal of Constructional Steel Research*, 45(1), 39–65.

[32] Agheshlui H., Goldsworthy H., Gad E., Mirza O. (2017). "Anchored blind bolted composite connection to a concrete filled steel tubular column." *Steel and composite structures*, 23(1), 115-130.

[33] Yao, H., Goldsworthy, H., Gad, E., Mirza, O., and Uy, B. (2010). "Moment Connections to Circular and Square Composite Columns Using Blind Bolts." *Australian Earthquake Engineering Society 2010 Conference*, Perth, Western Australia, 9.

[34] Chunhaviriyakul, P., MacRae, G.A., Anderson, D., and Leon, R.T. (2013). “Composite Steel-Concrete Construction for New Zealand.” *Steel Innovations Papers*, 1-30.

[35] Robert, F., and Simmons, J. (2005). “Innovative Connections.” *Journal of Modern Steel Construction*, 45(8), 38–41.

[36] Kurobane, Y., Packer, J. A., Wardenier, J., and Yeomans, N. (2004). Design Guide 9: For Structural Hollow Section Column Connections. (TÜV Verlag, ed.), CIDECT.

[37] AISC. (1997). Hollow Structural Sections Connections Manual, AISC 310:1997. Chicago, IL.

[38] AISC. (2010a). Specification for Structural Steel Buildings, AISC 360:2010a. Chicago, IL: American Institute of Steel Construction.

[39] AISC. (2010b). Prequalified Connections for Special and Intermediate Steel Moment Frames for Seismic Applications (AISC 358:2010b), Chicago, IL: American Institute of Steel Construction.

[40] BSI. (2000). Structural Use of Steelwork in Building, BS 5950, part 1. London, UK: British Standards Institute.

[41] CSA. (2001). Steel Structures for Buildings (limit State Design), CSA-S16-01. Toronto, ON: Canadian Standards Association.

[42] NZS. (1997). Steel Structures Standard, NZS 3404, part 1. Wellington, New Zealand: Standards New Zealand.

[43] Standards Australia. (1998). Structural Steel Hollow Sections, Australian Standard AS 4100. Sydney, Australia: Standards Australia.

[44] Eurocode 3: Design of steel structures - part 1.1: General Rules and Rules for Buildings. Brussels, Belgium: European Committee for Standardization.

[45] AIJ. (1990). Standard For Limit State Design of Steel Structures. Tokyo, Japan: Architectural Institute of Japan. (In Japanese)

[46] Bruneau, M., Uang, C.M., and Whittaker, A. (1998). Ductile Design of Steel Structures, McGraw Hill, Boston, Massachusetts.

[47] Kunnath, S.K., and Malley, J.O. (2002). "Advances in Seismic Design and Evaluation of Steel Moment Frames: Recent Findings from FEMA/SAC Phase II Project." *Journal of Structural Engineering*, 128(4), 415-419.

[48] Kishi, N. and Chen, W.F. (1986): Data Base of Steel Beam-to-Column Connections, Structural Engineering Report No. CE-STR-86-26, School of Civil Engineering, Purdue University, West Lafayette, IN.

[49] Gerardy, J.C. and Schleich, J.B. (1991): Semi-Rigid Action in Steel Frame Structures, Report on ECSC Agreement, No. 7210-SA/507, Arbed Recherches, Luxembourg, November.

[50] Weinand, K. (1992): SERlCON - Databank on Joints in Building Frames. Proceedings of the 1st COST Cl Workshop, Strasbourg, October 28-30.

[51] Wang J, Chen L. Experimental investigation of extended end plate joints to concrete-filled steel tubular columns. J. Constr. Steel Res. 2012;79:56–70.

[52] Latour M, Piluso V, Rizzano G. Experimental behaviour of friction T-stub beam-to-column joints under cyclic loads. Steel Construction. 2013;6(1):11–8.

[53] Wang Z-Y, Wang Q-Y. (2016). Yield and ultimate strengths determination of a blind bolted endplate connection to square hollow section column. *Eng Struct*, 111, 345–69.

[54] Huang S-S, Davison B, Burgess IW. (2013) Experiments on reverse-channel connections at elevated temperatures. *Engineering Structures*, 49, 973–82

[55] Torabian S, Mirghaderi SR, Keshavarzi F. (2012). Moment-connection between I-beam and built-up square column by a diagonal through plate. *Journal of Constructional Steel Research*, 70, 385–401.

[56] Attiogbe E., and Morris G. (1991). "Moment–Rotation Functions for Steel Connections." *Journal of Structural Engineering*, 117(6), 1703–18.

[57] Shi, G., Shi, Y.J., Wang, Y.Q., Chen, H. (2004). "Numerical Simulation and Experimental Study on Bolted End-Plate Connections." In: *The Eighth International Symposium on Structural Engineering for Young Experts*, 1, 137–42.

[58] Chen, W.F., and Lui, F.M. (1991). Stability Design of Steel Frames. Boca Raton (FL): CRC Press.

[59] Douty, R.T., and McGuire, W. (1965). "High Strength Bolted Moment Connections." *Journal of the Structural Division*, 91(ST2), 101–28.

[60] Nair, R.S., Birkemoe P.C., Munse, W.H. (1974). "High Strength Bolts Subject To Tension and Prying." *Journal of the Structural Division*, 100(ST2), 351–72.

[61] Kato, B., McGuire, W. (1973). "Analysis of T-Stub Flange-to-Column Connections." *Journal of the Structural Division*, 99(ST5); 865–88.

[62] Agerskov H. (1976). “High-Strength Bolted Connections Subject to Prying.” *Journal of the Structural Division*, 102(ST1), 161–75.

[63] Zoetemeijer P. Summary of the research on bolted beam-to-column connections (period 1978–1983). Delft: Stevin II Laboratory; 1983.

[64] Wales MW, Rossow EC. (1983). Coupled moment-axial force behaviour in bolted joint. *Journal of Structural Engineering*, 109(5), 1250–66.

[65] Tschemmernegg F. (1988). On the nonlinear behaviour of joints in steel frames. In: *Connections in Steel Structures: Behaviour, Strength and Design (ed. R. Bjorhovde et al.)*. Elsevier Applied Science Publishers, London, 158-165.

[66] Tschemmernegg F, Humer C. (1988). The design of structural steel frames under consideration of the non-linear behaviour of joints. *Journal of Constructional Steel Research*, 11, 73-103.

[67] Jaspart JP. (1991), “Etude de la semi-rigidité des nœuds poutre-colonne et son influence sur la résistance et la stabilité des ossatures en acier”, PhD Thesis, Université de Liège.

[68] Jaspart JP. (1997), “Recent advances in the field of steel joints: Column bases and further configurations for beam-to-column joints and beam splices”, Universite de Liege.

[69] Lopes F, Santiago A, Simões da Silva L, Heistermann T, Veljkovic M, Guilherme da Silva J. (2013). Experimental behaviour of the reverse channel joint component at elevated and ambient temperatures. *International Journal of Steel Structures*, 13(3), 459–72.

[70] Málaga-Chuquitaype C, Elghazouli AY. (2010). Component-based mechanical models for blind-bolted angle connections. *Engineering Structures*, 32(10), 3048–67.

[71] Jaspart JP, Weynand K. (2015). Design of hollow section joints using the component method. *Proceedings of the 15th International Symposium on Tubular Structures*, Rio de Janeiro, Brazil, 405–10.

[72] Krishnamurthy, N. (1976). “Correlation between 2- And 3-Dimensional Finite Element Analyses of Steel Bolted End-Plate Connections.” *Computers & Structures*, 6, 381–9.

[73] Krishnamurthy, N., Huang, H.T., Jefferey, P.K., and Avery, L.K. (1979). "Analytical M-θ Curves for End-Plate Connections." *Journal of the Structural Division*, 105(ST1), 133–45.

[74] Krishnamurthy, N. (1980). "Modeling and Prediction of Steel Bolted Connection Behaviour." *Computers & Structures*, 11, 75–82.

[75] Sherbourne, A.N., and Bahaari, M.R. (1994). "3D Simulation of End-Plate Bolted Connections." *Journal of Structural Engineering*, 120(11), 3122–36.

[76] Bahaari, M.R., and Sherbourne, A.N. (1996). "3D Simulation of Bolted Connections to Unstiffened Columns-II. Extended Endplate Connections." *Journal of Constructional Steel Research*, 40(3), 189–223.

[77] Sherbourne, A.N., and Bahaari, M.R. (1997). "Finite Element Prediction of End Plate Bolted Connection Behavior I: Parametric Study." *Journal of Structural Engineering*, 123(2), 157–64.

[78] Bahaari, M.R., and Sherbourne, A.N. (1997). "Finite Element Prediction of End Plate Bolted Connection Behavior II: Analytic Formulation." *Journal of Structural Engineering*, 123(2), 165–75.

[79] Shi, G., Shi, Y.J., Wang, Y.Q., Li, S., and Chen, H. (2004) "Finite Element Analysis And Tests on Bolted End-Plate Connections in Steel Portal Frames." *Advances in Structural Engineering*, 7(3), 245–56.

[80] Shi, G., Shi, Y.J., and Chen, H. (2004). "Finite Element Analysis of Beam–Column Bolted End-Plate Connections in Steel Frames." In: *Seventh pacific structural steel conference*.

[81] Shi, G., Shi, Y., Wang, Y., and Bradford, M. a. (2008). "Numerical Simulation of Steel Pretensioned Bolted End-Plate Connections of Different Types And Details." *Engineering Structures*.

[82] Shi, Y., Shi, G., and Wang, Y. (2007). "Experimental and Theoretical Analysis of the Moment-Rotation Behaviour of Stiffened Extended End-Plate Connections." *Journal of Constructional Steel Research*, 63(9), 1279–1293.

[83] Yang C, Yang J-F, Su M-Z, Liu C-Z. (2016). Numerical study on seismic behaviours of ConXL biaxial moment connection. *Journal of Constructional Steel Research*, 121, 185–201.

[84] AlHendi H, Celikag M. (2015). Finite element prediction of reverse channel connections to tubular columns behavior. *Engineering Structures*, 100, 599–609.

[85] Heistermann T, Koltsakis E, Veljkovic M, Lopes F, Santiago A, Simões da Silva L. (2015). Initial stiffness evaluation of reverse channel connections in tension and compression. Journal of Constructional Steel Research, 114, 119–28.

[86] Kataoka MN, El Debs ALHC. (2014). Parametric study of composite beam-column connections using 3D finite element modelling. *Journal of Constructional Steel Research*, 102, 136–49.

[87] Esfahanian A, Mohamadi-shooreh MR, Mofid M. (2015). Assessment of the semi-rigid double-angle steel connections and parametric analyses on their initial stiffness using FEM, 22, 2033–45.

[88] Kataoka MN, El Debs ALHC. (2014). Parametric study of composite beam-column connections using 3D finite element modelling. Journal of Constructional Steel Research, 102, 136–49.

[89] Kukreti, A.R., Murray, T.M., and Abolmaali, A. (1987). "End-Plate Connection Moment–Rotation Relationship." *Journal of Constructional Steel Research*, 8, 137–57.

[90] Bose, B., Wang, Z.M., and Sarkar, S. (1997). "Finite-Element Analysis of Unstiffened Flush End-Plate Bolted Joints." *Journal of Structural Engineering*, 123(12), 1614–21.

[91] ANSYS Multiphysics 16.0. Canonsburg, Pennsylvania, USA: Ansys Inc; 2015.

[92] ABAQUS 6.14-1. Providence, RI, USA: Dassault Systèmes; 2014.

[93] Mirghaderi, S. R., Torabian, S., and Keshavarzi, F. (2010). "I-Beam to Box-Column Connection by a Vertical Plate Passing Through the Column." Engineering Structures, Elsevier Ltd.

[94] Yeomans, N. (1996). Flowdrill Jointing System: Part 1 - Mechanical Integrity Tests (No. 6F-13A/96): CIDECT.

[95] Yeomans, N. (1996). Flowdrill Jointing System: Part 2 - Structural Hollow Section Connections (No. 6F-13B/96): CIDECT.

[96] Korol, R.M., Ghobarah, A., and Mourad, S. (1993). "Blind Bolting W-Shape Beams to HSS Columns." *Journal of Structural Engineering*.

[97] Mourad, S., Korol, R.M., and Ghobarah, A. (1996). "Design of Extended End-Plate Connections for Hollow Section Columns." *Canadian Journal of Civil Engineering*.

[98] Ghobarah, A., Mourad, S., and Korol, R.M. (1993). "Behaviour of Blind Bolted Moment Connections for HSS Columns." *Tubular structures V*, M. G. Coutie and G. Davies, eds., E & FN Spon, 125–132.

[99] Lindapter International. Type HB Hollo-Bolt for Blind Connection to Structural Steel and Structural Tubes. 1995.

[100] Barnett, T.C. (2001). The Behaviour of a Blind Bolt Moment Resisting Connections in Hollow Steel Sections. Ph.D. Thesis, University of Nottingham, UK.

[101] Ajax Engineered Fasteners (2002). ONESIDE Brochure. B-N012 Data Sheet, Victoria, Australia.

[102] Gardner, A. P., and Goldsworthy, H. M. (2005). "Experimental Investigation of the Stiffness of Critical Components in a Moment-Resisting Composite Connection." *Journal of Constructional Steel Research*, 61(5), 709-726.

[103] Lee, J. (2011). "Blind Bolted Connections for Steel Hollow Section Columns in Low Rise Structures." The University of Melbourne.

[104] Lee, J., Goldsworthy, H. M., and Gad, E.F. (2011). "Blind Bolted Moment Connection to Sides of Hollow Section Columns." *Journal of Constructional Steel Research*, Elsevier Ltd, 67(12), 1900–1911.

[105] Ghobarah, A., Mourad, S., and Korol, R.M. (1993). "Behaviour of Blind Bolted Moment Connections for HSS Columns." *Tubular structures V*, M. G. Coutie and G. Davies, eds., E & FN Spon, 125–132.

[106] Mourad, S., Korol, R.M., and Ghobarah, A. (1996). "Design of Extended End-Plate Connections for Hollow Section Columns." *Canadian Journal of Civil Engineering*, 23(1), 277–286.

[107] Ghobarah, A., Mourad, S., and Korol, R.M. (1996). "Moment-Rotation Relationship of Blind Bolted Connections for HSS Columns." *Journal of Constructional Steel Research*, 40(1), 63–91.

[108] Wheeler, A.T., Clarke, M.J., Hancock, G.J., and Murray, T.M. (1998). "Design Model for Bolted Moment End Plate Connections Joining Rectangular Hollow Sections." *Journal of Structural Engineering*, 124(2), 164–173.

[109] Wheeler, A.T., Clarke, M.J., and Hancock, G.J. (2000). "FE Modeling of Four-Bolt, Tubular Moment End-Plate Connections." *Journal of Structural Engineering*, 126(7), 816–822.

[110] ACI-ASCE Committee 352 (1985). "Recommendations for Design of Beam-Column Joints in Monolithic Reinforced Concrete Structures." *ACI Journal*, 82(3), 266-283

[111] Denavit, M.D., and Hajjar, J.F. (2014). Characterization of Behavior of Steel-Concrete Composite Members and Frames with Applications for Design. Urbana, IL.

[112] Tanaka, T., Tabuchi, M., Maruyama, M., Furumi, K., Morita, T., Usami, K., and Matsubara, Y. (1996). "Experimental Study on End Plate to SHS Column Connections Reinforced By Increasing Wall Thickness with One Sided Bolts." *Proc. of 7th International Symposium on Tubular Structures*, Miskolc, Hungary, 253– 260.

[113] Elghazouli, A.Y., and Packer, J.A. (2014). "Seismic Design Solutions for Connections to Tubular Members." *Steel Construction*, 7(2), 73–83.

[114] Ricles, J.M., Peng, S.W., and Lu, L.W. (2004). "Seismic Behaviour of Composite Concrete Filled Steel Tube Column-Wide Flange Beam Moment Connections." *Journal of Structural Engineering, American Society of Civil Engineers*, 130(2), 223–232.

[115] Wu, L.Y., Chung, L.L., Tsai, S. F, Shen, T. J., and Huang, G.L. (2005). "Seismic Behaviour of Bolted Beam-to-Column Connections for Concrete Filled Steel Tube." *Journal of Constructional Steel Research*, 61(10), 1387–1410.

[116] Van-Long, H., Demonceau, J., and Jaspart, J. (2013). "Innovative Bolted Beam-To-Column Joints in Moment Resistant Building Frames: From Experimental Tests to Design Guidelines." *International Workshop HSS-SERF High Strength Steel in Seismic Resistant Structures*, Naples, Italy, 2013.

[117] Wu, L.Y., Chung, L.L., Tsai, S.F., Lu, C.F., and Huang, G.L. (2007). "Seismic Behavior of Bidirectional Bolted Connections for CFT Columns and H-Beams." *Engineering Structures*, 29(3), 395–407.

[118] Ding, J. (2007). "Behaviour of Restraint Concrete Filled Tubular (CFT) Columns and Their Joints in Fire." PhD thesis, School of Mechanical, Aerospace and Civil Engineering, University of Manchester.

[119] Jones, M.H. (2008). "Tensile and Shear Behaviour of Fin-Plate Connections to Hollow and Concrete-Filled Steel Tubular Columns at Ambient and Elevated Temperatures." PhD thesis, School of Mechanical, Aerospace and Civil Engineering, University of Manchester.

[120] Ding, J., and Wang, Y.C. (2007). “Experimental Study of Structural Fire Behaviour of Steel Beam to Concrete Filled Tubular Column Assemblies with Different Types of Joints.” *Engineering Structures*, 29(12), 3485–3502.

[121] Elsawaf, S., and Wang, Y.C. (2012). “Methods of Improving the Survival Temperature in Fire of Steel Beam Connected to CFT Column Using Reverse Channel Connection.” *Engineering Structures*, 34, 132–146.

[122] Elsawaf, S., and Wang, Y.C. (2013). “Behaviour of Restrained Structural Subassemblies of Steel Beam to CFT Column in Fire during Cooling Stage.” *Engineering Structures*, 46, 471–492.

[123] Elsawaf, S., Wang, Y.C., and Mandal, P. (2011). “Numerical Modelling of Restrained Structural Subassemblies of Steel Beam and CFT Columns Connected Using Reverse Channels in Fire.” *Engineering Structures*, 33(4), 1217–1231.

[124] Málaga-Chuquitaype, C., and Elghazouli, A. Y. (2010). “Behaviour of Combined Channel/Angle Connections to Tubular Columns under Monotonic and Cyclic Loading.” *Engineering Structures*, 32(6), 1600–1616.

[125] Wang, Y.C., and Xue, L. (2013). “Experimental Study of Moment–Rotation Characteristics of Reverse Channel Connections to Tubular Columns.” *Journal of Constructional Steel Research*, 85, 92–104.

[126] Tizani, W., Al-Mughairi, A., Owen, J. S., and Pitrakkos, T. (2013). “Rotational Stiffness of a Blind-Bolted Connection to Concrete-Filled Tubes Using Modified Hollo-Bolt.” *Journal of Constructional Steel Research*, 80, 317–331.

[127] Tizani, W., Wang, Z.Y., and Hajirasouliha, I. (2013). “Hysteretic Performance of a New Blind Bolted Connection to Concrete Filled Columns under Cyclic Loading: An Experimental Investigation.” *Engineering Structures*, 46, 535–546.

[128] Shahidi, F., Rezaeian, A., Jamal-Omidi, M., and Shahidi, F. (2015). “Investigation of the ConXL Moment Connection Cyclic Behavior in Box Columns without Filling Concrete with Different Arrangement of Collar Bolts.” *The Structural Design of Tall and Special Buildings*, 24(5), 317–350.

[129] Rezaeian, A., Jamal-Omidi, M., and Shahidi, F. (2014). “Seismic Behavior of ConXL Rigid Connection in Box-Columns Not Filled With Concrete.” *Journal of Constructional Steel Research*, Elsevier B.V.

[130] He, W.H., Yang, C.Q., Yi, Y.Y., Tang, Z.H., He, P.C., and Weng, H.B. (2013). “Analytical Investigation on Concrete Filled Double-Skinned Steel Tubular

Column Composite Frame with Bolted End-Plate Connections." *Advanced Materials Research*, 639-640, 220–224.

[131] Li, Y., He, Y.B., Guo, J., Zhou, H.B., and Huang, P. (2010). "Force Mechanism and Nonlinear Finite Element Analysis on the Behaviour of CFDSST Column-to-Beam Connections." *Proceedings Of The International Conference On Modelling And Computation In Engineering, CMCE 2010*, J. Zhu, ed., Taylor and Francis Group, LLC, Hong Kong, 51–55.

AN INNOVATIVE I-BEAM TO HYBRID FABRICATED COLUMN CONNECTION: EXPERIMENTAL INVESTIGATION

CHAPTER 2

This chapter has been published in the Journal of *Engineering Structures*, Volume 148, 1 October 2017, Pages 907-923. DOI: 10.1016/j.engstruct.2017.07.029.
Reprinted here with the Author Rights granted by Elsevier.

Table of Contents

Abstract

Hybrid fabricated columns (HFCs) have been investigated by researchers during the past two decades. Many researchers have reported higher load-bearing capacity, post-buckling strength and better energy absorption as the main advantages of this type of column compared to other structural sections. This provides an opportunity for the construction industry and designers to utilise these superior properties in building more reliable structures. However, no matter how capable and reliable a column is, it still needs a robust connection to make the use of this column in construction viable. Since the topic of connections between these columns and I-beams has been untouched, the authors decided to study this knowledge gap. In this research, a new generation of modular connections is proposed by the authors, referred to hereafter as M-HFC. The performance of this connection has been tested experimentally. In addition, a three-dimensional finite element model has been developed to simulate the behaviour of the connection. The results show that this connection is a fully resistant and semi-rigid connection according to the standard classifications, which makes it a good choice for use in moment frames.

Keywords: hybrid fabricated column, modular connection, bolted connection, ductility, ultra-high strength, moment-rotation

2.1 Introduction

Today's construction industry demands structural members with very high capacity. Cold-formed sections, such as rectangular or circular hollow sections, which are currently available in the market, have limitations on the member dimensions [1 - 5]. On the other hand, fabricated sections appear to have the capacity of meeting these higher demands. Considering the closed profile of the fabricated members, additional stresses resulting from special loading cases such as torsion, warping and biaxial moments are less of an issue, while these stresses can lead to the reduced load-bearing capacity of open sections [6]. The concept of hybrid sections composed of thin plates and tubes welded together to form a closed section was first studied by Aoki [7]. In this research, stub columns with triangular cross-sections were fabricated by welding three plates to three tubes at each apex and tested under uniform and eccentric compressive loading. It was found that the capacity of the stub columns was far greater than the sum of the individual member's capacities. Numerous researchers have worked on this concept and have made considerable developments in terms of finding the behaviour of the new configuration of fabricated columns under different loading conditions, materials, and temperatures using experimental and numerical methods [8 - 13].

Based on the previous research, the greater load-bearing capacity, post-buckling strength, ductility, and energy dissipation of hybrid fabricated columns make them suitable for use in moment-resisting frames. However, although they possess the aforementioned advantages, the development of suitable beam-to-fabricated column connections is challenging.

The difficulty of access to the internal space of the hollow columns can result in reluctance in using bolted connections for hollow columns. However, different methods, including blind bolting systems such as Flowdrill, Hollobolt, and ONESIDE, have been developed in order to resolve this issue [17 - 27]. On the other hand, while the majority of conventional steel frames are constructed using welded connections, on-site welding errors, and labour costs make using bolted connections more appealing.

In addition to research on beam to I-shaped column end-plate connections, particular studies have focused on this type of connection between I-beam to rectangular hollow sections. For example, Ghobara et al. investigated this connection with high-strength bolts and blind bolts [28]. Later, they proposed a design procedure together with an analytical

moment-rotation relationship for extended end-plate connections to hollow rectangular sections [29]. A design guide for bolted end-plate connections for hollow rectangular sections [30] and a finite element (FE) model for the design of bolted hollow structural sections joints [31] have been proposed by Wheeler et al. Achieving a full-resistance connection by attaching the connection directly to the rectangular column face usually needs local strengthening of the face. One of the methods used is locally thickening the face using a special procedure invented in Japan [32]. However, without stiffening of the hollow section column face, deformation of the flexible column face may be the governing failure mode, irrespective of the type of fastener used [20].

Moment-frame connections with traditional welded or bolted connection were extensively used from the 1960s to the early 1990s due to the belief that they can show enough ductility. After the Northridge, California earthquake (January 17, 1994) this belief came under scrutiny as a result of the brittle fracture observed in nearly 150 buildings [33]. A 5-year investigation was initiated by FEMA [1] to discover the causes and find the required solutions. Design recommendations and state-of-the-art reports were published in 2000 [34]. In spite of the extent of studies that have been carried out, which have led to several new connection details being proposed for the connection of I-beams to wide flange columns since the 1994 Northridge earthquake, research on the connection of I-beams to box columns has been limited [35]. Since box columns have not been a common choice for construction (particularly in the US) the pre-qualified connections for these columns are very limited [36]. Therefore, the lack of a suitable connection that can be used in practice has encouraged researchers to propose different types of connection between I-beams and rectangular tubular columns using structural components such as plates, angles, and tees. Efforts to improve the connections have not been limited to the structural scale, and many researchers have investigated the material scale behaviour of different grades of steel in order to gain a better understanding of their characteristics under different loading conditions [37 - 40]. Hitherto, the challenging problem of connecting beams to hybrid fabricated columns consisting of mild-steel plates and ultra-high strength (UHS) corner tubes has not been investigated. In this research work, an innovative type of connection is proposed for connecting I-beams to hybrid fabricated columns. The connection behaviour

[1] U.S. Federal Emergency Management Agency

is investigated through experimental and numerical studies in order to extract moment-rotation curves for the connection, which can be used to find out how the connection behaves under quasi-static monotonic loading compared to the requirements specified by the relevant codes and standards for moment resisting frame connections.

2.2 Proposed connection

2.2.1 Description

Conventional connections may not be a suitable choice to transfer the loads from an I-beam to the hybrid fabricated column effectively. Therefore, it is necessary to design a new connection from scratch, based on the characteristics of the hybrid fabricated column (Fig. 2-1).

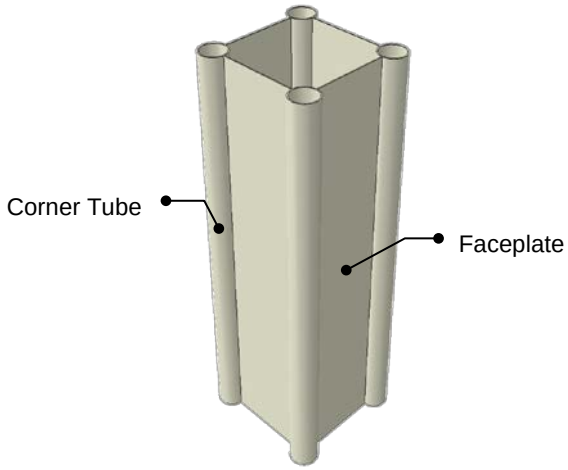

Fig. 2-1. Hybrid fabricated column

This new connection should be capable of taking most advantage of the significantly higher capacities of the corner tubes in hybrid fabricated columns. Obviously, the connection should demonstrate enough ductility and moment capacity in such a way that a weak member-strong connection relation exists. A new connection has been recently proposed for this type of column by the authors and has been investigated numerically [42]. The proposed connection is modular to make construction quicker, easier, and safer. The modular connection reduces the necessity of on-site welding, increases safety, and provides the building with better construction tolerances, which makes the jobs of different trades easier and improves the overall quality of the structure. It will also provide the possibility

of retrofitting the building by replacing only the damaged parts or erecting temporary moment frames. The connection parts are also re-usable in new constructions if a structure built with these connections were demolished. This connection is also flexible enough to cover a wide range of column and beam sizes with minimum modifications in the components or by changing the distance between the top and bottom segments. Although the connection has fascinating characteristics, it nevertheless requires more investigation in areas such as geometrical optimisation and ease of production of connection parts. Fig. 2-2 shows a representation of the proposed connection. Each part of the proposed connection is separately displayed in Fig. 2-3.

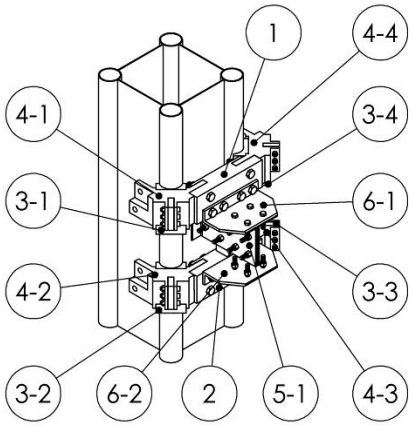

Fig. 2-2. Proposed I-beam to hybrid fabricated column modular connection

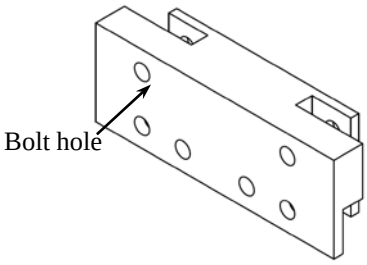

(a) Part No.1- Top collar

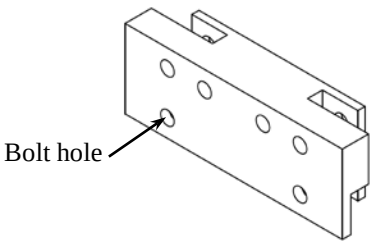

(b) Part No.2- Bottom collar

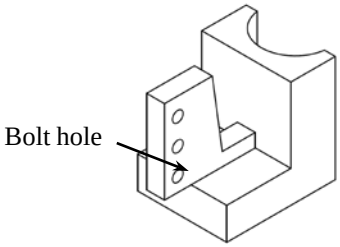

(c) Part No.3- Bottom corner

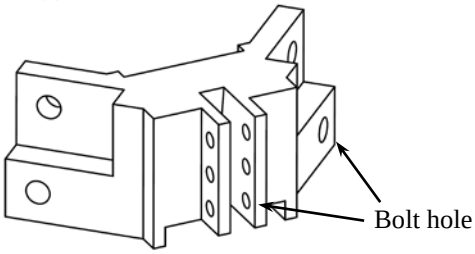

(d) Part No.4- Top corner

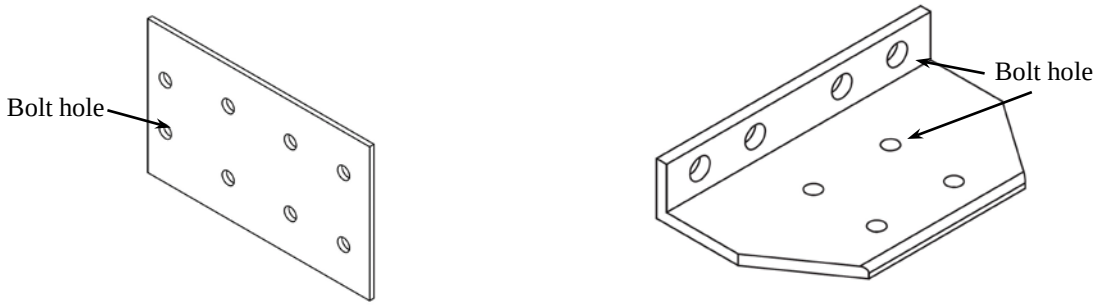

(e) Part No. 5- Side plate (f) Part No.6- Top/Seat angle

Fig. 2-3. Different parts of the proposed modular connection

2.2.2 Connection parts

The proposed connection comprises fifteen components. These components form two solid segments through the assembly of parts 1,3-1,3-4,4-1,4-4 at the top and parts 2,3-2,3-3,4-2,4-3 at the bottom, as shown in Fig. 2-2. These two segments are distanced from each other depending on the size of the beam that is to be used with this connection in the structure. Four parts of this connection (3-1 to 3-4 as shown in Fig. 2-3 (c)) are welded to the column tubes and transfer the load from the connection to the column. These parts are strong bases for the corner parts (4-1 to 4-4 as shown in Fig. 2-3 (d)) of top and bottom segments. The slot in the middle of this part (Fig. 2-3 (d)) works as a guide for easier assembly of the parts and in interaction with the previously-mentioned part prevents the lateral movement of the top corner part under loading. After the installation of the top and bottom corner parts, the inclined surface in the middle slot of the top corner part engages with the similar but negative surface on the bottom corner part and acts as a wedge lock. This guarantees the continual interaction of these two parts. The design of the top corner part has been made with the bilateral connection capability of the connection in mind. The design provides engineers with the possibility of using this connection on every column in the structure and attaching up to four beams to the same connection simply by adding a few more components. These two corner parts are attached together using bolts that resist the upward movement of the connection if any upward force is transferred to the connection.

In both segments, an interconnecting member (parts No. 1 and 2) joins the two adjacent top corner parts. These middle parts complete segments of the connection at the top and bottom and are the components to which the beams are connected using the angle-shaped parts (6-1 and 6-2). The top and bottom collars are identical blocks, but the locations of the

holes are different. The top and bottom flanges of the beam are bolted to two angle-shaped parts (parts 6-1 and 6-2). The resultant assembly of the two angle parts and the beam is then bolted to the top and bottom collars. A plate called a web extension is also welded between parts 1 and 2 at each end. This interconnecting part acts along with the top and the bottom segments and transfers shear between them as well as contributing to the ductility of the connection. A side plate (parts 5-1 and 5-2) is bolted to each side of the beam web and the web extension. The last row of bolts in the side-plates is bolted to two angles that are welded to the column face. This arrangement increases the interaction between the beam and the column and utilises the ductility of the column face to improve the connection's overall performance. The collar and the top corner parts have matching steps that result in a stable assembly after installation. The collars are bolted to the top corner parts to avoid undesirable movement in the case of unexpected or extreme conditions.

2.3 Experimental Phase

2.3.1 Specimen geometry and material properties

An experimental test set-up was designed and prepared in order to investigate the performance of the connection described in the previous section. Three different tests were performed on the proposed connection connecting the I-beams to the hybrid fabricated columns. The column height is one meter and fabricated by fillet-welding the mild steel (Grade 250) flat plates to the corner tubes that were of two different materials UHS steel (Grade 1200) or mild steel (Grade 250) in different tests. The welding method used for fabrication of the column is gas tungsten arc welding (GTAW) using ER2209 filler rods with 0.2% proof stress and tensile strength of 560–620 MPa and 800–835 MPa, respectively. The properties of the mild steel and UHS steel materials can be found in detail in data published by Javidan et al. [11]. M16 bolts that connect the beam assembly to the connection and M10 bolts that secure corner parts together are Grade 8.8 while M12 bolts used to attach side plates to the beam web are Grade 12.9.

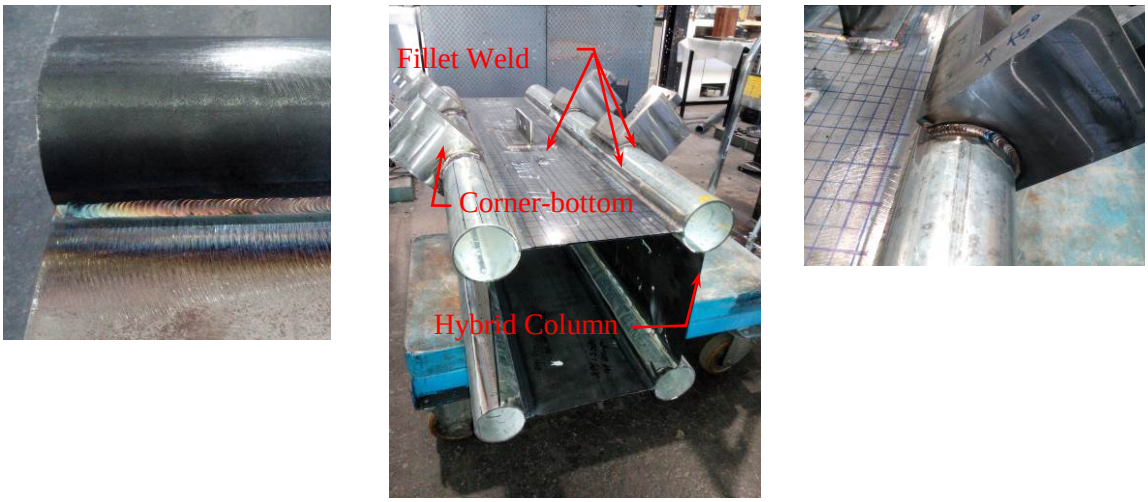

(a) (b) (c)

Fig. 2-4. Hybrid fabricated column and corner bottom parts after welding (a) Corner tube weld (b) Hybrid column and corner bottom parts assembly (c) Corner bottom part weld

As shown in Fig. 2-4, the corner-bottom parts of the connection are also welded to the corner tubes using the tungsten inert gas (TIG) welding method. The components of the connection are fabricated by machining and are made of Grade 250 mild steel. The beam is 1.2 meters long and is of 200UB22.3 type [36]. The section geometry of the hybrid fabricated column is presented in Fig. 2-5 and Table 2-1.

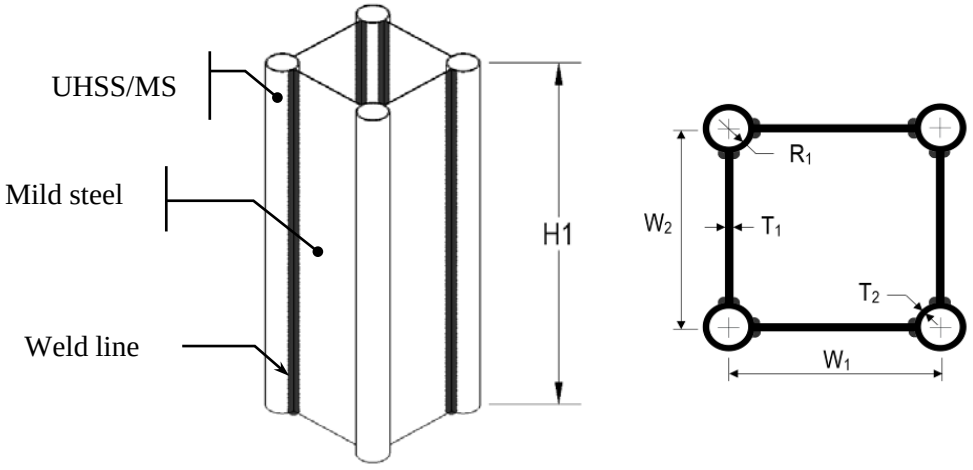

(a) (b)

Fig. 2-5. (a) Schematic of hybrid fabricated column and (b) Column cross-section

Table 2-1. Dimensions of the hybrid fabricated column cross-section

Symbol	Value mm	Symbol	Value mm
W_1	286	T_1	3
W_2	286	T_2	3.2
H_1	1000	R_1	34.8

2.3.2 Test set-up

The bottom end of the column is welded to a thick plate. This plate is securely bolted to the laboratory strong floor, which as a result maintains the encastre boundary conditions all the time during the tests at the bottom end of the column. The column is axially loaded under a constant load of 50 kN during the course of testing using a manually-controlled hydraulic jack through a thick plate placed on the top end of the column. This plate distributes the hydraulic load evenly on the top surface of the column. This axial load, which is well below the capacity of the column (1523 kN [11]), is expected to have the least effect on the connection behaviour [26] while ensuring the continuous establishment of the only-vertically-free boundary condition at the top end and also simulating gravity load on the column.

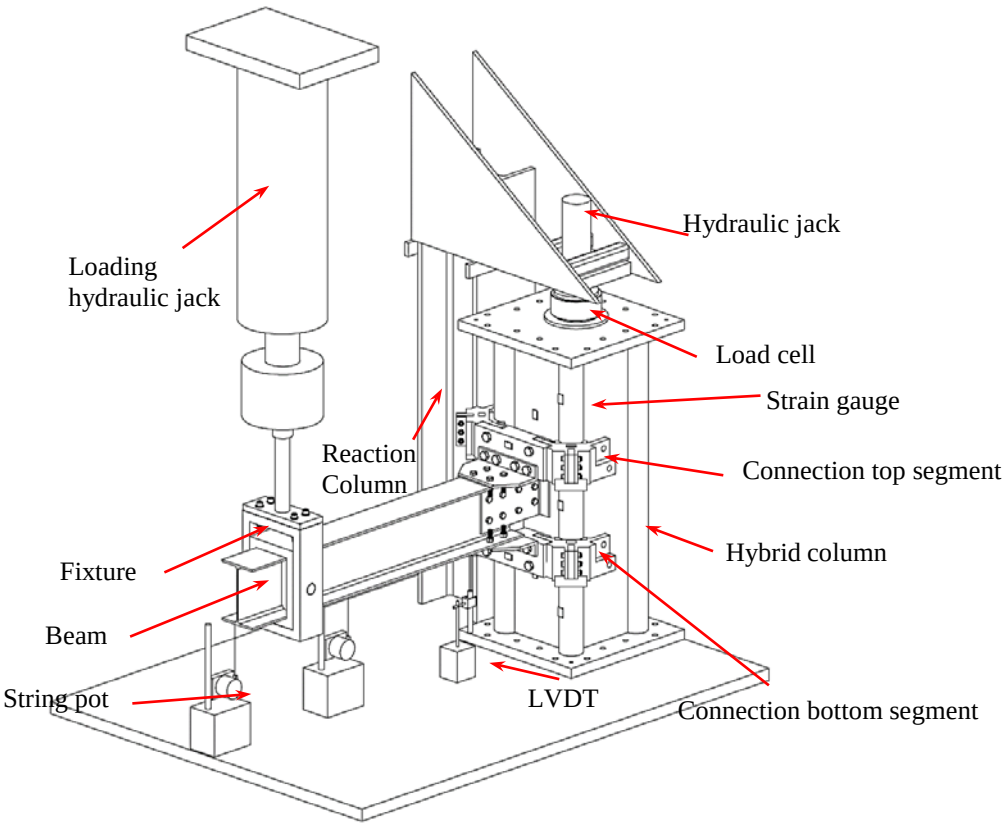

Fig. 2-6. Schematic of the test set-up

A reaction column is placed adjacent to the hybrid fabricated column. This column serves as the point of the reaction of the hydraulic jack applying the axial load. Several strain gauges are installed on the column and connection components to monitor the behaviour of these parts during the application of the load at the free end of the beam. Multiple linear and string pots are placed in different places to capture the displacements of the beam for further extraction of the moment-rotation curves. The displacement measured by the loading machine, LVDTs, and string pots is used to regenerate the rotation in the studies (Fig. 2-7).

Rotation of a connection at each deformation stage (elastic or plastic) can be resulted from global or local rotation of each component; however, in this study the overall rotation of the connection is being investigated. Whereas the angle θ is relatively small, the rotation at each point on the beam can be accurately estimated by the following relation (Eq. 2.1) between the vertical displacement and the distance from the connection face, assuming that the beam does not bend considerably and the rotation of the connection face and column are negligible:

$$\theta = \tan^{-1}\left(\frac{Veritical\ displacement}{Distance\ from\ the\ connection\ face}\right) \qquad \text{Eq. 2.1}$$

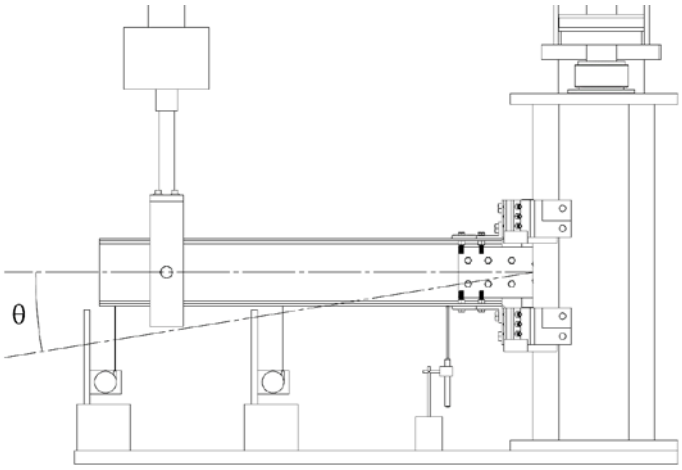

Fig. 2-7. Rotation measurement

Although the angle θ does not exactly represent the actual rotation of the column face or connection components, it can be used for comparative study between different connections, which is in accordance to FEMA350 [44]. The quasi-static load was applied in displacement control mode at a rate of 1mm/min. Loading was applied using a 250kN Instron machine equipped with a special fixture mounted close to the free end of the beam

at a one-meter distance from the connection face. This fixture transfers the downward movement of the hydraulic ram to the beam while letting the beam end rotate following the deformation in the connection assembly.

2.4 Numerical Modelling

Parallel to the experimental work, a numerical model was developed using Abaqus [43] to simulate the connection's behaviour. The robust model developed and verified in this stage provides a basis for further parametric investigation of the connection's performance with different geometry and materials. The column, beam, and connection components were modelled as three-dimensional objects in the software. The geometry of the beam and column is the same as those described in section 3 (Experimental phase). The element type used for meshing the parts was C3D8R, which is an eight-node brick element with reduced integration and hourglass effect control. This type of element is recommended for the simulation of models with high degrees of non-linearity such as large deformation problems, contact, plasticity, and failure [43]. Geometrical and material non-linearities were taken into account in the modelling procedure. Mild steel and ultra-high strength steel mechanical properties considered in the simulation are presented in Table 2-2. The details of the material properties of the column and connection were extracted from the experimental data [11]. Bolts and weld material properties have been introduced in the previous sections.

Table 2-2. Material properties

Material	Modulus of Elasticity	Poisson's Ratio	Yield Stress
	GPa	-	MPa
Mild Steel (Grade 250)	195	0.29	266
Ultra-high Strength Steel	210	0.3	1260

In an effort to enhance the capability of the model to capture the real behaviour of the connection, the material ductile damage criteria and damage evolution law were defined in Abaqus for different steels. These properties were obtained from the data acquired from the material tension test and fed to the software in the form of tabular data or exponential laws. The contacts between different parts of the connection assembly are of very great importance in the modelling of bolted connections, and these contacts were defined using surface-to-surface interaction and finite sliding formulation. A detailed discussion on the numerical part can be found in [42]. The results presented in this research work are Von

Mises stress distribution in the test assembly. Von Mises stress, which is in direct proportion to the deviatory strain energy, is a common criterion for investigating the stress state and prediction of the failure of ductile materials under complex loading conditions.

2.5 Results and discussion

This section presents the results of three tests conducted on the proposed I-beam to hybrid fabricated column connection.

2.5.1 Test No. 1: Connection with bolted angles

In the first test, each of the top and bottom angles (parts 6-1 and 6-2 in Fig. 2-2) were attached to one flange of the beam using four bolts. The connection setup for this test is shown in Fig. 2-8. The column corner tubes are Grade 1200 UHS steel.

Fig. 2-8. Test No.1 set-up

The moment-rotation curve for this test can be found in Fig. 2-9. In this test, the failure occurred in the two top rows of bolts attaching the beam flange to the angle-shaped part. The first major drop in the curve (point A) corresponds to the point where two of the bolts far from the connection face failed and dropped off. The second major drop (point B) relates to the failure of the second pair of bolts. Using the moment-rotation curve and the beam dimensions, this connection falls into the category of semi-rigid connections, based on the definitions and classifications of Eurocode3[45]. Fig. 2-10 displays the profile of the beam in different situations of the loading from the start to the end of the test. It can be observed

that the beam local deformation compared to the overall displacement of the connection is negligible and the linear relation for approximation of the drift angle is reasonable.

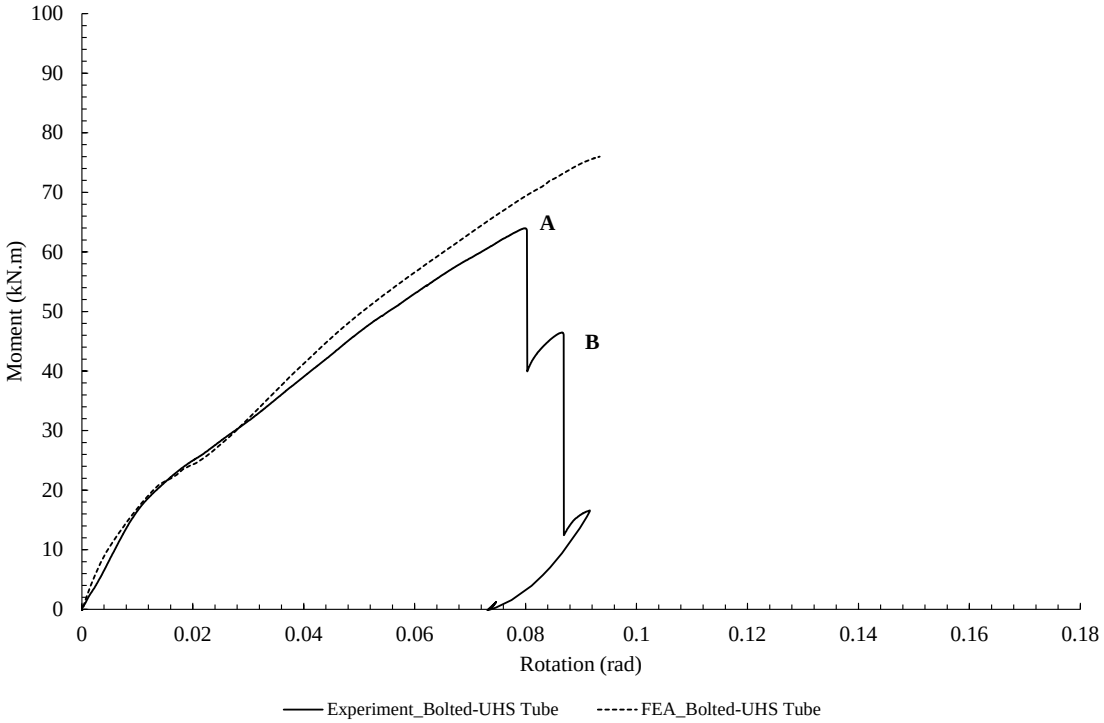

Fig. 2-9. Test No.1 Moment-rotation curve

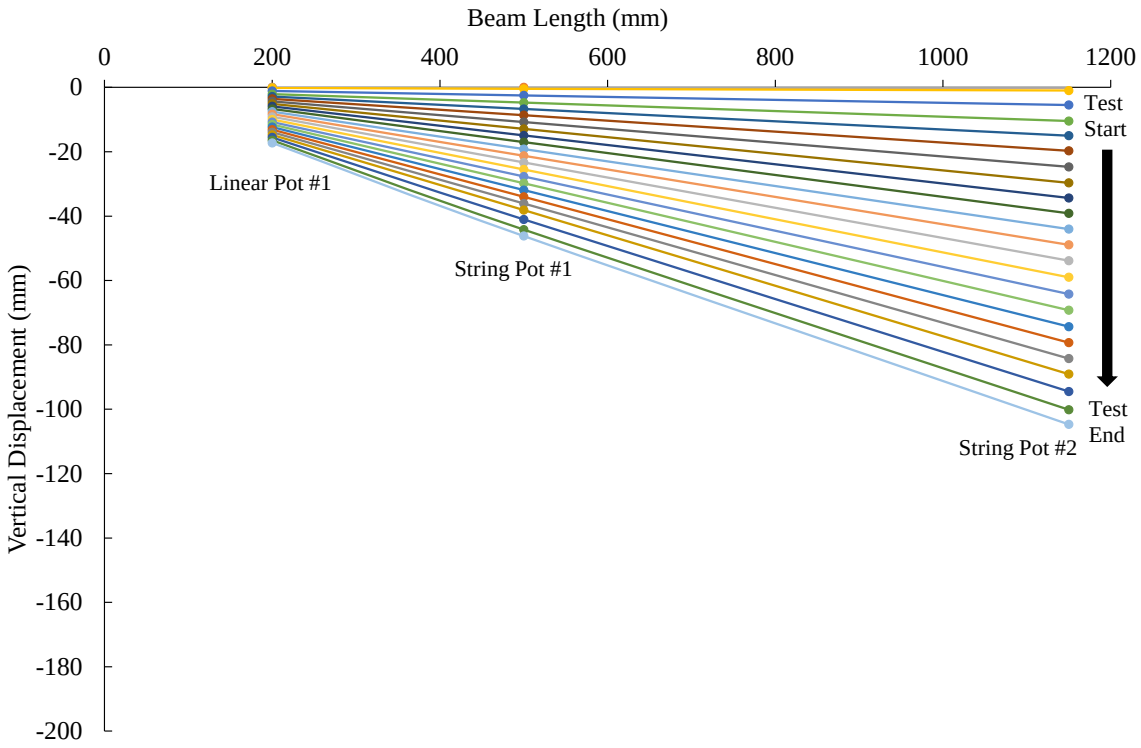

Fig. 2-10. Test No.1 Beam deflection profile during the test

The failed bolts are shown in Fig. 2-11. The fracture started from one thread root and developed further in a slope until the complete failure of the bolt, which suggests the failure was a result of a combination of tension and shear actions. The fracture surface roughness indicated that the fracture was mostly a brittle phenomenon rather than a ductile and smooth fracture, which is in accordance with the test observations.

Fig. 2-11. Test No.1Failed bolts of the top angle side

The final stage of the connection after failure is presented in Fig. 2-12.

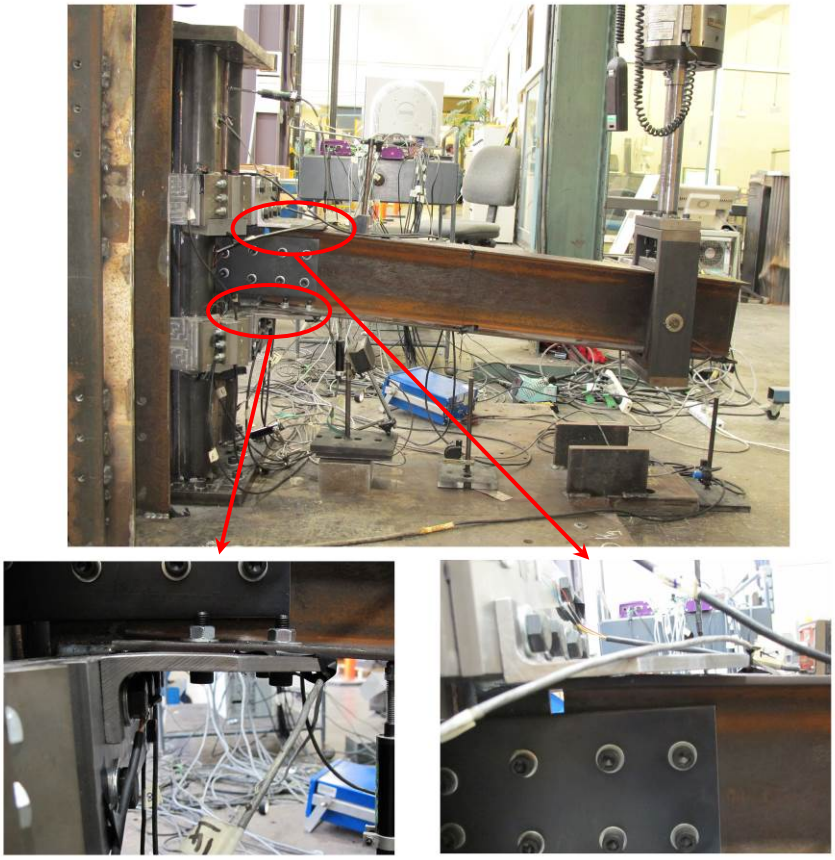

Fig. 2-12. Test No.1Displacement of different components of the connection

The top and bottom flanges of the beam also underwent plastic deformation, as shown in Fig. 2-13. The bolts passing through the web of the beam also crushed their holes. The direction of the deformation of the holes shows the line of action of this group of bolts in response to the rotation of the beam under loading.

(a) Web holes

(b) Top flange holes

(c) Top flange

Fig. 2-13. Test No.1 Deformations of different components of the beam

The proposed connection components moved relative to each other following the response of the beam-column assembly (Fig. 2-14) but no plastic deformation was evident. This relative displacement was observed in the top segment of the connection, which was subject to the tensile force applied to the top flange of the beam, while the bottom segment parts remained in their initial arrangement. After removing the beam and cutting off the welds of the web extension (the part connecting the top and bottom segments) all the components sprang back into place.

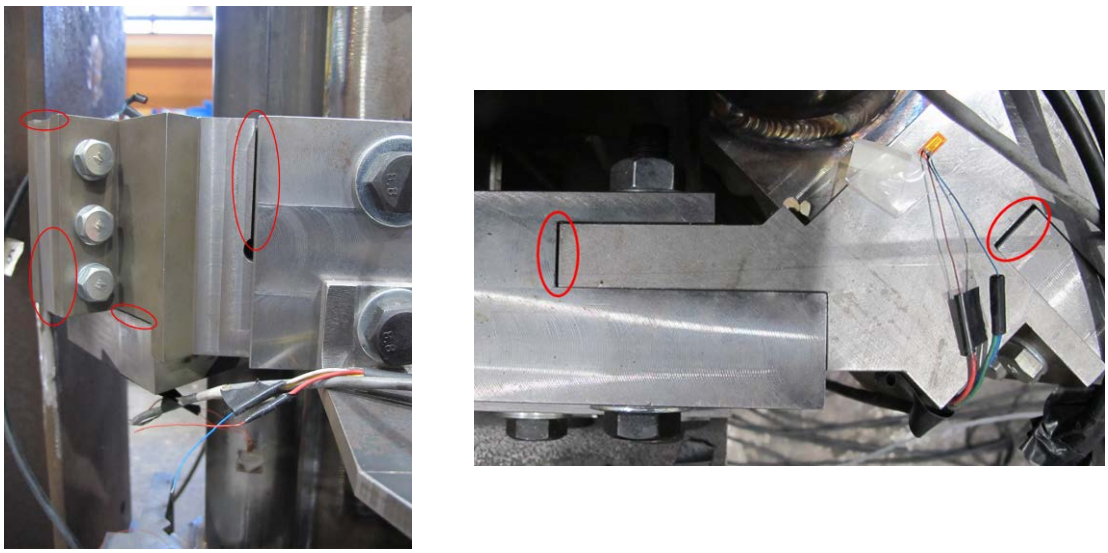

Fig. 2-14. Test No.1 Relative displacements of the top segment of the proposed connection

The FEA stress levels in the connection components (as can be seen in Fig. 2-15) are below the yield limit of their material that comply with this spring-like behaviour. The fact

that the connection components were within their elastic limits and the beam deformed plastically shows that the connection worked well, consistent with the weak beam-strong column design philosophy. In this test, the moment capacity of the connection was nearly 95% of the plastic moment capacity of the beam.

The unwanted behaviour of the connection is the abrupt failure of the bolts, which is not a favourable behaviour in structures. In order to tackle this issue, the connection was modified and a new test was performed. The results of the simulation presented in Fig. 2-15 can be used for visual comparison between the FEA deformations of the different parts of the connection and the test results.

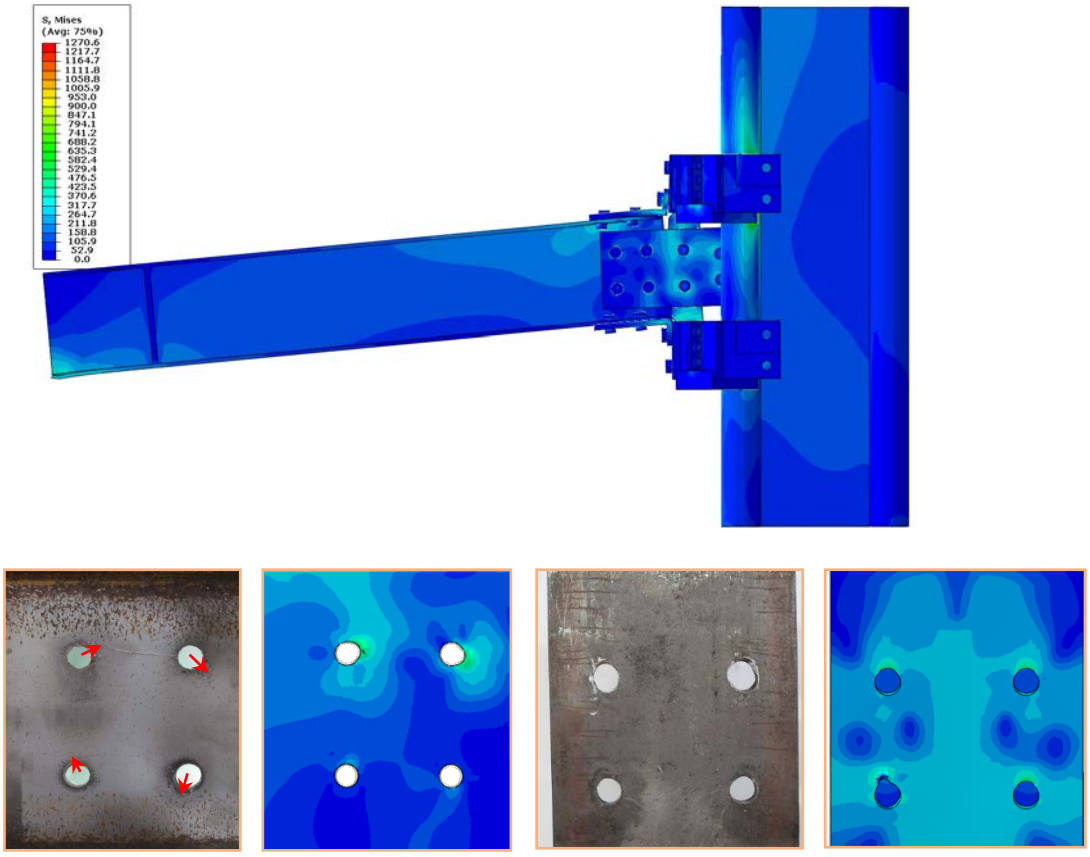

(a) (b)

Fig. 2-15. Test No.1 Deformations of the connection predicted by FE model (a) Beam web (b) Beam top flange

As Fig. 2-15 shows, the model is able to capture the deformations of the connection parts successfully. The moment-rotation curve generated using the data extracted from the FE simulation is also able to predict the connection behaviour accurately (Fig. 2-9). Magnitude of the maximum Von Mises stress in this case is 1270 MPa, which is observed in the front corner tubes.

2.5.2 Test No. 2: Connection with welded angles and UHSS tubes

In this connection set-up, based on the results of the previous test the design was modified such that the bolts connecting the top and bottom angles to the beam flanges were omitted and the aforementioned parts were connected to the beam using fillet welds. This measure was taken to avoid the sudden failure of the connection. This beam assembly was bolted to the proposed connection collars similar to the previous test. The column was also the same as that in the previous test and was composed of four UHS steel corner tubes and mild steel flat faces. The test assembly is shown in Fig. 2-16.

Fig. 2-16. Test No.2 set-up

The connection performance in this test was better than that in the previous test in the sense that both the ductility and capacity of the connection improved significantly (around 44%). In addition, the change made to the connection to eliminate the sudden drop in the capacity in the advent of failure improved the connection behaviour, in that this sudden failure did not happen again. The moment-rotation curve of the connection is presented in Fig. 2-17.

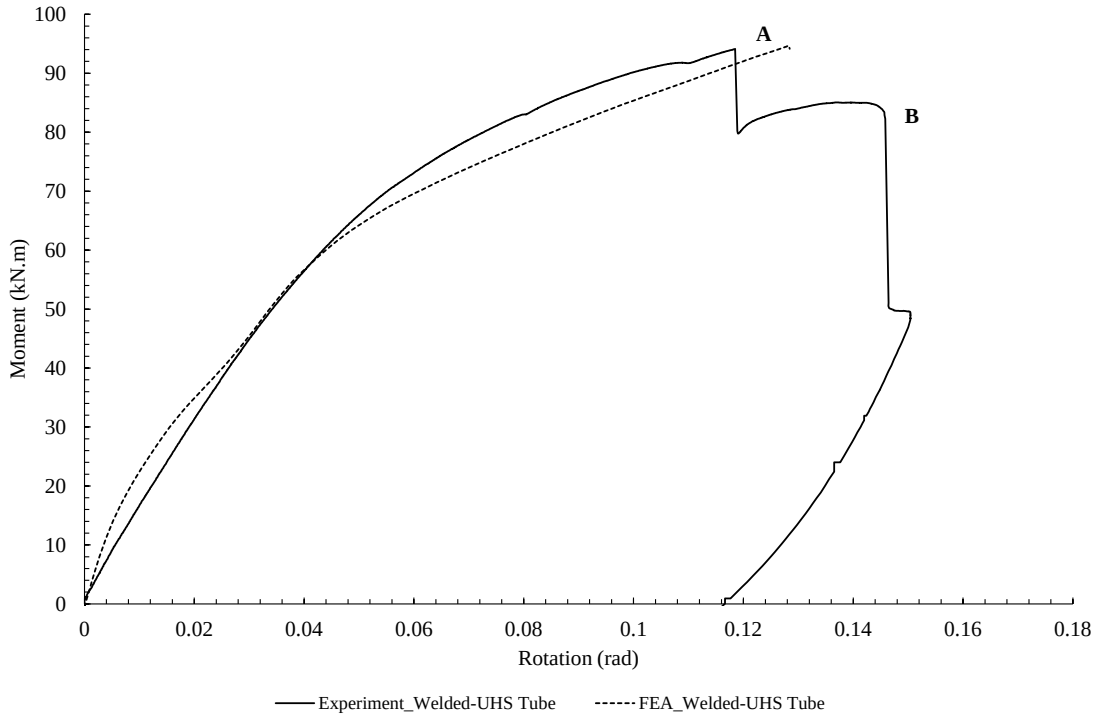

Fig. 2-17. Test No.2 Moment-rotation curve

Point A in Fig. 2-17 corresponds to the first sign of the failure of the connection, which is the failure of the right side of the top angle part, as indicated in Fig. 2-19. After this point, the connection still has the majority of its capacity and shows a ductile behaviour until the next failure point. At point B, the middle part of the top angle fails and the capacity drops significantly. Shortly after this point, the hydraulic jack of the testing machine reaches almost the end of its ram stroke. The testing was therefore stopped for safety reasons and avoiding any damage to the machine.

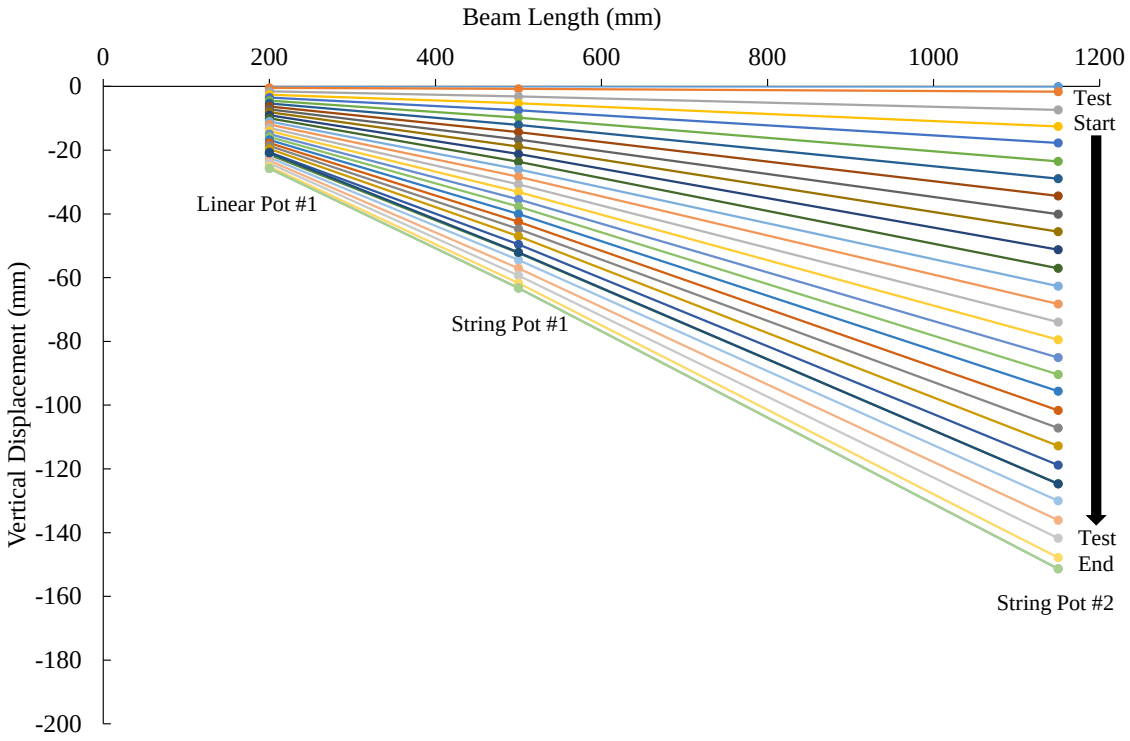

Fig. 2-18. Test No.2 Beam deflection profile during the test

The beam's profile during the test is presented in Fig. 2-18. As the curves show, the beam local deflection is negligible and it can be regarded as a straight beam for the purpose of calculating the drift angle.

This connection also is a semi-rigid connection according to Eurocode3[45], but compared to the previous connection, the initial stiffness of the connection is greater.

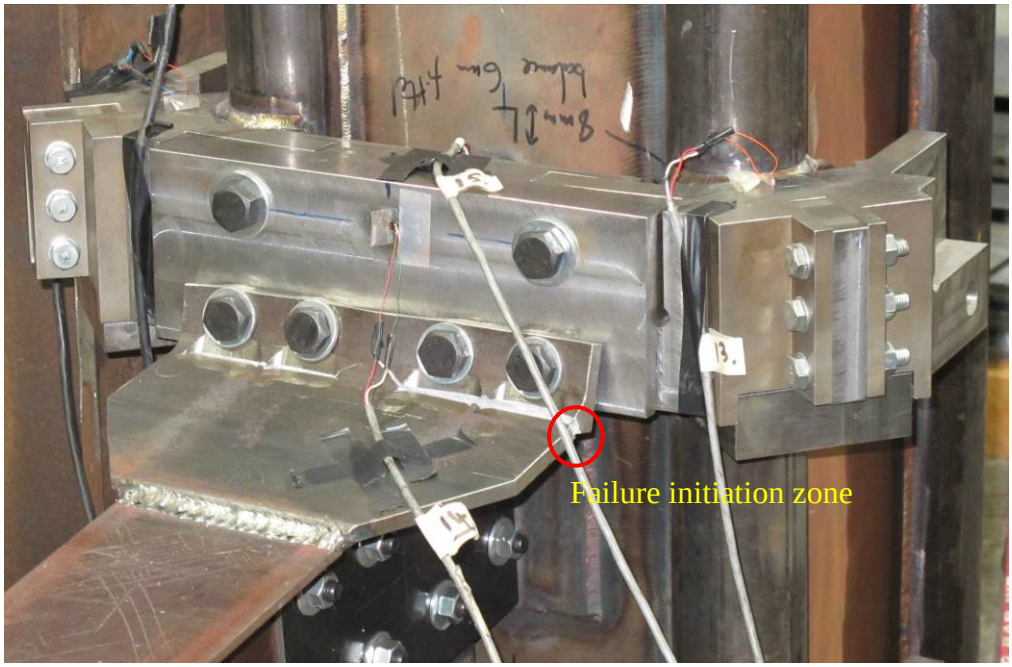

Fig. 2-19. Test No.2 Failed top angle

The final stage of the connection is presented in Fig. 2-20. In addition to the rupture of the top angle, the bottom angle also experienced plastic deformation, and the bottom flange of the beam buckled locally adjacent to the weld line of the bottom angle.

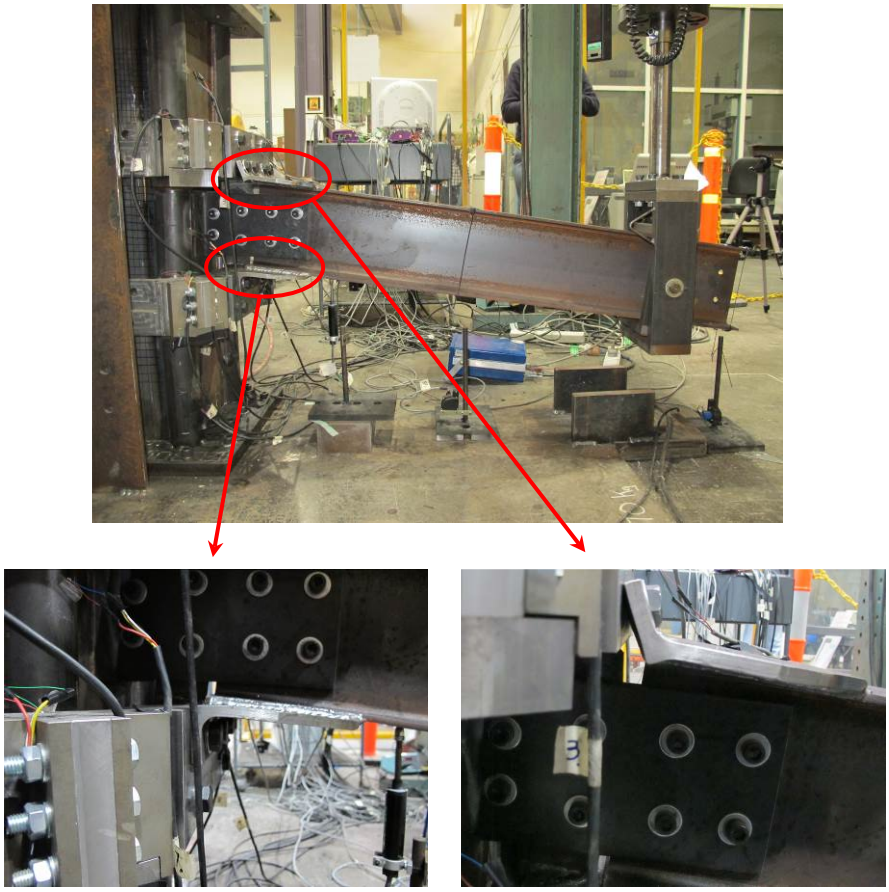

Fig. 2-20. Test No.2 Displacement of different components of the connection

The M16 bolts attaching the top angle to the top collar underwent a large amount of load and deformed considerably, as shown in Fig. 2-21. Number 1 indicates the bolt on the very left side of the top collar and number 4 is the last bolt located on the right (see Fig. 15).

Fig. 2-21. Test No.2 Deformed bolts from the top segment

The deformations of different parts of the connection are presented in Fig. 2-22.

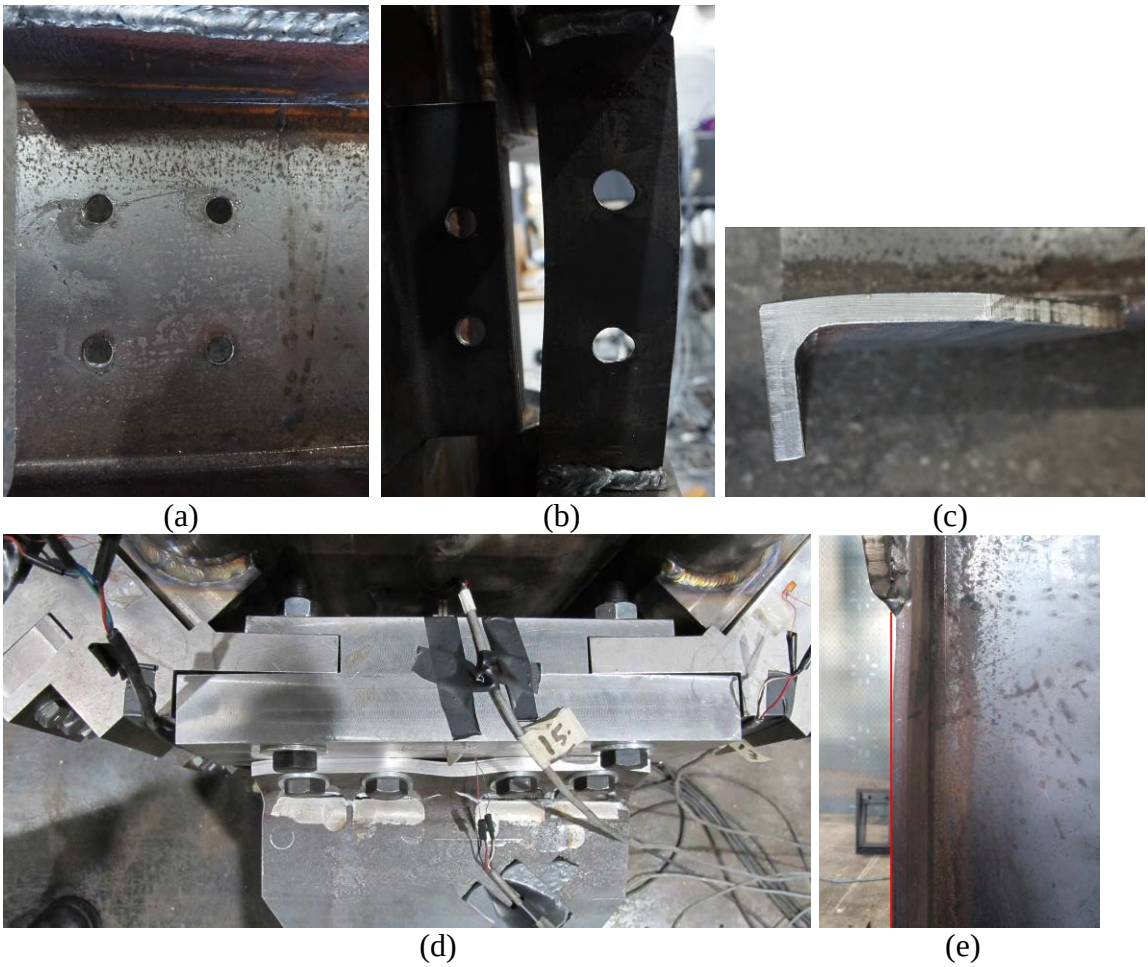

Fig. 2-22. Test No.2 Deformation of different parts of connection (a) Beam web (b) Web extension (c) Bottom flange (d) Top segment (e) Beam bottom flange buckling

Samples of the deformation of different parts of the connection, which was analysed using FE modelling, can be found in Fig. 2-23. This simulation was able to capture the deformation of the different parts of the connection with a good approximation. In addition, as can be seen in Fig. 2-17, the moment-rotation curve of the connection predicted by the FE model was able to predict the connection behaviour reasonably accurately. Maximum Von Mises stress level reached in this simulation is 1340 MPa that similar to the previous test is in the front corner tubes.

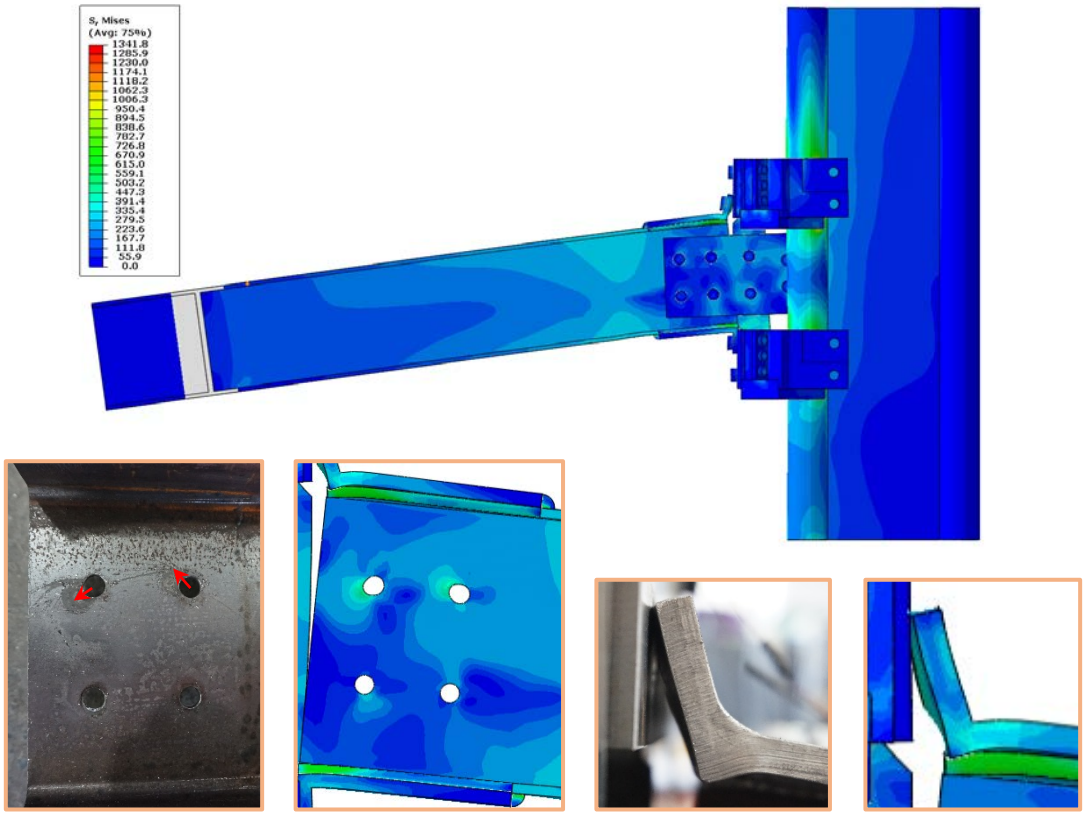

Fig. 2-23. Test No.2 Deformations of connection predicted by FE model (a) Beam web (b) Top angle

2.5.3 Test No. 3: Connection with welded angles and MS tubes

This test set-up was similar to that described in Section 2.5.2 with the difference being the material properties of the corner tubes. In this test, the corner tubes were made of mild steel material (Grade 250) instead of UHS steel, in order to explore the effect of corner tube material on the connection's performance. The moment-rotation diagram of the connection can be found in Fig. 2-24. The initial stiffness of this connection, similar to the previous connections, puts this connection in the semi-rigid connections category. However, this

connection had the lowest initial stiffness of the three different tests discussed in this research work.

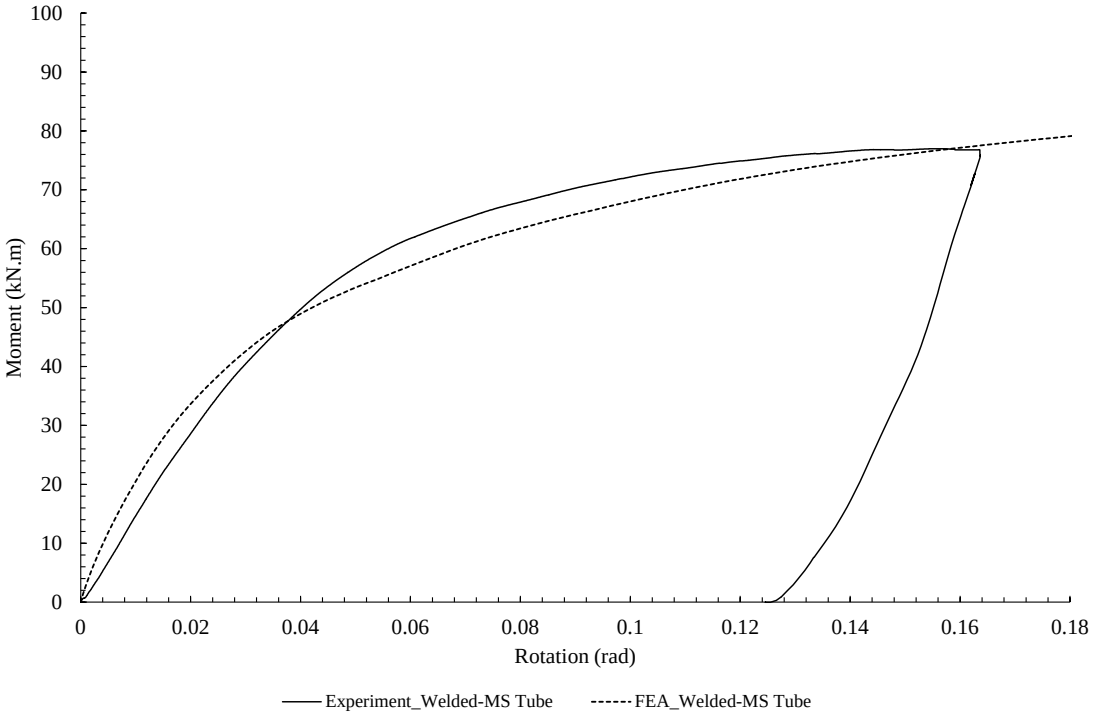

Fig. 2-24. Test no.3 Moment-rotation curve

The moment capacity of the connection was around 10% lower than the connection attached to the column with UHS corner tubes but the connection showed a higher degree of ductility, as the rotation capacity of the connection was 12% higher. This higher ductility could be the result of the crushing of corner tubes and warping of the side plates under the load that allowed the column-connection to deform relatively significantly while the load level increased slowly.

Fig. 2-25 shows the deflection profile of the beam in different stages of the test based on the data acquired from the instruments. The beam remains straight throughout the test. The last three profiles seem to be curved at their first portion, which can be interpreted as the slip of the head of LVDT at its point of contact with the beam due to high displacement of the beam in this particular test, which has caused this bend in the profiles.

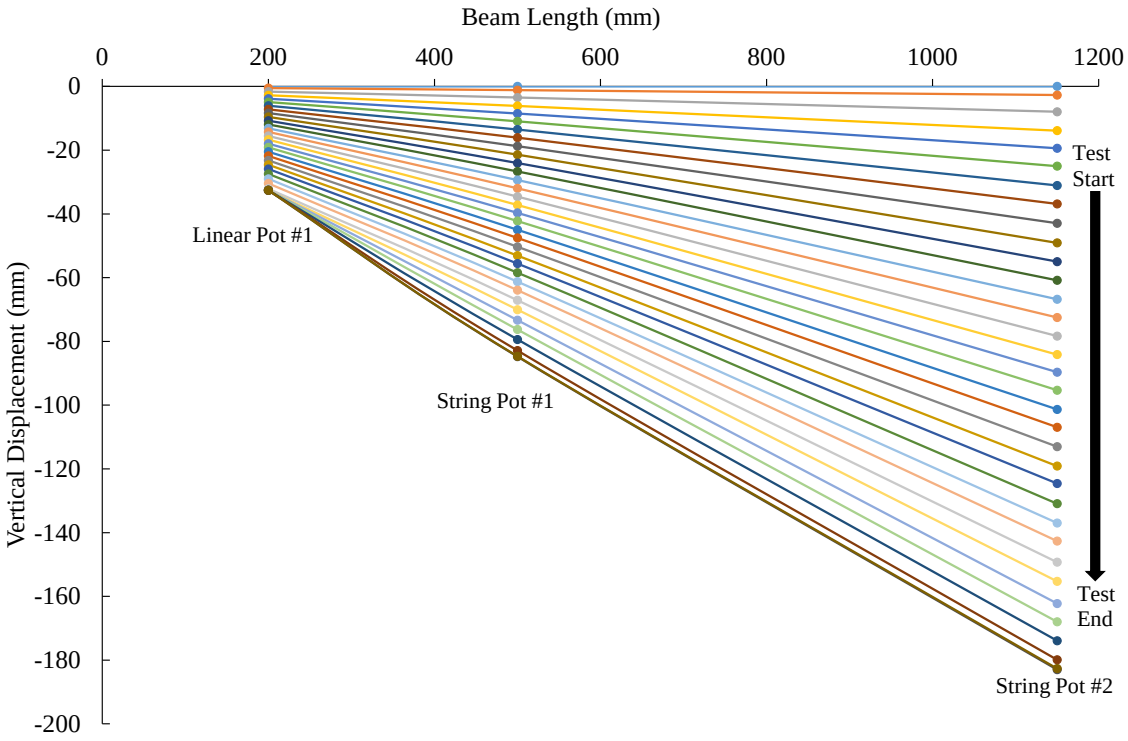

Fig. 2-25. Test No.3 Beam deflection profile during the test

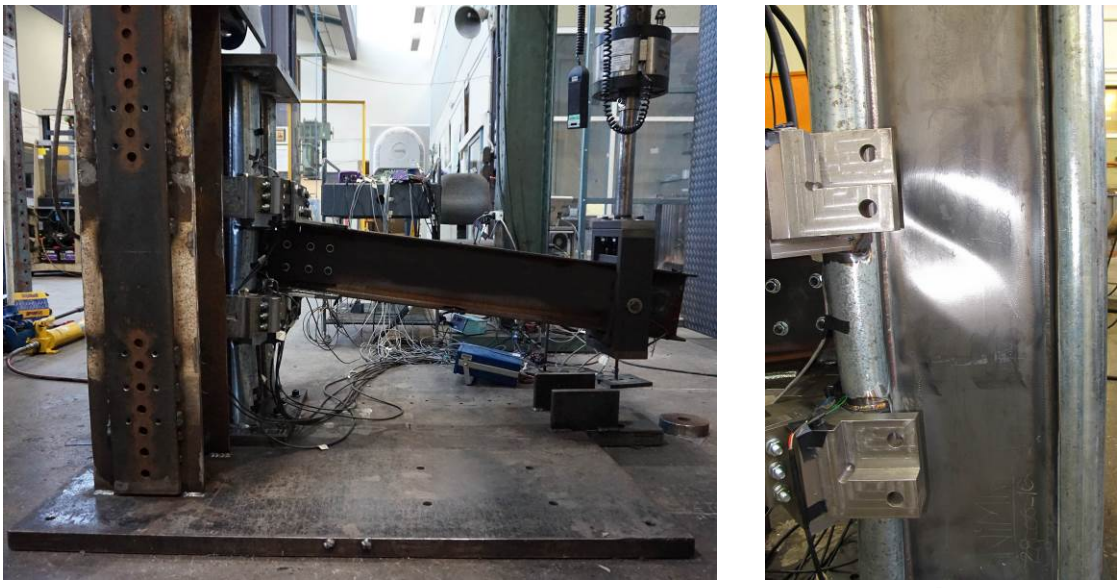

(a) (b)

Fig. 2-26. Test No.3 (a) Final state of the connection (b) Column lateral face

Further loading of the connection was not possible, as the full course of action of the hydraulic ram was almost used. The final state of the connection is presented in Fig. 2-26. As shown in this figure (Fig. 2-26), the column deformed noticeably compared to the previous tests. Unlike the previous tests in which the corner tubes underwent very limited

deformation, in this case, the corner tubes deformed significantly. In addition, the lateral plates of the column crumpled and deformed visibly. As shown in Fig. 2-27 (c), the column tubes at the point where the bottom segment is connected to them were considerably squashed. The tube at the top segment of the connection was also distorted and pulled outward. The top and bottom angle parts, which are welded to the beam, were bent but no other sign of damage was visible in them (Fig. 2-27 (d), (e)). The holes on the web of the beam, web extension and the side plates were also not noticeably deformed, as they were in the previous tests. Fig. 2-27 (f) shows the holes on the web extension as a sample. In this test, due to the huge deformation of the corner tubes, the bottom collar part was also bent inward, as shown in Fig. 2-27 (b).

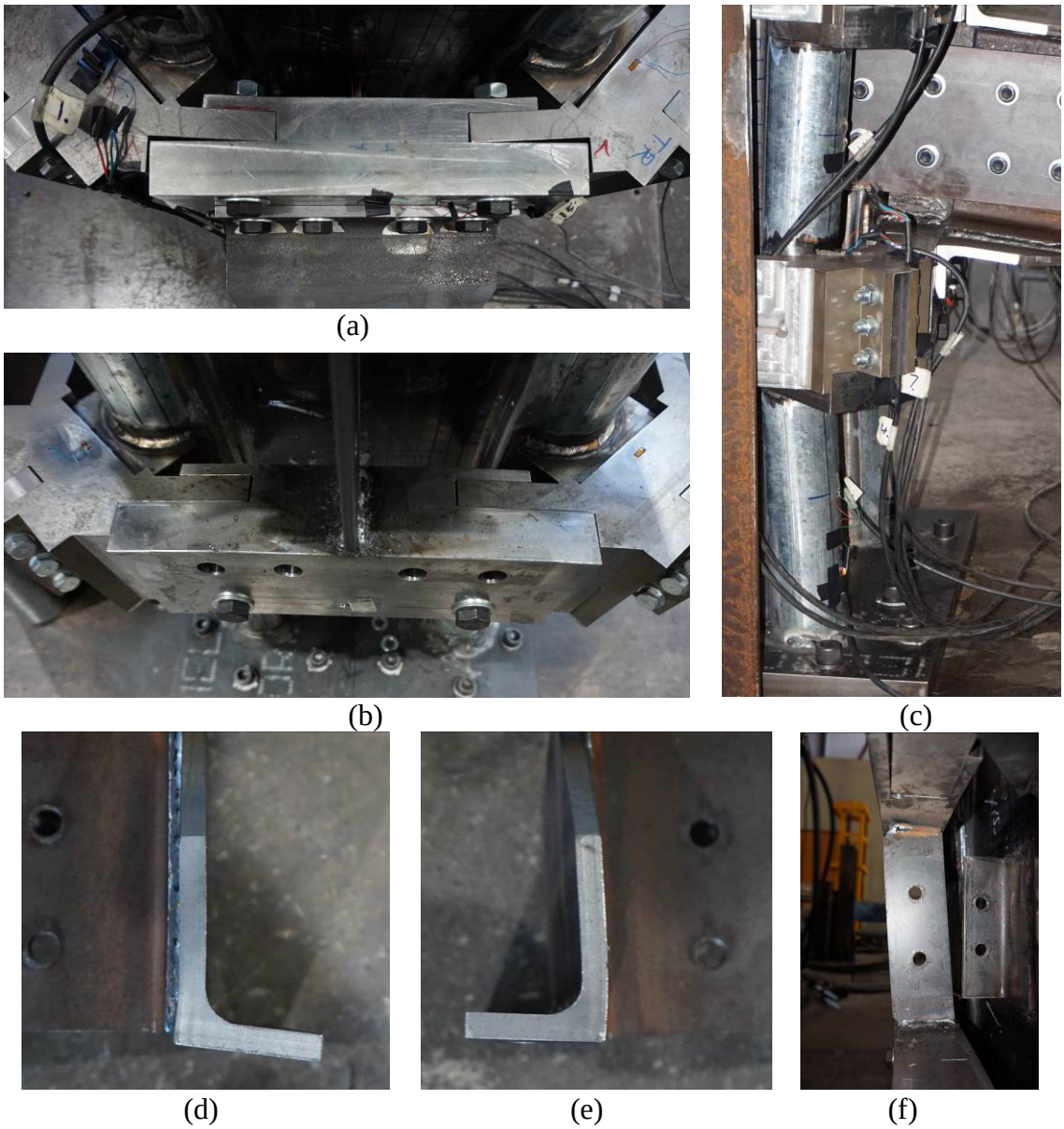

Fig. 2-27. Test No.3 Deformation of different parts of connection (a) Top collar (b) Bottom collar (c) Corner tube (d) Top angle (e) Beam angle (f) Web extension and angles

Similar to the previous experiments, this test was also numerically simulated, and the quantitative results in the form of moment-rotation curve are presented in Fig. 2-24 along with the experimental results for comparison. The deformation predicted by the FE model can be found in Fig. 2-28. As in previous tests, the model was able to predict the deformations of the connection parts accurately. A comparison of the experimental moment-rotation curve and the FEA results suggests that the model was able to predict the connection behaviour successfully.

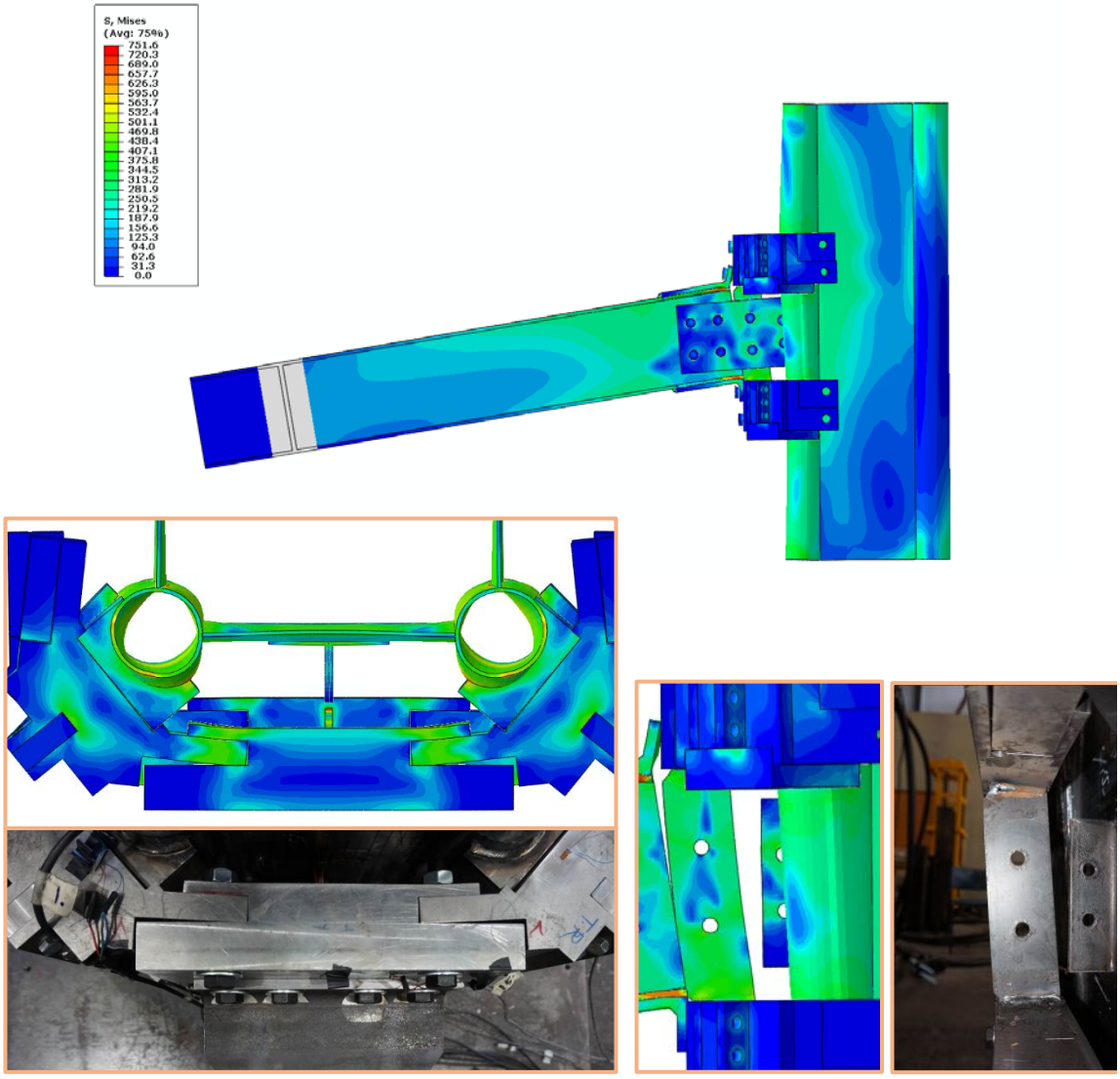

(a) (b)

Fig. 2-28. Test No.3 Deformations of the connection predicted by FE model (a) Bottom part bending (b) Web extension

Maximum Von Mises stress in this test is around 750 MPa happening in the M16 bolts connecting the top angle to the connection. The moment-rotation curves of all three connections are presented in Fig. 2-29 to make the comparison of their behaviour easier. The replacement of the bolts on the beam flanges with welds increased the initial stiffness and moment capacity. The hybrid column with mild steel corner tubes and attached to the beam with welded angles still had higher moment capacity than the connection with a bolted beam, but its initial stiffness fell below that of both other connections.

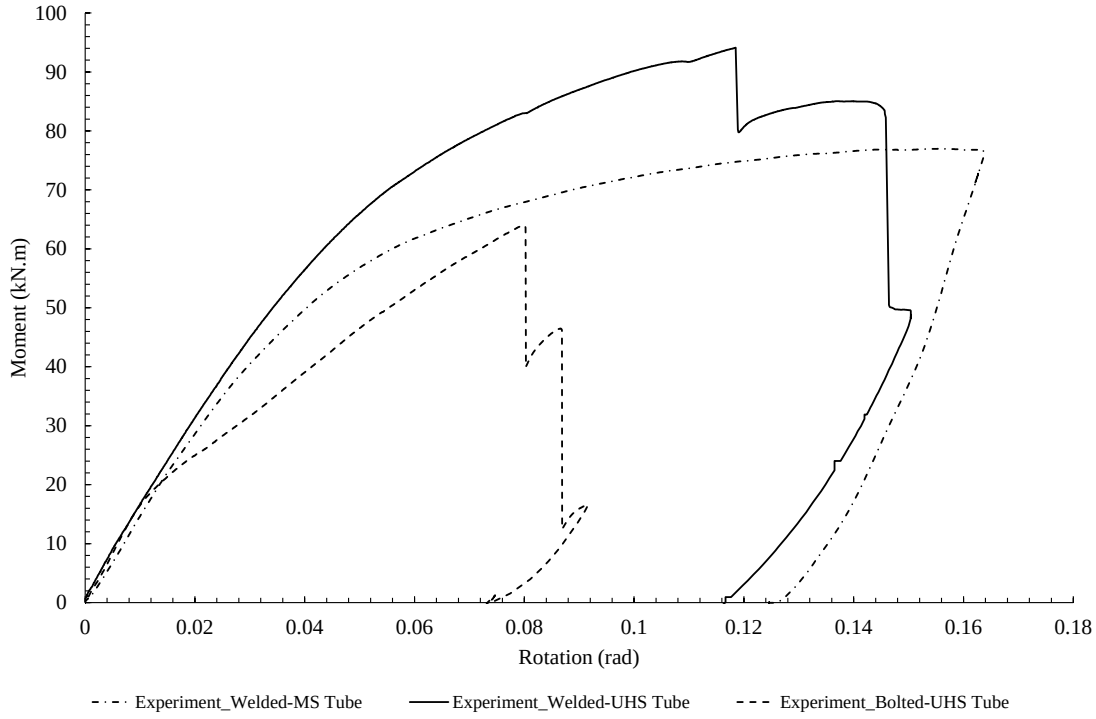

Fig. 2-29. Comparison of moment-rotation behaviour of three tests

Table 2-3 summarizes the values of beam plastic moment capacity, and moment capacity, rotation capacity and initial stiffness obtained from each test.

Table 2-3. Test results summary

Test No.	Initial Stiffness ($S_{j,ini}$)	Moment Capacity	Rotation Capacity	Beam Plastic Moment Capacity
	kN.m/rad	kN.m	rad	kN.m
1	1582.41	63.54	0.092	66.53
2	1850.01	94.13	0.150	66.53
3	1404.93	76.68	0.163	66.53

It is noted that EI_b/L_b is the parameter that is used as the criterion to determine whether a connection is pinned, semi-rigid or rigid. In these tests, the value of EI_b/L_b is 2100 kN.m. According to Eurocode3 [45] the connections with initial stiffness within the range of $0.5EI_b/L_b < S_{j,ini} < k_bEI_b/L_b$ are semi-rigid, in which $k_b = 8$ for frames with a bracing system reducing the horizontal displacement by at least 80% and $k_b = 25$ for other frames.

Connections with stiffness higher than $k_b E I_b / L_b$ are classified as rigid. Comparing the values in Table 2-3, this connection could be classified as a rigid connection but since this connection is not used in a frame and the ratio of K_b / K_c ($K_b = I_b / L_b$ and $K_c = I_c / L_c$) [45] is less than 0.1 for this test, it is assumed that the connection is a semi-rigid connection.

2.6 Conclusion

In this research work, a new connection is proposed for use with hybrid fabricated columns. Three experimental tests were performed on the connection to investigate the performance of the connection under static loading. Moreover, a three-dimensional finite element model was developed in Abaqus [43] to simulate the experiments.

As the results of the experiments suggest, the moment-bearing capacity is at least as high as 95% of the plastic moment capacity of the beam. When the beam flanges were bolted to the connection parts, the bolts failed and an abrupt change in the capacity was observed. As this is not a favourable failure, the bolts were replaced by welding. In this new version, the connection showed almost 50% higher moment capacity while maintaining the high ductility. Replacing the UHS corner tubes with mild steel tubes reduced the capacity by around 10% but notable deformation of the column suggests that the UHS material offers superior performance. The rotation capacity of the connection was also well beyond the thresholds suggested by different standards. A typical value for the rotation capacity of connections to make them qualified for moment frames is usually around 0.04 rad, and in this connection, the capacity is far beyond this threshold.

This connection can be used for different sizes of columns and beams. In order to modify the connection for different column sizes, the diameter of the backside of the corner bottom parts (parts 3-1 to 3-4 in Fig. 2-2) and the length of the collars, (parts 1 and 2 in Fig. 2-2) need to be altered. The distance between the top and bottom segments of the connection can also be changed to fit different beam sizes onto the connection.

The modularity of the connection reduces the need to have extensive on-site welding, as the main welding would be done in the factory while the parts would only be assembled on-site. Another feature of this connection is the re-usability of the connection, which has also been practically verified. All three tests were conducted using the same set of components and the connection components are re-usable in further tests, in spite of the

large deformations in the hybrid fabricated column. Although the current set of the connection parts are machine cut but the suggested method of mass production is casting which could lower the price and make the connection more feasible for widespread use in the construction industry.

The numerical simulation results presented, show that the model has been able to predict the behaviour of the connection successfully. The moment rotation curves generated from the data acquired from the numerical simulation can predict the initial stiffness and follow the actual behaviour with less than 15% deviation in the majority of the loading range, especially for the connections connected to the columns with UHSS corner tubes. It means that this model can be used in further investigation of the connection.

The connection is still under further experimental investigation in order to improve its characteristics. These improvement tasks include testing the connection with other hybrid fabricated columns, such as columns consisting of corrugated plates with/without corner tubes and optimisation of the connection geometry. The connection is designed in a way to maintain its integrity and capabilities under load reversal, too; however, the connection behaviour under cyclic loading needs to be thoroughly investigated.

Acknowledgement

The research work presented in this research work is supported by the Australian Research Council through a Discovery Project (DP150100442) awarded to the authors. The experiments were performed in the Structures Laboratory of the Civil Engineering Department at Monash University, and the contribution of the staff is highly appreciated. The columns were fabricated by CrossLine Engineering Pty Ltd and the connection components by Fetha Engineering. The SSAB steel manufacturer in Finland provided the ultra-high strength steel tubes.

References

[1] Rasmussen KJR, Hancock GJ. Geometric imperfections in plated structures subject to interaction between buckling modes. Thin-Walled Struct. 1988;6:433–52.

[2] Degée H, Detzel A, Kuhlmann U. Interaction of global and local buckling in welded RHS compression members. J Constr Steel Res. 2008;64:755–65.

[3] Schillinger D, Papadopoulos V, Bischoff M, Papadrakakis M. Buckling analysis of imperfect I-section beam-columns with stochastic shell finite elements. Comput Mech. 2010;46:495–510.

[4] Lotfi S, Azhari M, Heidarpour A. In-elastic local buckling of skew thin thickness tapered plates with and without intermediate supports using the isoparametric spline finite strip method. Thin-Walled Struct. 2011;49:1457–82.

[5] Kasaeian Sh, Azhari M, Heidarpour A, Hajiannia A. In-elastic local buckling of curved plates with or without thickness-tapered sections using finite strip method. Int J Steel Struct. 2012;12:427–42.

[6] Valeš J. Effect of random axial curvature on the performance of open and closed section steel columns. AIP Conference Proceedings. 2013. 2512-2515. Print..

[7] Aoki T, Ji B. Experimental study on buckling strength of tri-tube steel members. The 3rd International Conference on Coupled Instabilities in Metal Structures, Lisbon, Portugal; 2000. p. 283–90.

[8] Zhao XL, Van Binh D, Al-Mahaidi R, Tao Z. Stub column tests of fabricated square and triangular sections utilizing very high strength steel tubes. J Constr Steel Res. 2004; 60:1637–61.

[9] Van Binh D, Al-Mahaidi R, Zhao XL. Finite element analysis (FEA) of fabricated square and triangular section stub columns utilizing very high strength steel tubes. Adv Struct Eng. 2004;7:447–57.

[10] Javidan F, Heidarpour A, Zhao X-L, Hutchinson CR, Minkkinen J. Effect of weld on the mechanical properties of high strength and ultra-high strength steel tubes in fabricated hybrid sections. Engineering Structures. 2016;118:16–27.

[11] Javidan F, Heidarpour A, Zhao XL, Minkkinen J. Performance of innovative fabricated long hollow columns under axial compression. J Constr Steel Res. 2015;106:99-109.

[12] Heidarpour A, Cevro S, Song QY, Zhao XL. Behaviour of innovative stub columns utilising mild-steel plates and stainless steel tubes at ambient and elevated temperatures. Eng Struct. 2013;57:416–27.

[13] Heidarpour A, Cevro S, Song QY, Zhao XL. Behaviour of stub columns utilising mild-steel plates and VHS tubes under fire. J Constr Steel Res. 2014;95:220–9.

[14] Nassirnia M, Heidarpour A, Zhao XL, Minkkinen J. Innovative Hollow Columns Comprising Corrugated Plates and Ultra High-Strength Steel Tubes. Thin-Walled Struct. 2016;101:14–25.

[15] Nassirnia M, Heidarpour A, Zhao XL, Minkkinen J. Innovative hollow corrugated columns: a fundamental study. Eng. Struct. 2015;94:43–53.

[16] Farahi M, Heidarpour A, Zhao XL, Al-Mahaidi R. Compressive Behaviour of Concrete-Filled Double-Skin Sections Consisting of Corrugated Plates. Eng Struct. 2016;111:467–77.

[17] Yeomans N. Flowdrill jointing system: Part 1- Mechanical intregrity tests. CIDECT Report: 6F-13A/96; 1996.

[18] Yeomans N. Flowdrill jointing system: Part 2- Structural hollow section connections. CIDECT Report: 6F-13B/96; 1996.

[19] Korol RM, Ghobarah A, Mourad S. Blind Bolting W-Shape Beams to HSS Columns. Journal of Structural Engineering. 1993;119(12):3463–81.

[20] Kurobane Y, Packer JA, Wardenier J, Yeomans N. Design Guide 9: For Structural Hollow Section Column Connections. 1st ed. Koln, Germany: TÜV-Verlag; 2004. 213 p.

[21] Song QY, Heidarpour A, Zhao XL. Han LH. Performance of Double-Angle Bolted Steel I-Beam to Hollow Square Column Connections Under Static and Cyclic Loadings. International Journal of Structural Stability and Dynamics. 2016;16(2):1-20.

[22] Barnett, T.C. (2001). The Behaviour of a Blind Bolt Moment Resisting Connections in Hollow Steel Sections. Ph.D. Thesis, University of Nottingham, UK.

[23] Ajax Engineered Fasteners (2002). ONESIDE Brochure. B-N012 Data Sheet, Victoria, Australia.

[24] Gardner AP, Goldsworthy HM. Experimental investigation of the stiffness of critical components in a moment-resisting composite connection. Journal of Constructional Steel Research. 2005;61(5):709–26.

[25] Lee J, Goldsworthy HM, Gad EF. Blind bolted moment connection to sides of hollow section columns. Journal of Constructional Steel Research. 2011;67(12):1900–11.

[26] Wang J, Spencer BF. Experimental and analytical behavior of blind bolted moment connections. Journal of Constructional Steel Research. 2013;82:33–47.

[27] Wang Z-Y, Wang Q-Y. Yield and ultimate strengths determination of a blind bolted endplate connection to square hollow section column. Engineering Structures. 2016;111:345–69.

[28] Ghobarah A, Mourad S, Korol RM. Behaviour of blind bolted moment connections for square HSS columns. In: Coutie MG, Davies G, editors. Tubular structures V. Nottingham, United Kingdom: E & FN Spon; 1993. p. 269.

[29] Mourad S, Korol RM, and Ghobarah A. Design of Extended End-Plate Connections for Hollow Section Columns. Canadian Journal of Civil Engineering. 1996;23(1), 277–286.

[30] Wheeler AT, Clarke MJ, Hancock GJ, and Murray TM. Design Model for Bolted Moment End Plate Connections Joining Rectangular Hollow Sections. Journal of Structural Engineering. 1998;124(2), 164–173.

[31] Wheeler AT, Clarke MJ, and Hancock, GJ. FE Modeling of Four-Bolt, Tubular Moment End-Plate Connections. Journal of Structural Engineering. 2000;126(7), 816–822.

[32] Tanaka T, Tabuchi M, Maruyama M, Furumi K, Morita T, Usami K, and Matsubara Y. (1996). Experimental Study on End Plate to SHS Column Connections Reinforced By Increasing Wall Thickness with One Sided Bolts. Proc. of 7th International Symposium on Tubular Structures, Miskolc, Hungary, 253– 260.

[33] Bruneau M, Uang CM, and Whittaker A (1998). Ductile Design of Steel Structures, McGraw-Hill, Boston, Massachusetts.

[34] Kunnath SK, and Malley JO. Advances in Seismic Design and Evaluation of Steel Moment Frames: Recent Findings from FEMA/SAC Phase II Project. Journal of Structural Engineering. 2002;128(4), 415-419.

[35] Mirghaderi SR, Torabian S, Keshavarzi F. I-beam to box–column connection by a vertical plate passing through the column. Engineering Structures. 2010;32(8):2034–48.

[36] Federal Emergency Management Agency (FEMA) (2000). State of the art report on connection performance. Prepared by the SAC Joint Venture for the Federal Emergency Management Agency. FEMA-355D, September. Washington, DC: FEMA.

[37] Mirmomeni M, Heidarpour A, Zhao XL, Hutchinson C, Packer J, and Wu C. Fracture behaviour and microstructural evolution of structural mild steel under the multi-hazard loading of high-strain-rate load followed by elevated temperature. Construction and Building Materials. 2016;122:760-771.

[38] Hosseini S, Heidarpour A, Collins F, and Hutchinson C. Strain ageing effect on the temperature dependent mechanical properties of partially damaged structural mild-steel induced by high strain rate loading. Construction and Building Materials. 2016:123:454-463.

[39] Azhari F, Heidarpour A, Zhao XL, and Hutchinson C. Mechanical properties of ultra-high strength (Grade 1200) steel tubes under cooling phase of a fire: An experimental investigation. Construction and Building Materials. 2015;93:841-850.

[40] Sinaie, S., Heidarpour, A. , and Zhao, XL. Stress-strain-temperature relation for cyclically-damaged structural mild steel. Engineering Structures. 2014;15:84-94.

[41] AS/NZS 3679.1:2016 Structural steel - Hot-rolled bars and sections. Standards Australia; 2016.

[42] Sadeghi N, Heidarpour A, Zhao XL, Al-Mahaidi R. Numerical investigation of innovative modular beam-to-fabricated column connections under monotonic loading. In: Zingoni A, (ed.) Insights and Innovations in Structural Engineering, Mechanics and Computations. Cape Town, South Africa: Taylor and Francis Group, LLC; 2016. p. 1247–52.

[43] ABAQUS 6.14-1. Providence, RI, USA: Dassault Systèmes; 2014.

[44] Federal Emergency Management Agency (FEMA) (2000). Recommended seismic design criteria for new steel momentframe buildings. Prepared by the SAC Joint Venture for the Federal Emergency Management Agency. FEMA-350, June. Washington, DC: FEMA.

[45] European Committee for Standardisation (CEN). (2005). Eurocode 3. Design of Steel Structures, Part 1-8: Design of Joints. Brussels: CEN.

A COMPARATIVE NUMERICAL STUDY ON THE INNOVATIVE I-BEAM TO THIN-WALLED HYBRID FABRICATED

CHAPTER 3

This chapter has been published in the Journal of *Thin-Walled Structures*, Volume 127, June 2018, Pages 235-258. DOI: 10.1016/j.tws.2018.02.007.
Reprinted here with the Author Rights granted by Elsevier.

Table of Contents

Abstract

Hybrid fabricated columns (HFCs) consisting of mild-steel thin plates connected to ultra-high strength thin-walled tubes at corners have exhibited superior performance compared to the equivalent conventional tubular columns. The higher load-bearing capacity, energy absorption, and post-buckling strength of these columns provide designers with new possibilities in the construction of high-rise buildings. Although several studies have been conducted on these columns, the connection between I-beams and this type of column is challenging. In this research work, using 3-D finite element modelling a numerical study is conducted to compare the behaviour of recently patented bolted modular M-HFC connection between I-beams and HFCs with the welded non-modular type of this connection (called as W-HFC). The performance of the W-HFC connection is also compared with four different types of common conventional connections currently in use in the industry. Moreover, a topology optimisation has been performed on the M-HFC connection in order to reduce the overall weight of the connection components while keeping the moment- rotation characteristics of the connection as close as possible to the originally proposed connection.

Keywords: Hybrid fabricated column, connection, ultra-high strength, moment rotation, numerical study, topology optimisation

3.1 Introduction

The concept of fabricated sections composed of thin plates and tubes welded together to form a closed section was first studied by Aoki [1]. In this research, stub-columns with triangular cross-sections were fabricated by welding three plates to three tubes at each apex and tested under uniform and eccentric compressive loading. It was found that the capacity of the stub-columns was far greater than the sum of each individual member's capacities. Based on investigations by different researchers on the behaviour of these fabricated columns with various configurations (Fig. 3-1), including square hybrid fabricated columns (HFCs) consisting of mild-steel plates and very high strength tubes [2 - 7], and square hybrid columns consisting of corrugated plates with or without corner tubes [8 - 10], their load-bearing capacity, post-buckling strength, ductility, and energy absorption compared to those of equivalent conventional sections are significantly improved. This makes HFCs suitable for the construction of moment frame structures.

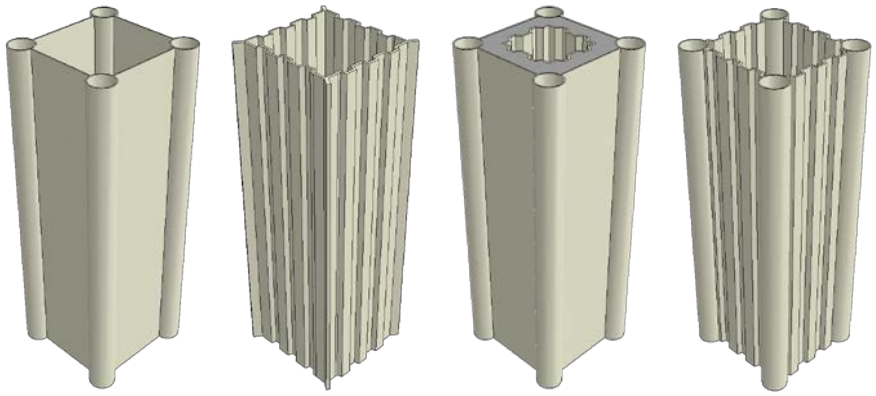

Fig. 3-1. Various types of HFCs (a) Flat face with corner tubes (b) Corrugated face without corner tubes (c) Concrete-filled double skin sections with corner tubes (d) Corrugated face with corner tubes

One major challenge limiting the widespread commercial use of HFCs in construction is the lack of suitable robust connections between beams and these columns. In order to tackle this issue, the authors recently proposed an innovative **m**odular type of connection, named the **M**-HFC connection (Fig. 3-2), that can be used with this type of column, and its

mechanical performance under static loading was experimentally and numerically analysed [11 , 12].

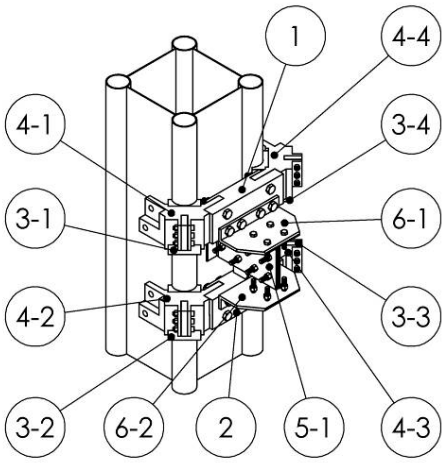

Fig. 3-2. M-HFC connection

The results of the experimental tests conducted on the M-HFC connection have demonstrated that this patented connection can deliver a high moment capacity and also more ductility compared to the requirements of the different codes of practice [13 , 14]. The modular nature of the connection also allows for faster and more reliable construction, while eliminating the need to perform extensive on-site welding. Furthermore, it has been designed to be re-usable after the occurrence of extreme events that could lead to the demolition of the structure.

Although the superior behaviour of the proposed M-HFC connection was demonstrated in the recent study conducted by the authors [11 , 12], a study on possible variations of the proposed connection is still required. Hence, in order to explore the mechanical performance of the non-modular type of the proposed connection, welds replace some of the bolts in the M-HFC connection. The performance of the proposed connection should also be compared with conventional connections currently in use in industry. Moreover, the connection topology should be optimised in a way that whilst showing a high performance, it is more economical to manufacture and use in the construction.

In this research work, the moment-rotation curve is used to compare the performance of various connections. The moment-rotation curve of a connection is a direct indicator of its actual behaviour and is used to classify the connections. For instance, according to

Eurocode 3: Part 1-8 (2005)[13] connections are classified based on their initial rotational stiffness as rigid, semi-rigid, and nominally pinned. Also, based on the strength criterion and comparing the design moment resistance of the connection with connected members, they are classified as full strength, partial strength and nominally pinned.

In practice, connections behave as semi-rigid and the relative deformation of their components should be taken into account. To this end, many experimental efforts have been dedicated to explore the moment-rotation relationship of several types of connections [15]. Several non-experimental methods have also been developed to predict the moment-rotation curves of end-plate connections, including the T-stub model, yield line model, and finite element (FE) analysis. The T-stub model was the outcome of early efforts to find semi-analytical methods for analysing end-plate connections [16 , 17]. Methods based on refined yield-line analysis have also been suggested and are widely accepted and employed by design procedures for end-plate connections [13]. Shi et al. performed several experiments and developed a new analytical model based on component-based method to evaluate the moment–rotation relationship for stiffened and extended steel beam–column end-plate connections [18]. The FE models and softwares have also gained more popularity over time and played a major role in determining the behaviour of different connections and producing their moment-rotation curves [19 - 29].

Many researchers have investigated the connections between I-beams and rectangular hollow sections. These studies are ranging from methods of stiffening the face of the column (such as welded plates around or through the column or flow drill) to the use of end-plate connections with different types of bolts, and new connections such as through plates or through bolts connections [30 - 46]. Reverse channel connection is also another type of connection between I- beams and hollow or concrete-filled columns in which the flanges of the channel section are shop-welded to the column while an end-plate is welded to the beam, and the beam-end-plate assembly is bolted to the reverse channel. A limited number of research studies, such as those conducted by Wang and Xue [47], Heistermann et al.[48], and Al-Hendi and Celikag[49 , 50] , have studied the fundamental behaviour of reverse channel connection using experimental tests, FE analysis, and analytical investigations.

ConXL is another connection which was proposed in 2005 [51]. The purpose of this connection has been to omit on-site welding, which increases weld quality and introduces more industrialisation to construction projects. This connection is a pre-qualified connection in AISC 358 [14] for a specific size of I-beams and rectangular hollow section columns. Rezaeian et al. [52] numerically investigated eleven types of ConXL connections, including reduced beam section (RBS) and normal beams with hollow columns. Recently, Yang et al.[53] developed a non-linear FE model in ABAQUS[29] to investigate the seismic behaviour of this connection.

This research work reports a comparative study on the innovative modular connection (M-HFC) between a typical I-beam and the HFC recently developed by the authors [11]. Three-dimensional FE models are developed to compare the behaviour of M-HFC connections with non-modular welded (called as W-HFC) type of this connection using ABAQUS[29]. Moreover, the mechanical performance of both M-HFC and W-HFC connections are compared with four conventional connections currently available in the construction industry, including flush and extended end-plate connections, reverse channel connections, and ConXL connections. The choice of these conventional connections was made based on their prevalence and the mechanism of transferring load from the beam to the HFC. In order to make the connection more economically feasible, the connection is subjected to an optimisation task to reduce its weight. This topology optimisation is performed in ANSYS [28] and subsequently the optimised connection performance is investigated in ABAQUS [29]. It is shown that the optimisation task resulted in 26% reduction in the connection weight. Despite of this noticeable reduction in the weight it is shown that the connection retains at least 82% of its moment capacity and full ductility.

In the following sections, first, the W-HFC connection is introduced in detail and its performance is investigated. Afterwards, the performance of aforementioned conventional connections is studied and compared to those of M-HFC and W-HFC connections. Finally, after proving the superior performance of the innovative connections, the topology optimisation is performed on M-HFC connection.

3.2 Numerical Modelling

The geometry of a typical hollow HFC that is of interest in this research work is presented in Fig. 3-3(a). The corner tubes can be of different grades of steel, but in this study, mild steel (MS) (Grade 250) and ultra-high strength (UHS) steel (Grade 1200) were chosen. The flat plates connecting the tubes were made of Grade 250 mild steel. The length of the column and beam was assumed to be 1m. Considering the column length and cross-section dimensions, the location of the connection is far enough from both ends to avoid any end effects on the behaviour of the connection. The beam is a 360UB56.7 standard universal I-beam [54]. The dimensions of the column and its cross-section can be found in Fig. 3-3 and Table 3-1.

The numerical study on the connections under static loading was conducted in ABAQUS[29]. According to the literature [54], models with three-dimensional (3D) geometry give reasonable accuracy of the connection and the behaviour of its different parts. Therefore, all connections investigated in this research work were modelled using 3D model. Both material and geometric non-linearities were taken into account in order to capture the actual performance of the connections.

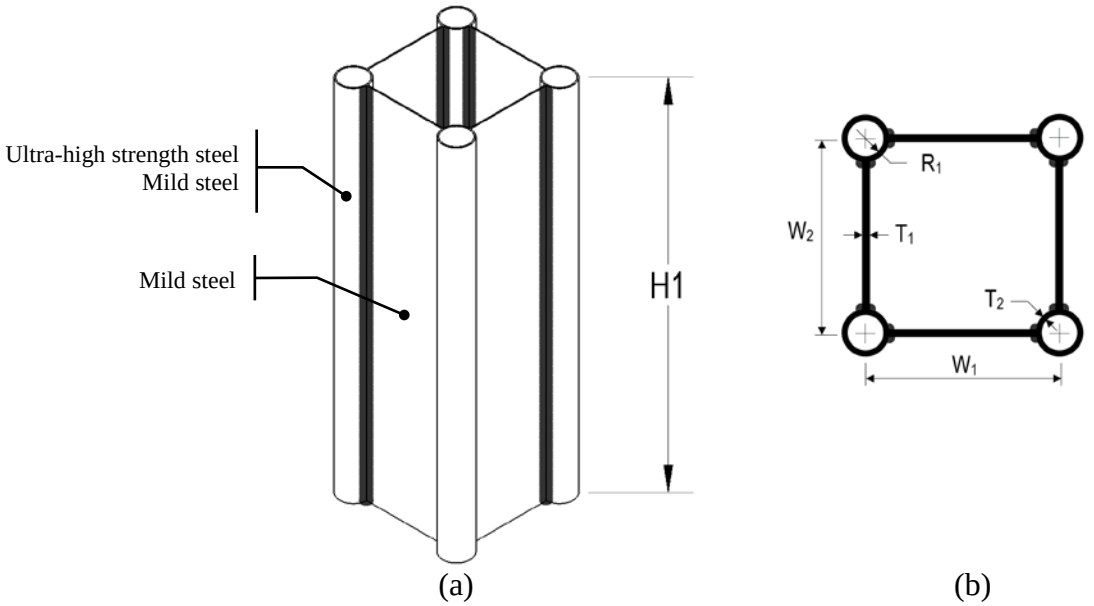

Fig. 3-3. (a) Hybrid fabricated column and (b) Column cross-section

Table 3-1. Dimensions of the hybrid fabricated column cross-section

Symbol	Value mm	Symbol	Value mm
W_1	286	T_1	3
W_2	286	T_2	3.2
H1	1000	R_1	34.85

3.2.1 Material properties

The material behaviour of the MS plates, MS and UHS steel tubes, connection parts (except for fasteners), and the I-beam were modelled considering both elastic and inelastic deformations of these components. In order to take into account the material non-linearity, the ductile damage behaviour of the materials was taken into consideration. The properties of the MS and UHS steel materials are based on the previous experimental data published by Javidan et al.[4].The material behaviour of fasteners (bolts and nuts) was modelled using the multi-linear material behaviour reported for Grade 8.8 bolts [50].

3.2.2 Element and meshing

The C3D8R element, which is an eight-node brick element with reduced integration and hourglass effect control, was used to mesh the different parts of the model. This element, in combination with appropriate meshing, can provide good results within a reasonable computational time, especially for the simulation of large deformation problems, contact, plasticity, and failure [29]. Meshing was done based on the criticality of each zone. For example, contact zones such as the area around bolts and nuts were meshed with a fine mesh to ensure the elements' density and size were suitable to capture the interaction between two adjacent surfaces. This was one of the strategies used to control the mesh size and avoid having fine meshes in unnecessary areas. The other strategy was to use tie constraint between neighbouring parts with different mesh densities. A sample of the different sections created in the different parts of the connection to control the mesh size in critical areas can be found in Fig. 3-4. Based on previous research [50], the thin components such as end-plates, column tubes and column faces have at least three elements through the thickness. Fig. 3-5 shows samples of meshing on connection components. It is worth noting that although Fig. 3-4 and Fig. 3-5 depict the components of a typical extended end-plate

connection, the aforementioned element type and size were used for all connections in this research work.

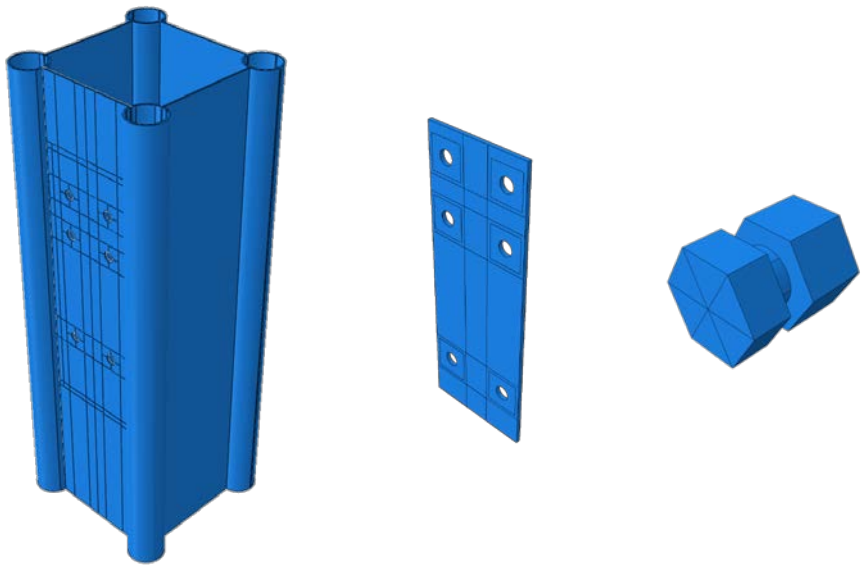

(a) (b) (c)

Fig. 3-4. Samples of the sections created (a) HFC (b) Extended end-plate (c) Fastener

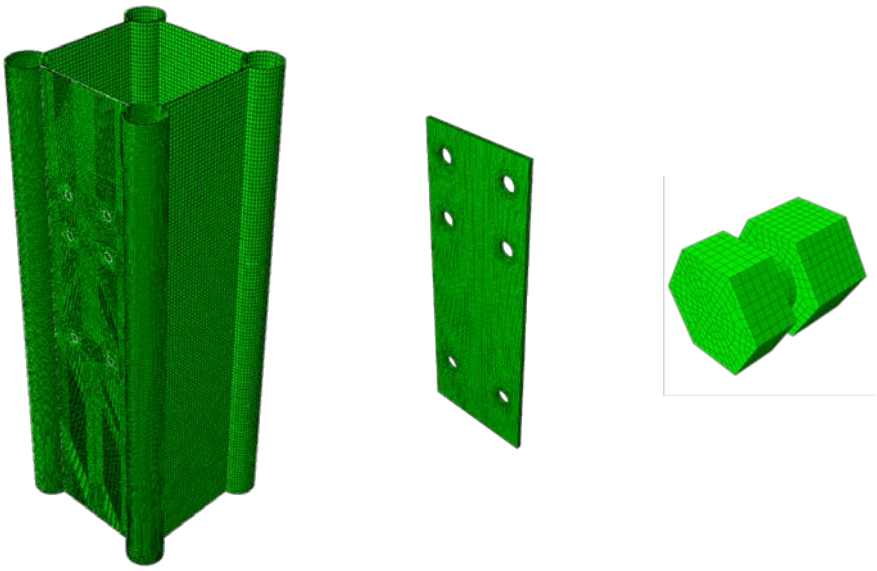

(a) (b) (c)

Fig. 3-5. Samples of the meshing on (a) HFC (b) Extended end-plate (c) Fastener

1.1. Constraints and interactions

Modelling the contact between different components is of crucial importance. In this study, different parts of the connection were assembled in their correct position in ABAQUS [29] and the essential contacts between the adjacent areas were then made. It is necessary to pay particular attention when choosing the master and slave surfaces, since these can affect the numerical stability. It is also recommended that areas in contact should have similar meshing geometry, while the slave surface must have a higher mesh density than that of the master surface. The beam is attached to the connection using tie constraint, which best defines the welded condition that the beam and the connection have in reality and allows a sudden change in the mesh size in their interface. The same approach was used in attaching corner tubes to the column plates of HFC that are also welded together in reality.

The interactions between the fasteners, the connection parts, and the column were defined as contact interaction. This interaction is of the surface-to-surface type with the finite sliding formulation. This means that the parts in contact can have relative arbitrary displacement. The tangential behaviour was modelled using Coulomb friction where the behaviour in the normal direction is hard contact, which allows for separation of the parts after contact. Interactions were defined in a separate step from the loading to ensure the contacts were in action well in advance. Bolts and nuts were modelled as a single united part. This reduces the number of interaction definitions in the simulation, which leads to less computational time, while the accuracy of the simulation is not affected significantly.

3.2.3 Boundary conditions and loading

The bottom end of the column was fully constrained, while the top end could slide only in the axial direction. A constant axial compressive force of 50kN was applied on the column's top surface. This load simulates a level of gravity load well below the compressive capacity of the column. Note that the capacity of a 1m HFC consisting of MS plates and UHS steel tubes is about 1523kN[6]. Since the axial load on column can affect the behaviour of the connection by changing its rotation capacity [56], ductility [57] or initial stiffness [54 , 58] and makes it impossible to study the true contribution of connection components , the applied level of axial load is kept well below the predicted

maximum level of gravity load in high-rise buildings (%15 of the column capacity [56]). Bolts were preloaded using the bolt load definition in ABAQUS[29] by applying a displacement proportional to the bolt pitch dimension. Loading was in the form of a downward displacement applied at the free end of the beam. The model configuration for a typical flush end-plate connection is presented in Fig. 3-6.

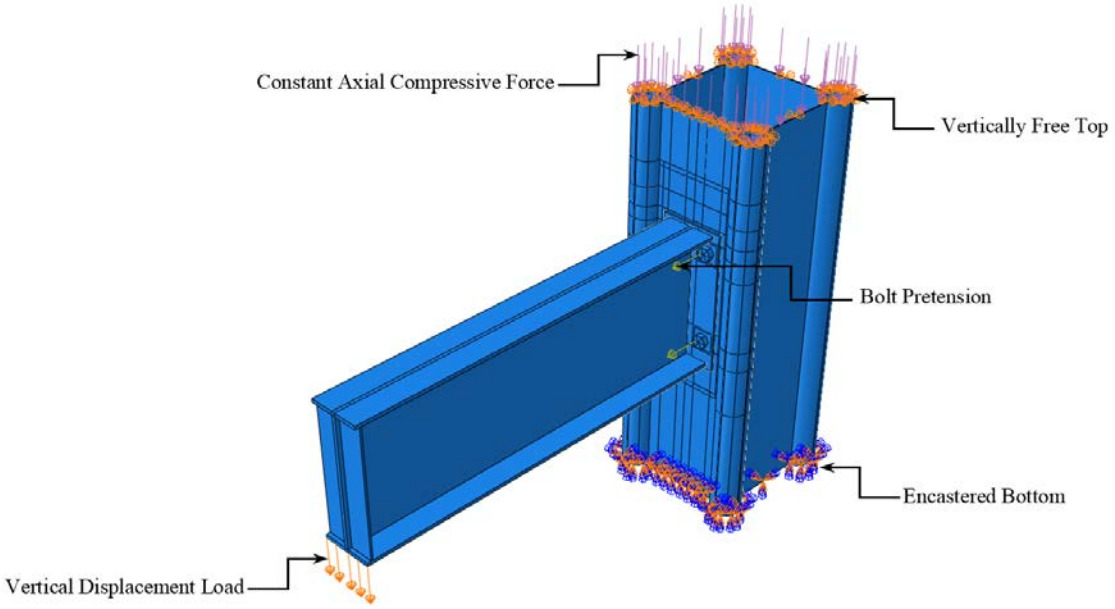

Fig. 3-6. Loading and boundary conditions of a typical flush end-plate connection

The rotation of a connection in reality is composed of elastic and plastic parts, which happen in different components of a connection at different stages of the loading. However, for the purpose of this study since the rotation angle is relatively small, the angle shown in Fig. 3-7 (as an example for W-HFC connection) is opted which represents the overall rotation of the connection and has been used in reference codes and standards [59].

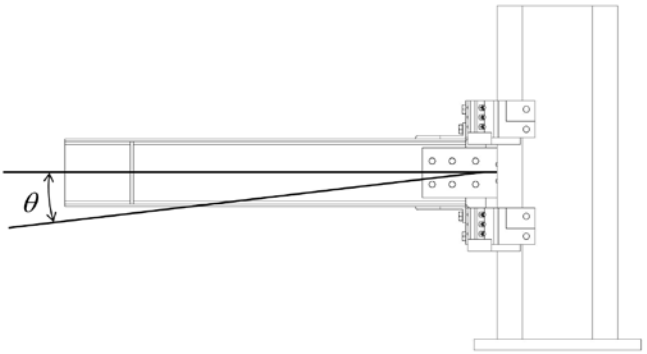

Fig. 3-7. Rotation of the W-HFC connection

This rotation angle can effectively be used for comparison between different connections. In order to measure the rotation of connection the definition presented in Eq. 3.1 is used.

$$\theta = \tan^{-1}\left(\frac{\Delta}{d}\right) \qquad \text{Eq. 3.1}$$

where Δ is the vertical displacement at measurement point and d is the distance from the measurement point to the connection face. In this research work, the point where the load is applied (200 mm from the I-beam tip) is chosen as the measurement point.

3.3 W-HFC connection

Fig. 3-8 shows a representation of the proposed W-HFC connection. As the figure shows, compared to the M-HFC connection (see Fig. 3-2), parts 6-1 and 6-2 and the middle bolts on parts 1 and 2 of the M-HFC connection have been removed and replaced by welds. It means that the resulting connection is no longer a kind of modular connection. Thus, the comparison between the proposed connection and conventional connections will mainly be based on the performance characteristics. Fig. 3-9 depicts each part of the welded connection.

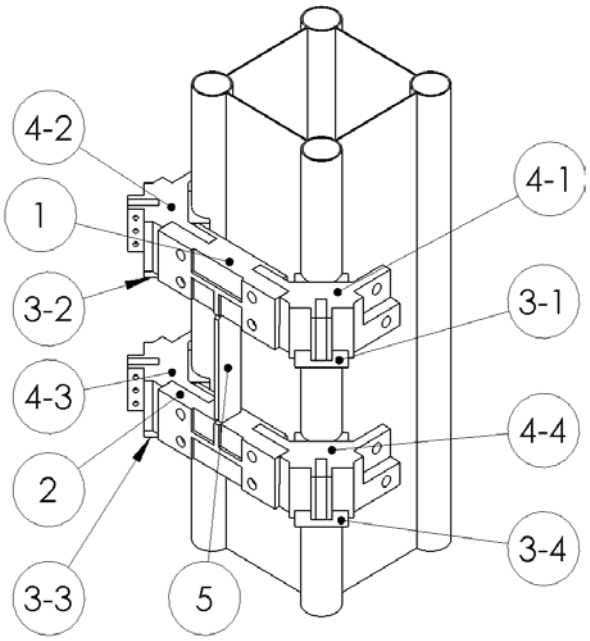

Fig. 3-8. Proposed W-HFC connection for I-beam to HFC connection

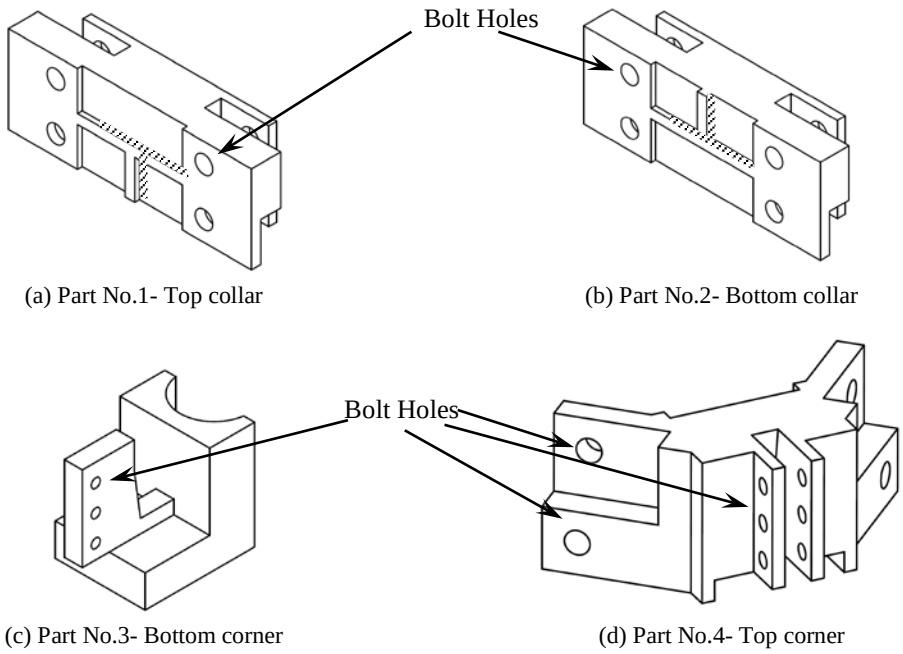

(a) Part No.1- Top collar (b) Part No.2- Bottom collar

(c) Part No.3- Bottom corner (d) Part No.4- Top corner

Fig. 3-9. Different parts of the W-HFC connection

3.3.1 Connection parts

As shown in Fig. 3-8, the W-HFC connection has eleven components. The assembly of parts 1,3-1,3-2,4-1,4-2 at the top and parts 2,3-3,3-4,4-3,4-4 at the bottom forms two solid segments separated from each other by a distance based on the size of the beam that is attached to the column. The points of interaction of this connection with the column are four parts (3-1 to 3-4), which are welded to the column tubes. These parts provide a solid foundation for the top corner parts (4-1 to 4-4). The top corner parts (Fig. 6d) are designed to provide bilateral connection capability. This means that up to four beams can be connected to a single hybrid fabricated column at the same connection, simply by adding a few more components. The top corner and bottom corner parts, for instance parts 3-1 and 4-1, are fixed together using bolts that prevent unwanted movement of the top corner part in case of unexpected or extreme conditions that might push the connection upward.

In both segments, the collar parts (1 and 2) connect two adjacent top corner parts of the connection in each segment and are the components to which the beam is connected. For instance, part 1 fits in the space between parts 4-1 and 4-2 in the top segment. The top and bottom collars are identical, except at the face to which the beam is connected. The beam is welded to these parts. The hatched area in Fig. 3-9(a) and (b) on the front face of the

collars is where the beam flange and a portion of the web are welded. The web extension (Part No.5) is welded at each end between parts 1 and 2. This part interconnects the top and the bottom segments and transfers the shear force between them. The remaining portion of the beam web that is not welded to the top and bottom collars is welded to the web extension. Each collar and its adjoining top corner parts have steps that match each other and form a stable assembly after installation. The collars are secured to the top corner parts using bolts. This guarantees the engagement of the connection parts during its service life.

3.3.2 Numerical modelling of the proposed W-HFC connection

As Fig. 3-10 shows, the finite element model has a pair of L-shaped plates connected to web extensions on one side (the long leg) and to the column faceplate on the other side. The reason is that although the thin faceplates of the column make much less contribution to the load-bearing capacity of the column, especially in the case of the column with UHS corner tubes, they can contribute significantly to the ductility of the connection. These two additional parts help the column faceplates to engage and contribute to the ductile behaviour of the connection.

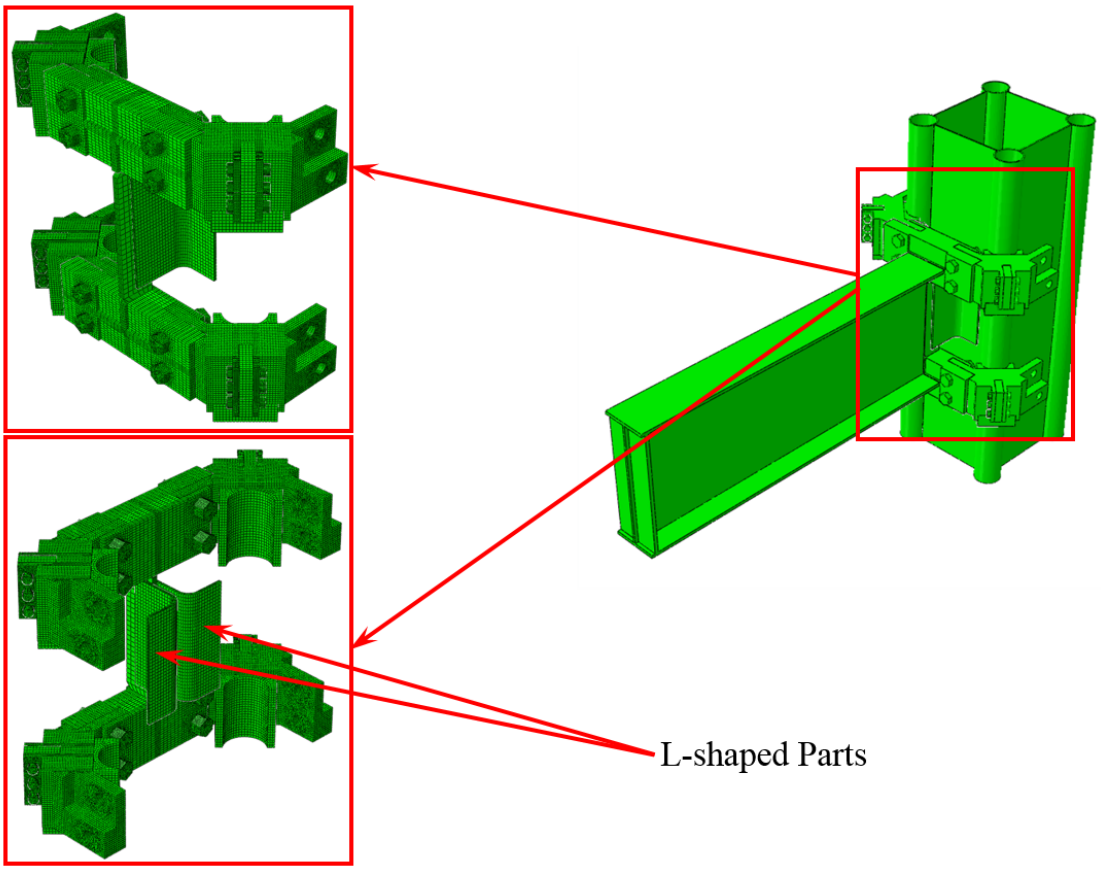

Fig. 3-10. Proposed connection model configuration

The moment-rotation curves for the W-HFC connection between the I-beam and HFCs with UHS and MS corner tubes are depicted in Fig. 3-11.

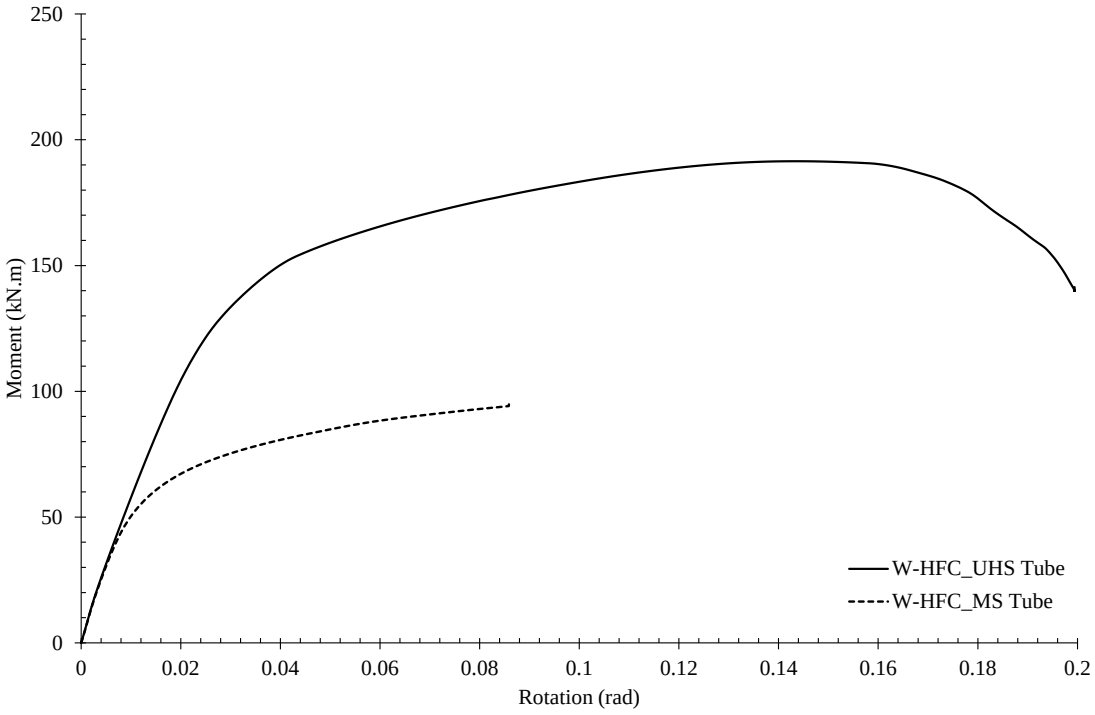

Fig. 3-11. Moment-rotation behaviour of W-HFC connection

The point where the moment-rotation curve of the W-HFC- MS Tube connection is terminated relates to a state of the simulation where the bottom edge of the bottom segment has collided with the column tubes, which could be considered as the endpoint of the connection displacement range. The decreasing part of the moment-rotation curve of the W-HFC-UHS Tube connection displays the connection behaviour after the point at which the bottom flange of the beam buckles and fails at the end of the beam close to the connection. A comparison of the curves in Fig. 3-11 suggests that while the initial stiffness of both W-HFC connections is the same, both ductility and strength improve significantly in the case with corner tubes of UHS material. The von Mises stress distributions on different parts of the column and connection at the final step of each simulation can be found in Fig. 3-12 and Fig. 3-13.

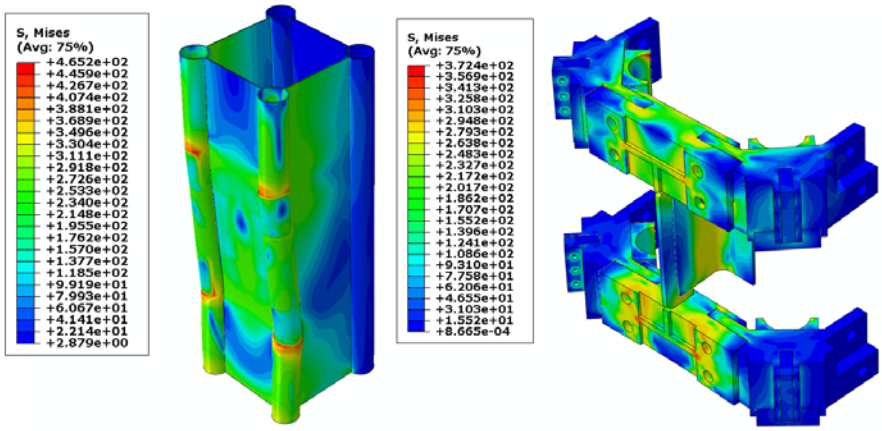

(a) (b)

Fig. 3-12. von Mises stress (MPa) distribution in the (a) column (b) W-HFC connection parts for HFC with mild steel corner tubes

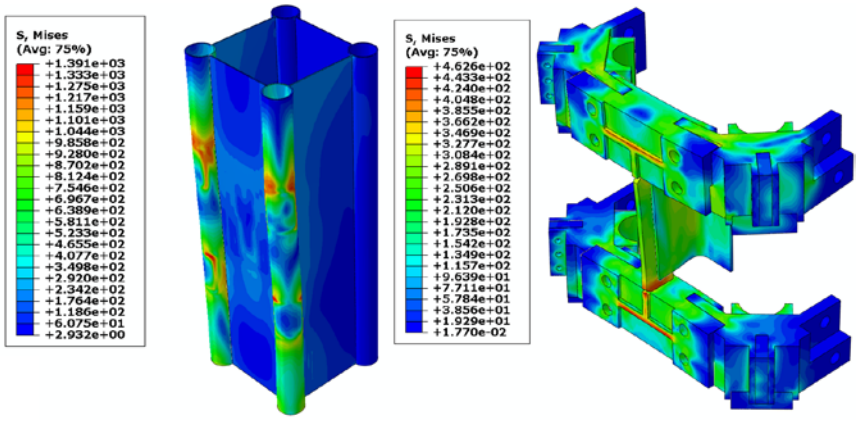

(a) (b)

Fig. 3-13. von Mises stress (MPa) distribution in the (a) column (b) W-HFC connection parts for HFC with ultra-high strength steel tubes

The stress distributions show that the proposed welded connection has the capability of getting the most out of the material properties of the corner tubes, as the levels of stress in both the column and connection are close to the yield stress levels of the constituent material. The two front corner tubes in the case of the HFC with MS corner tubes have crushed, while the UHS steel tube has deformed less and can still bear more load. The stress distribution shows that the steel corner tubes are highly engaged in the load transfer from the beam to the column, since the stress levels in a portion of the tubes are relatively high and around the material's ultimate stress level. The angles that connect the web extension to the column face have also engaged the MS plates and contributed to the ductility of the connection. In the case of the column with MS corner tubes, the mild steel tubes fail much

earlier than the UHS tubes. The significant deformation of the corner tubes leads to the column's partial collapse and results in the termination of the solution. This is due to the collision of the bottom segment and the corner tubes, which renders the continuation of the solution unnecessary. Although the tubes in the column with UHS corner tubes deform under load, they do not crush and provide a strong base for the connection to bear more load. This also allows the connection to engage the L-shaped parts and the column's flat face in order to utilize their ductility. Therefore, in addition to showing a higher load-bearing capacity compared to the column with MS corner tubes, more ductility is observed in the case of the column with UHS corner tubes. It is worth noting that according to the moment-rotation curves depicted in Fig.8, the W-HFC connection falls into the semi-rigid category of connections classified by Eurocode 3 [13].

The FEA model developed by authors and verified by the experimental test results for investigating the behaviour of M-HFC [11] can be used to compare the behaviour of W-HFC with M-HFC. For this comparison, the beam used in the previous simulation of the W-HFC is replaced with 200UB22.3 type beam as used for M-HFC in Ref. [11]. The result of this comparison is presented in Fig. 3-14. The terms R1 and R2 relate to the different variations of the M-HFC experimentally tested by the authors. In R1 case, the beam flanges are bolted to the connection angles (parts 6-1 and 6-2 in Fig. 3-2) but in R2 case, the beam flanges are welded to the aforementioned parts. From Fig. 13 it can be seen that W-HFC has a lower initial stiffness compared to M-HFC connection in all cases. W-HFC connection, similar to M-HFC connection, can be categorised as semi-rigid according to Eurocode 3 [13]. The moment capacity of W-HFC is lower than the M-HFC but it is higher than the capacity of the beam attached (66.5 kN.m). Ductility is also comparable with M-HFC variations and more than the 0.04 rad threshold, generally required by the standards for connections used in moment resisting frames [59].

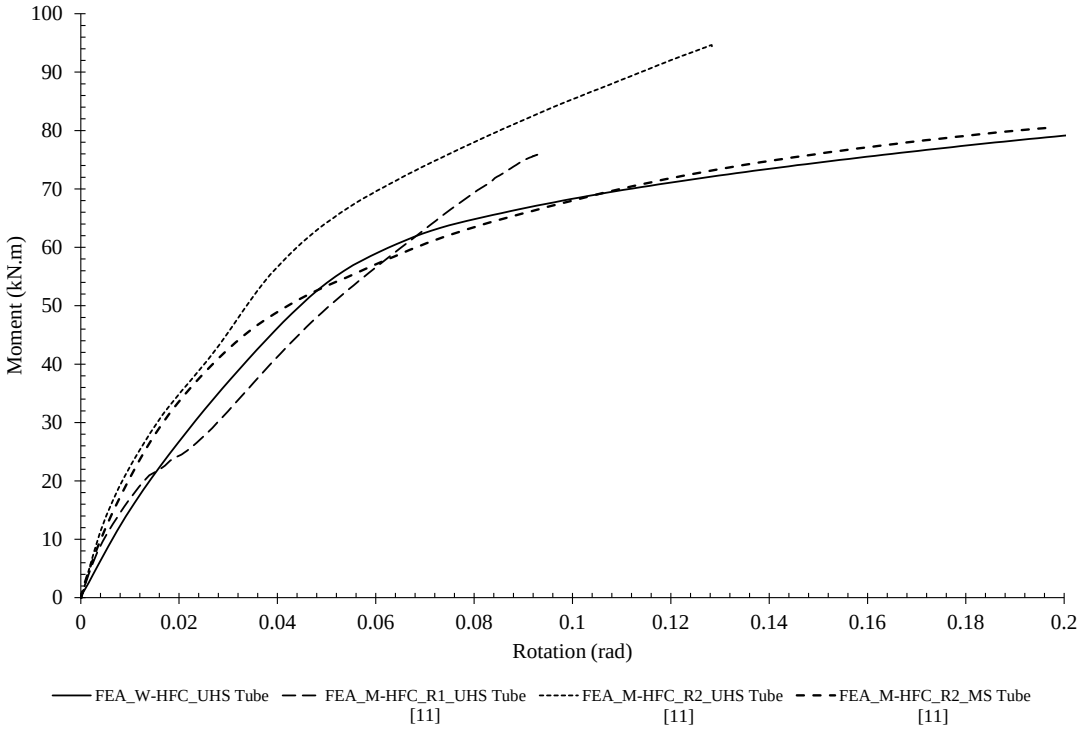

Fig. 3-14. Comparison of moment-rotation behaviour of W-HFC and M-HFC connections

3.4 Conventional connections

In this section, the results of the simulations of four types of conventional connections between an I-beam and the HFC are presented and compared with those obtained for the proposed M-HFC and W-HFC connections. As explained in the previous sections, moment-frame connections should have specific characteristics in terms of capacity and rotation in order to be qualified as suitable connection for moment-resisting structures [14]. Therefore, an understanding of the mechanical performance of the popular conventional connections is essential to investigate the suitability of these connections for use with HFCs. In all cases, the beam and column considered henceforth are the same as those used in the previous sections.

3.4.1 Flush endplate connection

Fig. 3-15 shows a typical view of the flush end-plate. In this connection, an end-plate is welded to one end of the beam and the assembly of the beam-end-plate is bolted to the face of the column. It is assumed that the end-plate has four holes and the bolts are of M20 size. Bolts and nuts are modelled as a single unit. The dimensions of the end-plate are presented in Table 3-2.

Table 3-2. Dimensions of the flush end-plate connection

Symbol	Value mm	Symbol	Value mm
W_3	160	T_3	6
W_5	365	R_2	11

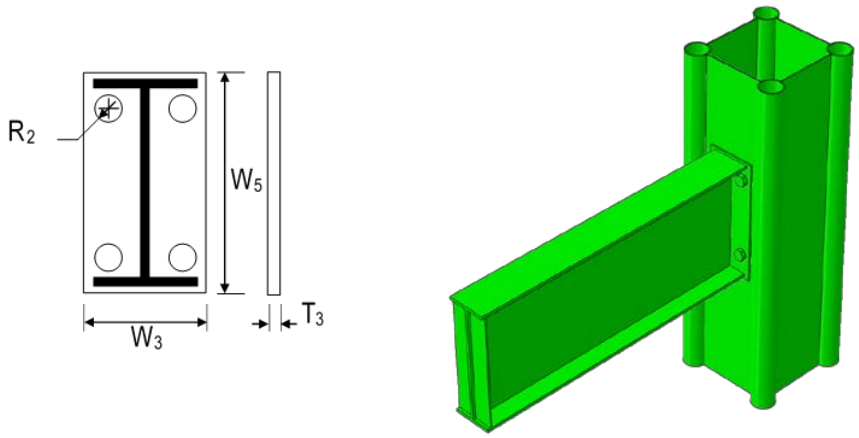

(a) (b)

Fig. 3-15. Flush end-plate (a) parametric dimensions of the end-plate and (b) isometric view

It is assumed that the beam, end-plate and column flat face are made of Grade 250 mild steel while the fasteners are Grade 8.8 bolts. Similar to the W-HFC connection proposed in the previous section, the corner tubes of the HFC are made of either MS (Grade 250) or UHS steel (Grade 1200) to investigate how the material properties of the corner tubes contribute to the connection performance. Fig. 3-16 depicts the moment-rotation curves of the simulations.

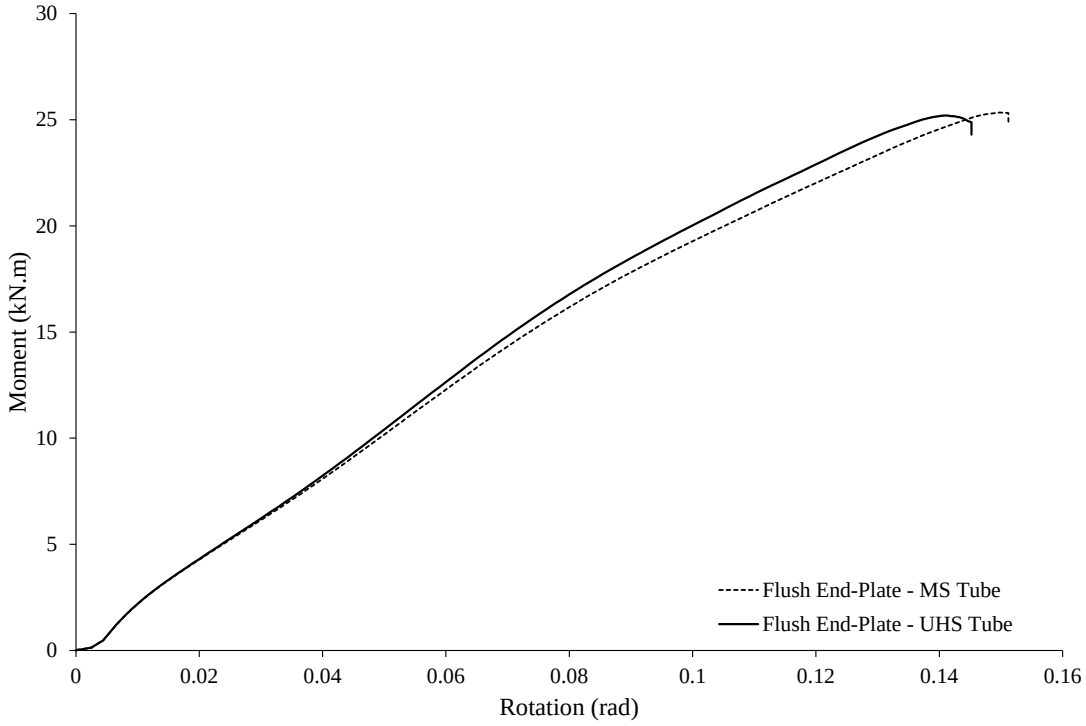

Fig. 3-16. Moment-rotation curves for I-beam to HFC flush end-plate connection

As can be seen in Fig. 3-16, the effect of different materials for corner tubes on the mechanical performance of the flush end-plate connection is not significant, demonstrating the fact that this type of connection cannot effectively benefit from the superior strength of UHS corner tubes. Although the connection shows a reasonable amount of ductility, the load-bearing capacity is not considerable. The end of the simulation is where the damage index and the large deformation of the column face around the bolt holes indicate the bearing failure of the column face. The magnitude of the damage index reported by ABAQUS [29] for the flush end-plate connection in the column with MS corner tubes is 78% around holes. This index for the column with UHS steel corner tubes is 85%. The von Mises stress distributions in the column and the end-plate are presented in Fig. 3-17 and Fig. 3-18, respectively, which show the maximum stress in the corner tubes of the HFC does not exceed the yield stress of their constituent material. It is noted that according to Eurocode3 [13], this connection is classified as a pinned connection.

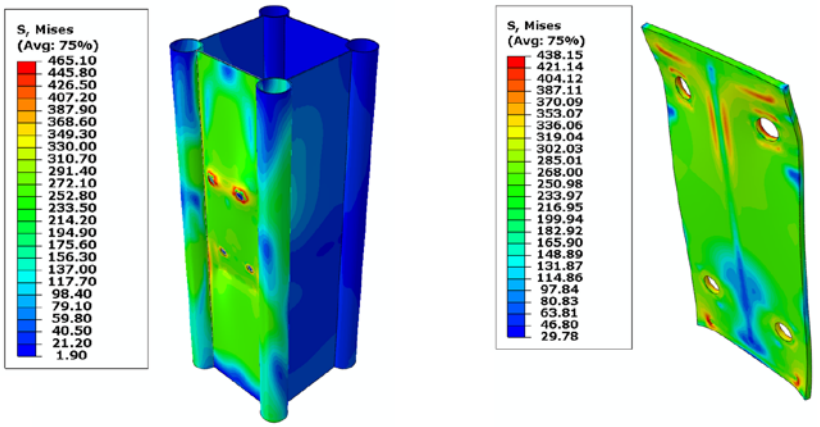

(a) (b)

Fig. 3-17. von Mises stress (MPa) distribution in the (a) HFC with mild-steel corner tubes, and (b) flush end-plate

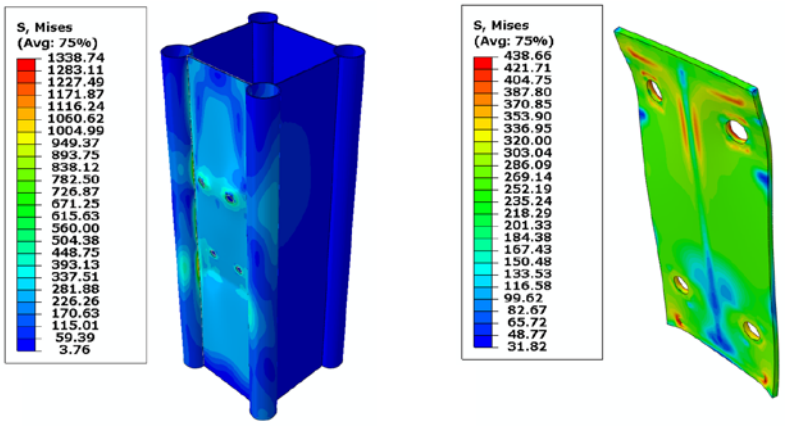

(a) (b)

Fig. 3-18. von Mises stress (MPa) distribution in the (a) HFC with ultra-high strength corner tubes, and (b) flush end-plate

3.4.2 Extended end-plate connection

The isometric view and the dimensions of the extended end-plate connection used in this study are presented in Fig. 3-19 and Table 3-3. This connection is similar to the flush end-plate connection, with the difference being that the end-plate is extended at the top end, making enough room for extra bolts to be placed in this area.

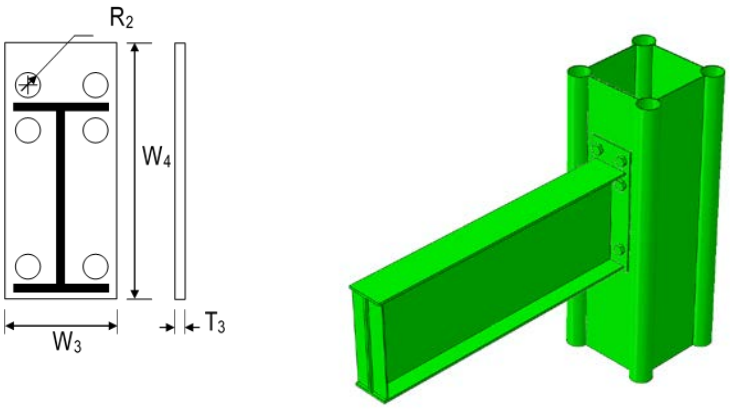

(a) (b)

Fig. 3-19. Extended end-plate (a) parametric dimensions and (b) isometric view

Table 3-3. Dimensions of the extended end-plate connection

Symbol	Value mm	Symbol	Value mm
W_3	160	T_3	6
W_4	435	R_2	11

The material properties of the connection parts, the beam, and the HFC are similar to those used for the flush end-plate connection explained in the previous section. The results of the numerical simulations for two cases with different corner tube materials can be found in Fig. 3-20.

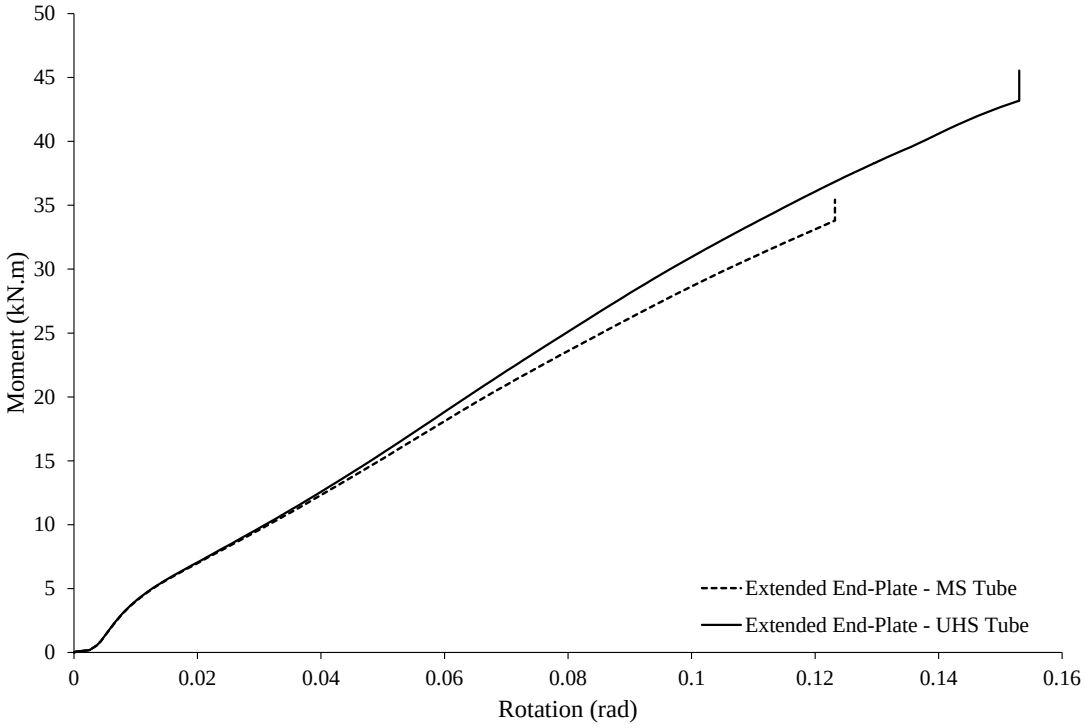

Fig. 3-20. Moment-rotation curves for the I-beam to HFC extended end-plate connection

Fig. 3-20 indicates that the stiffness and moment capacity of the extended end-plate connection are higher than those for the flush end-plate. The effect of corner tube material is more significant, indicating that the corner tubes are slightly more engaged. For instance, at 0.12 rad rotation of the beam, the difference between the moment capacities of the connection with two different column materials is about 10% in favour of the connection with the UHS steel corner tubes. Nevertheless, similar to the flush end-plate connection, the maximum stress developed in the corner tubes does not exceed their yield stress as depicted in Fig. 3-21 and Fig. 3-22. The damage is similar to that of the flush end-plate connection, and is located mostly around the bolt holes and around the weld lines of the column thin faceplate in the area close to the bottom of the end-plate. The values of the damage index for the connection containing HFC with the MS and UHS steel corner tubes are 42% and 59%, respectively. Like the flush end-plate connection, this connection based on Eurocode 3 [13] is classified as a pinned connection.

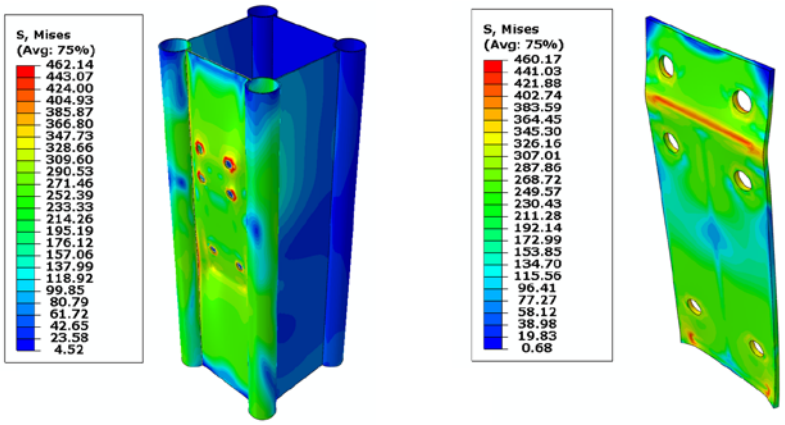

(a) (b)

Fig. 3-21. von Mises stress (MPa) distribution in the (a) HFC with mild-steel corner tubes, and (b) extended end-plate

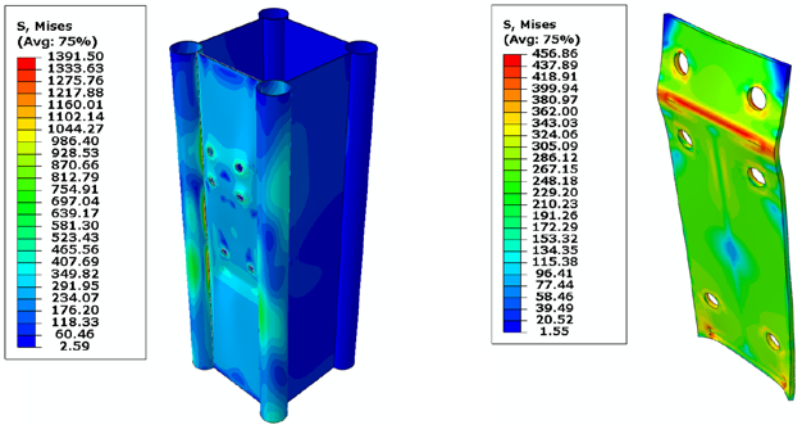

(a) (b)

Fig. 3-22. von Mises stress (MPa) distribution in the (a) HFC with ultra-high strength corner tubes, and (b) extended end-plate

3.4.3 Reverse channel

Since the column faceplate in the hybrid fabricated columns is made of a thin steel plate, according to the numerical results presented in the previous sections, it appears not to be a suitable choice to engage it as the main load-bearing component in the connection between this type of column and an I-beam. An alternate path for transferring the load and minimising the role of the column faceplate in controlling the connection capacity is through the corner tubes. The reverse channel connection is a conventional connection, which is used for connecting I-beams to hollow sections. The shape of the connection and the way it is attached to the column is more promising than the previously-discussed end-

plate connections, for which the load can be transferred from the beam to the column directly through the corner tubes. Fig. 3-23 and Table 3-4 show a schematic view of the reverse channel connection and the dimensions used in the simulations, respectively. As briefly explained in previous sections, in this type of connection, a standard C-section is attached to the column such that the free ends of the section flanges are welded to the column corner tubes. The beam is welded to a flush end-plate and the assembly of the beam and end-plate is then bolted to the C-section. The dimensions of this end-plate are identical to the connection investigated in Section 4.1.

Table 3-4. Dimensions of the reverse channel connection

Symbol	Value mm	Symbol	Value mm
W_6	296	T_4	10
W_7	90	R_3	15
W_8	400		

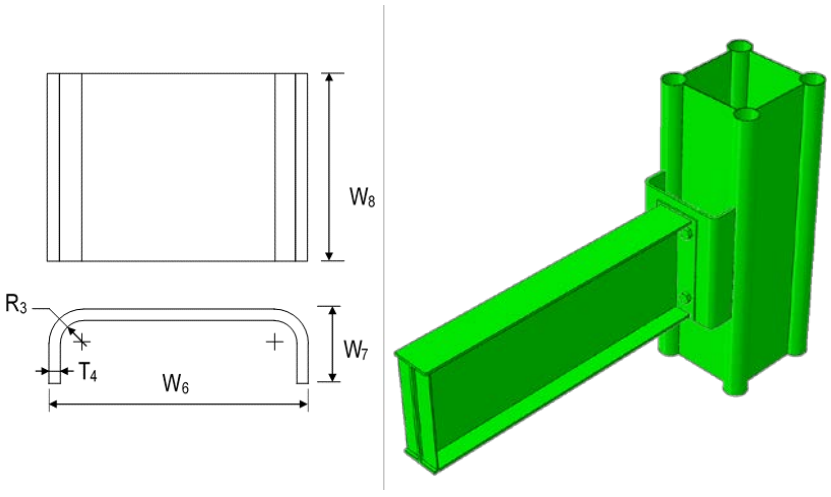

(a) (b)

Fig. 3-23. Reverse channel connection: (a) parametric dimensions and (b) isometric view

The material properties are similar to the connections investigated in the previous sections. The C-section is assumed to be of MS material. Fig. 3-24 shows the moment-rotation curves for the reverse channel connection under static loading.

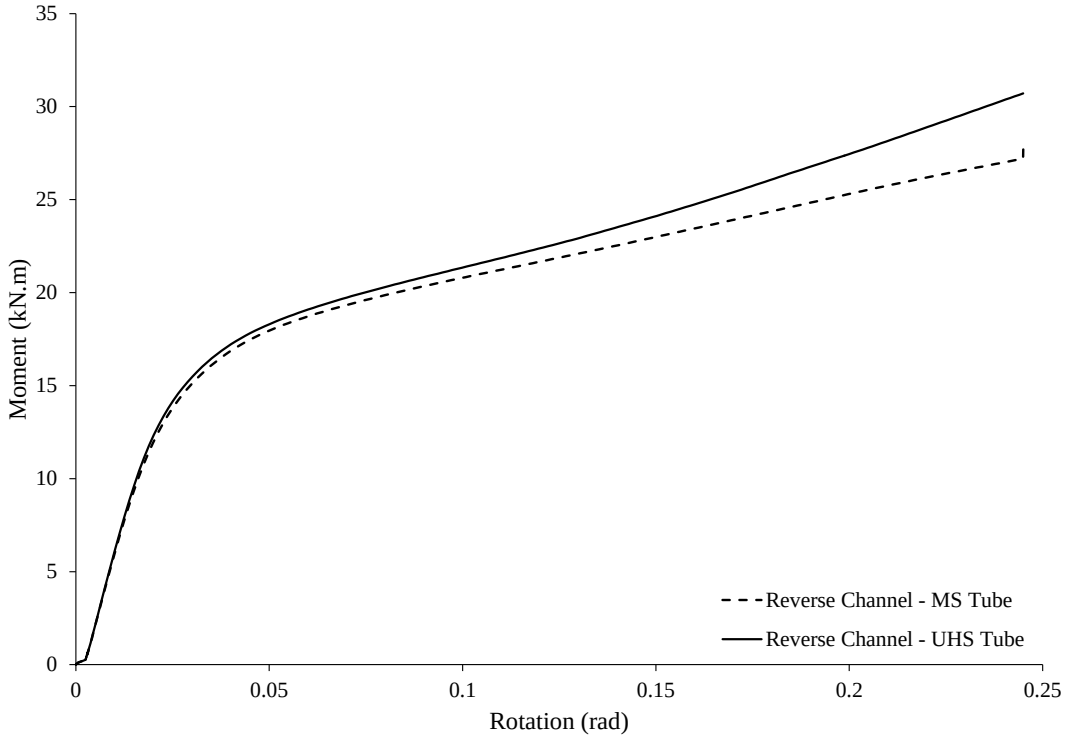

Fig. 3-24. Moment-rotation curves for the I-beam to HFC reverse channel connection

The figure shows that the reverse channel connection has a higher initial stiffness than the flush and extended end-plate connections. This connection shows considerably more ductility, while not having a significant change in the moment-bearing capacity compared to end-plate connections. Fig. 3-25 and Fig. 3-26 show the von Mises stress distribution on different components of this connection.

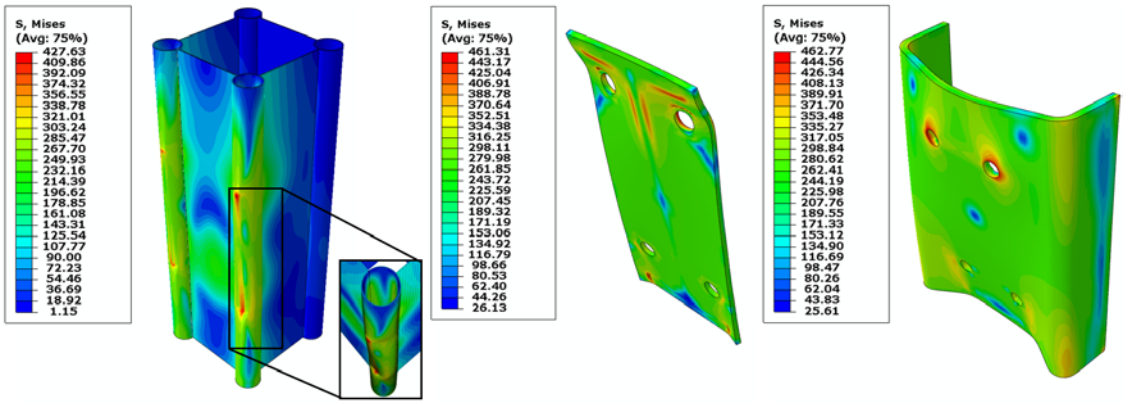

(a) (b) (c)

Fig. 3-25. von Mises stress (MPa) distribution in (a) HFC with mild-steel corner tubes, (b) end-plate, and (c) C-section

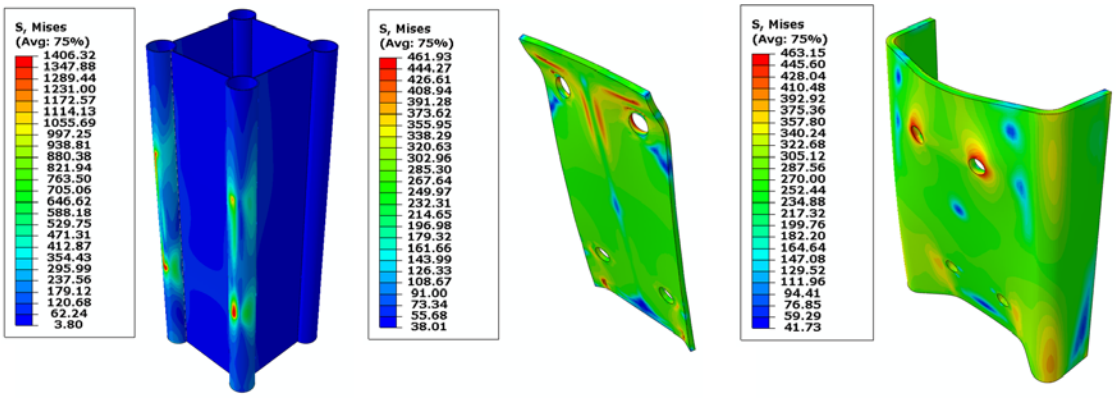

(a) (b) (c)

Fig. 3-26. von Mises stress (MPa) distribution in (a) HFC with ultra-high strength corner tubes, (b) end-plate, and (c) C-section

As depicted in Fig. 3-25 (a), in the HFC with MS corner tubes, the tube has buckled locally under the compressive load applied by the connection, while no such deformation can be observed in the column with UHS steel corner tubes. In terms of maximum utilisation of the superior material properties of the UHS steel corner tubes, this connection performs better than the other two end-plate connections presented in the previous section. A larger portion of the corner tubes undergoes higher levels of stress and this zone of high-stress level is shifted from the interface of the tube and faceplate towards the zone where the C-section is attached to the column. The reverse channel connection investigated here is also classified as a pinned connection [13].

3.4.4 Modified ConXL connection

As explained in Section 1, the ConXL connection was designed to be used for rectangular hollow sections. Since the load transfer mechanism from the I-beam to HFC through a ConXL connection appears to be a favourable method, this connection was chosen for analysis. The dimensions of this connection given in AISC358 [14] are for larger members; accordingly, modification of the connection sizes was necessary. In addition, to attach the connection to the HFC, the geometry of some of the components needed to be changed. Fig. 3-27 depicts the typical views of the standard ConXL connection and also the modified version used for simulations in this study. Note that the views in Fig. 3-27 are not to the same scale.

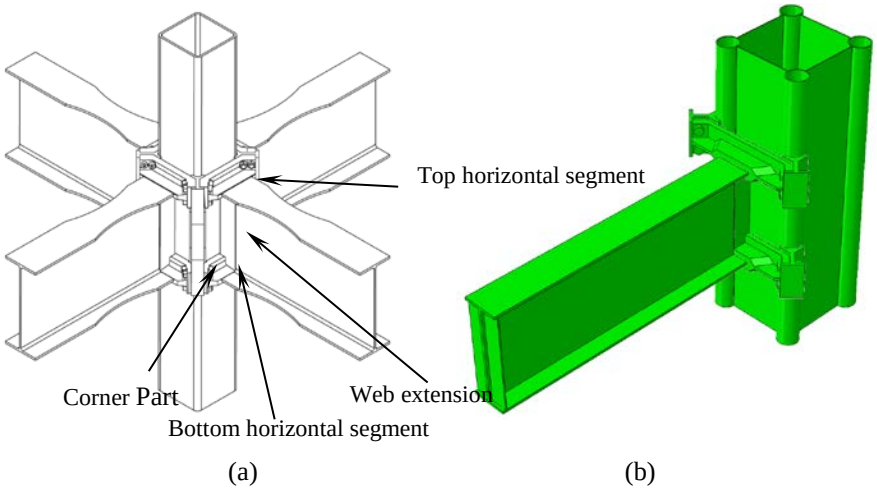

Fig. 3-27. (a) Standard ConXL connection [14] (b) isometric view of the modified ConXL connection used in the present study

In this type of connection, the beam is welded to the horizontal parts at top and bottom, and a web extension is welded between the top and bottom horizontal segments and to the beam web. The resulting assembly is lowered between the corner parts and then secured in place using bolts. In the simulations, the beam and web extension are attached to the top and bottom horizontal members and to each other using tie constraint. The mechanism of load transfer in this connection, similar to the reverse channel connection, is through the corner tubes; hence, it is expected to engage the corner tubes of HFC more significantly compared to the flush and extended end-plate connections. The results of the connection performance under static loading are presented in Fig. 3-28.

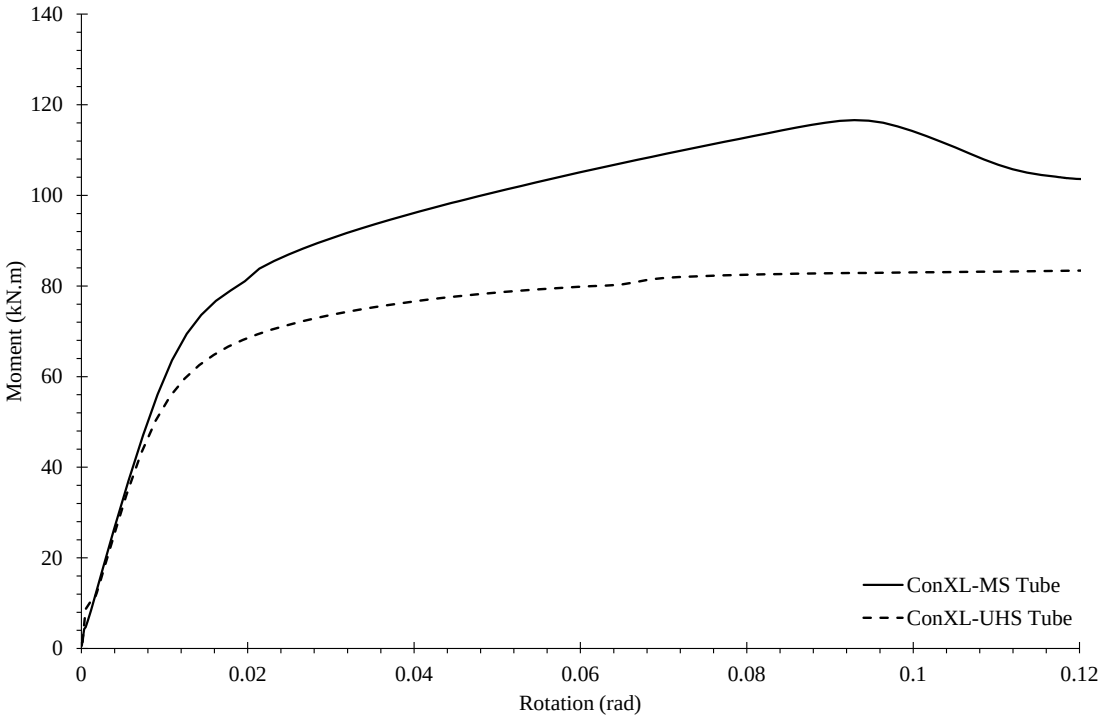

Fig. 3-28. Moment-rotation curves for the I-beam to HFC modified ConXL connection

According to the figure, in addition to showing ductile behaviour, the connection's moment capacity is significantly higher than that of the reverse channel and end-plate connections discussed in previous sections. In addition, the material properties of the corner tubes have a massive increasing effect on the moment capacity of the connection. This supports the idea of utilising the corner tube as the main load path to transfer the load from the beam to the HFC. The end-point of the curves is the point at which the bottom collar of the connection with MS corner tubes hits the corner tubes. The peak in the curve corresponding to the connection of the column with UHS corner tubes is due to the initiation of ductile damage at the top collar of the connection. The von Mises stress distributions on the different parts of the connection are presented in Fig. 3-29 and Fig. 3-30. The damage zone can be seen in Fig. 3-30 (b) as the blue areas on both sides of the thick section in the middle of the top collar.

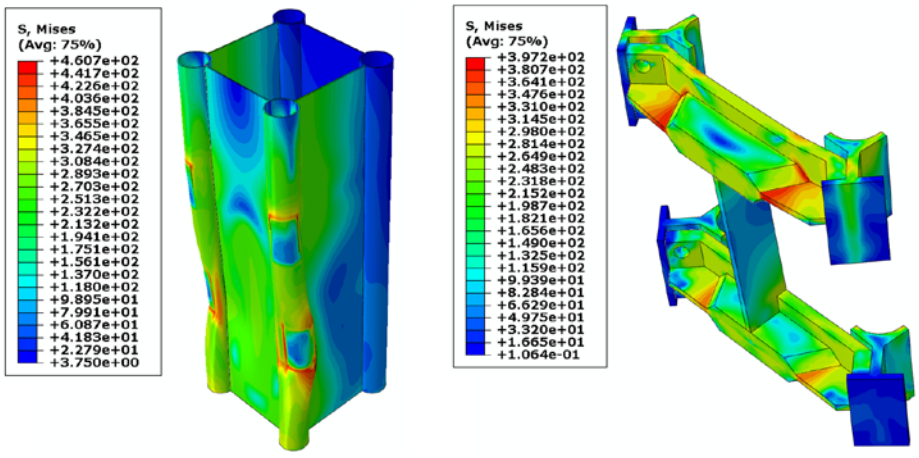

(a) (b)

Fig. 3-29. von Mises stress (MPa) distribution in the (a) HFC with mild-steel corner tubes, and (b) modified ConXL connection

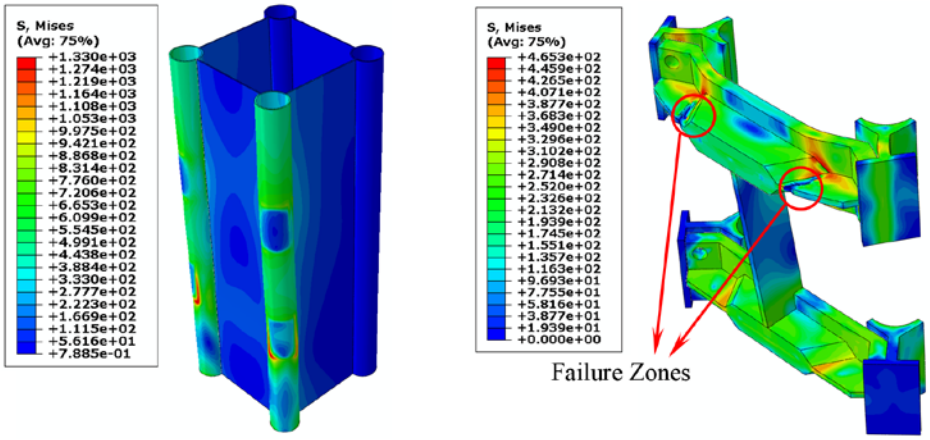

(a) (b)

Fig. 3-30. von Mises stress (MPa) distribution in the (a) HFC with ultra-high strength corner tubes, and (b) modified ConXL connection

The front tubes of the column with MS corner tubes have crushed under load, while the UHS tube is still capable of bearing more load. The stress distribution in columns with UHS corner tubes shows that a larger portion of the tube is under higher stress, which implies that the superior material property of the tubes is more in use. It is noted that this connection based on Eurocode 3 [13] is classified as a semi-rigid connection.

3.5 Comparison of the M-HFC and W-HFC connections with conventional connections

The results of the conventional connection simulations support the idea that a robust connection between HFCs and I-beams is essential in order to transfer the load effectively through to the column tubes while engaging the column faceplate to contribute to connection ductility. The end-plate connections presented in the previous sections are not capable of reaching high moment capacities proportional to the higher capacity of the column. Moreover, they directly engage the thin faceplate of the column, which is another weak point for these connections. From the construction perspective, access to the inside space of the hollow columns is limited. Therefore, end-plate connections are not favourable in construction when HFCs are involved as they cost more to install because of the special tools and parts needed (e.g. blind bolting systems), and require workforce training.

The reverse channel connection shows good characteristics in applications such as design for fire and provides easy access for installation. In the case of connection to the HFC, while showing good ductility, it does not reach high moment capacity. The distribution of the stress on corner tubes does not show promising signs of the capability of the connection to utilise the material properties of the UHS corner tubes.

The modified version of the ConXL appears to have better performance, but the number of changes made to the original design to make it a suitable connection for the HFC is considerable. Furthermore, in the case of the column with UHS corner tubes, the top collar part of the connection deformed significantly and signs of permanent ductile damage appeared in the simulation (Fig. 3-30 (b)). Although the ConXL connection is a pre-qualified connection, it is only applicable for a limited type of beams and only for rectangular columns with conditions described in the AISC 358 standard [14]. The ConXL connection parts are complex in shape and difficult to manufacture. All of these reasons justify moving towards designing a new connection for HFCs.

Table 3-5 shows the initial stiffness, moment capacity, and rotation capacity of W-HFC connection compared to the four different conventional connections analysed in this study. As the table shows, the initial stiffness, and moment and rotation capacities of W-HFC connection are higher than those of other connections are, demonstrating the utilisation of

material properties in the enhancement of the performance of the connection in terms of both load-bearing capacity and ductility.

Table 3-5. Comparison of properties of connections

Connection Type	Initial Stiffness (kN/mm)	Moment Capacity (kN.m)		Rotation Capacity (rad)	
		MS	UHS	MS	UHS
Flush end-plate	0.24	25.33	25.19	0.151	0.145
Extended end-plate	0.53	33.65	43.11	0.123	0.153
Reverse channel	0.78	27.2	30.63	0.244	0.244
Modified ConXL	5.52	83.3	116.61	0.127	0.127
W-HFC	6.44	93.74	191.46	0.084	0.199

3.6 Topology optimisation

The collar parts in the top and bottom segments of the M-HFC connection constitute a large portion of the weight of the connection. Thus, any reduction in the weight or volume of these parts may result in a noticeable drop in the overall weight of the connection. Therefore, this section is dedicated to optimising the M-HFC connection mainly in order to decrease its weight. It is noted that among size, shape and topology optimisation the latter is the highest level in the optimisation efforts hierarchy [60]. The topology optimisation presented in this section was performed using ANSYS [28] which is done through discretising the optimisation domain and maximising the stiffness of the part being optimised or minimising its compliance with a quality distribution function of the structure as the optimisation parameter. Afterwards, ABAQUS [29] was used to investigate the performance of the optimised connection. In the case of this study, the collar top and bottom parts (parts 1 and 2 in Fig. 3-2) are chosen as optimisation domain.

In order to find out the extreme level of the material that could be removed from the parts, apart from the practicality of the solution, optimisation goal in ANSYS [28] was set to be 40% reduction in the weight of the collars. In order to decrease the time needed for the optimisation process, the former loading condition used in the previous sections has been replaced with a tensile load applied on the free edge of the top angle (part 6-1 in Fig. 3-2) and only the top half of the column and connection has been modelled.

The results of optimisation conducted by ANSYS [28] can be found in Fig. 3-31.

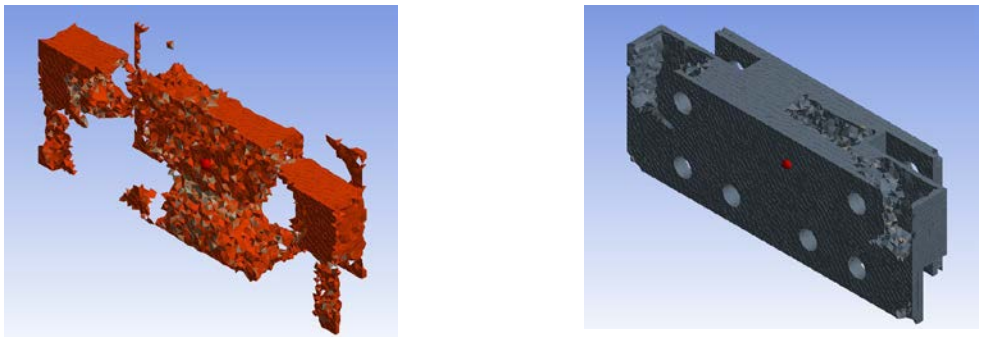

(a) elements that can be removed (b)elements that must remain

Fig. 3-31. ANSYS optimisation results- Non-reduced thickness

As it can be seen in Fig. 3-31 (a), the centre of the part and a portion of the thick flaps located in front of the collars can be removed. The connection was modified based on these results and turned into the part presented in Fig. 3-32 (b). The core of the collar part is modified such that it can be practical for manufacturing, without changing any other dimensions in the connection parts. The weight at this stage is reduced around 6.2%.

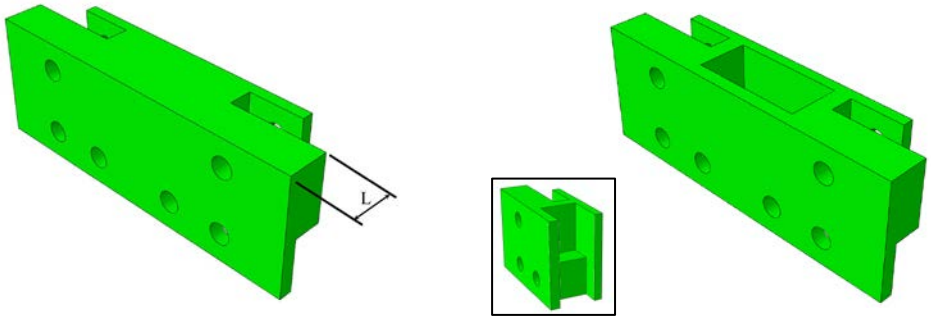

(a) Original part (b) Optimised original part and cutaway view

Fig. 3-32. Optimisation geometries of non-reduced thickness case

Moreover, in addition to the aforementioned optimisation, another variation of M-HFC connection with a smaller thickness of the collar parts was also investigated and the results were compared with those obtained from ANSYS optimisation. Therefore, the thickness of the collar (dimension L in Fig. 3-32 (a)) is 12 mm reduced. The reduced-size collar is optimised again to investigate how the resulting collar will turn out.

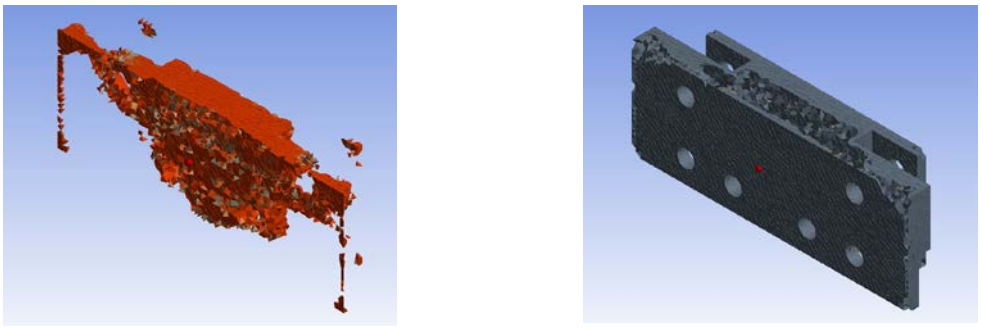

(a) elements that can be removed (b)elements that must remain

Fig. 3-33. ANSYS optimisation results- Reduced thickness

The results of optimisation on the reduced part can be found in Fig. 3-33. The collar with reduced thickness is presented in Fig. 3-34 a. As it can be observed in Fig. 3-33, this time the thickness of the flaps is almost fully contributing in load bearing and its size cannot be reduced. Nevertheless, the centre of the part is still a domain that allows for further material removal. The geometry of the collar part with the hollowed core can be found in Fig. 3-34 (b).

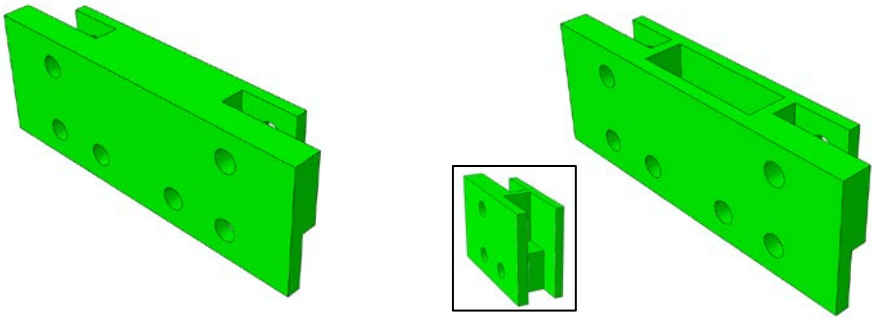

(a) Reduced size part (b) Reduced and optimised part and cutaway view

Fig. 3-34. Optimisation geometries of reduced thickness case

Altering the thickness of the collar requires the dimensions of the other parts to be updated accordingly, which results in further reduction in the weight. The connection with the reduced-size collars (Fig. 3-34 (a)) is 21.7% lighter than the original design and becomes around 26.8% lighter than the original design when it is optimised (Fig. 3-34 (b)).

Once the optimum topology was found in ANSYS [28], the new geometry of M-HFC connection was modelled in ABAQUS [29] with loading and boundary conditions similar to the conditions described in Section 2. The beam attached to these connections is of

200UB22.3 [54] type and is 1.2 m long with the load applied at 0.2 m far from the free end applied in displacement control form. The results of the simulations are presented in Fig. 3-35 and Fig. 3-36 for the connection connected to the HFC with MS and UHS corner tubes, respectively.

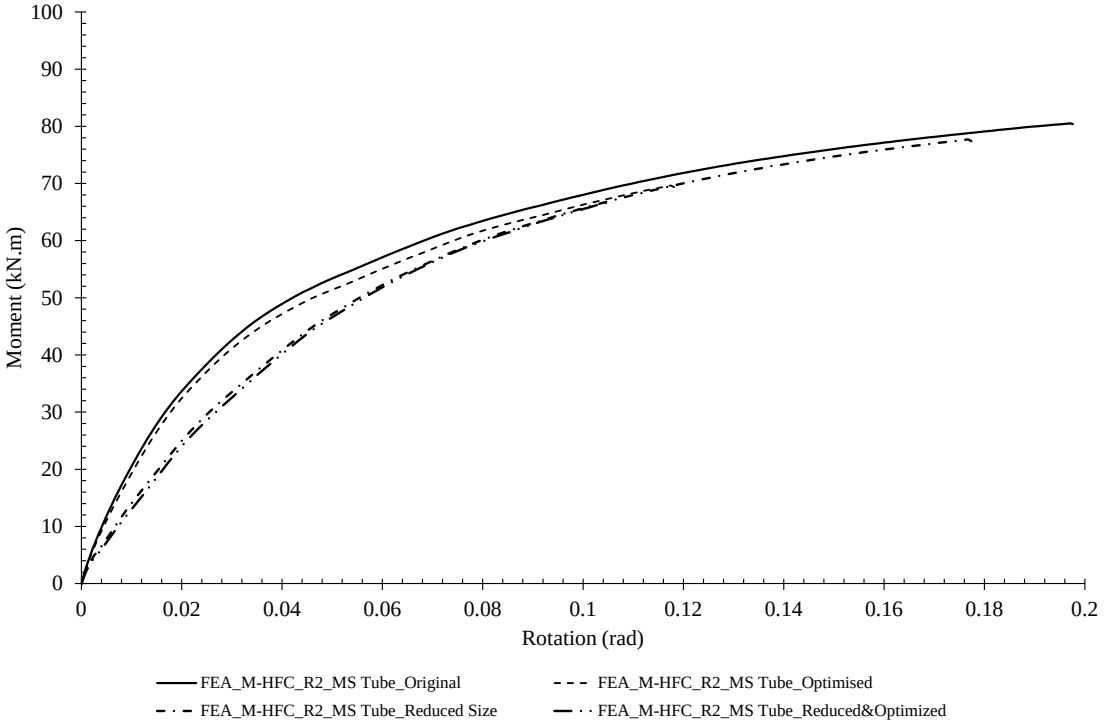

Fig. 3-35. Comparison of performance of different variations of the connection attached to column with MS corner tubes

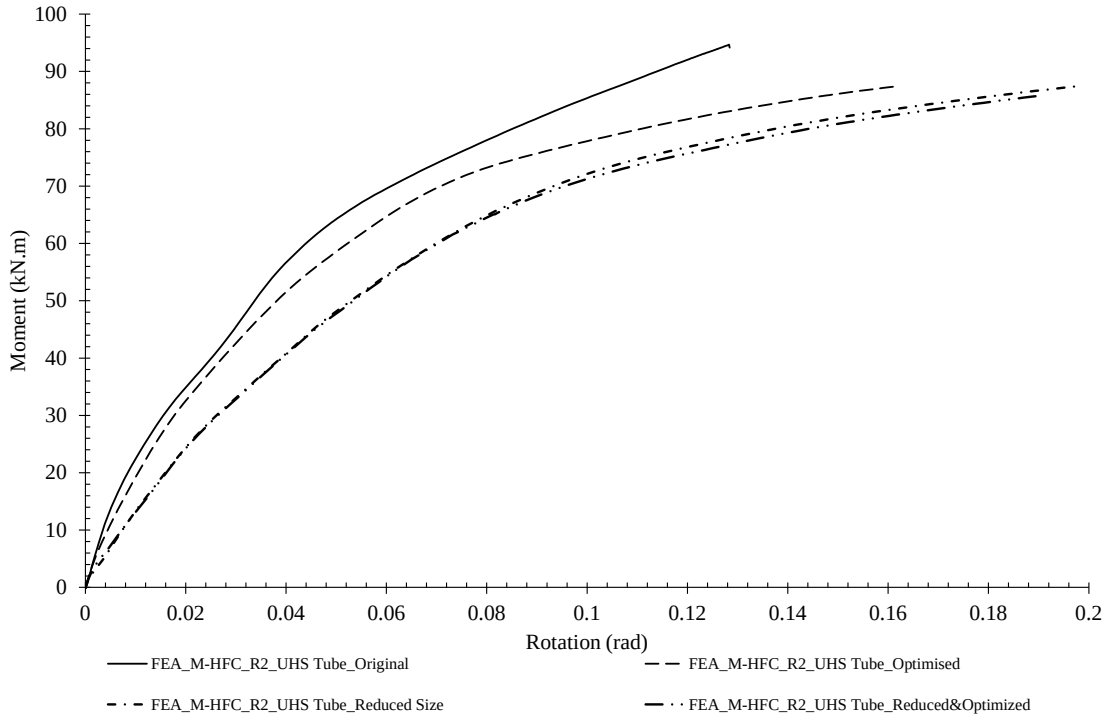

Fig. 3-36. Comparison of performance of different variations of the connection attached to column with UHS corner tubes

It can be observed that in the case of MS corner tubes the moment capacity and initial stiffness of the connection is not significantly affected by changing the thickness or geometry of the collar parts. In the case of UHS corner tubes, the difference in moment capacity is noticeably higher. The optimised connection with reduced thickness attached to the column with UHS corner tubes shows the highest level of difference in the capacity compared to the other variations of the connection. In this case, the moment capacity at 0.12 rad (which is the point of failure in the experiment on M-HFC_R2_UHS Tube connection) rotation has 18% decreased compared to the original connection. However, it is yet greater than the beam plastic moment capacity.

As expected, the stiffness of the optimised connections with the reduced thickness collar segments is less than the original connection. In the connection with reduced thickness collar, the difference between the performance of the connection before and after optimisation is negligible. It demonstrates the fact that the optimisation process has progressed in the right direction and although the final design (Fig. 3-34 (b)) is the lightest of all variations it still can reach a moment capacity, which matches that of the reduced size connection before optimisation.

The failure mode observed in the experiments was fracture in the top angle along with excessive deformation of the bolts attaching this part to the top collar part [11]. In order to investigate whether this failure happens in the optimised connection the von Mises stress distribution on the aforementioned parts is compared with those of the original connection at the first point of failure in the test. Since the model has been verified with the experimental results for the case of original connection [11], the stress levels in that analysis can be regarded as the benchmark for assessing the situation in other cases. Fig. 3-37 and Fig. 3-38 present the stress distribution contours on the bolts. As can be seen in these figures, the maximum stress level in all cases is less than that of the connection with the original size. A similar trend can be observed with the comparison of the stress levels in the top angle (Fig. 3-39 and Fig. Fig. 3-40). Therefore, since the stress levels in the optimised cases are less than the original connection case, it can be concluded that the optimised variations may fail at slightly higher than that of the original connection .

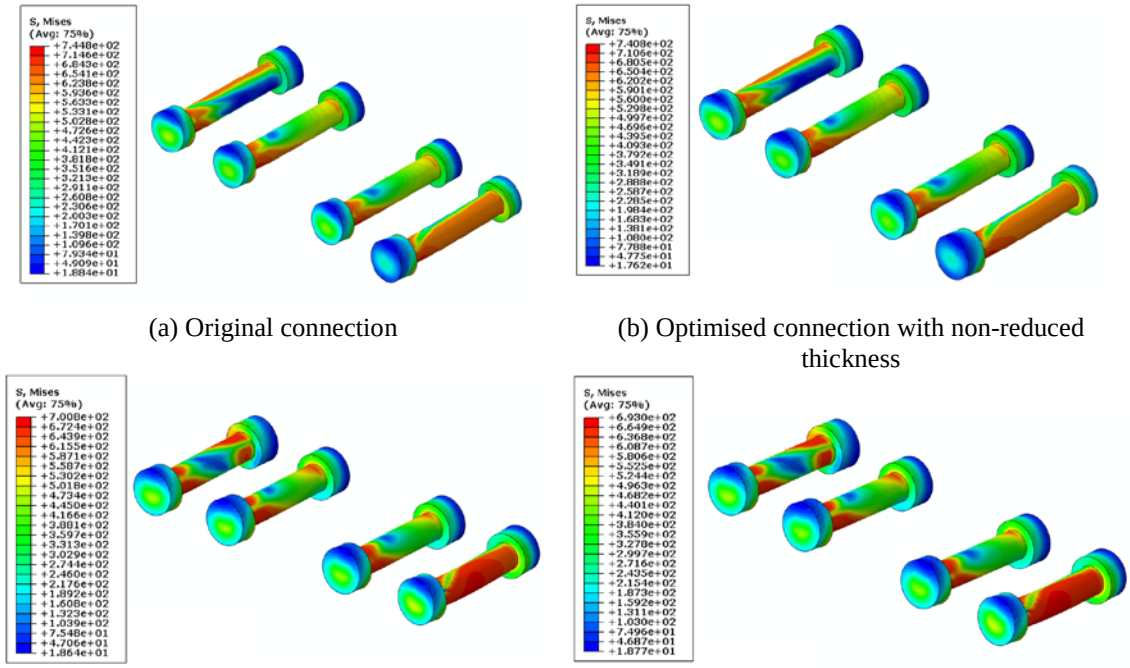

(a) Original connection

(b) Optimised connection with non-reduced thickness

(c) Reduced thickness connection

(d) Optimised connection with reduced thickness

Fig. 3-37. von Mises stress distribution on bolts connecting the top angle to the collar part (column with UHS tube)

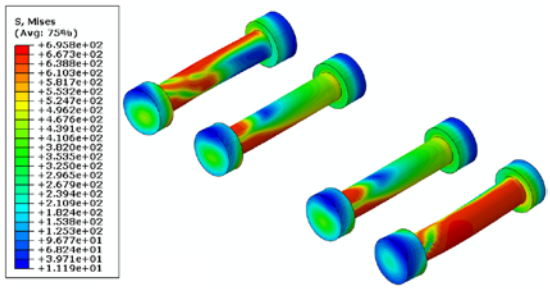

(a) Original connection

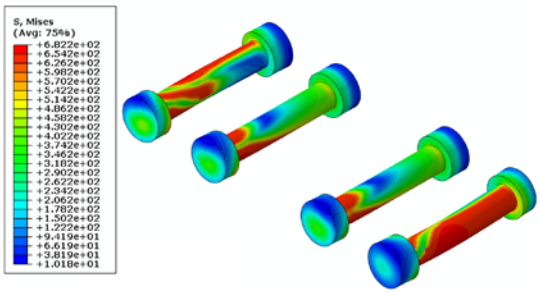

(b) Optimised connection with non-reduced thickness

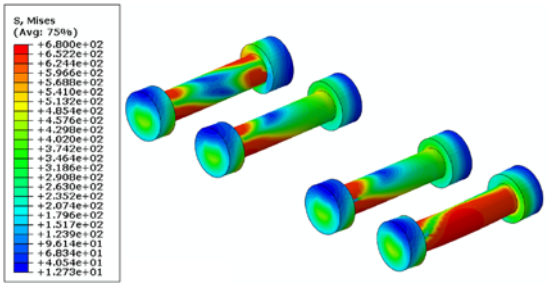

(c) Reduced thickness connection

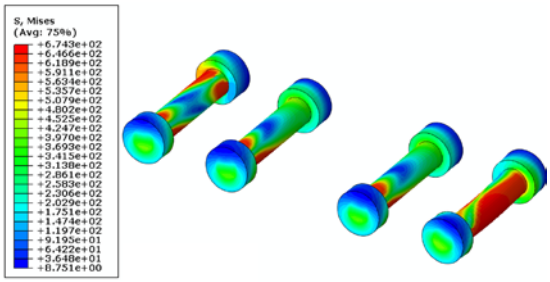

(d) Optimised connection with reduced thickness

Fig. 3-38. von Mises stress distribution on bolts connecting the top angle to the collar part (column with MS tube)

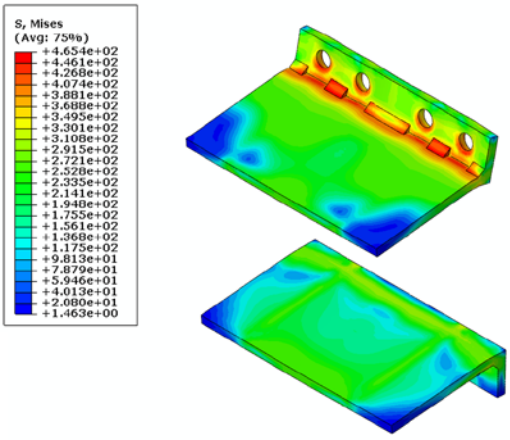

(a) Original connection

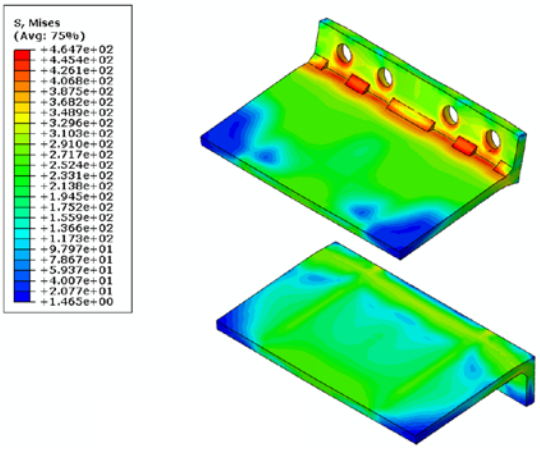

(b) Optimised connection with non-reduced thickness

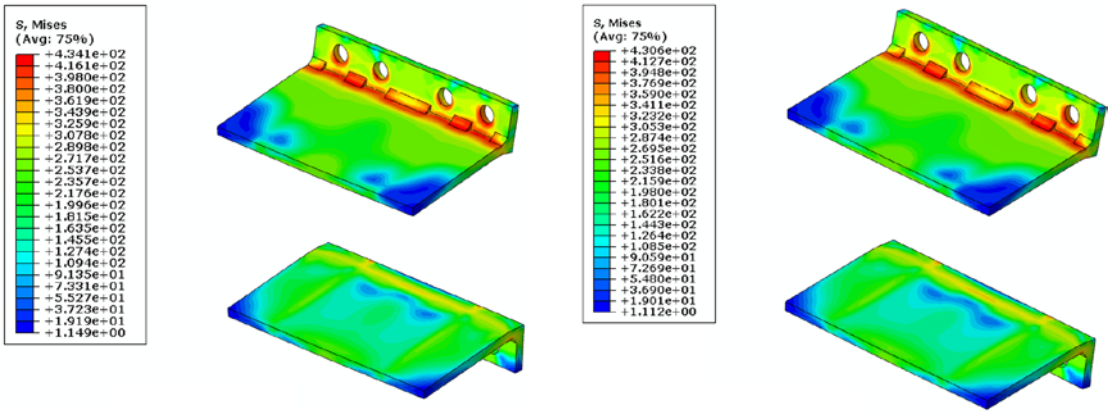

(c) Reduced thickness connection (d) Optimised connection with reduced thickness

Fig. 3-39. von Mises stress distribution on top angle bolted to the collar part (column with UHS tube)

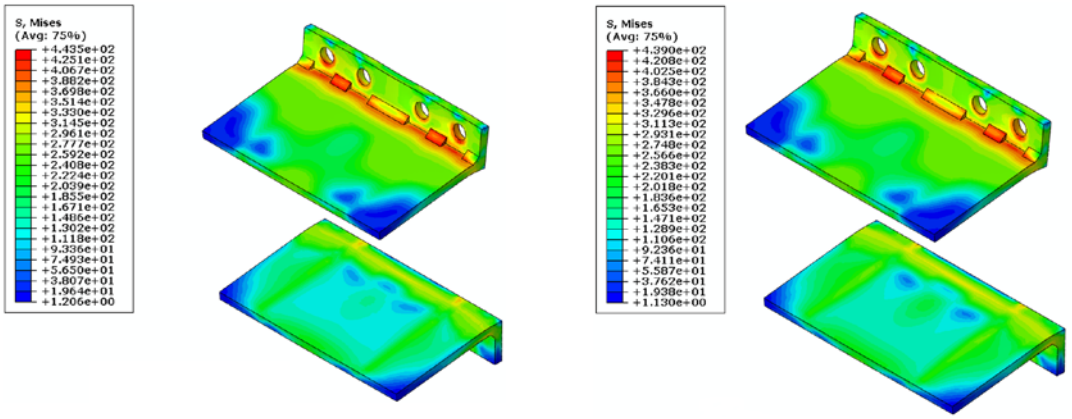

(a) Original connection (b) Optimised connection with non-reduced thickness

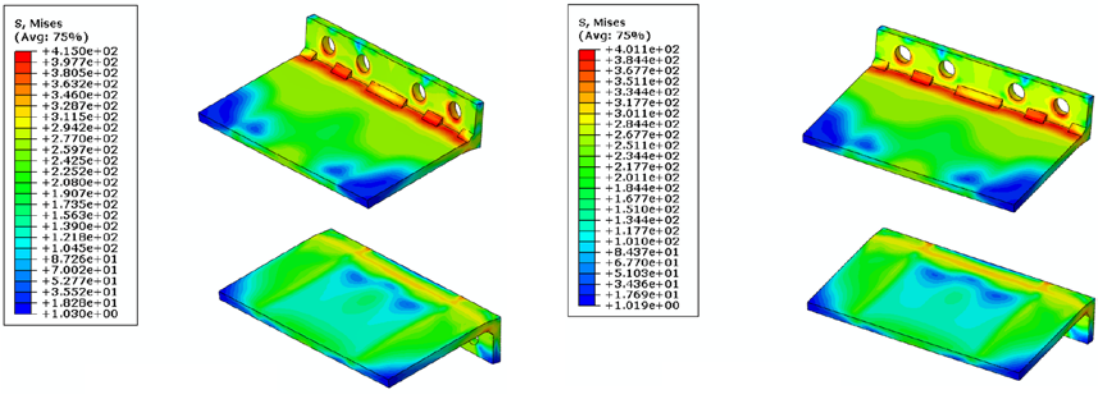

(c) Reduced thickness connection (d) Optimised connection with reduced thickness

Fig. 3-40. von Mises stress distribution on top angle bolted to the collar part (column with MS tube)

One of the characteristics of the original connection was reusability of its components. As reusability depends on the stress level and degree of plastic deformations in the parts, comparing the distribution of equivalent plastic strain (PEEQ) variable on different components, among the aforementioned connections can be used to investigate whether or not the optimised variations of the M-HFC connection are reusable. Note that the original connection components were reusable after experiments [11]. Whereas the collar undergoes larger loads and larger deformations, the reusability of this part is more of interest. Fig. 3-41 and Fig. 3-42 present the distribution of PEEQ variable on the collar parts at the rotation in which the first fracture initiated in the experiments [11] in the connection attached to the column with UHS corner tubes.

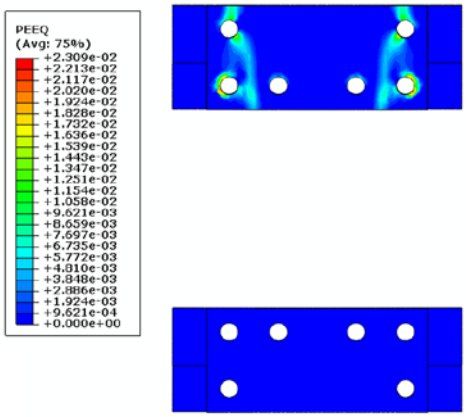

(a) Original connection

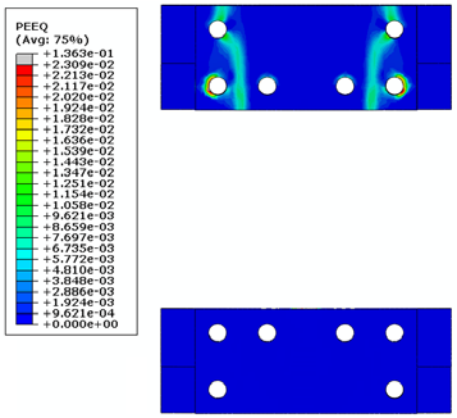

(b) Optimised connection with non-reduced thickness

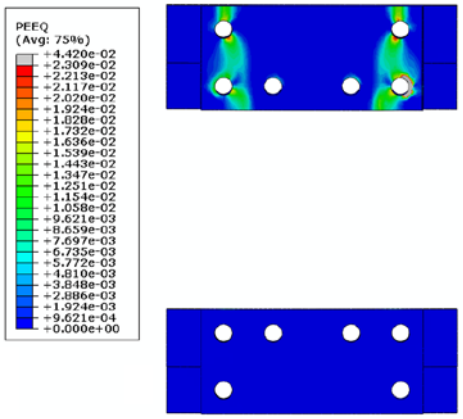

(c) Reduced thickness connection

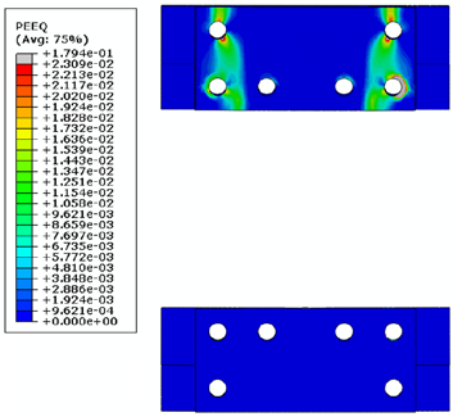

(d) Optimised connection with reduced thickness

Fig. 3-41. PEEQ distribution on top and bottom collar parts (column with UHS tube)

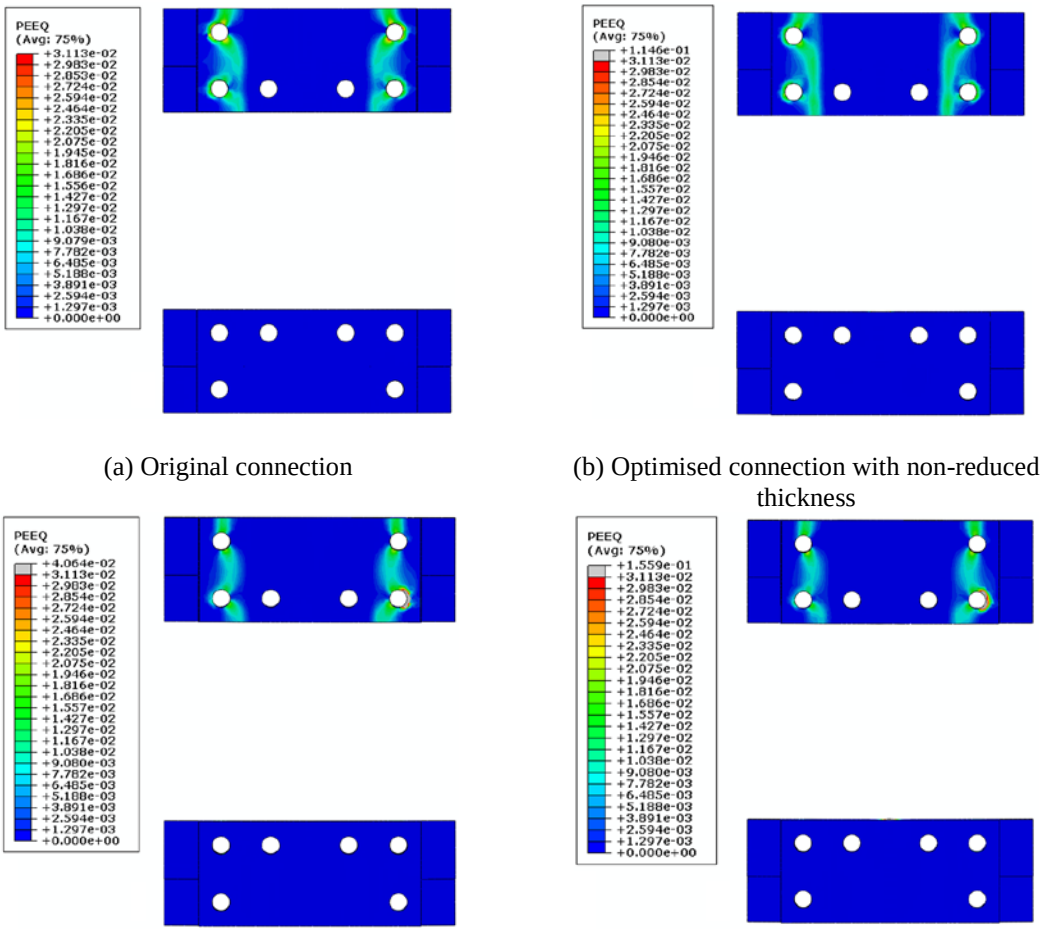

(a) Original connection

(b) Optimised connection with non-reduced thickness

(c) Reduced thickness connection

(d) Optimised connection with reduced thickness

Fig. 3-42. PEEQ distribution on top and bottom collar parts (column with MS tube)

The grey areas in the collars show that the variable magnitude is more than the top limit of the spectrum, which is set to be the maximum PEEQ value in the original connection's collar part. These areas are mostly located around the boltholes, where the bolt after deformation touches the collar. Also in the cases that the collar is optimised and the mid-section of the collar is hollowed, as a result of smaller weld area, the surface that is tied to the extension part undergoes higher levels of strain and consequently shows higher levels of PEEQ variable. These local phenomena can be avoided by using washers (that are not modelled but were used in the experiments conducted on the original M-HFC connection) and slight modifications of the extension part such that it can have more common surface with the collars for better interaction. In spite of these local high strains, the collar parts are within the limits set from the results of the simulation of the original connection and can be regarded as reusable.

3.7 Conclusion

In this research work, a comprehensive numerical study was conducted to compare the performance of recently developed M-HFC connection with the welded type of this connection (W-HFC) and also four types of conventional connections. A detailed three-dimensional FE model was developed in ABAQUS [29] to simulate the connection behaviour under static loading. It was demonstrated that the conventional types of connections could not effectively benefit from the material properties of the corner tubes utilised in the HFC. The flush and extended end-plate connections exhibited low initial stiffness and very limited load-bearing capacity. The reverse channel connection indicated a higher initial stiffness but still failed to provide enough capacity to satisfy the weak member-strong connection design condition. A modified version of the ConXL connection was also simulated as one of the conventional types of connections. This connection exhibited a higher initial stiffness and a relatively higher load-bearing capacity; however, the major modifications required to adapt it for the HFC is a major drawback to the potential usage of this connection. However, the welded W-HFC connection consisting of eleven components has demonstrated a high initial stiffness and has the highest moment capacity of all the studied connections.

An optimisation task was also done on the M-HFC. This task included a parametric study to see how different dimensions and geometries of the connection can influence its behaviour. Nevertheless, a more thorough parametric study including other components of the connection could be a topic for further investigations. The results show up to 26% reduction in the connection weight with 18% reduction in the capacity (in the case of connection to UHS corner tubes) but the capacity still satisfies the strong connection-weak beam design philosophy. The optimised connection reusability was also investigated through comparison of plastic deformation levels in the connection variations with the levels in the original connection.

The advantages of a highly ductile behaviour along with the notably high moment capacity make the HFC connection an excellent choice for high-rise buildings. This connection also utilises the superior material properties of HFCs with UHS corner tubes.

Acknowledgement

The research work presented in this research work is supported by the Australian Research Council through a Discovery Project (DP150100442) awarded to the authors.

References

[1] Aoki T, Ji B. Experimental study on buckling strength of tri-tube steel members. The 3rd international Conference on Coupled Instabilities in Metal Structures, Lisbon, Portugal; 2000. 283–90.

[2] Zhao XL, Van Binh D, Al-Mahaidi R, Tao Z. Stub column tests of fabricated square and triangular sections utilizing very high strength steel tubes. J Constr Steel Res. 2004;60:1637–61.

[3] Van Binh D, Al-Mahaidi R, Zhao XL. Finite element analysis (FEA) of fabricated square and triangular section stub columns utilizing very high strength steel tubes. Adv Struct Eng. 2004;7:447–57.

[4] Javidan F, Heidarpour A, Zhao X-L, Hutchinson CR, Minkkinen J. Effect of weld on the mechanical properties of high strength and ultra-high strength steel tubes in fabricated hybrid sections. Engineering Structures. 2016;118:16–27.

[5] Javidan F, Heidarpour A, Zhao X-L, Hutchinson CR, Minkkinen J. Application of high strength and ultra-high strength steel tubes in long hybrid compressive members: Experimental and numerical investigation. Thin-Walled Structures. 2016;102:273-285.

[6] Heidarpour A, Tofts NS, Korayem AH, Zhao X-L, Hutchinson CR. Mechanical properties of very high strength steel at elevated temperatures. Fire Safety Journal. 2014; 64:27-35.

[7] Heidarpour A, Cevro S, Song QY, Zhao XL. Behaviour of stub columns utilising mild-steel plates and VHS tubes under fire. J Constr Steel Res. 2014;95:220–9.

[8] Nassirnia M, Heidarpour A, Zhao XL, Minkkinen J. Innovative Hollow Columns Comprising Corrugated Plates and Ultra High-Strength Steel Tubes. Thin-Walled Struct 2016;101:14–25.

[9] Nassirnia M, Heidarpour A, Zhao XL, Minkkinen J. Innovative hollow corrugated columns: a fundamental study. Eng. Struct. 2015;94:43–53.

[10] Farahi M, Heidarpour A, Zhao XL, Al-Mahaidi R. Compressive Behaviour of Concrete-Filled Double-Skin Sections Consisting of Corrugated Plates. Eng Struct. 2016;111:467–77.

[11] Sadeghi SN, Heidarpour A, Zhao XL, Al-Mahaidi R. An innovative I-beam to hybrid fabricated column connection: Experimental investigation. Engineering Structures, 2017;148:907-923.

[12] Sadeghi N, Heidarpour A, Zhao XL, Al-Mahaidi R. Numerical investigation of innovative modular beam-to-fabricated column connections under monotonic loading. In: Zingoni A, (ed.) Insights and Innovations in Structural Engineering, Mechanics and Computations. Cape Town, South Africa: Taylor and Francis Group, LLC; 2016. p. 1247–52.

[13] European Committee for Standardisation (CEN). (2005). Eurocode 3. Design of Steel Structures, Part 1-8: Design of Joints. Brussels: CEN.

[14] AISC. (2010b). Prequalified Connections for Special and Intermediate Steel Moment Frames for Seismic Applications (AISC 358:2010b), Chicago, IL: American Institute of Steel Construction.

[15] Chen W.F. (2000). Practical analysis for semi-rigid frame design. Singapore: World Scientific.

[16] Douty RT, and McGuire W. (1965). High Strength Bolted Moment Connections. Journal of the Structural Division, 91(ST2), 101–28.

[17] Agerskov H. (1976). High-Strength Bolted Connections Subject to Prying. Journal of the Structural Division, 102(ST1), 161–75.

[18] Shi Y, Shi G, and Wang Y. (2007). Experimental and Theoretical Analysis of the Moment-Rotation Behaviour of Stiffened Extended End-Plate Connections. Journal of Constructional Steel Research. 63(9);1279–1293.

[19] Krishnamurthy N. Correlation between 2- And 3-Dimensional Finite Element Analyses of Steel Bolted End-Plate Connections. Computers & Structures. 1976;6:381–9.

[20] Krishnamurthy N, Huang HT, Jefferey PK, and Avery LK. Analytical M-θ Curves for End-Plate Connections. Journal of the Structural Division. 1979;105(ST1):133–45.

[21] Krishnamurthy N. Modeling and Prediction of Steel Bolted Connection Behaviour. Computers & Structures. 1980;11:75–82.

[22] Sherbourne AN, and Bahaari MR. 3D Simulation of End-Plate Bolted Connections. Journal of Structural Engineering. 1994;120(11):3122–36.

[23] Bahaari, M.R., and Sherbourne, A.N. 3D Simulation of Bolted Connections to Unstiffened Columns-II. Extended Endplate Connections. Journal of Constructional Steel Research. 1996;40(3):189–223.

[24] Sherbourne AN, and Bahaari MR. Finite Element Prediction of End Plate Bolted Connection Behavior I: Parametric Study. Journal of Structural Engineering. 1997;123(2):157–64.

[25] Bahaari MR, and Sherbourne AN. Finite Element Prediction of End Plate Bolted Connection Behavior II: Analytic Formulation. Journal of Structural Engineering. 1997;123(2):165–75.

[26] Kukreti AR, Murray TM, and Abolmaali A. End-Plate Connection Moment–Rotation Relationship. Journal of Constructional Steel Research. 1987;8:137–57.

[27] Bose, B., Wang, Z.M., and Sarkar, S. Finite-Element Analysis of Unstiffened Flush End-Plate Bolted Joints. Journal of Structural Engineering. 1997;123(12):1614–21.

[28] ANSYS Multiphysics 16.0. Canonsburg, Pennsylvania, USA: Ansys Inc; 2015.

[29] ABAQUS 6.14-1. Providence, RI, USA: Dassault Systèmes; 2014.

[30] AISC, Steel Construction Manual, 13th ed. Chicago, IL: American Institute of Steel Construction; 2006.

[31] Agheshlui H, Yao H, Goldsworthy HM, and Gad EF. (2011). Anchored Blind Bolted Connections within SHS Concrete Filled Columns : Group Performance. Australian Earthquake Engineering Society 2011 Conference, Novotel Barossa Valley Resort, South Australia, 1–9.

[32] Yao H, Goldsworthy H, Gad E, Mirza O, and Uy B. (2010). Moment Connections to Circular and Square Composite Columns Using Blind Bolts. Australian Earthquake Engineering Society 2010 Conference, Perth, Western Australia,1-9.

[33] Tanaka T, Tabuchi M, Maruyama M, Furumi K, Morita T, Usami K, and Matsubara Y. (1996). Experimental Study on End Plate to SHS Column

Connections Reinforced by Increasing Wall Thickness with One Sided Bolts. Proc. of 7th International Symposium on Tubular Structures, Miskolc, Hungary, 253– 260.

[34] Mirghaderi SR, Torabian S, Keshavarzi F. I-beam to box–column connection by a vertical plate passing through the column. Engineering Structures. 2010;32(8):2034–48.

[35] Yeomans N. Flowdrill jointing system: Part 1- Mechanical intregrity tests. CIDECT Report: 6F-13A/96; 1996.

[36] Yeomans N. Flowdrill jointing system: Part 2- Structural hollow section connections. CIDECT Report: 6F-13B/96; 1996.

[37] Korol RM, Ghobarah A, Mourad S. Blind Bolting W-Shape Beams to HSS Columns. Journal of Structural Engineering. 1993;119(12):3463–81.

[38] Lindapter International. Type HB Hollo-Bolt for Blind Connection to Structural Steel and Structural Tubes. 1995. Lindapter International Ltd, Bradford, England.

[39] Ajax Engineered Fasteners (2002). ONESIDE Brochure. B-N012 Data Sheet, Victoria, Australia.

[40] Lee J, Goldsworthy HM, and Gad EF. Blind Bolted Moment Connection to Sides of Hollow Section Columns. Journal of Constructional Steel Research. 2011;67(12):1900–1911.

[41] Wang Z-Y, Wang Q-Y. Yield and ultimate strengths determination of a blind bolted endplate connection to square hollow section column. Engineering Structures. 2016;111:345–69.

[42] Wheeler AT, Clarke MJ, Hancock GJ, and Murray TM. Design Model for Bolted Moment End Plate Connections Joining Rectangular Hollow Sections. Journal of Structural Engineering. 1998;124(2):164–173.

[43] Wheeler AT, Clarke MJ, and Hancock GJ. FE Modeling of Four-Bolt, Tubular Moment End-Plate Connections. Journal of Structural Engineering. 2000;126(7):816–822.

[44] Elghazouli AY, Packer JA. Seismic Design Solutions for Connections to Tubular Members. Steel Construction. 2014;7(2):73–83.

[45] Hoang VL, Demonceau JF, Jaspart JP. Innovative bolted beam-to-column joints in moment resistant building frames: from experimental tests to design guidelines . In Dubina, D., et al. (eds.), “Application of High Strength Steel in Seismic-resistant Structures”, “Orizonturi Universitare” Pub. House, Romania, 2014:1-17.

[46] Wu LY, Chung LL, Tsai SF, Lu CF, and Huang GL. Seismic Behavior of Bidirectional Bolted Connections for CFT Columns and H-Beams. Engineering Structures. 2007;29(3):395–407.

[47] Wang YC, and Xue L. Experimental Study of Moment–Rotation Characteristics of Reverse Channel Connections to Tubular Columns. Journal of Constructional Steel Research. 2013;85:92–104.

[48] Heistermann T, Koltsakis E, Veljkovic M, Lopes F, Santiago A, Simões da Silva L. Initial stiffness evaluation of reverse channel connections in tension and compression. Journal of Constructional Steel Research. 2015;114:119–28.

[49] Al Hendi H, Celikag M. Finite element prediction of reverse channel connections to tubular columns behavior. Engineering Structures. 2015;100:599–609.

[50] Al Hendi H, Celikag M. Parametric study on moment–rotation characteristics of reverse channel connections to tubular columns. Journal of Constructional Steel Research. 2015;104:261–73.

[51] Robert F, and Simmons J. Innovative Connections. Journal of Modern Steel Construction. 2005;45(8):38–41.

[52] Rezaeian A, Jamal-Omidi M, Shahidi F. Seismic behavior of ConXL rigid connection in box-columns not filled with concrete. Journal of Constructional Steel Research. 2014;97:79–104.

[53] Yang C, Yang JF, Su MZ, Liu CZ. Numerical study on seismic behaviours of ConXL biaxial moment connection. Journal of Constructional Steel Research. 2016;121:185–201.

[54] AS/NZS 3679.1:2016 Structural steel - Hot-rolled bars and sections. Sydney, Australia: Standards Australia; 2016. 47 p.

[55] Wang J, Spencer BF. Experimental and analytical behavior of blind bolted moment connections. Journal of Constructional Steel Research. 2013;82:33–47.

[56] Shen J, Akbas B, Seker O, Doran B, Wen R, Uckan E. Seismic axial loads in steel moment resisting frames. International Journal of Steel Structures. 2015;15(2):375–87.

[57] FEMA-350, 2000, Recommended Seismic Design Criteria for New Steel Moment-Frame Buildings, prepared by the SAC Joint Venture for the Federal Emergency Management Agency, Washington, DC.

[58] Peters, J. W. and Driscoll, George C. Jr., "A study of the behavior of beam-to-column connections, May 1968 " (1968). Fritz Laboratory Reports. 293.

[59] American Institute of Steel Construction (AISC). Seismic Provisions for Structural Steel Buildings (AISC 341), Chicago, IL: American Institute of Steel Construction; 2016.

[60] Rothwell. A. (2017), *Optimization Methods in Structural Design*, Springer International Publishing AG, Switzerland.

A COMPONENT-BASED MODEL FOR INNOVATIVE PREFABRICATED BEAM-TO-HYBRID TUBULAR COLUMN CONNECTIONS

CHAPTER 4

This chapter has been submitted for publication in the Journal of *Thin-Walled Structures*.

Table of Contents

Abstract

This research work presents the results of a component-based model developed for an innovative type of connection, recently proposed by the authors, for beam-to-hybrid fabricated column (HFC) connections. The active constitutive components of the connection are identified and their relevant resistance and flexural stiffness are presented. The moment-rotation curve of the joint is reproduced using the assembly of these components. The failure point of the connection is also predicted using the failure modes observed in the experimental tests. The results obtained from the developed component-based model are then compared to those provided by a three-dimensional (3-D) finite element (FE) model. It is shown that the component-based model shows good accuracy in the prediction of the initial stiffness, rotation capacity and failure of the connection.

Keywords: hybrid fabricated column, modular bolted connection, component-based model, ductility, ultra-high strength, moment-rotation curve, hybrid tubular column

Nomenclature

A_s	Thread area of bolt
A_{vc}	Shear area of the column
b_1	Width of bottom corner part
$b_{eff,ta}$	Effective width of angle in bending
b_{wx}	Thickness of web extension
D	Flexural rigidity of tube
D_{tb}	Tube external diameter
d_0	Diameter of bolt hole
d_{M16}	Diameter of M16 bolt
d_b	Bolt diameter
E	Modulus of elasticity
e_b	Distance of bolt line to free edge in the direction of applied load
e_p	Distance from bolt line to the free edge of T-stub
e_1	Distance from bolt line to the free edge of angle
e_2	Distance between bolt holes in top/seat angle
F_{Rd}^i	Component plastic resistance
F_{Rd}^{Tr}	Plastic resistance at bolt row *r*
F_{Total}	Total external force
$F_{at,Rd}$	Resistance of angle leg in tension
$F_{bs,Rd}$	Resistance of bolt row in shear
$F_{bt,Rd}$	Resistance of a single bolt
$F_{ctc,Rd}$	Resistance of corner tube in compression
$F_{ctt,Rd}$	Resistance of corner tube in tension
$F_{cw,Rd}$	Resistance of column web
$F_{pb,Rd}$	Resistance of plate in bending
$F_{tab,Rd}$	Resistance of angle in bending
$F_{wat,Rd}$	Resistance of web angle in tension
$F_{wxt,Rd}$	Resistance of web extension in bending

f	Summation of thickness and fillet size of web angle
f_{ub}	Ultimate strength of bolt
f_{up}	Ultimate strength of plate
f_{uw}	Ultimate strength of weld
f_{uwa}	Ultimate strength of web angle
f_{uwx}	Ultimate strength of web extension
f_{ya}	Yield strength of angle
f_{yb}	Design shear stress of the bolt
f_{ycw}	Yield strength of the column web
f_{ytb}	Yield strength of the tube material
g	Gap between the beam end and face of column/connection
g_1	Distance from the bolt hole centre to the face of beam on the outstanding leg of angle
g_a	Gauge length of the angle
H_1	Column height
H_{ep}	Height of bottom corner part
h_r	Component lever arm
h_{wx}	Height of web extension
h_t	Tension lever arm
I	Second moment of inertia of the angle leg
I_{wx}	Second moment of inertia of the cross section of web extension
K1, K2,…, K37	Component reference number in the model (Fig. 4-5)
K^c	Overall equivalent stiffness of the compression zone
K^t	Overall equivalent stiffness of the tension zone
k^i, k^i_j	Component extensional deformability
k_{at}	Stiffness of angle leg in tension
k_{bs}	Stiffness of bolt row in shear
k_{bt}	Stiffness of bolt in tension
k_{ctc}	Stiffness of corner tube in compression
k_{ctt}	Stiffness of corner tube in tension
k_{cw}	Stiffness of column web
k_{pb}	Stiffness of plate in bending
k_r^T	Total extensional deformability of row number *r*
k_{tab}	Stiffness of angle in bending
k_{wat}	Stiffness of web angle in tension
k_{wxb}	Stiffness of web extension in bending
L	Effective length measured along the mid-line of angle leg along the leg
L_a	Full length of the outstanding legof an gle
L_b	Grip length of bolt
L_{ta}	Length of top/seat angle
$L_{eff,a}$	Effective length of angle leg
$L_{eff,p}$	Effective length of plate
L_{cw}	Column faceplate width
L_{wa}	Length of the web angle along the length of column
L_{wx}	Length of the web extension
$M_{bp,Rd}$	Flexural resistance of plate
$M_{j,Rd}$	Flexural resistance of the joint
$M_{tab,Rd}$	Plastic moment of the angle leg
M_{Total}	Total external moment
M_u	Ultimate moment of connection
m_p	Distance from bolt line to the corner of T-stub
m_{ta}	Characteristic length of angle
n	Number of components in row *r*
n_b	Number of bolts

n_c	Number of bolt rows in compression zone
n_s	Number of shear planes passing through the bolt
n_t	Number of bolt rows in tension zone
P	Force
p_b	Spacing between bolts
r_w	Column faceplate weld radius
T_1	Column plate thickness
T_2	Tube thickness
t_a	Thickness of angle leg
t_{ep}	Thickness of bottom corner part
t_p	Plate thickness
t_{pb}	Thickness of the plates subjected to bolt shear force
t_{ta}	Angle thickness
t_{wa}	Thickness of web angle
$S_{j,ini}$	Initial rotational stiffness of the joint
V_{cws}	Design shear resistance of the panel zone
W_1	Width of column measured between tube axes
W_2	Depth of column measured between tube axes
w	Distance between internal bolt lines of angle
w_p	Vertical distance between bolt lines
Δ_{sh}	Deformation capacity of angle
α	Angle of engagement of corner tube in compression
γ_{M0}	Partial safety factor for design shear resistance of panel zone
γ_{M5}	Partial safety factor for resistance of corner tube in tension
γ_{Mb}	Partial safety factor for resistance of bolt in tension
ε_u	Ultimate tensile strainof material
θ_{Cd}	Rotation capacity of connection

4.1. Introduction

Of the different types of closed section columns, hybrid fabricated columns (HFCs) are a reliable alternative to conventional tubular box columns. HFCs (part 7 in Fig. 4-1) are composed of structural mild steel plates, which may be flat or corrugated, welded to hollow thin-walled tubes at two opposite edges. The concept of HFC was first introduced by Aoki [1]; however, since then it has been studied by many researchers [2 - 13]. HFC columns exhibit higher load-bearing capacity, and better post-buckling strength and energy absorption compared to the equivalent tubular columns [2 - 4]. Javidan et al. [2] have demonstrated that the capacity of hybrid fabricated columns is significantly higher than the corresponding conventional welded box column. For instance, when ultra-high strength tubes with external diameter of 76.1mm and wall thickness of 3.2mm are added to the corners of a 2-meter 210mm×210mm×3mm welded box column, its axial capacity increases at least 10 times. The ductility of this HFC section is also 200% more than the welded box column. An HFC with high strength or ultra-high strength corner tubes can carry two to three times more axial load compared to an HFC with mild steel tubes, respectively [2]. Thus, considering the high capacity to weight ratio and economic benefits [2], the application of these columns in high-rise buildings sounds reasonable and feasible. The main obstacle to the broad usage of these columns in construction has been the issue of a lack of a robust connection, for which the authors of the present research work have recently proposed a solution (Fig. 4-1) that can be effectively used along with HFCs [14],[15]. In spite of the complex look of the connection components, the manufacturing of the components is rather easy and quick. In the experimental tests conducted on the connection, the parts were machine cut from mild steel (Grade 250). However, the recommended manufacturing process for large-scale production is “casting”. Having this perspective in mind, different components of the connection have been designed in a way that poses no difficulties in the casting process. Avoiding complex shapes or cavities, not having sharp edges or very thin features are among these measures. Therefore, achieving a consistent and production tolerance is possible. The design philosophy behind this connection is ‘weak beam-strong column’ which aims at shifting the failure from the column and connection towards the beam ends such that the connection is the latest component which may fail. In these research studies, the behaviour of an innovative modular connection under monotonic loading has been studied experimentally

and numerically using finite element (FE) analysis. The FE model, which was verified against the data extracted from the experimental tests, can accurately predict the overall behaviour of the connection [14]. However, the FE model is a full three-dimensional (3-D) representation of the joint, which is computationally expensive.

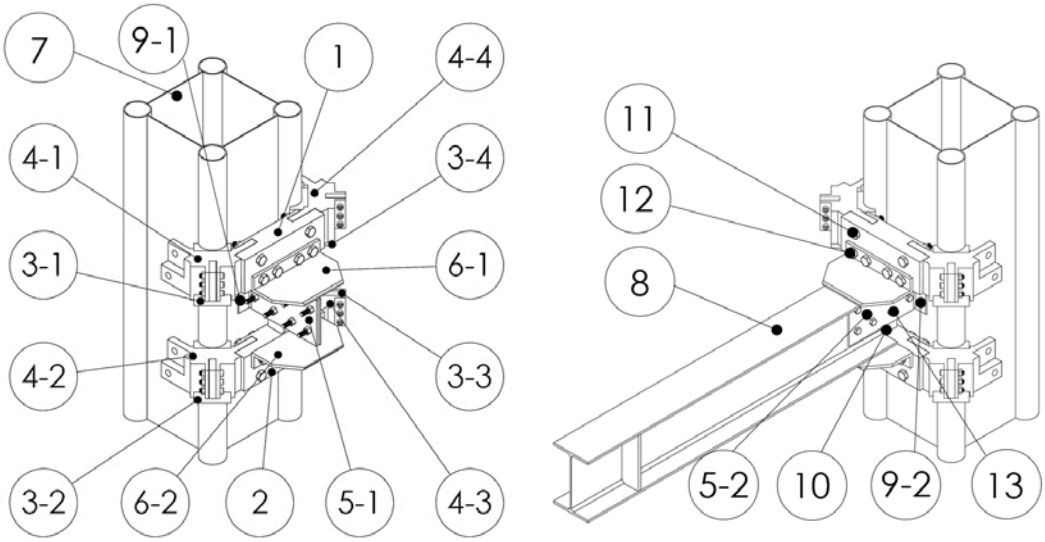

(a) Isometric views

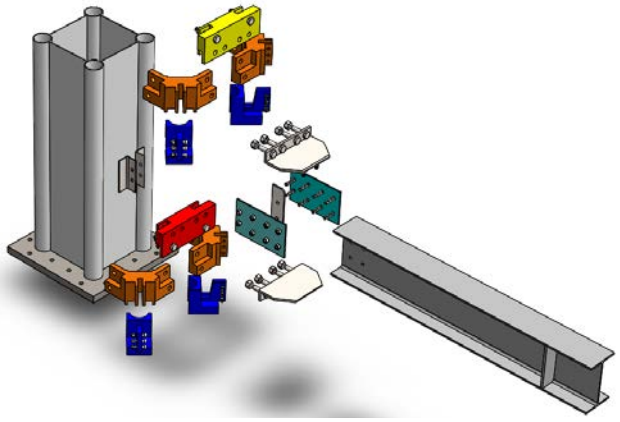

(b) Exploded view

Fig. 4-1. Innovative connection and hybrid fabricated column

The behaviour of a connection is generally reflected in its moment-rotation (M-θ) curve (Fig. 4-2) by providing essential parameters such as initial stiffness ($S_{j,ini}$), moment resistance ($M_{j,Rd}$), and rotation capacity (θ_{Cd}). Many researchers try to relate these parameters to the mechanical and geometrical properties of the joint's components. The

moment-rotation curve or its characteristics can be used in structural analysis packages for design purposes or global analysis of moment-resisting frames.

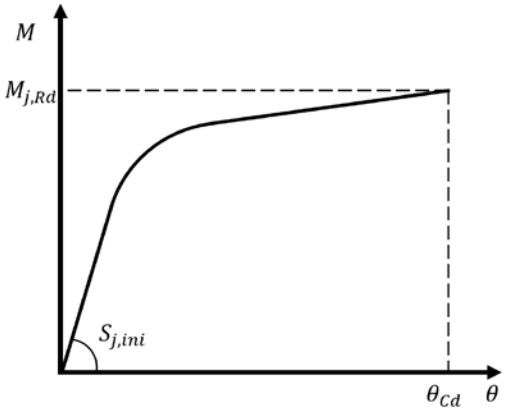

Fig. 4-2. Typical moment-rotation curve

There are different ways of extracting the moment-rotation curve of a connection, including experimental testing, empirical models, analytical models, mechanical models, numerical models, and informational models [17]. Experimental testing is the most accurate method to find the actual behaviour of a joint, but it is costly and time-consuming to conduct for different types of joints. Empirical models are a mathematical representation of the moment-rotation curves in which the mathematical parameters are related in terms of the mechanical and geometrical properties of the joints. The main disadvantage of these models is that they are mainly applicable to the joints used for the calibration of their formulations [18]. Analytical models use equilibrium, compatibility and material constitutive relations as the basis to build a model for the prediction of the rotational stiffness or moment resistance of joints. The reliability of the results provided by this method is based on how consistent they are with the results of the available experimental data [18].

Numerical models are a reliable alternative to experimental testing, but they may be computationally expensive, particularly when a complex joint with multiple components (such as bolts, end plates, column web, etc.) and their various interactions is modelled. If the material and geometrical non-linearities are also included, the analysis is even more time-consuming although more accurate results are anticipated. Nevertheless, FE analysis has been widely used by researchers to investigate the behaviour of joints since the early 1970s [19],[20].

Mechanical models, also known as spring models or component-based models, are efficient methods for analysing beam-to-column connections. These models can be

considered as a trade-off between semi-empirical and complicated 3-D FE models [21]. In this method, the connection is decomposed into multiple rigid or flexible components. Each component has stiffness, strength or deformability. The first step in developing a component-based model is to identify the important components which contribute to the deformation or failure of the connection. The second step is to find the flexural resistance and rotational stiffness of the essential components. In the last step, these components are assembled in order to provide the moment-rotation curve of the joint. The basics of the component method are based on the analytical and experimental tests performed by Zoetemeijer [22]. Wales and Rossow investigated the behaviour of double-web angle connections using a rigid bar connected by two non-linear springs [23]. Tschemernegg investigated unstiffened welded connections [24]. Tschemmernegg and Humer studied end-plate bolted connections with this method [25]. Jaspart [26],[27] combined the available component data and provided a practical tool for designing semi-rigid joints. Based on these developments, this method was codified in Eurocode 3 (1997) for fully welded connections, end-plate connections and top and seat angle connections. Given the flexibility of component-based modelling, since then a great deal of research has been dedicated to developing component-based models for different types of connections [28 - 33]. Researchers have also investigated joint behaviour using this method under various loading conditions, such as cyclic loading [21],[34] and fire [35],[36].

In addition to joints with open sections, joints in hollow sections have also been investigated. Jaspart and Weynand [37] discussed the extension of the component method to the design of steel joints in tubular construction. Following their study, more research work was done in this regard, especially through Comité International pour le Développement et l´Etude de la Construction Tubulaire (CIDECT) research projects [37 – 42].

The aim of this research work is to develop a component-based model for the innovative beam-to-fabricated tubular connection shown in Fig.1. The model is capable of developing the moment-rotation curve of the connection and predicting its failure point. The tri-linear moment rotation curve proposed in this research work for the moment-rotation behaviour of the innovative connection, can predict the behaviour of this connection accurately. Whereas the majority of the connection parts are different to conventional connections, the required force/moment- displacement/rotation relations are either derived (e.g. the extension (part10 in Fig. 4-1 (a))) or extracted from the existing literature and

accommodated to the new parts. The results are compared with the results of the FE model, which was previously developed and verified by the experimental test data provided by the authors [14].

4.2. Component-based modelling

4.2.1 Component method

The component method has been adopted in Eurocode3 [44] and Eurocode4 [45] and can be used to reproduce the moment-rotation curve and predict the initial rotational stiffness and moment resistance of a wide variety of joints. As mentioned in the previous section, the first stage in the development of a component-based model is to break down the joint to its individual basic components. Many of the components have already been investigated and their characteristics are available in the literature [44],[45]. The new components could also be investigated analytically, numerically, or experimentally to identify their characteristics [18]. Each component has a force-displacement relationship which may be bi-linear, tri-linear or non-linear [21]. In the present research, the components are assumed to have elastic-perfectly plastic response curves. Therefore, each component has an extensional deformability k^i and a plastic resistance F_{Rd}^i (Fig. 4-3).

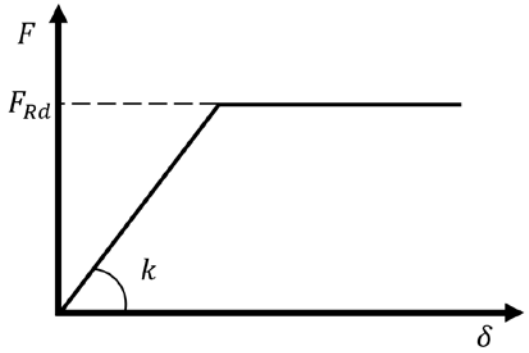

Fig. 4-3. Bi-linear behaviour of joint components

Each component is represented by a translational spring, which can undergo either tension or compression. It also has a lever arm (h_r), which is measured from the reference datum to the bolt row to which that specific component belongs. The datum in this study is chosen to be at the middle of the thickness of the outstanding leg of the bottom angle (part 6-2 in Fig. 4-1). The plastic resistance at each row (F_{Rd}^{Tr}) is obtained from:

$$F_{Rd}^{Tr} = \min_{i=1,\dots,n} F_{Rd}^{i} \quad \text{(Eq. 4.1)}$$

where, *n* is the number of components in row *r*. Moreover, the equation of equilibrium leads to the following equations:

$$F_{Total} = \sum F_{Rd}^{Tr} \quad \text{(Eq. 4.2)}$$

$$M_{Total} = \sum F_{Rd}^{Tr}.h_r \quad \text{(Eq. 4.3)}$$

in which F_{Total} and M_{Total} are total external force in both horizontal and vertical directions and moment applied to the joint, respectively.

The final stage is to assemble the springs in each row and eventually in the tension and compression zones. The resultant extensional deformability of each row is found based on the extensional deformability of all components, dependent on that bolt row. The relation is as follows:

$$\frac{1}{k_r^T} = \sum_{i=1}^{n} \frac{1}{k^i} \quad \text{(Eq. 4.4)}$$

where, k_r^T is the total extensional deformability of row number *r*, and *n* is the number of components in that row. Therefore, assuming the rigid rotation of the web about the compression centre leads to the overall equivalent stiffness of the tension zone (K^t) such that:

$$K^t = \frac{\sum_{r=1}^{n_t} k_r^T.h_r}{h_t} \quad \text{(Eq. 4.5)}$$

and

$$h_t = \frac{\sum_{r=1}^{n_t} k_r^T.h_r^2}{\sum_{r=1}^{n_b} k_r^T.h_r} \quad \text{(Eq. 4.6)}$$

in which h_t is the tension lever arm, and n_t is the number of bolt rows in the tension zone. In the compression zone, the equivalent extensional stiffness of the components (K^c) is evaluated based on the laws of mechanics for springs in parallel and series configurations as follows:

$$K^c = \sum_{j=1}^{n_c} \frac{1}{\sum_{i=1}^{n} \frac{1}{k_j^i}} \quad (4.7)$$

where k_j^i is the stiffness of the component i in row j and n_c is the number of bolt rows in the compression zone.Finally, the initial rotational stiffness of the joint ($S_{j,ini}$) can be found using the following expression:

$$S_{j,ini} = \frac{h_t^2}{\frac{1}{K^t} + \frac{1}{K^c}} \quad \text{(Eq. 4.8)}$$

Similarly, the flexural resistance of the joint ($M_{j,Rd}$) is determined from:

$$M_{j,Rd} = \sum_{r=1}^{n_t} F_{Rd}^{Tr}.h_r \quad \text{(Eq. 4.9)}$$

In this study, the moment-rotation curve of the joint is assumed to be a multi-linear curve, as depicted in Fig. 4-4.

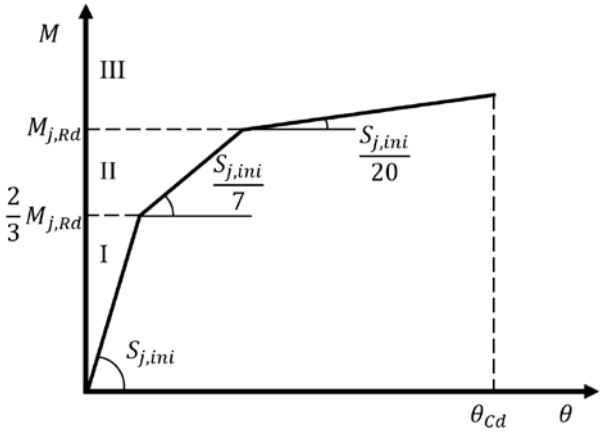

Fig. 4-4. Tri-linear moment-rotation curve of joint

The first range, which corresponds to the elastic range, varies linearly with a slope equal to the initial rotational stiffness of the joint [44]. This linear part is valid until the magnitude of moment reaches the value of $\frac{2}{3}M_{j,Rd}$ [44]. The second range is also assumed to be linear, but with a modified slope. This range is for the moment which is greater than the previous threshold and less than the flexural resistance of the joint ($M_{j,Rd}$). In the case of connections with top, seat and web angles, this slope can be taken as $\frac{S_{j,ini}}{7}$ [18]. The connection of the subject of this study can also be treated similarly in this respect. The last stage pertains to the plastic hardening stage of the connection. The slope in this zone is also taken to be linear. Where the moment exceeds the flexural resistance of the joint up to failure point, the slope can be taken as $\frac{S_{j,ini}}{20}$ [46]. There are major failure modes, such as top angle failure, corner tube crushing (in compression) or side plate wrinkling, of which only the first mode is included in this study. However, other modes also need to be considered in order to

improve the accuracy and reliability of the model. The group effect for bolts is also not included in the model, which presumably will enhance the model's ability to capture the joint behaviour accurately.

4.2.2 Characteristics of components in tension zone

The connection in the current study (Fig. 4-1) is decomposed to its components as shown in Fig. 4-5. From this figure it can be seen that the complexity of the connection requires a large number of components to be considered in the proposed component-based model. A summary of the joint components can be found in Table 4-1. The characteristics of the components are either taken from the literature (e.g. Eurocode 3 [44]) or are directly developed here when a similar component is not available in the literature. For example, the top/seat angles in Fig. 1 have four bolts which are different from the type of angle with two bolts included in Eurocode 3 [44]; therefore, their stiffness and geometrical parameters are taken into account using the adjustments suggested by Demonceau et al. [33]. Each component is explained in the following section.

Table 4-1. Breakdown of essential joint components

Component	**Part No. (Fig. 4-1)**	**Notation**	**Equations to calculate Stiffness & Resistance**
Plates in bending	1,2	K2,K5,K28,K31	Eq. 4.9 to Eq. 4.11
Angle bending	6-1,6-2	K7,K26	Eq. 4.12 to Eq. 4.15
Long bolts in tension	12	K6,K29	Eq. 4.16 & Eq. 4.17
Short bolts in tension	11	K3,K32	Eq. 4.16 & Eq. 4.17
Web bolts in shear	13	K12,K25	Eq. 4.18 & Eq. 4.19
Angle bolts in shear	13	K14,K18	Eq. 4.18 & Eq. 4.19
Side plate bearing-Beam web	5-1,5-2	K9,K22	Eq. 4.20 to Eq. 4.24
Side plate bearing-Web angle	5-1,5-2	K15,K19	Eq. 4.20 to Eq. 4.24
Beam web bearing	8	K8,K21	Eq. 4.20 to Eq. 4.24
Angle bearing	9-1,9-2	K13,K17	Eq. 4.20 to Eq. 4.24
Web extension in bearing	10	K10,K23	Eq. 4.20 to Eq. 4.24
Angle in tension	9-1,9-2	K16,K20	Eq. 4.25 & Eq. 4.26
Column web deformation	7	K36,K37	Eq. 4.27 & Eq. 4.28
Corner tube in tension	7	K1,K4	Eq. 4.29 & Eq. 4.30
Web extension in bending	10	K11,K24	Eq. 4.33 & Eq. 4.34
Angle leg in tension	6-1,6-2,9-1,9-2	K33,K34,K35	Eq. 4.35 & Eq. 4.36
Corner tube in compression	7	K27,K30	Eq. 4.37 & Eq. 4.38

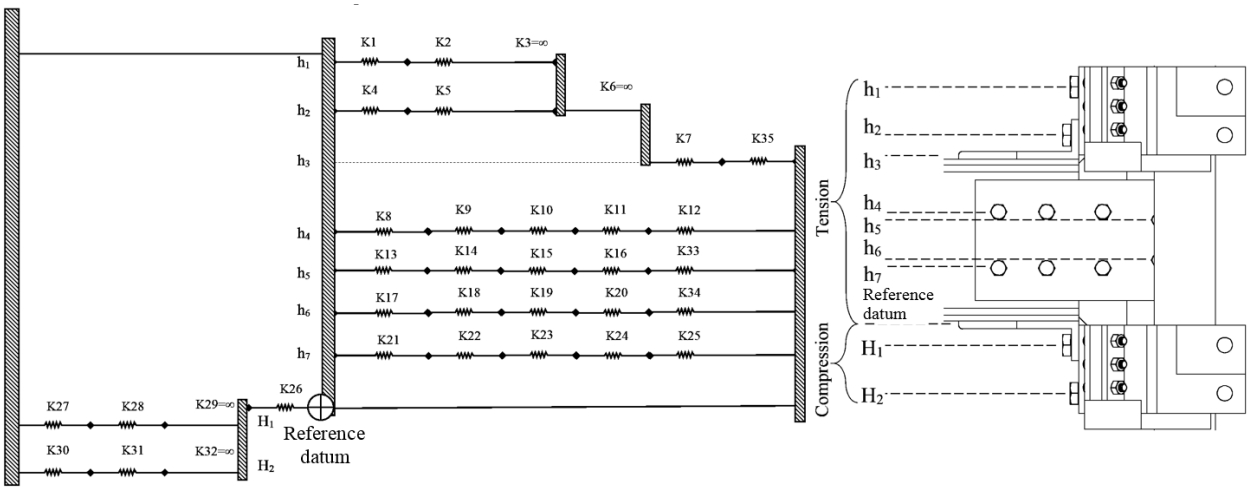

Fig. 4-5. Component model for innovative beam-to-hybrid fabricated column connection

4.2.2.1 Plates in bending

The thin metal flaps located at the back of the collar section of the connection (part 1 and part 2 in Fig. 4-1) behave similar to a T-stub such that the equivalent T-stub stiffness and flexural resistance are adopted here. The component resistance is chosen based on the possible collapse mechanisms observed in the experimental tests [47]. The top collar in the tension zone behaves differently to the bottom one in the compression zone. It is assumed (as observed in the experimental tests [14]) that the failure mode of the top collar flaps (shaded areas in Fig. 4-6) will be at the line where they are attached to the main body of the collar. The bolts will also be under significant amount of tension and will undergo a noticeable deformation. Each of the bottom collar flaps are expected to yield at two lines, one at the centre of the bolt and one at the line of attachment to the main body. Hence, the governing equations are obtained from:

$$k_{pb} = 0.5\frac{El_{eff,p}t_p^3}{m_p^3} \quad \text{(Eq. 4.10)}$$

$$Top\ collar: F_{pb,Rd} = \frac{2M_{bp,Rd} + 2F_{bt,Rd}}{m_p + e_p}$$
$$Bottom\ collar: F_{pb,Rd} = \frac{4M_{bp,Rd}}{m_p} \quad \text{(Eq. 4.11)}$$

$$l_{eff,p} = \min\begin{Bmatrix} 4m_p + 1.25e_p; e_x + 2m_p + 0.625e_p; \\ 0.5b_p; 0.5w_p + 2m_p + 0.625e_p \end{Bmatrix} \quad \text{(Eq. 4.12)}$$

in which m_p, t_p, and e_p are parameters displayed in Fig. 4-6. e_x is the vertical distance from the centre of the bolt hole to the edge of the plate and w_p is the distance between bolt lines. $M_{bp,Rd}$ and $F_{bt,Rd}$ are the flexural resistance of the plate and the ultimate resistance of a single bolt, respectively [18], and E is the modulus of elasticity of the collar material.

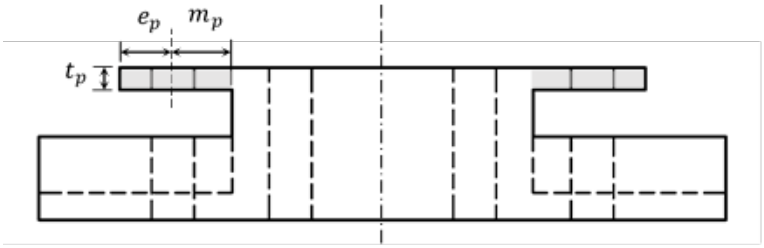

Fig. 4-6. Plate in bending

4.2.2.2 Angles in bending

The connection has top/seat angles (parts 6-1 and 6-2 in Fig. 4-1), for which the behaviour can be described based on the relations proposed by Faella et *al.* [48]. This model considers the increase of deformability due to the angle leg connected to the beam with the following relations:

$$k_{tab} = 0.5\frac{Eb_{eff,ta}t_{ta}^3}{m_{ta}^3}\left(\frac{4\lambda_{ta}}{4\lambda_{ta}+3}\right) \quad \text{(Eq. 4.13)}$$

$$F_{tab,Rd} = \frac{4M_{tab,Rd}}{m_{ta}} \quad \text{(Eq. 4.14)}$$

$$b_{eff,ta} = \min\begin{Bmatrix} 2m_x + 0.625e_x + (e_1+e_2); 4m_x + 1.25e_x + e_1; \\ 2m_x + 0.625e_x + (e_1 + 0.5w); 0.5(2e_1 + 2e_2 + w) \\ 8m_x + 2.5e_x \end{Bmatrix} \quad \text{(Eq. 4.15)}$$

$$\left.\begin{matrix} m_{ta} = L_{ta} - t_{ta} - e_{ta} - 0.8r_{ta} & for \;\; g \le 0.4t_{ta} \\ m_{ta} = L_{ta} - 0.5t_{ta} - e_{ta} & for \;\; g > 0.4t_{ta} \end{matrix}\right\} \quad \text{(Eq. 4.16)}$$

where, $\lambda_{ta} = \frac{I_2/L_2}{I_1/L_1}$ in which I and L relate to the legs of the angles, I is the second moment of inertia of the angle leg and L is its effective length measured along the mid-line of the angle leg along the leg, g is the gap between the end of the beam and face of the column, r_{ta} is the fillet radius of the angle, and $M_{tab,Rd}$ is the plastic moment of the angle leg [18]. Other parameters in Eqs. (Eq. 4.13)-(Eq. 4.16) can be found in Fig. 4-7.

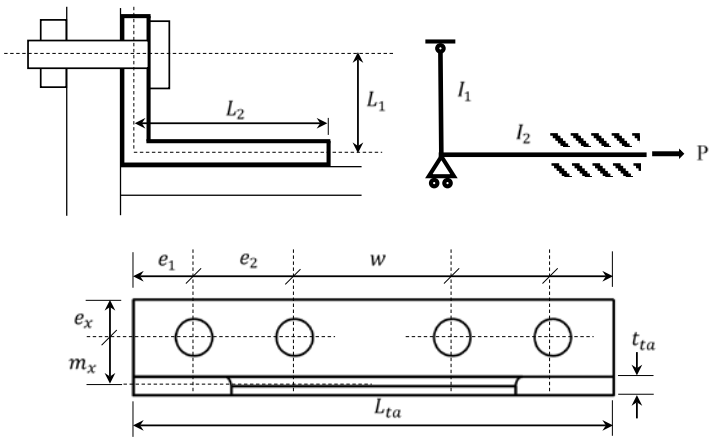

Fig. 4-7. Angle in bending

4.2.2.3 Bolts in tension

The stiffness of a single bolt row in tension and the resistance of each bolt can be calculated from [44]:

$$k_{bt} = 1.6\frac{EA_s}{L_b} \quad \text{(Eq. 4.17)}$$

$$F_{bt,Rd} = \frac{0.9A_s f_{ub}}{\gamma_{Mb}} \quad \text{(Eq. 4.18)}$$

where, A_s is the thread area of the bolt, L_b is the grip length of the bolt including the thickness of the plates held by the bolt plus washers and half of the thickness of the bolt head and nut, f_{ub} is ultimate strength of the bolt, and γ_{Mb} is the partial safety factor suggested by Eurocode [44].

4.2.2.4 Bolts in shear

In the case of bolted connections with angles, the flexibility and flexural resistance of the connection should be calculated accounting for the shear resistance of the bolts. For pre-loaded bolts, the stiffness is considered to be infinite (∞). However, the flexibility and resistance of bolt rows in shear can be determined from [18].

$$k_{bs} = 16\frac{n_b d_b^2 f_{ub}}{d_{M16}^2} \quad \text{(Eq. 4.19)}$$

$$F_{bs,Rd} = n_b n_s A_s f_{yb} \quad \text{(Eq. 4.20)}$$

where, n_b is the number of bolts, n_s is the number of shear planes passing through the bolt, f_{yb} is the design shear stress of the bolt which is taken as $0.6\,f_{ub}/\gamma_{Mb}$ based on the recommendation of Eurocode 3 [44], d_{M16} is diameter of the M16 bolt, and d_b is the bolt diameter.

4.2.2.5 Plate bearing

The members connected by bolts and under shear loads undergo large amounts of stress at the area where the members are in contact with the bolt shank. This effect is accounted for by using the following empirical formulations [18]:

$$k_{pb} = 24En_bk_bk_tf_{up} \quad \text{(Eq. 4.21)}$$

$$k_b = \min\left\{0.25\frac{e_b}{d_b} + 0.5; 0.25\frac{p_b}{d_b} + 0.375; 1.25\right\} \quad \text{(Eq. 4.22)}$$

$$k_t = \min\left\{1.5\frac{t_{pb}}{d_{M16}}; 2.5\right\} \quad \text{(Eq. 4.23)}$$

$$F_{pb,Rd} = 2.5\frac{n_b\xi f_{up}d_bt_{pb}}{\gamma_{Mb}} \quad \text{(Eq. 4.24)}$$

$$\xi = \min\left\{\frac{e_b}{3d_0}; \frac{p_b}{3d_0} - \frac{1}{4}; \frac{f_{ub}}{f_{up}}; 1\right\} \quad \text{(Eq. 4.25)}$$

where, t_{pb} is the thickness of the plates subjected to bolt pressure, f_{up} is the plate's ultimate strength, d_0 is the bolt hole diameter, p_b is the spacing between bolts, and e_b is the distance of the bolt line to the free edge in the direction of the applied load (Fig. 4-8).

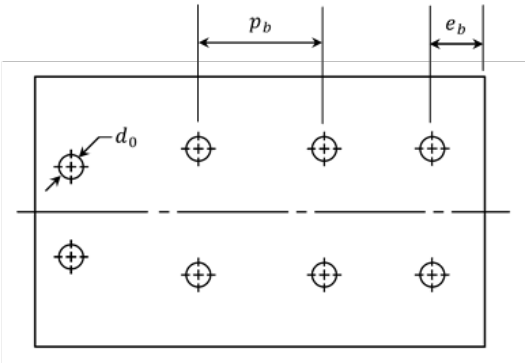

Fig. 4-8. Plate bearing

4.2.2.6 Angle in tension

The angles (parts 9-1 and 9-2 in Fig. 4-1) engaging the connection with the flat face of the column through the side plates (parts 5-1 and 5-2 in Fig. 4-1) are assumed to be under tension. Accordingly, the stiffness and resistance of this component are taken as [49]:

$$k_{wat} = \frac{6EI}{(L_a - f)^3} \quad \text{(Eq. 4.26)}$$

$$F_{wat,Rd} = \frac{L_{wa}t_{wa}^2 f_{uw} + 2L_{wa}t_{wa}^2 f_{uwa}}{8(L_a - f)} \quad \text{(Eq. 4.27)}$$

where, L_a is the full length of the outstanding leg, L_{wa} is the length of the web angle along the length of the column, t_{wa} is the thickness of the web angle, and f is the summation of the thickness and fillet size of the angle (Fig. 4-9). Moreover, f_{uw} and f_{uwa} are the ultimate strength of the weld and web angle, respectively.

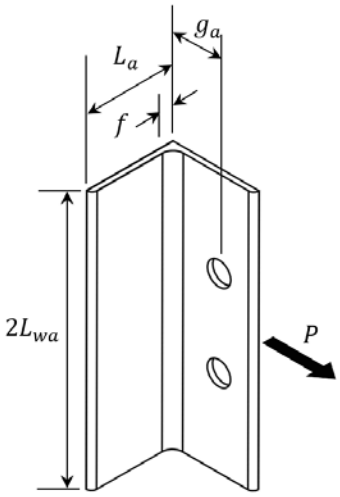

Fig. 4-9. Angle in tension

4.2.2.7 Column web deformation

For this component the relations suggested by Neves and Comes [50] is used. The conditions of the HFC's faceplate is shown in Fig. 4-10 which justifies using the formulation suggested by [50].

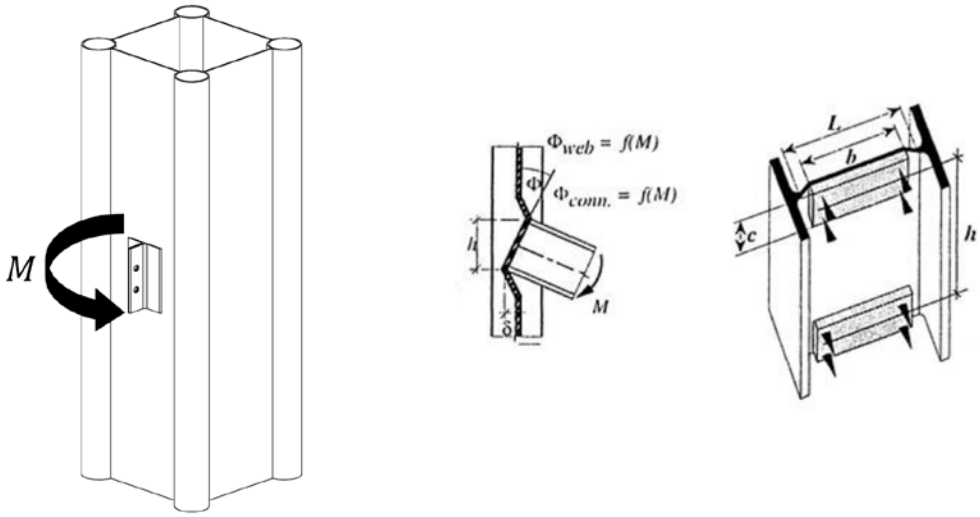

(a) Load case (b) Global mechanism of failure [50]

Fig. 4-10. Faceplate deformation

In order to derive the relations, it is assumed that the long edges of the faceplate are fixed and the other ends are free, which is the conditions that happens to the faceplate of the HFC. The load is applied thought the weld lines attaching the angles to the plate. The stiffness and resistance of the component can be found in [50], and Table 7.13 in [44], respectively:

$$k_{cw} = \frac{16ET_1^3}{(L_{cw} - 1.5r_w)^2}\left(\frac{\beta + (1+\delta)tan\theta}{(1-\delta)^3 + \frac{10.4(k_1 - k_2\delta)}{\mu^2}}\right) \quad \text{(Eq. 4.28)}$$

$$\beta = \frac{2L_a}{L_{cw} - 1.5r_w}, \delta = \frac{t_{wa}}{L_{cw} - 1.5r_w}, \theta = 35 - 10\beta$$

$$F_{cw,Rd} = min\left(\frac{f_{ycw}T_1^2}{\gamma_{M5}}.\frac{2 + 5.6\frac{L_a}{L_{cw}}}{\sqrt{1 - 1.8\frac{L_a}{L_{cw}}}}, f_{ycw}T_1(2t_{wa} + 10T_1)\right) \quad \text{(Eq. 4.29)}$$

where L_{cw} is the column faceplate width, r_w is the plate weld thickness, k_1=1.5, k_2=1.63, and γ_{M5} is a safety factor suggested by Eurocode3 [44].

4.2.2.8 Corner tubes in tension

The main load path for transferring the load from the connection to the column is through the corner tubes. It is assumed that while the connection is under bending moment, the corner tubes are locally under tension or compression. Since there is no case in the literature

which is exactly the same as the corner tubes used in this study, a similar case in which tubes are loaded through the bolts (rather than welds) [51 ,[52] are considered in the present study (Fig. 4-11). The effect of plates is replaced with a force for each plate. The interaction of the connection with the tube, which is through the weld lines is also replaced with a force per each weld line.

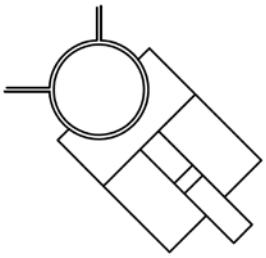

(a) Top View

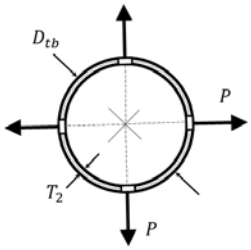

(b) Equivalent applied force diagram

Fig. 4-11. Tube under tension

Therefore, the initial stiffness [51] and resistance [44] (Table 7.4) respectively can be determined from the following relations:

$$k_{ctt} = \frac{D}{\gamma_s (D_{tb} - 2T_2)^2} \quad \text{(Eq. 4.30)}$$

$$F_{ctt,Rd} = k_p T_2^2 f_{ytb} \frac{(4 + 20\beta^2)(1 + 0.25\eta)}{\gamma_{M5}} \quad \text{(Eq. 4.31)}$$

$$D = \frac{E T_2^3}{12(1 - \upsilon^2)}$$

$$\beta = \frac{b_1}{D_{tb}} \quad \text{(Eq. 4.32)}$$

$$\eta = \frac{H_{ep}}{D_{tb}} \quad \text{(Eq. 4.33)}$$

where, D is the flexural rigidity, T_2 and D_{tb} are the tube thickness and external diameter, respectively (Fig. 4-11); γ_s is the deflection coefficient, which in this study equals 0.0005 and k_p for tension equals 1, γ_{M5} is a partial safety factor according to Eurocode 3 [44], f_{ytb} is the yield strength of the tube material, and b_1 and H_{ep} are shown in Fig. 4-12.

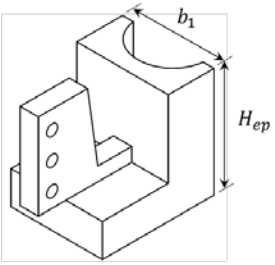

Fig. 4-12. Bottom corner part

4.2.2.9 Web extension in bending

The web extension (part 10 in Fig. 4-1) is a plate extended between the top and bottom collars (parts 1 and 2 in Fig. 4-1) which is welded to these parts. Hence, it can be assumed to be a beam fixed at both ends and under a loading condition as shown in Fig. 4-13, in which P is the load due to the relative displacement of the beam and the connection face, transferred from the beam web through the side plates (parts 5-1, 5-2 in Fig. 4-1) to the web extension.

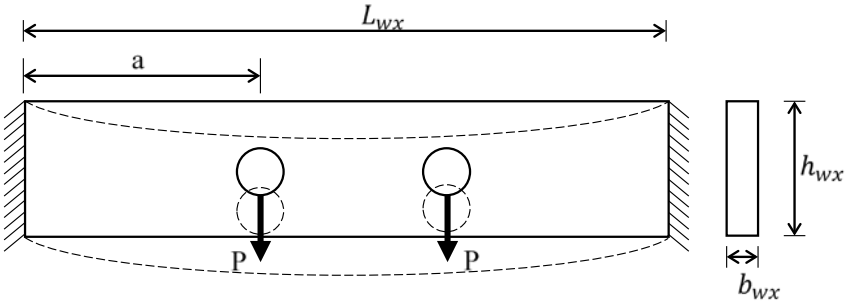

Fig. 4-13. Web extension component

The load-deflection relation for the loading condition shown in Fig. 4-13can be found using engineering mechanics in which the resistance is calculated based on the elastic moment capacity of the beam such that:

$$k_{wxb} = \frac{162EI_{wx}}{L_{wx}^3} \quad \text{(Eq. 4.34)}$$

$$F_{wxt,Rd} = \frac{81b_{wx}h_{wx}^2 f_{uwx}}{48L_{wx}} \quad \text{(Eq. 4.35)}$$

where, I_{wx} is the second moment of inertia of the cross-section of the web extension, L_{wx} is the length of the web extension, and b_{wx} and h_{wx} are cross-section dimensions shown in Fig. 4-13. The above relations are found taking $a = L_{wx}/3$, which is the case for the

connection of this study. It is noted that f_{uwx} is the ultimate strength of the web extension material.

4.2.2.10 Angle leg in tension

The top angle leg (part 6-1) and the web angle legs (parts 9-1,9-2) contribute to the ductility of the connection and their capacity should be taken into account in order to be able to have a more realistic model. The stiffness and resistance of these components are as follows [36]:

$$k_{at} = \frac{EL_{eff,a}t_a}{g_a} \quad \text{(Eq. 4.36)}$$

$$F_{at,Rd} = L_{eff,a}t_a f_{ya} \quad \text{(Eq. 4.37)}$$

in which $L_{eff,a}$ is the effective length based on the definitions of Eurocode 3 [44], g_a is the gauge length of the angle which is the length of the outstanding angle leg under tension measured in the load direction (Fig. 4-9), $f_{ya}$is the yield strength of the angle material, and t_a is the thickness of the angle.

4.2.3 Compression zone and shear behaviour

According to Fig.1, the seat angle in bending (part 6-2 in Fig. 4-1), and the corner tubes of the column in compression and the plate in bending (part 2 in Fig. 4-1) are chosen as the components representing the compressive behaviour of the joint. The seat angle in bending and the plate in bending are similar to the top angle in bending and the plate in bending, as explained in Section 2.2. However, the flexibility and resistance of the corner tubes of the column in compression can be obtained from [53] and Table 7.4 in [44], respectively:

$$k_{ctc} = \frac{\pi E \alpha H_{ep}(D_{tb} - 2T_2)}{360\left(t_{ep} + t_{tb}\right)} \quad \text{(Eq. 4.38)}$$

$$F_{ctc,Rd} = k_p T_2^2 f_{ytb} \frac{(4 + 20\beta^2)(1 + 0.25\eta)}{\gamma_{M5}} \quad \text{(Eq. 4.39)}$$

where, α, t_{ep} are shown in Fig. 4-14. It is assumed that the connection's corner part is bearing on the tube wall through applying a distributed pressure force.

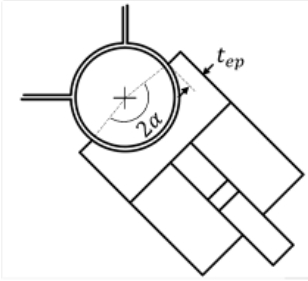

Fig. 4-14. Corner bottom part and tube assembly

It is assumed that the compressive force is distributed on the tube wall through the corner bottom part (parts 3-1 to 3-4 in Fig. 4-1) so that the tube wall acts as a bearing plate. The column side walls (i.e. the flat plates between corner tubes), deform noticeably less than other components of a joint, and therefore their contribution can be neglected in both tension and compressive behaviour of the joint [39]. In addition, web panel shear which happens in open sections is transferred to the side plates and the relevant formulation in the case of open section joints could be used for the hollow sections [39]. Neglecting the column axial load effects, the design shear resistance of the panel zone can be computed using the following equation [18]:

$$V_{cws} = \frac{f_{ycw} A_{vc}}{\sqrt{3}\gamma_{M0}} \qquad \text{(Eq. 4.40)}$$

$$A_{vc} = 2(W_1 + W_2 - 2D_{tb})T_1 + 4\pi T_2 \qquad \text{(Eq. 4.41)}$$

in which f_{ycw} is the yield strength of the column web, A_{vc} is the shear area of the column and γ_{M0} is the partial safety factor. W_1, W_2, T_1 are shown in Fig. 4-15.

4.2.4 Rotation capacity

The more complex a connection, the more complicated its behaviour. Bolts, angles, plates and each component of the connection may be a source for the failure of a joint. As the results of the experimental tests performed on the connection under investigation in this study suggest, the main source of failure is chosen to be the top angle seat. Therefore, the failure of this component has been investigated in the modelling of the joint. Different criteria have been proposed for the prediction of the axial deformation capacity of angle connections [54]. The criterion introduced by Shen and Astaneh-Asl [55] is adopted in the modelling in the present research. According to this method, the failure will happen in an angle under tension (which is the case in the joint in this study.) The rotation of the connection components compared to the top angle is negligible. Thus, the top angle is the

main source of deformation (Δ_t) in tension area. The compression area also undergoes deformation (Δ_c), which is more prominent in the case of corner tubes of mild steel material. These deformations occur in horizontal direction and therefore the rotation capacity of the connection before failure (θ_{Cd}) can be calculated using the following equation:

$$\theta_{Cd} = \tan^{-1}\left(\frac{(\Delta_t + \Delta_c)}{L}\right) \tag{4.42}$$

where L is the beam length and

$$\Delta_t = 2(g_1 - t_a)\varepsilon_u\sqrt{t_a/\big((g_1 - t_a)\varepsilon_u\big)} \tag{4.43}$$

$$\Delta_c = \frac{\sum_1^{n_c} F_{Rd}^{Tr}}{K_c} \tag{4.44}$$

in which ε_u is the ultimate tensile strain of the angle material taken as 0.35, g_1 is the distance from the centre of the bolt hole to the face of the beam on the outstanding leg of the angle, and t_a is the angle thickness. The above value is then used to predict the rotation capacity of the connection before failure (θ_{Cd}).

4.3. Illustration

In order to verify the results of the component-based model proposed in Section 2, finite element (FE) analysis was used using ABAQUS. FE analysis provides the opportunity to implement the idealisations used in the mechanical model, such as material properties and boundary conditions, or trace the onset of different events, like the yielding of different components. It is worth noting that the FE model used in this section has already been validated against the experimental results conducted on the connection under investigation in this study [14]. The FE model is a three-dimensional (3-D) representation of the joint with material and geometrical non-linearities included. Contacts between different parts of the connection are also modelled. The top and bottom surfaces of the column are fixed while the load is applied in displacement control mode at the free end of the attached beam. In order to be consistent with the assumption of the minimal contribution of side plates in the stiffness of the joint, the side plates of the column are assumed to be rigid. The element used for the simulation is C3D8R type, which is recommended for analyses with non-linear nature such as large deformations, contact, etc. [56]. C3D8R is a brick element with reduced integration and hourglass control. A schematic of the column cross-section,

loading and boundary conditions of the FE model is presented in Fig. 4-15. The column height is chosen to be 1m and the beam cross-section is taken as 200UB22.3 [57].

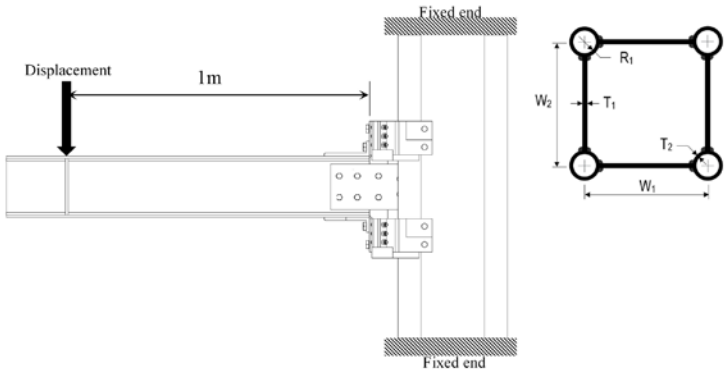

Fig. 4-15. FEA boundary conditions and column cross-section

Dimensions of the column are given in Table 4-2.

Table 4-2- HFC dimensions

Symbol	Value mm	Symbol	Value mm
W_1	286	T_1	3
W_2	286	T_2	3.2
		R_1	34.8

Numerical simulation was performed for the joint once with mild steel (MS) corner tubes and once with ultra-high strength steel (UHSS) corner tubes. The material properties can be found in Table 4-3 [14]. The same data were also used in the component-based modelling.

Table 4-3. Material Properties

Material	Modulus of Elasticity GPa	Poisson's Ratio -	Yield Stress MPa
Mild Steel (Grade 250)	195	0.29	266
Ultra-high Strength Steel	210	0.3	1260

The results of the component-based modelling and FE analysis for joints with MS corner tubes and UHSS corner tubes are presented in Fig. 4-16 (a) and (b), respectively. A summary of the results is also presented in Table 4-4.

Table 4-4. Summary of results

Corner Tube Material	Initial Stiffness $S_{j,ini}$ kNm/rad		Moment Resistance $M_{j,Rd}$ kNm	Rotation Capacity θ_{Cd} rad	Ultimate Moment M_u kNm
	Component	FEA			
Mild Steel (Grade 250)	3990.2	3465.2	62.8	0.088	71.0
Ultra-high Strength Steel	4008.3	3542.5	69.4	0.102	79.42

As the results suggest, the component-based model proposed here predicts the connection to respond more stiffly to the loading compared to the FE model. This over-estimation could be due to bolt slippage, bolt pre-tension, residual stresses or imperfections [36], which are modelled in the FE analysis but not in the component-based model. However, the discrepancies are not significant. Obviously, as a result of the tri-linear behaviour assumption in the model, it is not possible to capture the exact non-linear behaviour of the joint. Nevertheless, the post-yield section of the curve is close to the behaviour of the joint predicted by the FE model. Regarding the failure prediction, in the case of the column with UHSS corner tubes, the failure determined by the experimental test happens at 0.112 rad rotation [14], while the prediction given by the component-based model in this study is 0.102 rad, indicating a good estimate of the failure point. Moreover, the prediction based on Eurocode 3 [44] after the first linear zone is less accurate than the results of this study, and after the moment reaches the moment resistance of the connection, its results deviate even more from the FE model predictions and is not able to capture the non-linear behaviour of the connection.

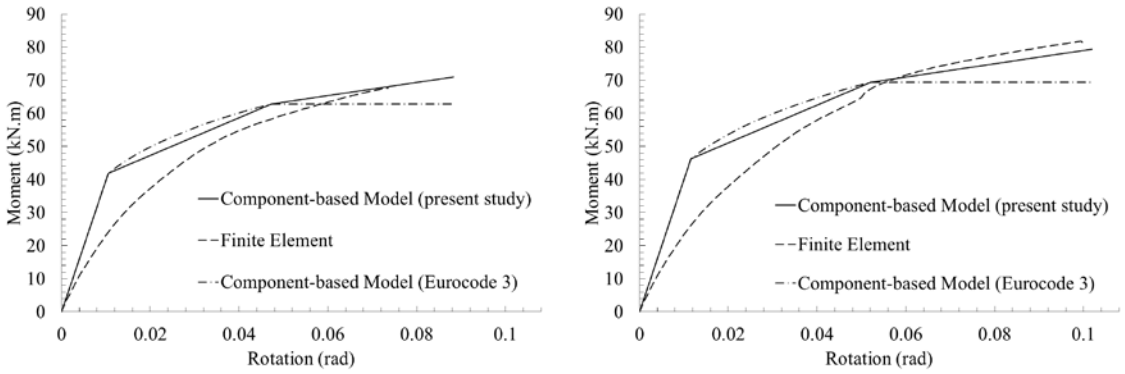

(a) Joint with column with MS corner tubes (b) Joint with column with UHSS corner tubes

Fig. 4-16. Comparison of results

4.4. Conclusion

Component-based modelling is proven to be a reliable and flexible method for the prediction of the behaviour of different connections. In this method, the joint is decomposed into its basic components with previously known behaviour. In the present research a component-based model was developed for an innovative connection, which has been recently proposed by the authors, for beam-to-hybrid fabricated column connections. The results of this model are compared with those of an FE model. The developed component-

based model is shown to be able to closely predict the initial stiffness, moment resistance and deformation capacity of the joint. The concept of the component model developed in this research work can be used to conduct a comprehensive parametric study where other failure modes and the geometry boundary for each failure mode can be thoroughly investigated. Although the modelling method is consistent with the approach included in Eurocode 3 [44], since the resultant model of this study accounts for the remaining strength of the parts in the plastic hardening region by adopting a tri-linear moment-rotation curve with non-zero slopes, it is able to predict the joint behaviour more accurately compared to the results provided by Eurocode 3 [44], which suggests using a constant value for moment in this region. The developed model is also capable of prediction of the failure of the connection accurately, verified by comparison to the previously published experimental results. The resultant model can be efficiently used for further studies of the joint, such as parametric studies, or the provision of design recommendations without need for extensive experimental work or time-consuming FE simulations. However, the model requires further improvements, such as including other possible failure modes, more experimental testing and the development of exclusive relations for other new components and other loadings such as cyclic, impact, fire, etc. The proposed model is based on the fact that failure occurs at top angle. The effect of various failure modes, geometry boundary of each failure, and dimensions of the connection components is being investigated at Monash University through a parametric study.

Acknowledgement

The research work presented in this research work is supported by the Australian Research Council through a Discovery Project (DP150100442) awarded to the authors.

References

[1] Aoki T, Ji B. Experimental study on buckling strength of tri-tube steel members. In: The 3rd international conference on coupled instabilities in metal structures, Lisbon, Portugal; 2000. p. 283–90.

[2] Javidan F, Heidarpour A, Zhao XL, Minkkinen J. Application of high strength and ultra-high strength steel tubes in long hybrid compressive members: Experimental and numerical investigation. Thin-Walled Structures 2016;102:273–285.

[3] Nassirnia M, Heidarpour A, Zhao XL, Minkkinen J. Innovative hollow columns comprising corrugated plates and ultra high-strength steel tubes. Thin-Walled Struct 2016;101:14–25.

[4] Nassirnia M, Heidarpour A, Zhao XL, Minkkinen J. Innovative hollow corrugated columns: a fundamental study. Eng Struct 2015;94:43–53.

[5] Zhao XL, Van Binh D, Al-Mahaidi R, Tao Z. Stub column tests of fabricated square and triangular sections utilizing very high strength steel tubes. J Constr Steel Res 2004;60:1637–61.

[6] Van Binh D, Al-Mahaidi R, Zhao XL. Finite element analysis (FEA) of fabricated square and triangular section stub columns utilizing very high strength steel tubes. Adv Struct Eng 2004;7:447–57.

[7] Javidan F, Heidarpour A, Zhao X-L, Hutchinson CR, Minkkinen J. Effect of weld on the mechanical properties of high strength and ultra-high strength steel tubes in fabricated hybrid sections. Eng Struct 2016;118:16–27.

[8] Heidarpour A, Cevro S, Song QY, Zhao XL. Behaviour of innovative stub columns utilising mild-steel plates and stainless steel tubes at ambient and elevated temperatures. Eng Struct 2013;57:416–27.

[9] Heidarpour A, Cevro S, Song QY, Zhao XL. Behaviour of stub columns utilising mild-steel plates and VHS tubes under fire. J Constr Steel Res 2014;95:220–9.

[10] Farahi M, Heidarpour A, Zhao XL, Al-Mahaidi R. Compressive behaviour of concrete-filled double-skin sections consisting of corrugated plates. Eng Struct 2016;111:467–77.

[11] Nassirnia M, Heidarpour, A, Zhao XL, Wang R, Li W, Han LH. Experimental behavior of innovative hollow corrugated columns under lateral impact loading. 2017 Proceediings of the 11th International Symposium on Plasticity and Impact Mechanics,

IMPLAST 2016: 11-14 December 2016, Indian Institute of Technology Delhi, New Delhi. Gupta, N. K. & Iqbal, M. A. (eds.). p. 383-390. (Procedia Engineering; vol. 173)

[12] Nassirnia M, Heidarpour A, Zhao XL. A benchmark analytical approach for evaluating ultimate compressive strength of hollow corrugated stub columns. Thin-Walled Structures 2017;117:127-139.

[13] Farahi M, Heidarpour A, Zhao X-L, Al-Mahaidi R. Effect of ultra-high strength steel on mitigation of non-ductile yielding of concrete-filled double-skin columns. Construction and Building Materials 2017;147:736-749.

[14] Sadeghi SN, Heidarpour A, Zhao XL, Al-Mahaidi R. An innovative I-beam to hybrid fabricated column connection: Experimental investigation. Engineering Structures, 2017;148:907-923.

[15] Sadeghi N, Heidarpour A, Zhao XL, Al-Mahaidi R. Numerical investigation of innovative modular beam-to-fabricated column connections under monotonic loading. In: Zingoni A, (ed.) Insights and Innovations in Structural Engineering, Mechanics and Computations. Cape Town, South Africa: Taylor and Francis Group, LLC; 2016. p. 1247–52.

[16] FEMA-350, 2000, Recommended Seismic Design Criteria for New Steel Moment-Frame Buildings, prepared by the SAC Joint Venture for the Federal Emergency Management Agency, Washington, DC.

[17] Daz C, Mart P, Victoria M, Querin OM. Review on the modelling of joint behaviour in steel frames. Journal of Constructional Steel Research, 2011;67(5):741–58.

[18] Faella C, Piluso V, Rizzano G. Structural steel semi-rigid connections : theory, design, and software. CRC Press, Boca Raton ; London, 2000.

[19] Bose SK, McNeice GM, Sherbourne AN. Column webs in steel beam to column connexions. Part I: formulation and verification. Computers & Structures 1972;2:253–72.

[20] Yang C, Yang JF, Su MZ, Liu CZ. Numerical study on seismic behaviours of ConXL biaxial moment connection. Journal of Constructional Steel Research. 2016;121:185–201.

[21] Alhasawi A, Guezouli S, Couchaux M. Component-Based Model Versus Stress-Resultant Plasticity Modelling of Bolted End-Plate Connection: Numerical Implementation. Structures 2017;164–77.

[22] Zoetemeijer P. Summary of the research on bolted beam-to-column connections (period 1978–1983). Delft: Stevin II Laboratory; 1983.

[23] Wales MW, Rossow EC. Coupled moment-axial force behaviour in bolted joint. Journal of Structural Engineering 1983;109(5):1250–66.

[24] Tschemmernegg F. On the nonlinear behaviour of joints in steel frames. In Connections in Steel Structures: Behaviour, Strength and Design (ed. R. Bjorhovde et al.). Elsevier Applied Science Publishers, London, 1988, pp. 158-165.

[25] Tschemmernegg F, Humer C. The design of structural steel frames under consideration of the non-linear behaviour of joints. Journal of Constructional Steel Research 1988;11:73-103.

[26] Jaspart JP. (1991), "Etude de la semi-rigidité des nœuds poutre-colonne et son influence sur la résistance et la stabilité des ossatures en acier", PhD Thesis, Université de Liège.

[27] Jaspart JP. (1997), "Recent advances in the field of steel joints: Column bases and further configurations for beam-to-column joints and beam splices", Universite de Liege.

[28] Lopes F, Santiago A, Simões da Silva L, Heistermann T, Veljkovic M, Guilherme da Silva J. Experimental behaviour of the reverse channel joint component at elevated and ambient temperatures. International Journal of Steel Structures 2013;13(3):459–72.

[29] Málaga-Chuquitaype C, Elghazouli AY. Component-based mechanical models for blind-bolted angle connections. Engineering Structures 2010;32(10):3048–67.

[30] Simões da Silva L. Towards a consistent design approach for steel joints under generalized loading. Journal of Constructional Steel Research 2008;64(9):1059–75.

[31] Del Savio AA, Nethercot DA, Vellasco PCGS, Andrade SAL, Martha LF. Generalised component-based model for beam-to-column connections including axial versus moment interaction. Journal of Constructional Steel Research 2009;65(8–9):1876–95.

[32] De Lima LRO, De Andrade SAL, Da PCG, Da Silva LS. Experimental and mechanical model for predicting the behaviour of minor axis beam-to-column semi-rigid joints. International Journal of Mechanical Sciences. 2002;44(6):1047–65.

[33] Demonceau JF, Weynand K, Jaspart JP, Müller C. Application of Eurocode 3 to steel connections with four bolts per horizontal row. In Proceedings of the SDSS'Rio 2010 conference 2010;199-206. Rio de Janeiro.

[34] Da Silva, Ahahbazian, Gentili, Augusto. Implementation of a component model for the cyclic behaviour of steel joints. Eighth international workshop on connections in steel structures, CONNECTIONS VIII Boston, Massachusetts, USA. 2016; 2016.

[35] Block FM, Davison JB, Burgess IW, Plank RJ. Principles of a component-based connection element for the analysis of steel frames in fire, Engineering Structures 2013;49:1059-1067.

[36] Sulong NR, Elghazouli AY, Izzuddin BA, Ajit N. Modelling of beam-to-column connections at elevated temperature using the component method. Steel and Composite Structures. 2010 Feb 1;10(1):23-43.

[37] Jaspart JP. Weynand K. 2001. Extension of the component method to joints in tubular construction, in Proceedings of the Ninth International Symposium and Euroconference on tubular structures. Düsseldorf, 517–523.

[38] Jaspart JP, Weynand K. Design of hollow section joints using the component method. Proceedings of the 15th International Symposium on Tubular Structures, Rio de Janeiro, Brazil, 27-29 May 2015. p. 405–10.

[39] Weynand K, Jaspart JP, Ly L. Application of the Component Method to Joints between Hollow and Open Sections (CIDECT Final Report : 5BM). Liège, Belgium; 2003.

[40] Weynand K, Busse E, Jaspart JP. First practical implementation of the component method for joints in tubular construction. Welding in the World. 2006. p. 126–32.

[41] Thai HT, Uy B. Rotational stiffness and moment resistance of bolted endplate joints with hollow or CFST columns. Journal of Constructional Steel Research 2016;126:139–52.

[42] Lee J, Goldsworthy HM, Gad EF. Blind bolted moment connection to sides of hollow section columns. Journal of Constructional Steel Research 2011;67(12):1900–11.

[43] Silva LAP, Neves LFN, Gomes FCT. Rotational Stiffness of Rectangular Hollow Sections Composite Joints. Journal of Structural Engineering 2003;129(4):487–94.

[44] European Committee for Standardisation (CEN). (2005). Eurocode 3. Design of Steel Structures, Part 1-8: Design of Joints. Brussels: CEN.

[45] European Committee for Standardisation (CEN). (2004). Eurocode 4: Design of composite steel and concrete structures - Part 1-1: General rules and rules for buildings. Brussels: CEN.

[46] Mohamadi-Shoore MR, Mofid M. New modeling for moment–rotation behavior of bolted endplate connections. Scientia Iranica 2011;18(4):827–34.

[47] Piluso, V, Faella C, RizzanoG. Ultimate behavior of bolted T-stubs. II: Model validation. J Struct Eng ASCE 2001;127(6):694–704.

[48] Faella C, Piluso V, Rizzzano G. A new method to design extended end plate connections and semi rigid braced frames. Journal of Constructional Steel Research 1997;41:61-91.

[49] De Stefano M, Astaneh A. Axial force-Displacement behavior of steel double angles. Journal of Constructional Steel Research 1991;20(3):161–81.

[50] Neves LC, Gomes F. Semi-Rigid behaviour of beam-to-column minor-axis joints. In: Eth-Honggerberg, Zurich, Switzerland, Proceedings of the IABSE International Colloquium on Semi-Rigid Structural Connections, Istanbul, Turkey, 1996. p. 207–16.

[51] Wang JF, Han LH, Uy B. Hysteretic behaviour of flush end plate joints to concrete-filled steel tubular columns. Journal of Constructional Steel Research 2009;65(8–9):1644–63.

[52] Ghobarah A, Mourad S, Korol RM. Moment-rotation relationship of blind bolted connections for HSS columns. Journal of Constructional Steel Research 1996;40(1):63–91.

[53] Yao H, Goldsworthy H, Gad E. Simplified component model for curved T-stub connection to concrete-filled steel tube with blind bolts and extensions. Earthquake Engineering in Australia. Canberra, Australia; 2006. p. 289–98.

[54] Gong Y. Ultimate tensile deformation and strength capacities of bolted-angle connections. Journal of Constructional Steel Research 2014;100:50–9.

[55] Shen J, Astaneh-Asl A. Hysteresis model of bolted-angle connections. Journal of Constructional Steel Research. 2000;54(3):317–43.

[56] ABAQUS 6.14-1. Providence, RI, USA: Dassault Systèmes; 2014.

[57] AS/NZS 3679.1:2016 Structural steel - Hot-rolled bars and sections. Standards Australia; 2016.

NUMERICAL INVESTIGATION OF THE BEHAVIOUR OF INNOVATIVE BEAM-TO-HYBRID CORRUGATED COLUMNS CONNECTION

CHAPTER 5

Table of Contents

Abstract

The hybrid-fabricated-columns (HFC) are known to show more load bearing capacity and better post buckling behaviour than conventional hollow sections. Among this new generation of columns, HFCs consisting of corrugated plates and corner tubes are known to have superior performance compared to the ones with flat plates. Several studies have been performed on the performance of this type of column with different configurations, corner tube materials and loading conditions. However, finding a proper connection for attaching I-beams to this type of column is challenging. The authors have recently proposed an innovative type of connection that can be used along with HFCs. The current research work presents the results of numerical simulations conducted on the behaviour of the aforementioned innovative connection under monotonic loading used along with HFCs with corrugated plates using a full 3-dimensional finite element model. Firstly, the behaviour of the original modular connection attached to the corrugated HFC is compared to that of the connection with flat plates HFC. Thus, a thinned version of the connection, which unlike the original connection is not reusable, is also investigated and compared with the original connection. Finally, considering the more flexible behaviour of the corrugated HFC, the behaviour of a bi-directional connection, which is one of the features of the innovative connection, is studied. It is demonstrated that this configuration of the connection has higher stiffness and reduces the lateral flexibility of the corrugated plates.

Keywords: hybrid fabricated column; corrugated plate; modular bolted connection; finite element method; ultra-high strength; moment-rotation curve; monotonic loading; bi-directional connection.

5.1 Introduction

Corrugated plates are known to have higher load bearing capacity compared to flat plates. Their specific shape gives them a continuous stiffening effect, which allows for using thinner plates than flat plates under similar conditions. Common patterns of corrugated used in different applications are shown in Fig. 5-1.

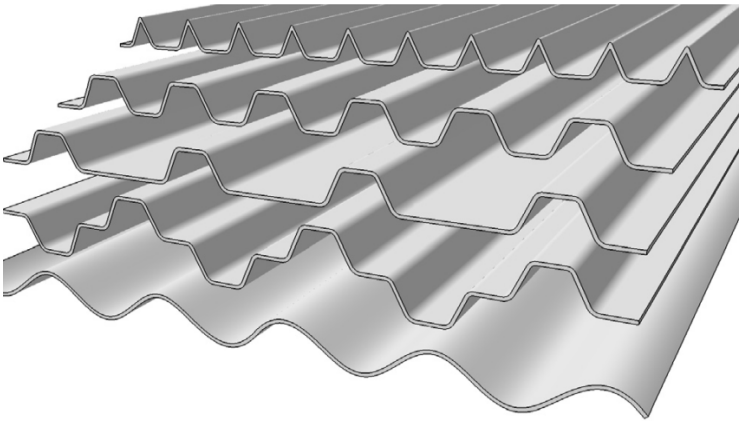

Fig. 5-1. Common corrugation patterns [1]

The higher stiffness and strength to weight ratios can be effectively used in many engineering applications, namely for structural applications. Many researchers have investigated the behaviour of individual corrugated plates while others have looked into the structural application of these plates as components in structural elements such as girders or columns [1 - 4].

In the past few years, hollow fabricated columns, among other structural elements, have gained more popularity due to higher load bearing capacity, energy absorption and better post-buckling behaviour. In general, fabricated columns, as the name suggests, are produced by putting different plates together through welding for forming the shape required by the designer. These plates can be corrugated or flat plates. The concept of using corrugated plates in fabricated columns was introduced and investigated by Nassirnia et al. [1]. A schematic view of the corrugated column used in this study is presented in Fig. 5-2.

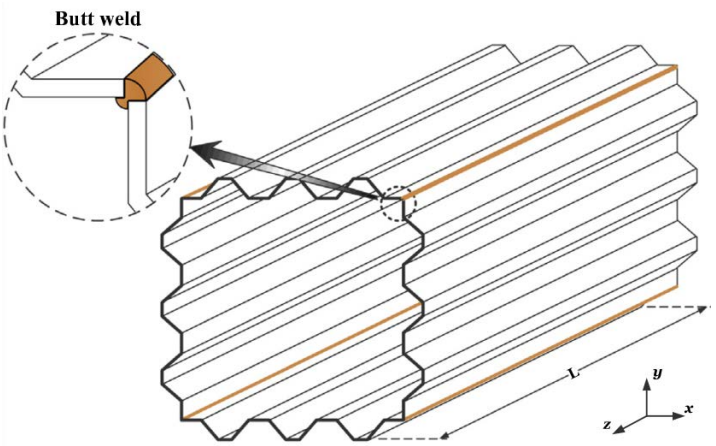

Fig. 5-2. Column consisting of corrugated plates [1]

The study conducted by Nassirnia et al. [1] has demonstrated the superior performance of this type of fabricated column, compared to the conventional rectangular flat hollow section in terms of load bearing capacity, energy absorption and even from economical point of view.

Another structural element that enjoys the benefits of using corrugated plates is hybrid fabricated column. This type of column is made of four plates attached to four corner tubes, forming a hollow closed section (Fig. 5-3).The performance of this column has been studied extensively at Civil Engineering Department of Monash University through an extensive experimental testing campaign and numerical simulations [5 - 12]. These investigations show that post buckling behaviour and load bearing capacity of hybrid fabricated columns could be improved by replacing the flat plates with corrugated ones.

(a) (b)

Fig. 5-3. Hybrid fabricated columns consisting of corner tubes and (a) flat plates (b) corrugated plates

Considering the superior performance of hybrid fabricated columns with corrugated plates, they could be a suitable choice in moment-resisting frames and in applications where there are needs for reliable members with superior performance. In order for so that these columns be used in construction, there should be a robust structural beam-to-column connection. The authors have recently proposed an innovative type of connection that can

be used along with hybrid fabricated columns [13],[14]. This modular connection shows high ductility while being able to deliver a high moment capacity, enabling the frame to satisfy the weak beam-strong column design philosophy.

In this work, the performance of hybrid fabricated column with corrugated plates in conjunction with the aforementioned innovative connection is investigated using finite element method. The moment-rotation curves of the connection attached to the corrugated hybrid column is compared with those of the connection attached to a hybrid column with flat plates in different cases including original connection, reduced size connection, and bidirectional connections.

5.2 Numerical modelling

The numerical model used in this study is a full three-dimensional (3D) finite element model, created in Abaqus [15] under static monotonic loading with displacement control. Both material and geometry non-linearities were included in the model in order to better capture the behaviour of the joint. The beam used in the simulations is of 200UB22.3 [16] type and 1.2m long. The column geometry and dimensions are presented in Fig. 5-4 (a). The corrugation type used in this study is shown in Fig. 5-4 (b) with the dimensions given in Fig. 5-4 (c). Plates of the column are modelled as mild steel (Grade 250), referred to as MS, and the corner tubes are made of either MS material or ultra-high strength steel (Grade 1200), referred to as UHSS.

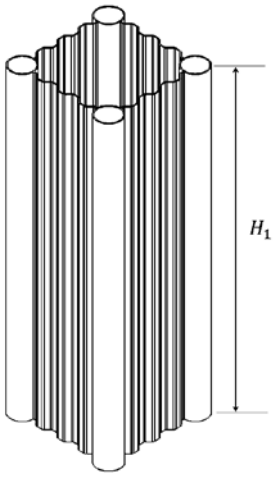

(a)

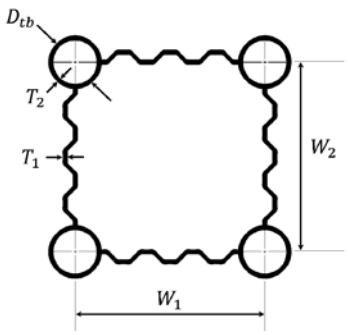

(b)

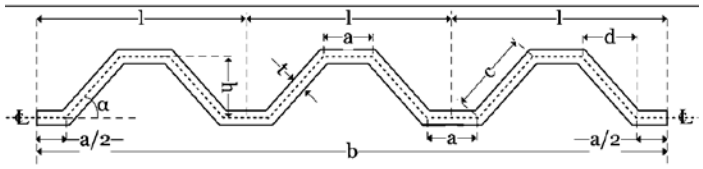

α (°)	a	h	t	l	d	c	b
45	20	15	3	70	15	21.21	210

(c)

Fig. 5-4. Dimensions used in the FE model

Table 5-1 presents the values of the parameters introduced in Fig. 5-4 (a) and (b).

Table 5-1. Dimensions of the hybrid fabricated column cross-section

Symbol	Value	Symbol	Value
	mm		mm
W_1	286	T_1	3
W_2	286	T_2	3.2
H_1	1000	D_{tb}	34.85

The external dimensions of this column are kept the same with the dimensions of the flat HFC used in the previous studies on the behaviour of the connection along with flat HFC to make the comparison of the results reasonable.

5.2.1 Material properties

The material properties of mild steel and ultra-high strength steel used in the simulations are taken form the experimental worked performed by Javidan et al [9] and given in Table 5-2.

Table 5-2. Material properties

Material	Modulus of Elasticity	Poisson's Ratio	Yield Stress
	GPa	-	MPa
Mild Steel (Grade 250)	195	0.29	266
Ultra-high Strength Steel	210	0.3	1260

In addition to the plates of the column, the connection components and the beam are also modelled using the Grade 250 mild steel properties. Ductile damage behaviour of these two grades of steel materials have been implemented in the modelling to ensure more realistic results. Bolts used in the simulations are assumed to be of Grade 8.8 with their multi-linear behaviour taken into account [17].

5.2.2 Meshing

The 3D model of the connection was meshed using C3D8R elements. This 8-node brick element with hour-glass effect control and reduced integration is the recommended element

for simulations with non-linear characteristics such as large deformation, contact or plasticity. Element sizing was controlled using the suitable sections created on different parts to ensure that the mesh size and density are sufficient to capture the interactions, especially in contact areas where the proper mesh sizing on slave/master surfaces is crucial for modelling the behaviour. Meshing of the corrugated HFC as a sample of meshing on the connection parts can be found in Fig. 5-5.

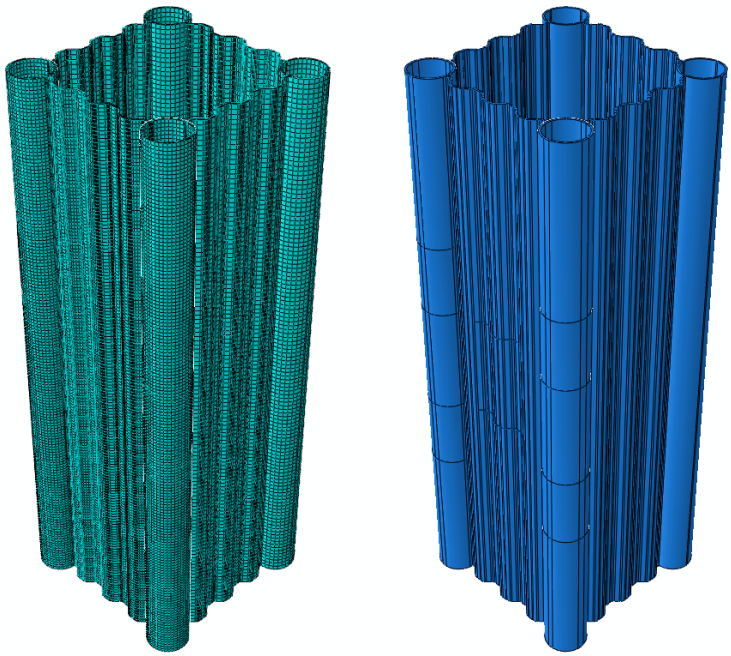

Fig. 5-5. Meshing samples

5.2.3 Interactions and constraints

In the connection of the subject of this study, bolts and also components of the connection are in direct contact with one another and therefore, the accurate modelling of the interaction between different parts of the connection is vital. Similarity of the meshing geometry and assigning a finer mesh to the slave surface in contact pairs is crucial. The contact definition in this model is done using surface-to-surface definition with finite sliding formulation. This definition allows for modelling the arbitrary relative motion of interacting parts. The normal behaviour is of hard contact type with separation after contact, allowed. The tangential behaviour is modelled using Coulomb friction. Since modelling the interaction of the bolts and nuts would have no significant effect on predicting the overall behaviour of the connection, but increasing the simulation time noticeably, they are modelled as unified items called fasteners. In order to ensure that the contacts are formed

and work as intended prior to the beginning of the loading, a separate load step, before the main loading step was dedicated to formation of the contacts. When connection parts are welded together, “Tie” constraint has been used to define the relevant interaction.

5.2.4 Boundary conditions and loading

Overview of the model used for FE analysis of the connection attached to the column with corrugated columns is shown in Fig. 5-6. The reason for choosing such setup is the possibility of comparing the results of current study with the pervious results obtained by the authors [13 , 14] on the connection attached the flat HFC. In this setup, the bottom plate as well as the base of the support structure are fully fixed. Top plate is under 50kN compressive axial force, which simulates the gravity load. This load level is chosen in a way to have the least effect on the behaviour of the connection while it is kept within the range of the gravity load on columns in high-rise buildings [18]. The loading ram is able to only move vertically and the loading is applied in displacement format in downward direction. Fasteners are loaded by an amount of displacement, which is proportional to their corresponding bolt pitch size.

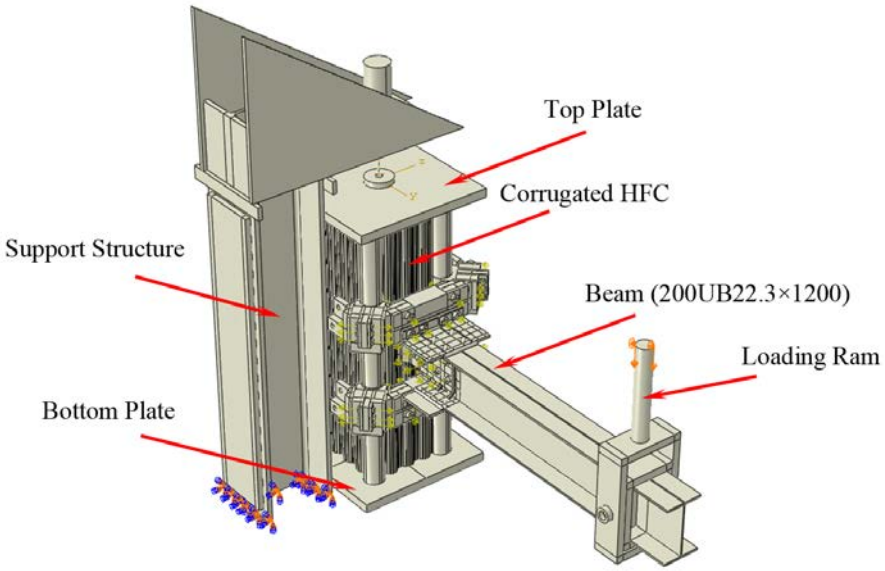

Fig. 5-6. Simulation setup

5.3 Results and discussion

In this study two different versions of the aforementioned innovative connection have been studied. The first version is called “original connection”, which has been simulated numerically and tested experimentally by authors recently [13 , 14]. The performance of this connection attached to the corrugated HFC is simulated and compared to the results of

the flat HFC in this section. The second version is a connection comprising of similar components but with thinner dimensions; so it is called “reduced-size connection”. One of the characteristics of the original connection is its reusability. The simulation of this second version is aimed at investigating the behaviour of a non-reusable version of the connection used along with HFCs. Since this version of the connection has not been analysed before, a simulation and comparison of the results with flat HFC is also included in this study.

The moment-rotation curve of the connections is used for the purpose of comparing the behaviour of different connections. The rotation of the joint at any stage of the loading of the connection could consist of elastic and plastic deformations, resulting from global or local deformations taking place in the joint. However, the rotation used in this study as shown in Fig. 5-7, is measured using the vertical displacement of a point and its distance from the face of the connection by utilising the relation presented in Eq. 5.1.

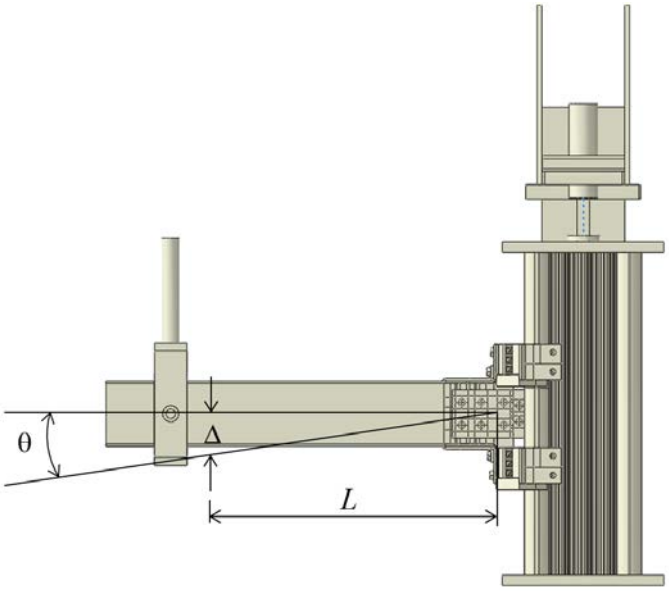

Fig. 5-7. Connection rotation

$$\theta = \tan^{-1}\frac{\Delta}{L} \qquad \text{Eq. 5.1}$$

In Eq. 5.1 L is the distance of the measurement point from the connection face and Δ is the vertical displacement measured at that point. This definition, which allows for the comparison of different connection using a uniform approach, is in accordance with globally accepted standards [19]. However, it is assumed that the rotation is small and the beam does not bend considerably.

5.3.1 Original connection

In this section the results of the simulation of the behaviour of the original version of the innovative connection used along with the corrugated HFC is presented. Considering the higher load bearing capacity and energy absorption and better post-buckling behaviour of the corrugated HFCs [7], the performance of the innovative connection used along with this type of HFCs is important. Details of the different parts of the connection are presented in Fig. 5-8.

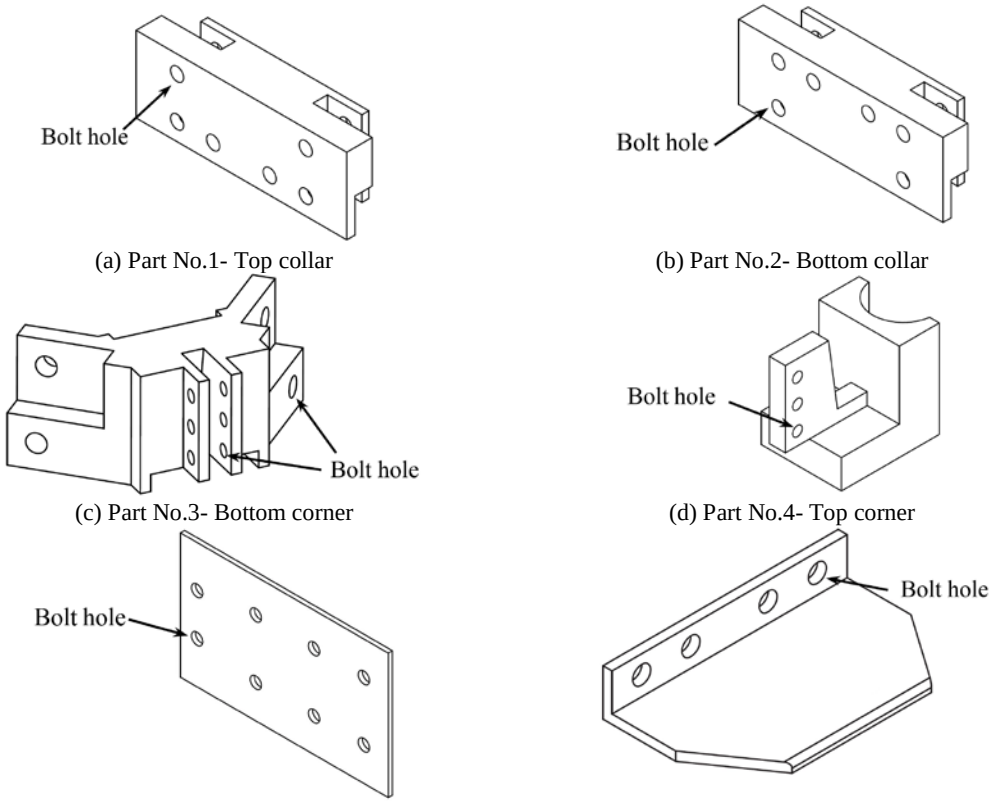

(a) Part No.1- Top collar (b) Part No.2- Bottom collar

(c) Part No.3- Bottom corner (d) Part No.4- Top corner

(e) Part No. 5- Side plate (f) Part No.6- Top/Seat angle

Fig. 5-8. Different parts of the innovative connection

The assembled connection has already been presented in Fig. 5-7. Four instances of Part No. 4 (Fig. 5-8 (d)) are welded to the corner tubes and other parts are assembled together and mechanically connected while being secured in their placed using bolts and nuts. Moment-rotation curve of the simulation in presented in Fig. 5-9. As the figure shows, the connection capacity is dropped compared to the connection attached to flat HFC, but in both cases (UHSS and MS corner tubes) the capacity is still more than the beam capacity (66 kN.m). The rotation capacity of the connection is beyond the 0.04 rad threshold [20] necessary for moment connections used in seismic applications.

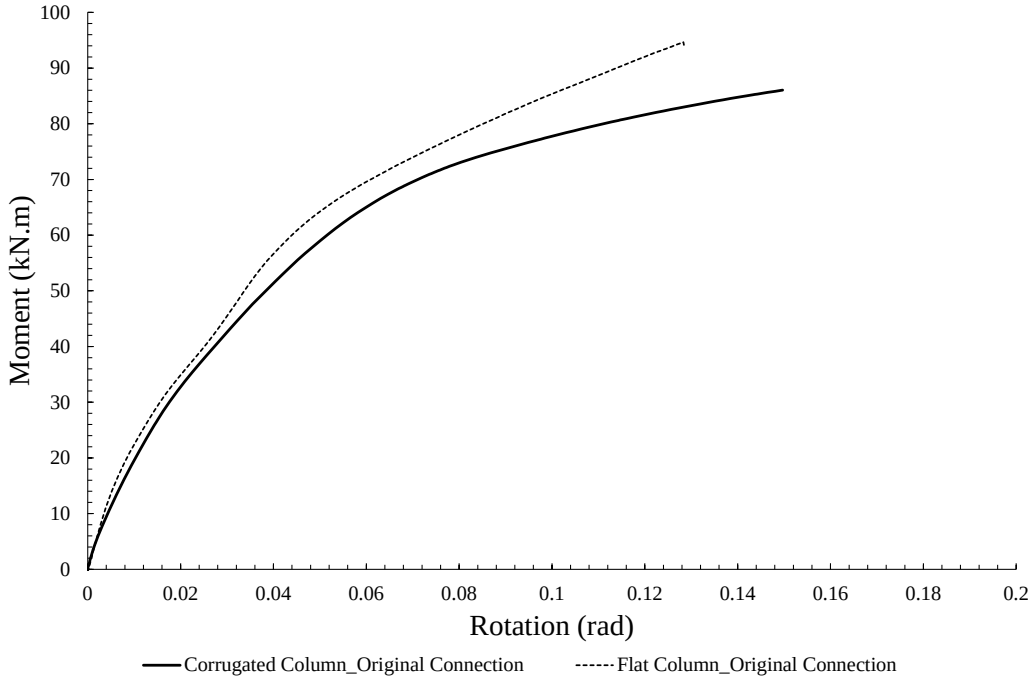

(a) Connection attached to HFC with UHSS corner tubes

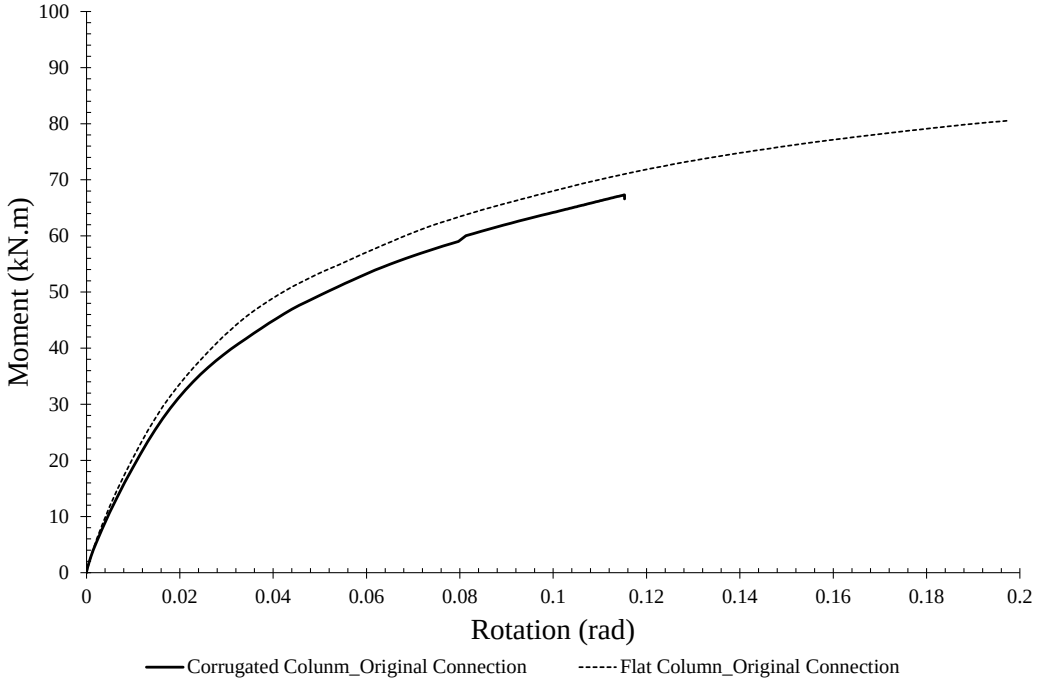

(b) Connection attached to HFC with MS corner tubes

Fig. 5-9. Comparison of behaviour of connection attached to corrugated HFC to flat HFC

The rotation capacity of the original connection attached to the corrugated HFC with MS tubes is less than the original connection used along with the flat HFC. The original connection possesses a similar initial stiffness to the one attached to the flat HFC. However, the general behaviour of the connection with corrugated HFC is less stiff. The reason could be attributed to the higher flexibility of the corrugated plate. It allows for a higher level of deformation in the column which eventually results in generally lower stiffness of the joint.

For instance, taking the corrugated plate attached to the side plates of the connection (part No. 5 in Fig. 5-8), and comparing its horizontal out of plane deformation (z direction) with that of the flat HFC, shows that a larger portion of the corrugated plate undergoes a higher amount of displacement (Fig. 5-10). It can also be observed how the area of greater displacements is localised in flat HFC compared to the corrugated one.

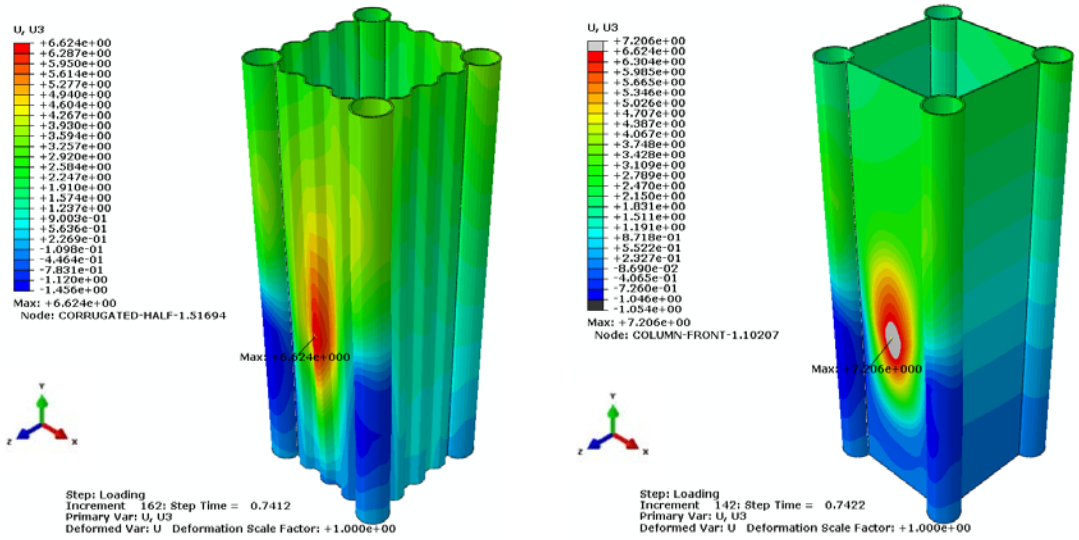

(a) Corrugated HFC (b) Flat HFC

Fig. 5-10. Z-direction displacement (mm)

The same phenomenon happens to the plates on the sides of the column. On the other hand, for the flat plate HFC, the plates on the sides of the column, due to the absence of corrugation are far stiffer. However, the maximum displacement on the flat column is slightly greater than the corrugated column, which is shown as the grey area in Fig. 5-10 (b).

Whereas the corner tubes are strong components of the HFCs, especially in the case of UHSS corner tubes, level of engagement of the corner tubes is important to be investigated to determine to what extent the capacity of these components has been used under loading. Fig. 5-11 shows the von Mises stress distribution on the columns in both MS and UHSS cases.

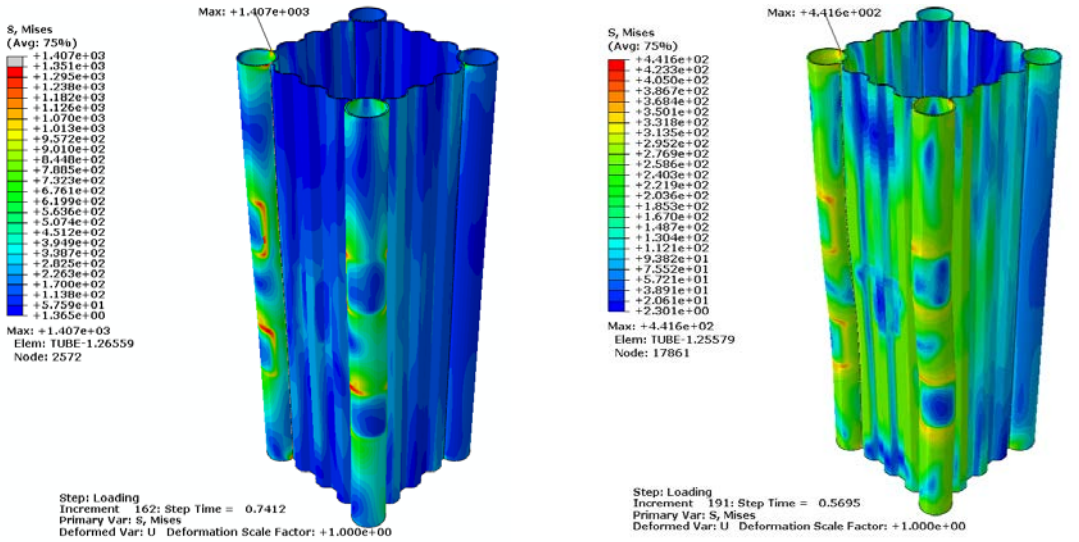

(a) UHSS corner tubes (b) MS corner tubes

Fig. 5-11. von Mises stress (MPa) distribution

It can be observed in these figures that the stress levels on the corner tubes are close to the ultimate strength of the corner tube materials in both cases, which shows that the connection has been able to utilise the material properties of the corner tubes effectively.

The aforementioned points in this section show that the performance of the original connection along with the corrugated column is as satisfactory and comparable to its performance along with the flat HFC.

5.3.2 Non-reusable connection

A topology optimisation and parametric study has been performed on the original connection used along with the flat HFC [13]. The goal of that study was reducing the weight of the connection while maintaining its main characteristics such as high capacity and reusability. In the current study, behaviour of a new version of the connection is investigated in which the components are thinned in a manner that they cannot be reused. For instance, the collar part of the connection in original and reduced-size versions is presented in Fig. 5-12. It can be seen that the connection thickness is reduced significantly but the minimum thickness is kept to the extent that the plate-like sections of the connection components can still be considered as thick to avoid local effects by bolts and nuts.

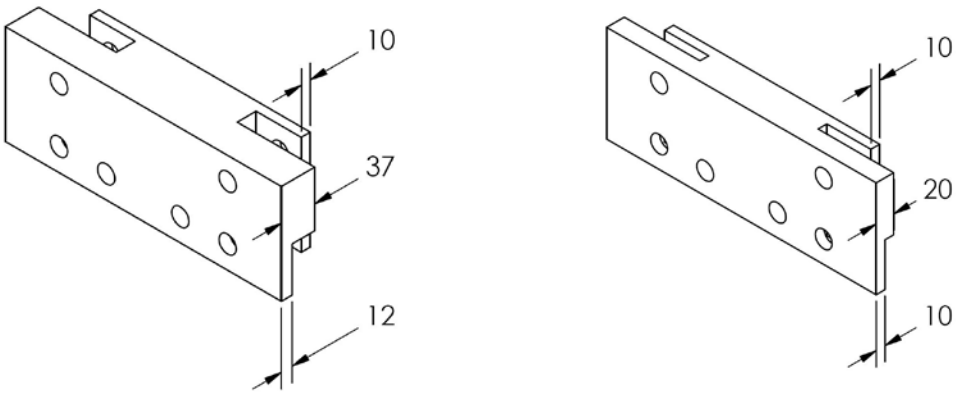

(a) Original connection (b) Thinned connection

Fig. 5-12. Top-collar parts

The weight of the non-reusable connection is 33.6% lower compared to the original connection. The modelling procedure and conditions are similar to what was explained in the previous sections. The result of the simulations is presented in Fig. 5-13. In order to be able to investigate the effect of corrugation on the performance of the non-reusable connection, its moment-rotation behaviour used along with HFC column consisting of flat plates was also investigated.

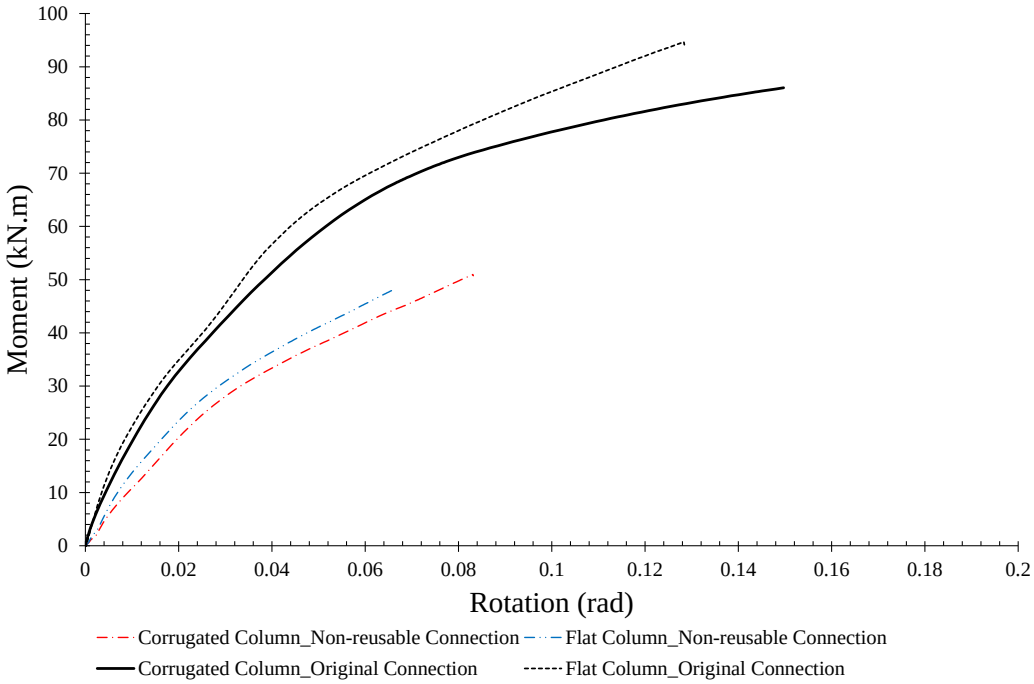

(a) Connection attached to HFC with UHSS corner tubes

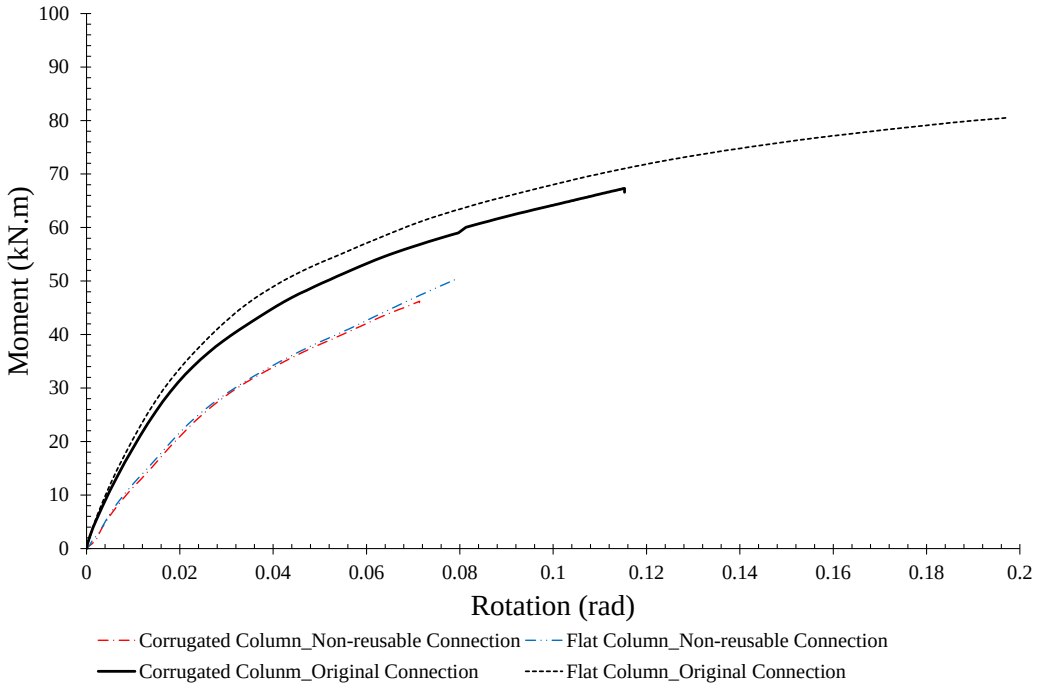

(b) Connection attached to HFC with MS corner tubes

Fig. 5-13. Behaviour of thinned connection attached to corrugated HFC and flat HFC

The results suggest that the capacity of the non-reusable connection is lower than the plastic moment capacity of the beam and thus, it is no longer a full resistance connection. The reduction in capacity is more noticeable in the HFCs with UHSS corner tube. The rotation of the non-reusable connection is also significantly less than the original connection; but in all cases it is still more than the 0.04 rad threshold recommended by AISC [20]. Comparison of the non-reusable connection attached to flat and corrugated HFCs shows that capacity and stiffness of the connection used along with the corrugated column is slightly lower, which in the case of HFC with UHSS corner tubes is more distinct. For instance at 0.04 rad rotation, the difference between capacity of flat HFC and corrugated HFC used along with the non-reusable connection in MS case is negligible while for UHSS case is about 9%. The lost capacity for corrugated HFC with UHSS corner tubes from original to non-reusable connection is 39%, while for MS case it is 25%. The effect of difference in material properties of the corner tubes is also negligible for the column with corrugated column, while for the flat HFC this difference is more evident. Moment capacity at 0.04 rad rotation is 16% increased for changing the corner tube material from MS to UHSS. A similar increase in capacity is observed for corrugated HFC used along with original connection.

The distribution of the equivalent plastic strain (PEEQ) on the collars of the connection can be used as an indicator of the reusability of the connection parts. The PEEQ distribution is presented in Fig. 5-14 for both flat and corrugated HFCs with MS and UHSS tubes.

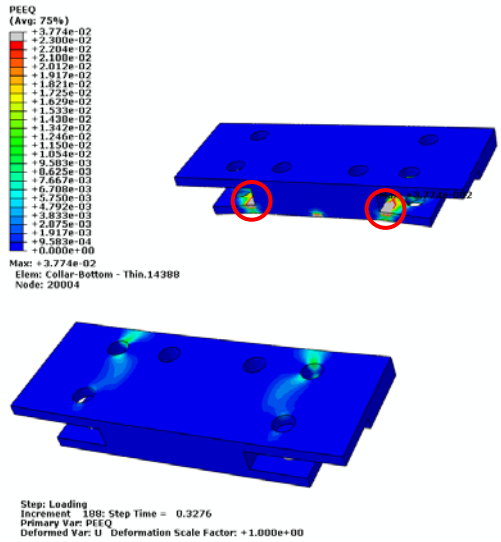

(a) Corrugated HFC with UHSS corner tubes

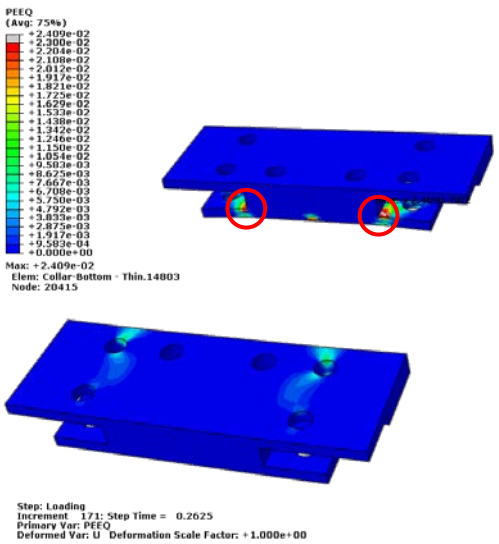

(b) Flat HFC with UHSS corner tubes

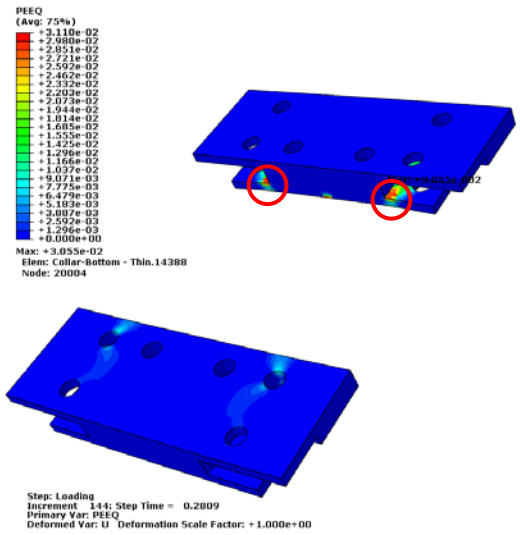

(c) Corrugated HFC with MS corner tubes

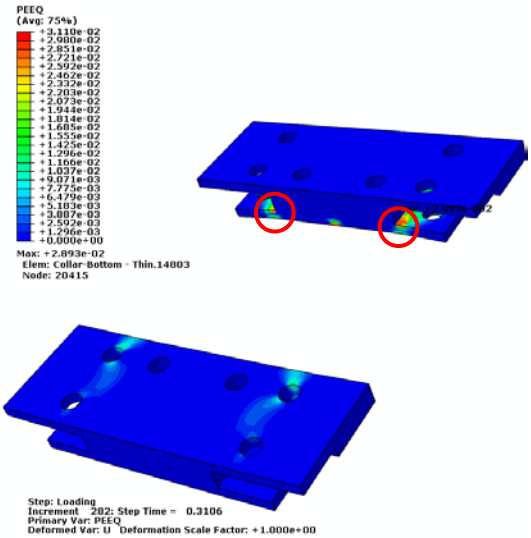

(d) Flat HFC with MS corner tubes

Fig. 5-14. PEEQ distribution on collars

The areas marked with circles are the zones in which the maximum level of PEEQ occurs and these levels are higher than the levels pertaining to the failure of the connection established in the previous studies by the authors [13]. This shows that the connection is not reusable at this stage. The connection components with the dimensions of the current version could be used in cases where reusability is not necessary but modularity and high rotation are required.

Similar to the past section, the level of engagement of the corner tube materials is important. Fig. 5-15 shows von Mises stress distribution on flat and corrugated HFC with MS and UHSS corner tubes.

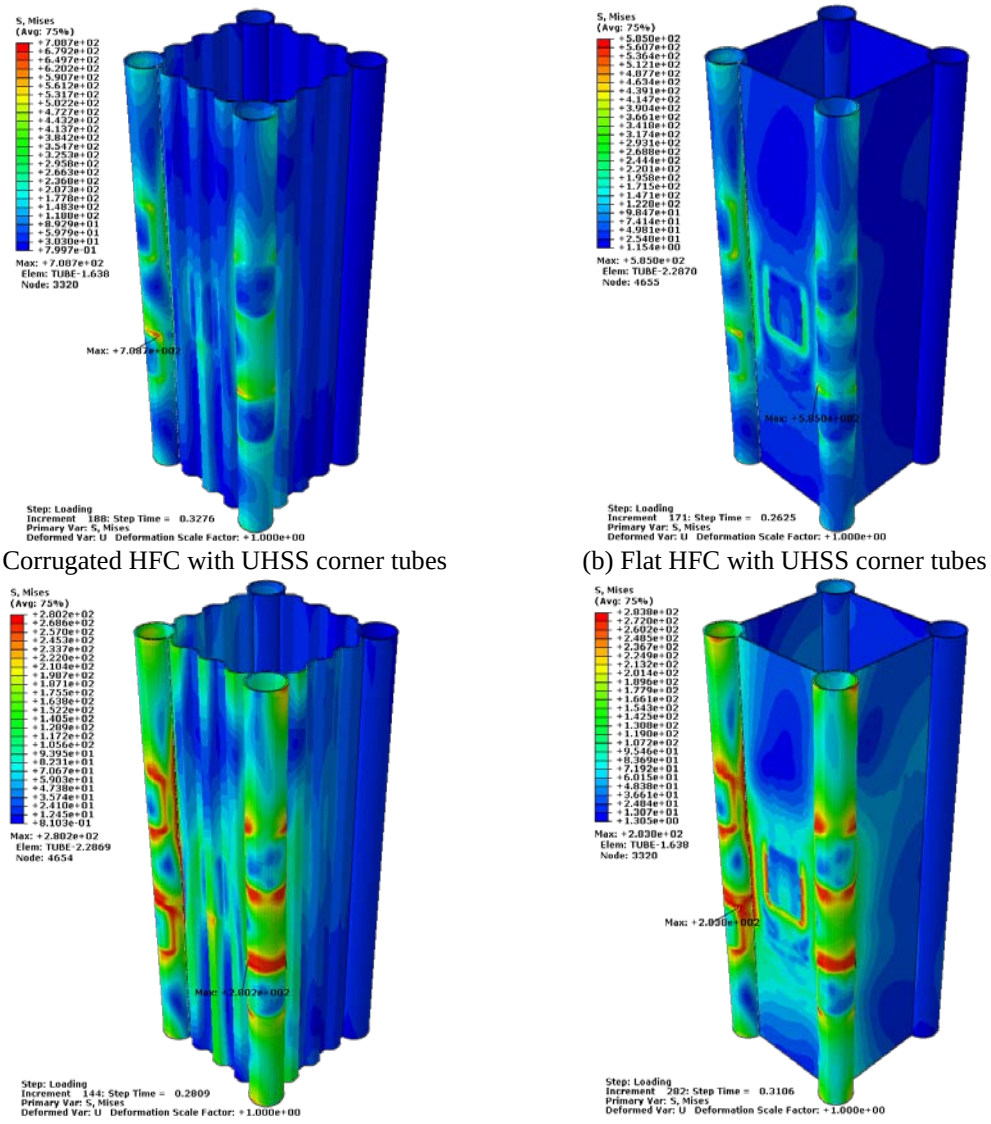

(a) Corrugated HFC with UHSS corner tubes (b) Flat HFC with UHSS corner tubes

(c) Corrugated HFC with MS corner tubes (d) Flat HFC with MS corner tubes

Fig. 5-15. von Mises stress (MPa) distribution on column

It can be observed that the level of von Mises stress on the corner tubes in all simulations performed on this non-reusable connection is lower than the ultimate strength of their material. It indicates that this version of the connection has not been able to utilise the material properties of the corner tubes, especially in the HFC consisting of UHSS corner tubes.

5.3.3 Bi-directional connection

One of the features of the innovative connection presented in this study is the capability of bi-directional connection i.e. attaching beam in perpendicular directions to the same connection. In this section the performance of a bi-directional connection is investigated. The ability of lateral in-plane deformation in the corrugated plates, as observed in the previous simulations, makes the study of the bi-directional connection attached to a

corrugated HFC very interesting. The limitation imposed by the connection on the deformation of the corrugated plates is expected to noticeably affect the connection performance. The model used in this simulation is presented in Fig. 5-16.

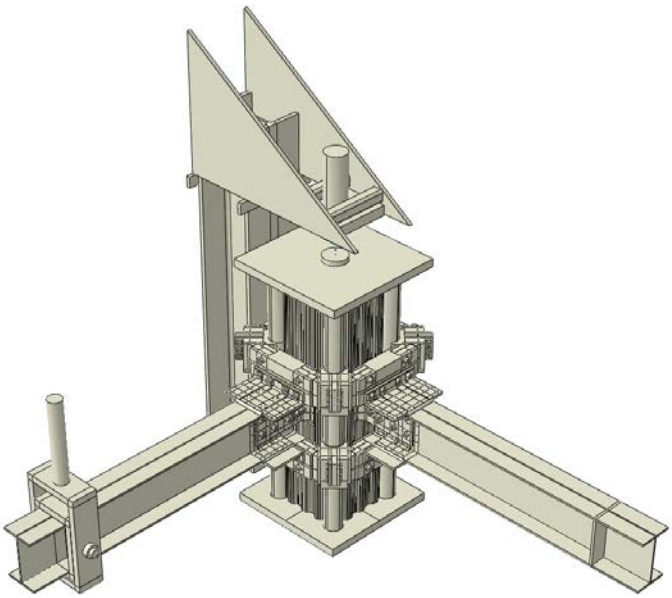

Fig. 5-16. Bi-directional connection simulation setup

Similar to the previous simulations, the load is applied on the ram rod and boundary conditions, material properties, and meshing properties are the same. The extra beam added to the connection is free of loading or constrains. This allows for investigating only the effect of additional components on the overall behaviour of the connection. The moment-rotation curves of the connection in both MS and UHSS cases are presented in Fig. 5-17.

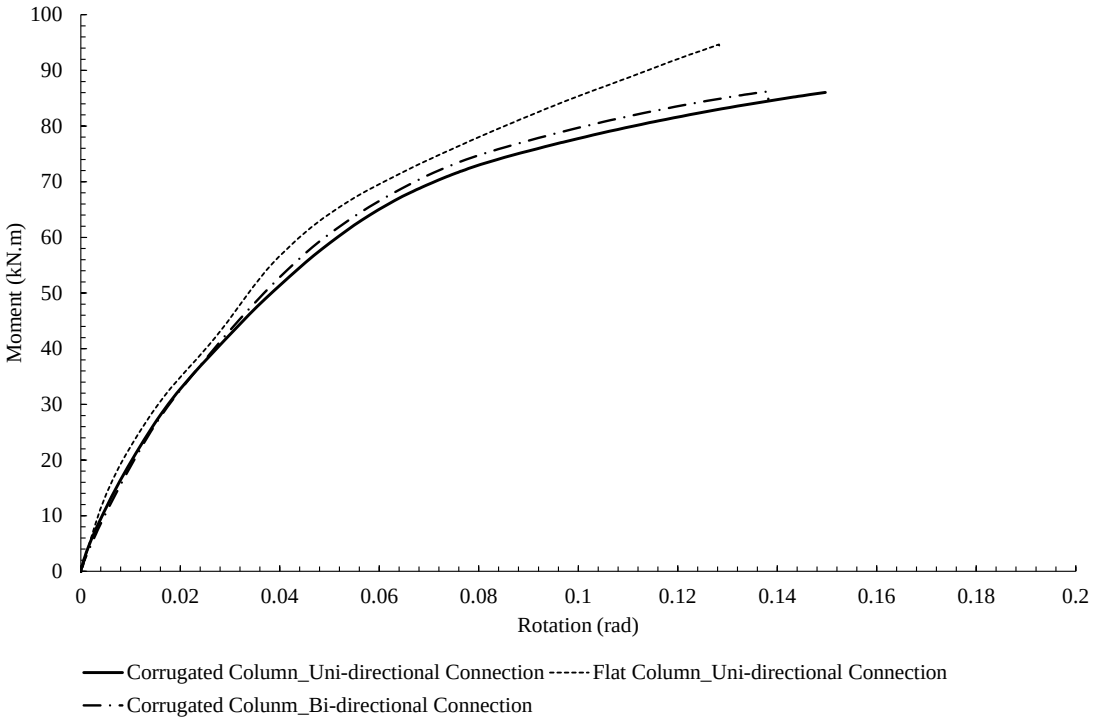

(a) Connection attached to HFC with UHSS corner tubes

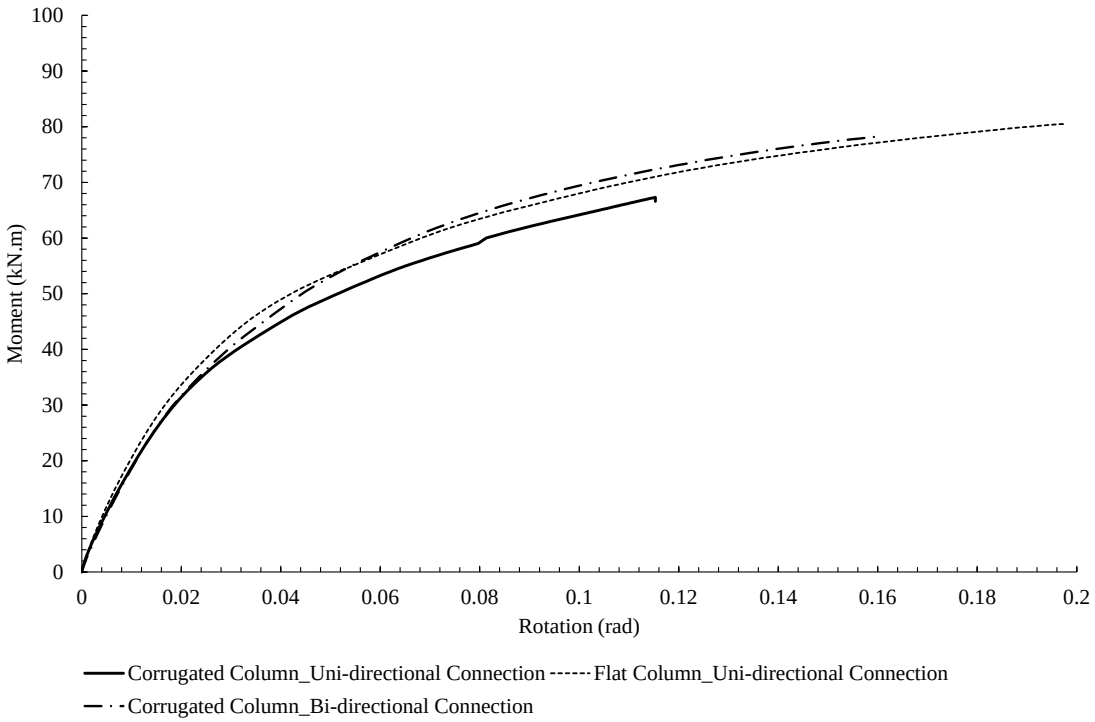

(b) Connection attached to HFC with MS corner tubes

Fig. 5-17. Behaviour of bi-directional connection attached to corrugated HFC

As it can be seen in Fig. 5-17, by adding the second set of connection components, the joint demonstrates a higher level of stiffness in general. The effect could be associated to the extra constraint that the added connection exerts on the deformation of the corrugated plate on the side to which the secondary connection is attached. This constrain is provided through the interaction of the collar part (Fig. 5-8 (a)) and top corner part (Fig. 5-8 (c)) and also shear resistance of the M16 bolts that connect the two aforementioned parts. This effect can also be observed in the way that the beam is deformed. For instance, in the corrugated column with UHSS corner tubes shown in Fig. 5-18, the beam bottom flange on the side to which the secondary connection is attached, shows more deformation than the other side which has no secondary parts attached.

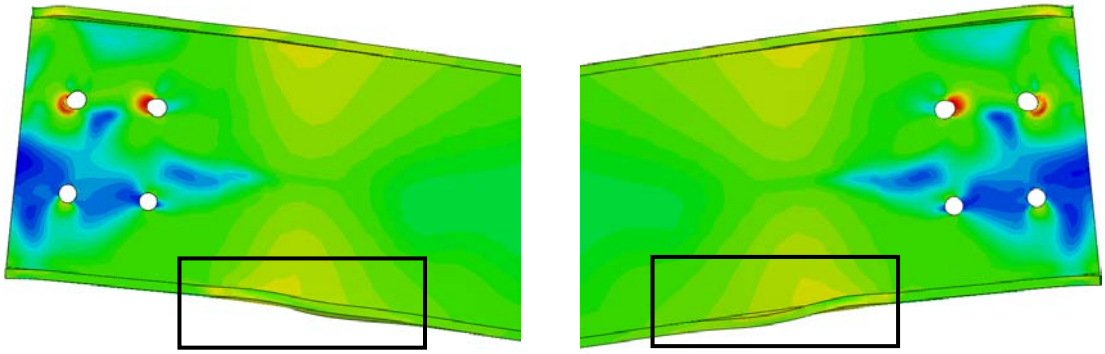

(a) No-connection side (b) Secondary connection side

Fig. 5-18. Comparison of beam deformation in bi-directional connection with UHSS corner tubes

The moment capacity of the connection also increases, which is more significant for the corrugated column with MS corner tubes. In other words, the effect of material properties of the corner tubes in the bi-directional connection is more significant. Taking the 0.1 rad rotation point, the capacity of the connection attached to the corrugated column with UHSS corner tubes has increased 2.6% but for the MS case this improvement is around 9.4%. The connection rotation is more than the 0.04 rad threshold and it is comparable to the uni-directional connections. The higher level of improvement in the MS case could be results of the support that the additional connection provides, which prevents the crushing of the corner tubes as happens for the uni-directional connection [14].

The von Mises stress distribution is presented in Fig. 5-19. The stress levels on the corner tubes which are supposed to be the main load path transfer shows that the stress levels on the corner tubes are very close to the ultimate strength levels of the corner tube materials in both MS and UHSS cases. This is the evidence that the connection has been able to take advantage of the material properties of the corner tube material, especially in the case of the UHSS corner tubes.

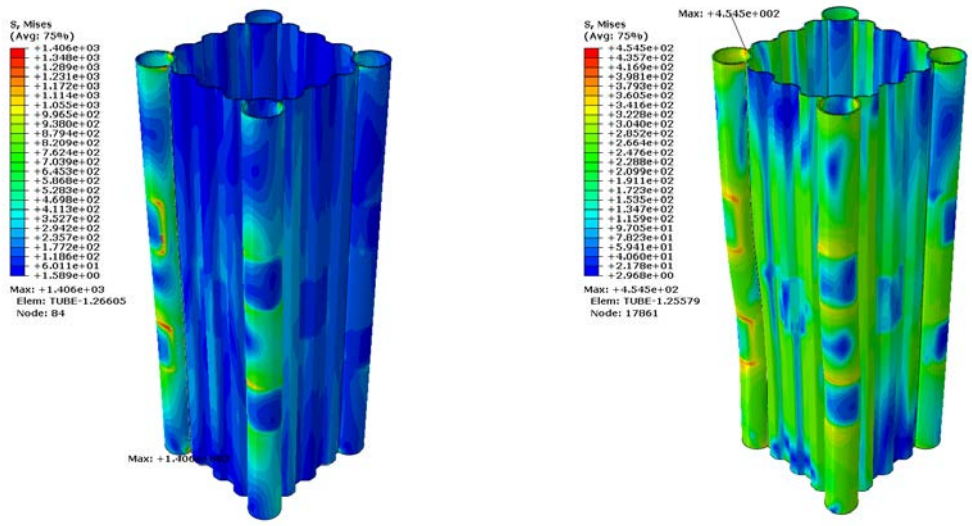

(a) UHSS corner tubes (b) MS corner tubes

Fig. 5-19. von Mises stress (MPa) distribution in bi-directional connection

The level of equivalent plastic strain on top angle and seat angle (Fig. 5-20), compared to the level of this parameter in the previous studies by the authors [13 , 14] show that although the levels of this variable are less than the failure limits extracted from previous studies, the top angles are very likely to be the first components of the connection that would fail under loading. This means the failure mode for bi-directional connection is expected to be similar to that of uni-directional connection.

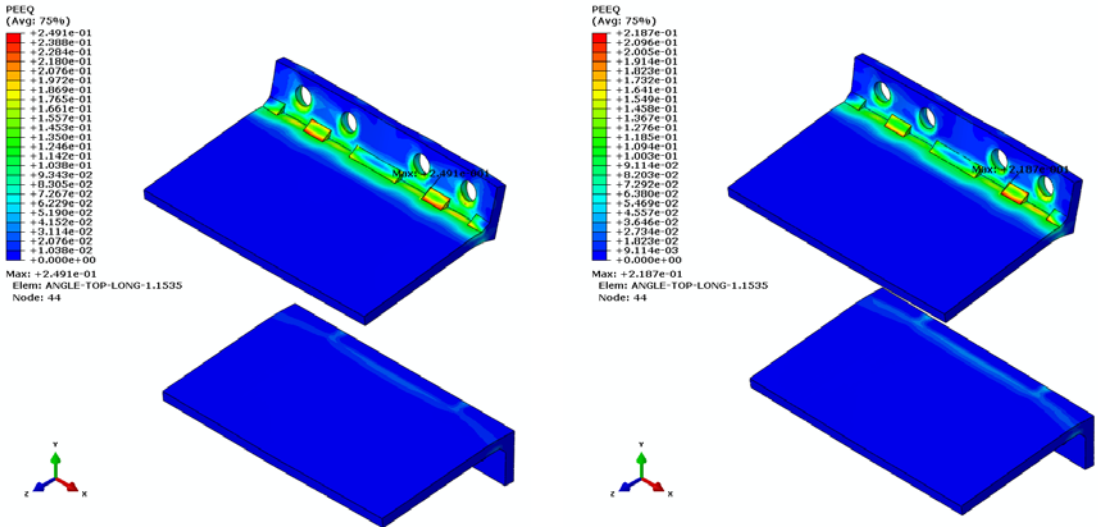

(a) UHSS corner tubes (b) MS corner tubes

Fig. 5-20. Equivalent plastic strain distribution in bi-directional connection on top and seat angles

5.4 Conclusion

In this research work, the performance of an innovative connection used along with corrugated hybrid fabricated columns was investigated. The simulation results showed that

the connection demonstrated less stiffness and moment capacity compared to the case where the flat column was investigated. The moment capacity was, however, more than the beam plastic capacity and the rotation was also more than the 0.04 rad threshold necessary for frames used in seismic applications.

A non-reusable version of the connection was also simulated. The moment capacity and stiffness of the connection dropped significantly and the connection lost its full-strength status. Nevertheless, the connection was still capable of rotations more than the 0.04 rad. In addition, the behaviour of this version of the connection was studied when used along with the HFC with flat plates. Setting the flat and corrugated HFCs side by side, it was shown that the effect of material properties on the performance of the connection in the HFCs with MS corner tubes was less significant compared to the case of the HFCs with UHSS corner tubes.

Considering the flexibility of the corrugated plates, it was expected that the effect of having a bi-directional connection on the connection performance would be noticeable. Thus, the behaviour of a bi-directional connection used along with the corrugated HFC was simulated. The results showed that the connection demonstrated more stiffness and possessed more capacity compared to the uni-directional connection used along with the corrugated HFC. The connection in this case was also able to utilise the material properties of the corner tubes. In addition, the effect of material properties for corrugated HFC with MS corner tubes was more significant on the behaviour of the connection compared to the HFC with UHSS corner tubes.

Acknowledgement

The research work presented in this research work is supported by the Australian Research Council through a Discovery Project (DP150100442) awarded to the authors.

References

[1] Nassirnia M, Heidarpour A, Zhao X-L, Minkkinen J. Innovative hollow corrugated columns: A fundamental study. Engineering Structures; 2015;94:43–53.

[2] Pignataro M, Pasca M, Franchin P. Post-buckling analysis of corrugated panels in the presence of multiple interacting modes. Thin Wall Struct 2000;36:47–66.

[3] Lotfi S, Azhari M, Heidarpour A. Inelastic initial local buckling of skew thin thickness-tapered plates with and without intermediate supports using the isoparametric spline finite strip method. Thin Wall Struct. 2011;49:1475–82.

[4] Kasaeian S, Azhari M, Heidarpour A, Hajiannia A. Inelastic local buckling of curved plates with or without thickness-tapered sections using finite strip method. Int J Steel Struct 2012;12:427–42.

[5] Nassirnia M, Heidarpour A, Zhao XL, Wang R, Li W, Han LH. Lateral impact response of innovative hollow corrugated members. International Journal of Impact Engineering. 2018;114:43–52.

[6] Farahi M, Heidarpour A, Zhao X, Al-mahaidi R. Compressive behavior of concrete filled double skin sections consisting of corrugated plates and ultra-high strength steel corner tubes. 2017;1(2):2120–7.

[7] Nassirnia M, Heidarpour A, Zhao X-L, Minkkinen J. Innovative hollow columns comprising corrugated plates and ultra high-strength steel tubes. Thin-Walled Structures. 2016;101:14–25.

[8] Farahi M, Heidarpour A, Zhao XL, Al-Mahaidi R. Compressive behaviour of concrete-filled double-skin sections consisting of corrugated plates. Engineering Structures. 2016;111:467–77.

[9] Javidan F, Heidarpour A, Zhao XL, Minkkinen J. Application of high strength and ultra-high strength steel tubes in long hybrid compressive members: Experimental and numerical investigation. Thin-Walled Structures. 2016;102:273–85.

[10] Javidan F, Heidarpour A, Zhao X-L, Hutchinson CR, Minkkinen J. Effect of weld on the mechanical properties of high strength and ultra-high strength steel tubes in fabricated hybrid sections. Engineering Structures. 2016;118:16–27.

[11] Farahi M, Heidarpour A, Zhao XL, Al-Mahaidi R. Parametric study on the static compressive behaviour of concrete-filled double-skin sections consisting of corrugated plates. Thin-Walled Structures. 2016;107:526–42.

[12] Javidan F, Heidarpour A, Zhao X, Minkkinen J. Performance of innovative fabricated long hollow columns under axial compression. Journal of Constructional Steel Research;2015;106:99–109.

[13] Sadeghi SN, Heidarpour A, Zhao XL, Al-Mahaidi R. A comparative numerical study on the innovative I-beam to thin-walled hybrid fabricated column connection. Thin-Walled Structures. 2018;127:235–58.

[14] Sadeghi SN, Heidarpour A, Zhao XL, Al-Mahaidi R. An innovative I-beam to hybrid fabricated column connection: Experimental investigation. Engineering Structures. 2017;148:907–23.

[15] ABAQUS 6.14-1. Providence, RI, USA: Dassault Systèmes; 2014.

[16] AS/NZS 3679.1:2016 Structural steel - Hot-rolled bars and sections. Sydney, Australia: Standards Australia; 2016. 47 p.

[17] Al Hendi, H, Celikag, M. Parametric study on moment–rotation characteristics of reverse channel connections to tubular columns. J. Constr. Steel Res. 2015;104:261–273.

[18] J. Shen, B. Akbas, O. Seker, B. Doran, R. Wen, E. Uckan, Seismic axial loads in steel moment resisting frames, Int. J. Steel Struct. 2015;15:375–387.

[19] FEMA-350, Recommended Seismic Design Criteria for New Steel Moment-Frame Buildings, Prepared by the SAC Joint Venture for the Federal Emergency Management Agency, Washington, DC, 2000.

[20] American Institute of Steel Construction (AISC), Seismic Provisions for Structural Steel Buildings (AISC 341), American Institute of Steel Construction, Chicago, IL, 2016.

SUMMARY AND FUTURE WORK

CHAPTER 6

Table of Contents

6.1 Summary of Outcomes

The main aim of this research has been developing a robust connection for hybrid fabricated columns. Several experimental tests have been conducted to validate the numerical models in order to investigate the behaviour of this innovative connection under quasi-static monotonic loading. The resutls of this study could be used for further study of the connection behaviour and provide a deeper insight into its performance. These resources could also be used to provide design formulae and recommendations for this type of connection. The summary of major outcomes and the suggestions for the future work are presented in this chapter.

6.1.1 Innovative modular connection

The conventional connections may not be a suitable choice to effectively transfer loads from an I-beam to the hybrid-fabricated column. Therefore, it seems necessary to design a new connection from scratch based on the characteristics of the hybrid-fabricated column. This new connection should be capable of getting the most out of the significantly higher capacities of the corner tubes in hybrid-fabricated columns. Obviously, the connection should demonstrate enough ductility and load-bearing capacity in such a way that a weak member-strong connection relation exists. The connection proposed in this thesis has been tried to be modular to make the construction quicker, easier, and safer. The modular connection annihilates the necessity of on-site welding, increasing the safety, and provides the building with better construction tolerances that make the jobs of different trades easier and improves the overall quality of the structure. It will also offer the possibility of retrofitting the building by just replacing the damaged parts or erecting temporary moment frames. The connection parts are also reusable in new constructions in the case of a structure built with these connections was deemed to be demolished. This connection is also flexible enough to cover a wide range of column and beam sizes with minimum modifications in the components or just changing the distance between the top and the bottom segments.

6.1.2 Numerical simulation of conventional and innovative connections

A 3D model that had been verified using the experimental data available from the tests and literature was used to investigate the behaviour of the innovative connection and four conventional types of connection (extended end plate, flush end plate, reverse channel, and

modified ConXL). This model can incorporate damage and non-linear deformations and material properties. The simulations showed that the conventional connection could not effectively utilise the superior behaviour of the HFCs and eventually a new connection was proposed that based on simulations was capable of reaching higher levels of moment capacity while showing a ductile behaviour. The flush and extended endplate connections exhibited low initial stiffness and insufficient load-bearing capacity. The reverse channel connection indicates a higher initial stiffness but still fails to provide a reasonably high capacity to satisfy the weak member-strong connection design condition. A modified version of the ConXL connection was also simulated as one of the conventional types of the connections. This connection exhibited a higher initial stiffness and a relatively higher load-bearing capacity; however, the major modifications required to adapt it for the HFC is a significant drawback in the potential use of this connection.

The innovative connection consisting of eleven components has demonstrated a high initial stiffness and has the highest moment capacity compared to all the studied connections. Having the advantage of showing a highly ductile behaviour along with the notably high moment capacity makes this connection an excellent choice for high-rise buildings. This connection also utilises the superior material properties of the hybrid-fabricated columns with ultra-high strength steel corner tubes.

6.1.3 Experimental investigation of innovative connection under monotonic loading

In this part of the research work, three experimental tests were performed under monotonic loading. The one-meter high columns were made of mild steel flat plates and mild steel or ultra-high strength steel corner tubes. The main aim of the tests was to extract the moment-rotation curve of the connection under static loading. The first test was performed on a column with ultra-high strength steel corner tubes attached to the first version of the connection. In this version, the beam is attached to the top and seat angles of the connection using bolts. In the second and third tests, the beam is welded to the top and seat angles of the connection. The corner tubes in the second and third tests are made of ultra-high strength steel and mild steel, respectively.

Results of the first test showed that the moment capacity of the connection could reach up to 90% of the capacity of the attached beam (200UB22.3 [52]). The connection failure was the sudden failure of the top/seat angle bolts. This failure caused a vast spontaneous drop in the moment capacity of the connection, which is not favourable in practice. The

connection components were in their elastic range and sprung back to their place upon removal of the beam. Moreover, the rotation capacity of the connection was more than 0.04rad, which is the recommended minimum rotation threshold for connections used in moment frames.

The second test was performed using a modified version of the connection in which the beam is welded to the top and seat angles of the connection. The column in this test, similar to the first test, had ultra-high strength corner tubes. Results of this test showed that the measure taken regarding replacing the bolts with welds for attaching the beam to the connection had fixed the issue with sudden connection failure and huge drop in its capacity. The moment capacity of the connection in this configuration went beyond the capacity of the beam (~1.5 times the beam capacity) while showing more ductility. Even after the failure initiation, which was in the top angle, the connection capacity did not drop significantly, and it was still higher than the beam capacity. The connection parts in this test were again reusable for the next experimental test.

The third test was performed using the same connection and a similar setup used in the second test. The difference was that the column corner tubes were made of mild steel material. The moment capacity of the connection, in this case, was also higher than the beam moment capacity (~1.2 times). The ductility of the connection was the highest among all three tests. In this test, the connection did not fail, and the test was stopped due to the hydraulic jack of the loading machine reaching its stroke limit. Unlike other tests that the columns were not noticeably damaged or distorted, the column in this test was heavily distorted. The faceplates on the sides were warped and the corner tubes were squashed close to the lower segment of the connection (compression zone). A part of the higher ductility of the connection in this test could be attributed to this phenomenon.

6.1.4 Topology optimisation of the innovative connection

In the experimental tests and numerical simulations, the performance of the innovative connection was investigated, and its advantages over the conventional connections were observed. One of the characteristics of the connection that has room for improvement is its weight. Among different parts of the connection, the collars are suitable candidates for topology optimisation and weight reduction. This is because of their relatively simpler shape compared to the other components and their contribution to a large portion of the

connection weight. Therefore, any change in their weight can have a major impact on the overall weight reduction of the connection.

Topology optimisation is defined as finding the optimal distribution of the material in the optimisation domain while satisfying certain conditions. This can be achieved by maximising the stiffness or minimising the compliance of the optimisation domain. The optimisation in this part was performed using ANSYS. In order to find the extreme levels that material could be removed from the collars, the optimisation goal was set at 40%. The optimisation was performed on the original connection and on a connection, which was 12mm thinner than the original. The optimisation results suggest that material at which areas can be removed and at which areas should be reserved. Obviously, the figures presented by the software are not of any practical use straightaway and need more processing to turn into practical solutions. However, it can be observed that the zone in the middle of the parts is the location where removing the material is mainly suggested.

Thus, the optimised components based on these suggestions were created, and a similar modification was done on the bottom collar as well. The resultant connection behaviour under monotonic loading was investigated. The loading conditions, boundary conditions, column geometry, and material definition were consistent with the previous simulations for comparison between the results being possible and meaningful.

In connection with original dimensions, the weight reduction was around 6% while in the case of the reduced size connection this reduction was almost 26%. In spite of these reductions in weight, the performance of the connection is still satisfactory. As the results showed, the connection has retained its high ductility and still can pass the 0.04rad threshold. The moment capacity is also comparably high, and the connection capacity in all cases is higher than the beam capacity. Although the initial stiffness in all cases is almost the same, the stiffness of the connection in reduced and reduced-optimised cases are noticeably lower in larger rotations, which is justifiable considering the lower thickness of the connection around the axis that it bends under loading. Therefore, the optimised connection can be a plausible option in practice by which the weight is reduced significantly while the capacity and ductility still meet the demands.

6.1.5 Developing a component-based model for the innovative connection

Although the developed numerical finite element model was capable of accurately predicting the behaviour of the connection, the complexity of the connection, non-linear

material properties, and contact definitions had made it computationally expensive. Therefore, a component-based model was developed in order to have an accurate representation of the moment-rotation curve of the connection at a lower computational cost. This model can be used in further parametric studies or design recommendations.

Due to the complexity of the connection, numerous components were identified and included in the model. It was assumed that the connection rotates about the reference datum, which is located at the mid-line of the seat angle's outstanding leg. The components above that line are in tension and the ones located lower are under compression.

A group of the connection components were already included in Eurocode3, and others were taken from the available literature or developed in this study. The geometrical and material properties of the components in the model were identical to the original connection.

The results of the component-based model were compared to the finite element results for columns with both mild steel and ultra-high strength steel corner tubes. The finite element model, similar to the previous simulations was a 3D model of the connection with the non-linearities (material, geometry, and contacts) included. The component-based model can capture the behaviour of the innovative connection. The initial stiffness was estimated accurately, and failure point prediction was close to the observations in the experimental tests.

The tri-linear model definition, chosen for the moment-rotation curve is more compatible with the joint behaviour in the plastic-hardening region of the curve, compared to that suggested by Eurocode3. The model can be used for further parametric studies, software implementation, or design recommendations.

6.1.6 Numerical analysis of the connection along with corrugated HFC

In this part of the research, the behaviour of the connection attached to the corrugated HFC was investigated. The finite element model developed for this analysis was similar to the model previously developed for the case of the column with flat plates (element type, loading conditions, etc.). The setup was identical to the previous simulations in which HFC with corrugated plates is replaced for HFC with flat faces.

In the first step, the original connection behaviour was studied. As the moment-rotation curve of the connection shows, the corrugation of the plates of the column reduces the moment capacity of the joint when compared to the original connection attached to HFC with flat plates. However, in both cases of MS or UHSS corner tubes, the connection retains

its full strength status. Although the ductility of the joint in both cases is still high and the rotation is far above the 0.04rad threshold, the rotation capacity in the MS tube case noticeably decreased.

The relatively lower stiffness of the joint with corrugated column could be attributed to the higher deformability of the corrugated plates on the sides of the column. Unlike the flat plates, the corrugated plates can expand when loaded transversely. In the column with flat plate, the front plate in the region close to the web-angles was locally more deformed to compensate for the required deformation, in spite of the higher stiffness of the column in that direction.

The connection was able to effectively utilise the UHSS corner tube's high capacity. Thus, HFC with corrugated plates could be used with this connection, and the resulting joint has high capacity (more than beam capacity) and rotation (higher than the 0.04rad threshold) similar to the connection with flat HFC.

In addition to the connection with the original size, a version of the connection with reduced thickness attached to the corrugated and flat connection was simulated as well. The dimensions of this new version of the connection were chosen so that its components, namely collars were not reusable. It was shown that the joint stiffness dropped significantly, and the connection's capacity was less than the beam capacity (partial strength). The effect of corrugation was less, compared to the case of original connection, but its effect was still more obvious in HFC with UHSS corner tubes compared to HFC with MS corner tubes. Finite element results showed that the UHSS corner tube capacity is utilised in neither the corrugated column nor the flat column. In MS corner tube case, the stress level in tubes was above the yield strength but did not reach the ultimate stress, so the capacity, in this case, was also not fully utilised.

Additionally, considering the bi-directional capability of the connection and the geometry of the corrugated plate of the HFC, which allows for more lateral plate deformation, the effect of attaching more than a beam to the same column on stiffness, capacity, and rotation of the joint was investigated. The results showed that the bi-directional connection capacity decreases compared to the uni-directional connection but the capacity is still above the beam capacity. The rotation of the connection is also more than the 0.04 rad threshold. Thus, this bi-directional connection could be used in seismic applications. However, the joint demonstrates a less stiff behaviour.

6.2 Future Works

The robustness and adequacy of the connection proposed in this PhD thesis have been demonstrated using experimental testing and numerical models. However, there are more steps needed to be taken before this connection can be used readily by the designers in practical applications.

6.2.1 Investigating the effect of fabrication method on the connection performance

Considering the shape and also volume of the connection components needed in construction, there might be more efficient and economically feasible methods (such as casting) to be used for fabrication of the connection. Finding the most efficient method and investigating the behaviour of the connection fabricated by such method could be beneficial for introducing the connection to the construction industry as a practicable option.

6.2.2 Cyclic behaviour

Since the connection proposed in this research might be used in seismic regions, it is necessary to investigate its behaviour under cyclic loadings. Full-scale cyclic loading for uni-directional and bi-directional connections could provide a deeper insight into how the connection behaves against load reversals and cumulative damage. This could be done individually or as a part of a hybrid simulation to investigate the response of a frame incorporating this type of connection.

6.2.3 Design recommendations

Although the moment-rotation curves of the connection behaviour for several cases have been extracted in this research, more simulations/experimental tests are required to provide enough data in order to be able to cover a wide range of column, beam and connection sizes. The component-method program that was developed during this research could be utilised to this end. Moment-rotation curves could be fed into major design software platforms (such as OpenSees) to be used in construction projects.